Ecole Thématique CNRS Spring School

IUEM PLOUZANE, FRANCE
11-14 MAI 2010

ICELAND

IN THE CENTRAL NORTHERN ATLANTIC

HOTSPOT, SEA CURRENTS AND CLIMATE CHANGE

IUEM-OSU
DOMAINES OCEANIQUES
CNRS-UBO

cnrs INSU
Observer & comprendre

TABLE DES MATIERES

All the communications and posters are in open access on the French repository HAL-UBO at the following address http://hal.univ-brest.fr/ICELAND/fr

ECOLE THEMATIQUE - CNRS - SPRING SCHOOL

Iceland in the central Northern Atlantic : Hotspot, sea currents and climate changes

11-14 Mai 2010 Institut Européen de la Mer, Plouzané, FRANCE

Avec le soutien du Laboratoire Domaines Océaniques, de l'UBO, de l'IUEM, du GIS Europôle Mer, de l'IPEV, du CNF-INQUA

Comité Scientifique- Scientific Commity :
Françoise Bergerat ; Yves Frenot, Louis Géli ; Hervé .Guillou , Paul Tréguer

Comité d'Organisation :
Brigitte Van Vliet-Lanoë, Dominique Gac ; Françoise Bergerat ; Gilles Chazot ; Olivier Dauteuil ; Christophe Hémond , Yves Frenot , Thierry Villemin

Responsable organisation : ***Brigitte van Vliet-Lanoë*** *avec Dominique .Gac, Agnès Agarla, Murielle Dubreule,*

Responsable publication : ***Dominique Gac*** *avec Brigitte Van Vliet-Lanoe*

PROGRAM

Tuesday 11th May: morning bus 8h15 at the hotel

9h00 Y.M. Paulet (Dir .IUEM) *Welcome*
C.David (Dir.Ad.IIPEV) *Arctic , a major research field*
9h30-10h: Th.Villemin *Iceland : inside the recent Earth geological story*

COFFEE BREAK

Hotspot, rifting and volcanism: A. Gudmundsson (Roy.Hol.London)
10h-10h 45 : L. Geoffroy (Le Mans) The North Atlantic System.
12h- 12h:45: Ch.. Hemond (LDO) Iceland, an anomalous Hot Spot.

BUFFET / POSTERS

Hotspot, rifting and volcanism: Chairman: M.Maia (LDO)
14h15-15h: F.Bergerat, (Paris VI): Recent and present-day tectonics near a hot spot: the transform zones of Iceland.
15h -15h45 : Garcia S (Berlin): Ridge jump process in Iceland.

COFFEE BREAK

Hotspot, rifting and volcanism: Chairman: A.Agranier (LDO)
16h15-17h: O.Sigmarsson (Clermont) Influence of tectonism on the composition of acid and basaltic lava.
17h-17h45: A.Gudmundsson .(Roy.Hol.London) Fluids and volcanism.

18h15 ICE BREAKER (bus departure at the IUEM: 20h)

Wednesday 12th May morning bus 8h15 at the hotel

Glaciology & Volcanism : Chairman G.Chazot

9h -9h45 : M.Menzies (Roy.Hol.London) Icelandic Tephrochronology - Matching the Provenance of Proximal and distal Volcanic Glasses Using La-Icpms Trace Element Data.
9h45-10h30: O. Dauteuil (Rennes) Enlargement of the active rift during Glaciations.

COFFEE BREAK

Glaciology & Volcanism : Chairman C.Delacourt

11h-11h45 H.Bjornsson (Univ.Reykjavik) Glaciers and jökulhlaups : the mechanisms.

11h45-12h30 J.L.Schneider (Pr .EPOC) Jokulhaup and climate change.

BUFFET / POSTERS

Glaciology & Volcanism : Chairman H.Belon
13h 45-14h30 T.Villemin (EDYTEM) Earth responses to Ice Mass Changing in Iceland.

14h30-15h15 H.Guillou (.LSCE) New unspiked K-Ar ages of Quaternary sub-glacial and sub-aerial volcanic activity in Iceland

COFFEE BREAK

Climate changes recorded in Iceland and offshore: Chairman J.Giraudeau
15h45-16h30 C.Hillaire-Marcel (GEOTOP) Sea Ice extent and global ice isotopic signal

16h30-17h15 N. Fagel (Ulg, B) Record of Glaciations Off the East Greenland Coast Over the Last 400 kyr:Sm-Nd Isotopic Signature of Marine Clays

17h15-18h00 F. Eynaud (EPOC) Paleohydrology around Iceland: microplanctonic proxies and the Last Glacial-Interglacial cycle

DINNER "on a boat" (Brest bay) bus departure IUEM : 18h30

Thursday 13th May: morning bus 8h15 at the hotel

Climate changes recorded in Iceland and offshore. Chairman C.Hillaire-Marcel

9h-9h45 Van Vliet-Lanoe B. (LDO) Glacier and Sea ice extent in Iceland during the Quaternary.

9h45-10h30 A. Gudmundsson (Reykjavik) Rock Glaciers and Relict Debris Bodies In Central North Iceland

COFFEE BREAK

Recent climate changes, sea ice and the ocean: chairman

11h00-11h45 M. Kirkbride (Dundee Univ.)Tephrochronological dating of Holocene moraines at icelandic glaciers, and climatic interpretations.

11h45-12h30 Strukell E. (Göteborg Univ.) Holocene Major Eruptions.

BUFFET

14h-16h Questions and discussion: importance of the volcanic forcing

Recent climate changes, sea ice and the ocean: Chairman N.Fagel (ULg)

16h30-17h15 J. Giraudeau (EPOC).The Holocene Climatic History of the Circum-Icelandic Oceanic Realms

17h15-18h N.Frank (LSCE): The Holocene Climatic History of the Circum-Icelandic Oceanic Realms

bus departure IUEM : 18h30 Free evening

Friday 14th May: morning bus 8h15 at the hotel

Recent climate changes, sea ice and the ocean: Chairman A.M.Tréguier (LPO)

9h-9h45 G. Massé (LOCEAN) Arctic Sea Ice: High Resolution Reconstructions

9h45-10h30 Huck Th. (LPO) Recent change in North Atlantic circulation

COFFEE BREAK

11h00 -11h45 C.Cassou (CERFACS, Toulouse) The North Atlantic Oscillation :Mechanisms And Spatio-Temporal Variability

12h-13 BUFFET

Workshop Discussion 13h-15h30 : T. Villemin, C.Cassou (CERFACS), C.Hillaire–Marcel (GEOTOP), O.Ragueneau (LEMAR), F.Eynaud (EPOC), M.Maia (LDO)

bus departure IUEM : 16h to the station; shuttle to the airport

THE TEACHING TEAM


Françoise Bergerat


Helgi Bjornsson


Christophe Cassou


Olivier Dauteuil


Fréderique Eynaud


Nathalie Fagel


Norbert Frank


Claude Hillaire Marcel


Sebastien Garcia


Laurent Geoffroy


Jacques Giraudeau


Agust Gudmundsson (Reykjavik)


Agust Gudmundsson (London)


Herve Guillou


Christophe Hémond


Thierry Huck

Martin Kirkbride

Guillaume Massé

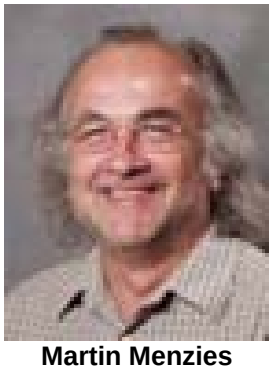

Martin Menzies

Jean-Luc Schneider

Olgeir Sigmarsson

Erik Sturkell

Brigitte Van Vliet-Lanoë

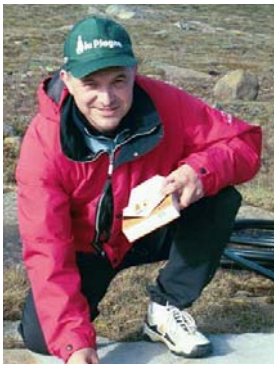

Thierry Villemin

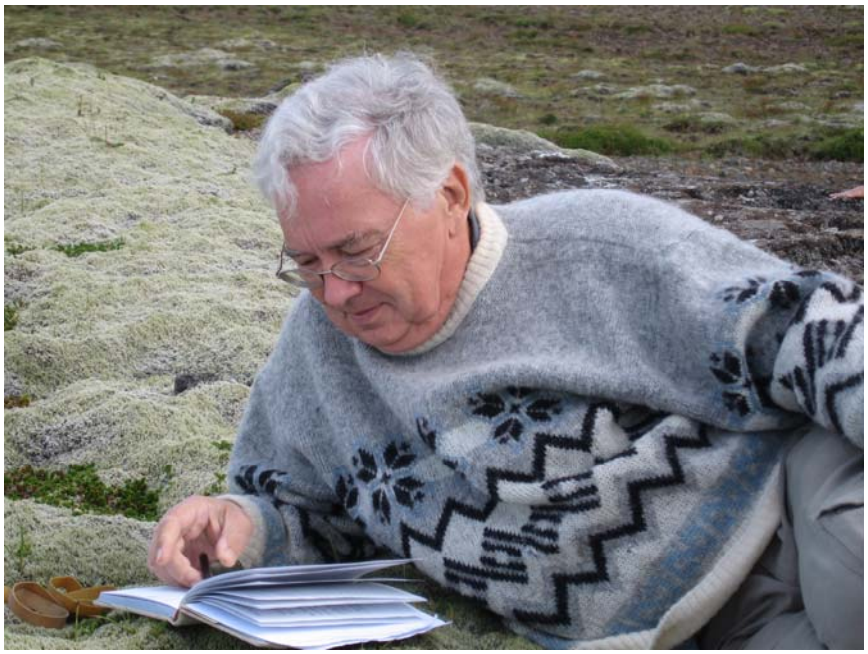

Jacques Angelier

1947 - 2010

Jacques Angelier devait présider cette Ecole sur l'Islande. Il nous a quittés le 31 janvier 2010 emporté en six mois par un cancer fulgurant.

Jacques Angelier est né le 2 mars 1947 à Alès. Elève de l'Ecole Normale Supérieure de Saint-Cloud de 1966 à 1970, il y acquiert le goût des tâches d'enseignement. Il entre comme Assistant à l'Université Pierre et Marie Curie en 1970, où il soutient une thèse de 3ème cycle sur la « Bande triasique de Barjols », puis il rejoint en 1971 l'Université d'Orléans. Il y restera, comme Assistant puis Maître-assistant, jusqu'en 1976, date à laquelle il revient à l'Université Pierre et Marie Curie, où il est nommé Professeur en 1981. Il a été pendant plus de vingt ans un des piliers du Laboratoire de Géologie Structurale puis de Tectonique avant de rejoindre, en 2003, l'Observatoire Océanologique de Villefranche-sur-Mer.

Il appréciait la chance qui lui avait été donnée de dispenser, au cours de sa carrière, des enseignements variés quant aux niveaux (tous les cycles universitaires), aux publics (étudiants, futurs enseignants, professionnels), aux nationalités (France, USA, Taiwan), et aux thèmes (tectonique, géophysique, informatique). Ceux qui ont suivi ses cours s'en souviennent comme d'un pédagogue de talent, il a certainement été à l'origine du goût pour la géologie de beaucoup d'étudiants.
Les travaux scientifiques de Jacques Angelier sont nombreux tant dans le domaine méthodologique que géodynamique.

Les « méthodes Angelier » d'analyse de la déformation cassante sont connues de tous ceux qui travaillent sur les déformations passées et présentes de la croûte terrestre et on ne compte plus le nombre de collègues qui les utilisent en France et dans de nombreuses universités sur tous les continents. Allant de l'approche théorique au développement de logiciels et aux applications de terrain, il travaillait sans cesse à les faire évoluer.

Ses recherches sur le terrain ont concerné des contextes variés de déformation, à la fois continentale et océanique. Sa thèse d'Etat sur « La néotectonique de l'arc égéen », soutenue en 1979, constitue le premier de ses grands travaux mêlant méthodologie et géodynamique. Il fut suivis d'autres sur l'Afrique du Nord, le Mexique, les Etats-Unis, le Japon, la Corée, la Russie, l'Ukraine, etc. Depuis le début des années 80, ses recherches s'étaient de plus en plus focalisées sur les déformations actives où ses travaux lui permettaient d'associer les études de terrain et l'analyse des séismes, en Islande et surtout à Taiwan, qui était le pays le plus cher à son cœur.
Ses recherches l'ont amené au cours de sa carrière à établir de nombreuses collaborations avec des Instituts géologiques ou géophysiques, tels que le Service Météorologique Islandais et l'*ISOR* à Reykjavik, *l'Academia Sinica* et le *Geological Survey* à Taipei, et bien d'autres. Il avait monté en 2007 un Laboratoire international France-Taiwan « ADEPT » (*Active Deformation and Environment*

Programme for Taiwan) soutenu par le CNRS et le *National Science Council*.

Jacques Angelier a été membre de diverses sociétés et académies en France et à l'étranger, ainsi que de l'Institut Universitaire de France ; il était membre correspondant de l'Académie des Sciences depuis 1997. Plusieurs prix avaient récompensé son activité scientifique : le prix Raulin de l'Académie des Sciences (1991), le prix Fourmarier de l'Académie Royale des Sciences de Belgique (1996), le prix de la Fondation franco-taiwanaise de l'Institut de France (1999).
Mais plus que de ces distinctions, Jacques Angelier était fier d'être resté un homme de terrain et prenait plaisir à transmettre et à partager ses connaissances tant avec ses nombreux thésards, qu'avec ses collègues, mais aussi avec les gens « du cru » rencontrés à l'occasion de ses campagnes. Ceux qui ont eu l'occasion de travailler avec lui garderont le souvenir d'un brillant scientifique et d'un homme toujours enthousiaste.

Françoise BERGERAT et Benoît DEFFONTAINES

RECENT AND PRESENT-DAY TECTONICS NEAR A HOT SPOT: THE TRANSFORM ZONES OF ICELAND.

F. Bergerat*, J. Angelier †, C. Homberg, S. Garcia, S. Verrier and M. Bellou
* CNRS, UMR 7193, ISTeP, Case 117, 4 place Jussieu, F-75252 Paris cedex 05, France.
Courriel : Francoise.bergerat@upmc.fr

Abstract

The two transform zones that connect the Icelandic rift segments and the mid-Atlantic Ridge close to the Icelandic hot spot, are described in terms of geometry of faulting and stress fields. They differ in age: 8-8.5 My in the north and 2-3 My in the south, illustrating the different stages of maturity in the transform process, from an immature stage illustrated by the South Iceland Seismic Zone to a mature stage shown by the Husavik-Flatey Fault.

Introduction

The existence of Iceland, as a major volcanic island on top of the Mid-Atlantic Ridge, results from the interaction between the Icelandic hot spot and the Mid-Atlantic Ridge across which spreading occurs at a rate of ~1.9 cm/yr. The boundary between American and Eurasian plates has moved westwards with respect to the Icelandic hot spot. However, due to successive rift jumps, the present-day axial rift zone in Iceland remains roughly centred above the apex of the hot spot (Fig.1a). Therefore, the Icelandic rift is shifted more than 100 km eastwards with respect to the general spreading axis.

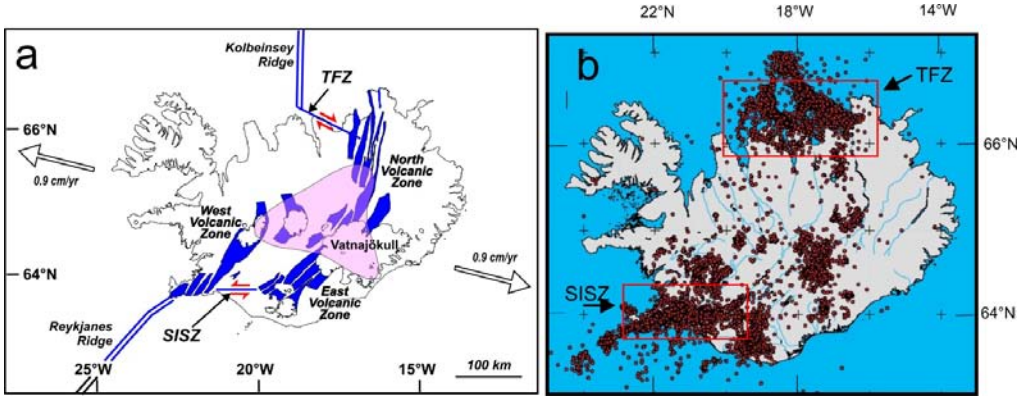

Figure 1 – (a) Iceland and the Mid-Atlantic Ridge. In black, the Icelandic rift. Grey triangular shape, extension of the hot spot at 400 km depth. Open arrows, direction and velocity of plate divergence. (b) Present day seismicity of Iceland: earthquakes of magnitude equal or superior to 1 for the period 1994-2002. SISZ : South Iceland Seismic Zone, TFZ: Tjörnes Fracture Zone.

The latest jumps differ in age in northern and southern Iceland: 8-8.5 My and 2-3 My, respectively. As a consequence, two major transform zones presently connect the Icelandic rift segments and the oceanic ridge, which are not at the same stage in their development and display different fault and stress patterns, highlighting the different stages of maturity in the transform process.

The two transform zones: the South Iceland Seismic Zone, in the south, and the Tjörnes Fracture Zone, in the north, are partly exposed on land and, in addition, the Icelandic Meteorological Office supplies a large database of earthquakes since 1991. Most of the seismicity in Iceland is located in these transform zones (Fig. 1b). The past and present fault geometry and the mechanical behaviour in both these areas can thus be analysed.

The South Iceland Seismic Zone (SISZ)

The Plio-Pleistocene fault pattern in the SISZ ranges in trend between N-S and ENE-WSW (Fig. 2c): the N30°E-N40°E trend mainly corresponds to normal faulting or tension fractures, whereas the N0°E-N20°E trend correspond to right-lateral strike-slip faults and the N60°E-N70°E trend to left-lateral faults. In detail, four brittle tectonic regimes were reconstructed in the whole SISZ (Fig. 2d). The primary stress regime is characterized, for both the strike-slip faulting and the normal faulting, by a NW-SE average direction of extension, compatible with left-lateral motion along the SISZ, and clearly prevails in terms of related brittle deformation (that is, numbers and sizes of minor faults). The second largest stress regime is characterised by a direction of extension NE-SW. Two other, less important, stress regimes display E-W and N-S directions of extension.

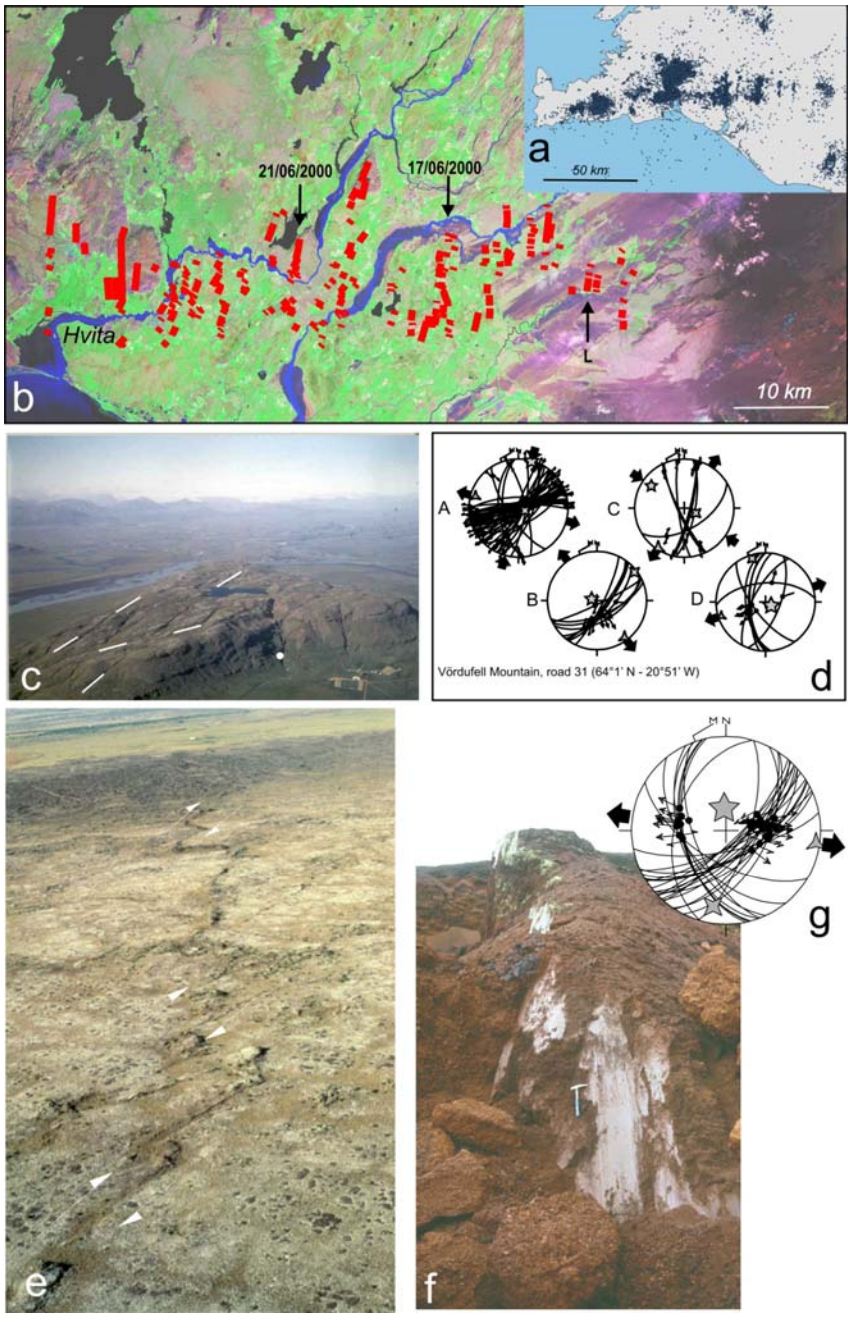

Figure 2 – Some aspects of the South Iceland Seismic Zone. (a) Earthquakes of magnitude equal or superior to 0.5 for the year 1995. (b) Surface traces of seismic strike-slip faults (in red) drawn on a Landsat image of the SISZ. The June 2000 earthquake (M = 6.6) are indicated as well as the Leirubakki Fault (L). (c) Example of the Holocene fault pattern in the SISZ: the Vördufell Mountain. White lines on the picture underline some major faults. (d) Paleostress determination in the Vördufell mountain. White dot on the photograph c indicates the measurement site. (e) Oblique aerial photograph of the Leirubakki Fault, a typical N-S trending right-lateral fault. (f) Outcrop photograph showing normal oblique-slip fault surfaces in scoriae of post-glacial volcano near Seydishólar. (g) Corresponding paleostress determination. Oblique aerial photograph c and e from A. Gudmundsson.

Considering the spatial distribution of earthquakes (Fig.2a-b), the SISZ is mainly affected by N-S major seismic faults. Some major fault ruptures, including the traces of the June 2000 large earthquakes (magnitude 6.6), have been mapped in detail. All these earthquake fault traces show right-lateral en-échelon patterns of fractures and push-up structures (Fig. 2e). The variety of focal mechanisms of earthquakes suggests that the whole set of mechanisms cannot correspond to a single stress regime. Mass inversions of large data sets of earthquake focal mechanisms in the SISZ indicate that a strike-regime with NW-SE extension and NE-SW extension clearly prevails, but however reveal a secondary, opposite, stress regime involving NE-SW extension and NW-SE extension.

The major fault geometry reveals consistency with a classical Riedel-type model of fault pattern in a left-lateral shear zone. The E-W trends are poorly developed in the brittle structures, despite the general E-W direction of the SISZ. The reason for this limited expression lies in the accommodation of the E-W lateral shear in a wide and diffuse zone of deformation (Fig. 4a).

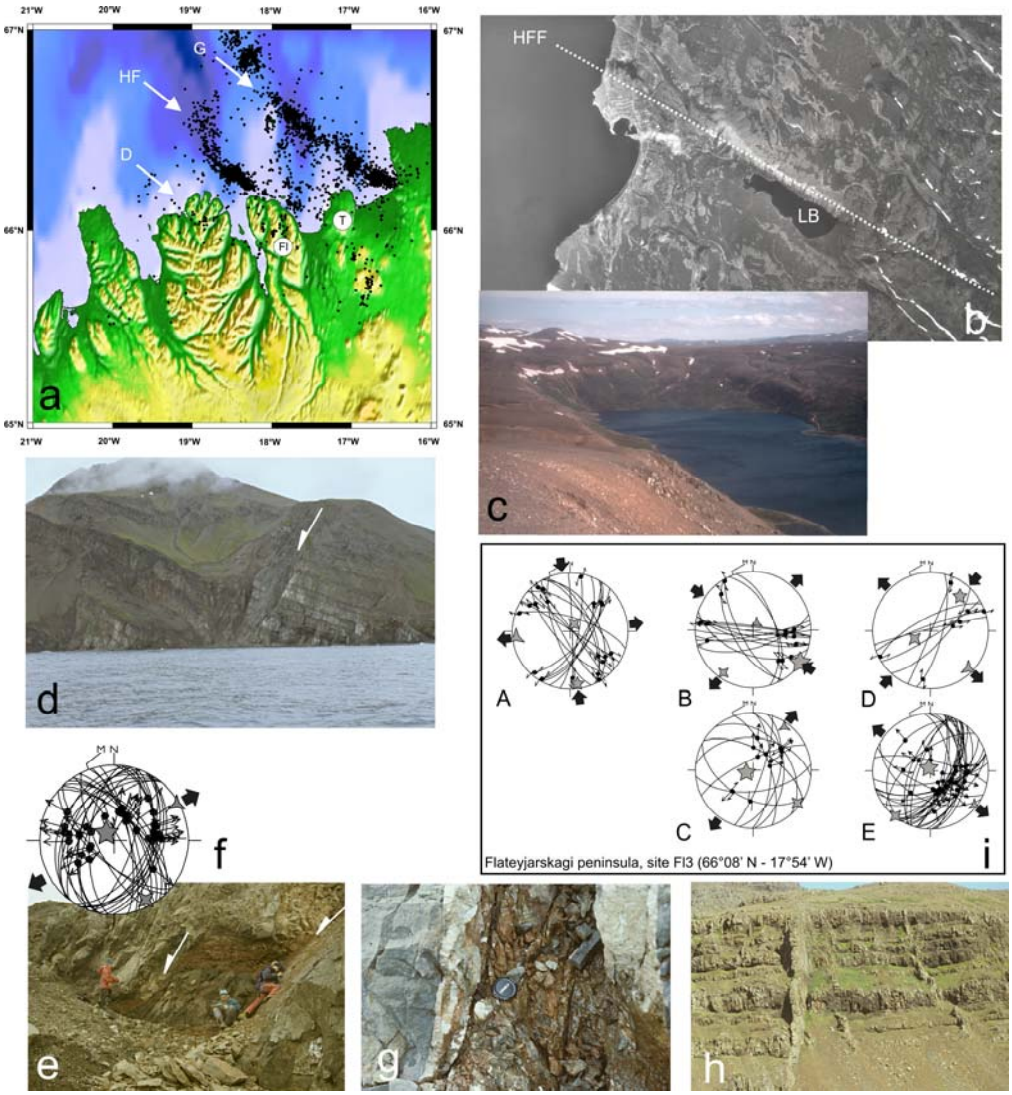

Figure 3 – Some aspects of the Tjörnes Fracture Zone. (a) Earthquakes of magnitude equal or superior to 1 for the period 1993-2002 in the Tjörnes Fracture Zone. G: Grimsey Seismic Zone, HF: Húsavík-Flatey Fault, D: Dalvik Lineament, Fl: Flateyjarskagi peninsula, T: Tjörnes peninsula. (b) Aerial photograph of the Húsavík-Flatey Fault (HFF) across the Tjörnes peninsula. The Lake Botnsvatn (BL) is interpreted as a pull-apart structure along the fault. (c) Photograph of the Botnsvatn pull-apart. (d) and (e) Photographs showing normal faults in the Upper Miocene tholeitic basalts, along the northeastern coast of the Flateyjarskagi peninsula. (f) Corresponding paleostress determination. (g) Crushed rocks along the Dalvik line. (h) Dykes trending parallel to the HFF. (i) Example of analysis of a heterogeneous data set of minor faults in Upper Miocene tholeïtic basalts, at the north-eastern coast of Flateyjarskagi.

The Törnes Fracture Zone (TFZ)

Three tectonic lines constitute the TFZ, from north to south, respectively: the Grimsey Line, the Húsavík-Flatey Fault (HFF) and Dalvik Line (Fig. 3a). They trend parallel to the whole transform zone that is WNW-ESE on average. However, no transform-parallel major faults could be recognised with the exception of the HFF.

The main onshore feature of the TFZ is the HFF, which can be followed as a 25 km long morphological feature across the Tjörnes peninsula (Fig. 3b-c) and is well marked on the northern coast of the Flateyjarskagi peninsula by a large zone of crushed rocks associated with tilted blocks of lava pile and numerous strike-slip and normal faults. The structural complexity of the TFZ results from the important right-lateral deformation that produced more or less important block rotation in the

vicinity of the major fault. All but few sites in the peninsula contain several fault subsets and thus reveal a high level of heterogeneity. As for the SISZ, four stress regimes can be identified (Fig. 3i), related to E-W, NE-SW, NW-SE and N-S extensions respectively. Each of these extensions is expressed through both strike-slip and normal-slip faulting and dykes. The most important extensions are compatible with the right-lateral general motion of the TFZ. One of these dominant stresses is characterised by an E-W extension, the other one corresponds to a NE-SW extension. The two other regimes are incompatible with the general motion of the TFZ, the trends of extension being N-S and NW-SE, respectively.

The HFF is characterised by a strong seismic activity (Fig. 3a) and some large magnitude earthquakes occurred (e.g., southwest of Húsavík in 1872, M = 6.3, and at its north-western tip in 1994, M = 5.5). Most seismic faults trend N122°E-N140°E and show right-lateral motion, however in its western part some N-S left-lateral seismic faulting also occurs. The two groups reflecting E-W and NE-SW extensions represent 43% and 39% of the total data set of seismic events.

The two dominant and transform-compatible stress states have been interpreted as revealing repeated changes from moderate mechanical coupling to very low across the transform fault zone. The two major directions of extension make angles of 20°-25° and 70°-85° with the transform direction. There is little evidence of intermediate situations, which suggests that the changes in coupling were abrupt rather than progressive during the transform history (Fig. 4b).

Conclusion

The fault patterns, as well as the related stress fields, show some similarities in both the SISZ and the TFZ. The most remarkable similarities are (i) the existence of extensional features accompanying strike-slip motion and (ii) the occurrence of minor stress states often opposite to the main ones (and thus incompatible with transform motion). However, major differences exist and reveal specific properties of these two zones. The general kinematics and geodynamics of Iceland did not change since, at least, the Miocene, so that these differences should be considered characteristic of the different stages in the transform process evolution. This contrast is a consequence of the difference in age between the two transform zones.

In terms of fault patterns, the organisation in the SISZ, that is youngest transform zone, may be characterised as diffuse in a wide area where no E-W trending major fault exists (Fig. 4a). Therefore, the SISZ can be considered as an immature transform zone and the geometrical pattern corresponds to the development of a classical Riedel-type pattern. Taking into account the southward propagation of the Easter Volcanic Zone in south Iceland, it is reasonable to predict a refocusing of the faulting activity towards a stronger consistency with the stress regime that prevails at the regional scale across the rift and transform zone segments, as might have happened in the TFZ.

In the Tjörnes fracture zone, which developed earlier, the earthquake distribution follows three major ESE-WNW trending lines. Especially, the HFF can be traced on land, as a tightly localised fault line. In detail, the geometrical fault pattern is certainly more complex as seismic faults characterised along the Dalvik and Grimsey alignments trend N-S to NNE-SSW, as left-lateral strike-slip faults. This complexity suggests that the TFZ actually includes different fault domains at different stages of maturity. The slip distribution and the crustal stress field geometry have been simulated using a 2D numerical modelling. It shows that, at any time during the development of the plate boundary, the plate motion is not distributed along each of the plate boundary faults but mainly occurs along a single master fault. The finite width of the TFZ results from slip transfer through time with locking of early faults, not from a permanent distribution of deformation over a wide area. Because of fault interaction, the stress field geometry within the TFZ is complex and includes stress deflections close to but also away from the major faults. Comparison between paleostress reconstructions and results of modelling suggests that the Dalvik Fault and the Husavik-Flatey Fault developed first, the Grismsey Fault being the latest active structure. Since initiation of the TFZ, the Husavik-Flatey Fault accommodated most of the plate motion and probably persists until now as the main plate structure. Because the Icelandic rift is propagating northward, the Grimsey Seismic Zone will probably reach to a major role in the transform process, developing as a true fault line and maybe replacing the HFF as the major structure of the TFZ in the future.

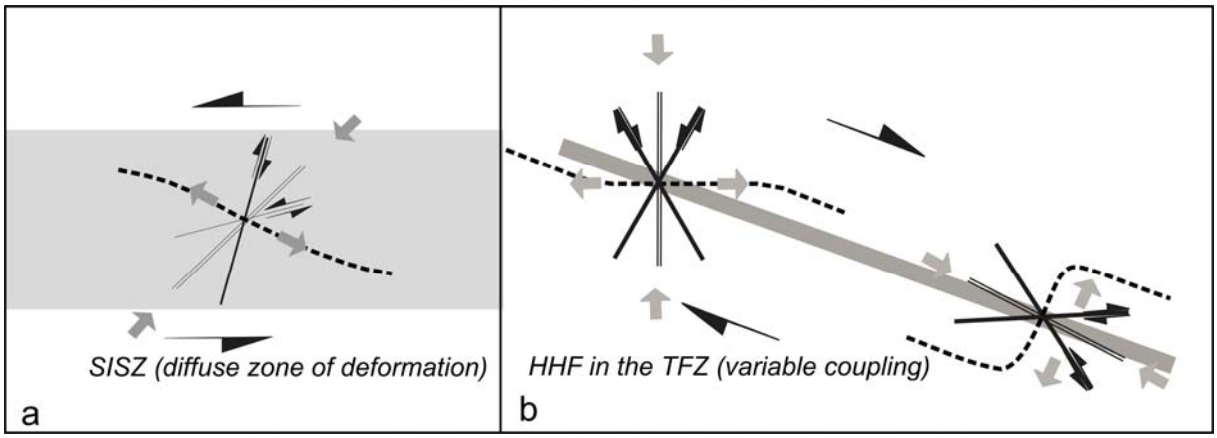

Figure 4 - Schematic pattern of faulting and associated average stresses (a) in the SISZ and (b) along the HFF. Solid lines with indication of the sense of shear: strike-slip faults; thin double lines: normal faults; convergent and divergent grey arrows: directions of compression and extension, respectively. Pairs of black arrows indicate the transform motion. The two fault and stress patterns along the HFF do not refer to different locations but illustrate the two major stress regimes.

To conclude, Iceland provides a unique opportunity to compare immature and mature transform zones on land (totally in the SISZ, partly in the TFZ) and using seismological data. This comparison demonstrates that the trend of the transform motion, as reflected in the major features, is hidden at the beginning of the transform process and develops when the transform zone becomes mature. The geometry related to the immature stage shows a diffuse shear zone with a Riedel-type pattern of faults, with a dominating stress field that reflects the behaviour of the transform zone. At the mature stage, the geometry becomes simpler, with the development of a well-localised shear fault zone where most of the transform process concentrates, but a complex stress pattern prevails with major variations in friction along the fault and different stress states that reflect abrupt changes in mechanical coupling, probably as a function of the major magmatic crises. To this respect, it is likely that not only does the Icelandic hot spot induce rift jumps; it also significantly influences the behaviour of the transform faults.

This abstract benefited from discussions and field investigations with some French and Icelandic colleagues, especially: O. Bourgeois, O. Dauteuil, A. Gudmundsson, K. Saemundsson, R. Stefansson, B. Van-Vliet-Lanoe and T. Villemin.

References

This abstract is based on the following works of F. Bergerat, J. Angelier†, C. Homberg, S. Garcia, S. Verrier and M. Bellou. Only some other relevant references are given herein, but complete reference lists can be found in the most recent papers.

Angelier J. and Bergerat F., 2002. Behaviour of a rupture of the 21 June 2000 earthquake in South Iceland as revealed in an asphalted car park. *Journ. Struct. Geol.*, 24, 1925-1936.

Angelier J., Bergerat F. and Homberg C., 2000. Variable coupling across weak oceanic transform fault : Flateyjarskagi, Iceland. *Terra Nova*,.12, 97-101.

Angelier J., Bergerat F., Stefansson R. and Bellou M.,2008. Seismotectonics of a newly formed transform zone near a hot spot: earthquake mechanisms and regional stress in the South Iceland Seismic Zone. *Tectonophysics,* 447, 95-116.

Angelier J., Slunga R., Bergerat F., Stefansson R. and Homberg C., 2004. Perturbation of stress and oceanic rift extension across transform faults shown by earthquake focal mechanisms in Iceland. *E.P.S.L.*, 219, 271-284.

Bellou M., Bergerat F., Homberg C. and Angelier J., 2005. Geometry and segmentation mechanisms of the surface traces associated with the 1912 Selsund Earthquake, Southern Iceland. *Tectonophysics*, 404, 133-149.

Bergerat F. and Angelier J., 2003). Mechanisms of the June 2000 earthquakes, southern Iceland : inferences from surface traces of the Arnes and Hestfjall faults. *Journ. Struct. Geol.*, 25, 1507-1523.

Bergerat F. and Angelier J., 2000. The South Iceland Seismic Zone : tectonic and sismotectonic analyses revealing the evolution from rifting to transform motion. *Journ. Geodynamics,* 29, 211-231.

Bergerat F., Angelier, J., 2008, Immature and mature transform zones near a hot spot: the South Iceland Seismic Zone and the Tjörnes Fracture Zone (Iceland). *Tectonophysics*, 447, 142-154.

Bergerat F., Angelier J. and Homberg C., 2000. Tectonic analysis of the Husavik-Flatey Fault (northern Iceland) and mechanisms of an oceanic transform zone, the Tjörnes Fracture Zone, *Tectonics.,* 19, 1161-1177.

Bergerat F., Angelier J. and Verrier S., 1999. Tectonic stress regimes, rift extension and transform motion : the South Iceland Seismic Zone. *Geodin. Acta*, 12, 303-319.

Bergerat F., Gudmundsson A., Angelier J., and Rögnvaldsson S.Th.,1998. Seismotectonics of the central part of the South Iceland Seismic Zone. *Tectonophysics,*298, 319-335.

Bergerat F., Angelier J., Gudmundsson A. and Torfason H., 2003. Push-ups, fracture patterns, and paleoseismology of the Leirubakki Fault, South Iceland. *Journ. Struct. Geol.*, 25, 591-609.

Einarsson, P., 1991. Earthquakes and present-day tectonism in Iceland. *Tectonophysics* 189, 261-279.

Einarsson, P., Khodayar, M., Clifton, A., Ófeigsson, B., Thorbjarnarson, S., Einarsson, B., Hjartardóttir, Á. R., 2005. A map of Holocene fault structures in the South IcelandSeismic Zone. *Geophysical Abstract Research*, vol. 7, Communication 08858.

Garcia S, Angelier J., Bergerat F. and Homberg C. ,2002. Tectonic analysis of an oceanic transform fault zone revealed by fault-slip data and earthquake focal mechanisms: the Husavik-Flatey Fault, Iceland. *Tectonophysics*, 344, 157-174.

Garcia S., Angelier J., Bergerat F., Homberg C. and Dauteuil O. , 2008. Influence of rift jump and excess loading on the structural evolution of Northern Iceland. *Tectonics*, 27, TC1006, doi: 10.1029/2006TC002029, 2008.

Garcia S., Arnaud N., Angelier J., Bergerat F. and Homberg C., 2003. Rift Jump process in Northern Iceland since 10 Ma from $^{40}Ar/^{39}Ar$ geochronology. *E.P.S.L.*, 214, 529-544.

Guðmundsson, Á., Brynjolfsson, S., 1993. Overlapping rift-zone segments and the evolution of the South Iceland Seismic Zone. *Geophys. Res. Lett*. 20, 18, 1903-1906.

Guðmundsson A., 2007, Infrastructure and evolution of ocean-ridge discontinuities in Iceland. *Journal of Geodynamics*, 43, 6-29.

Homberg C., Bergerat F., Angelier J., Garcia S.**,** 2010, Fault interaction and stresses along broad oceanic transform zone: Tjörnes Fracture Zone, north Iceland. *Tectonics*, 29, TC1002, doi:10.1029/2008TC002415.

Saemundsson, K., 1979. Outline of the geology of Iceland. *Jökull*, 29, 7-28.

Saemundsson, K. , 1974. Evolution of the Axial Rifting Zone in Northern Iceland and the Tjörnes Fracture Zone, *Geol Soc Am. Bull., 85,* 495-504.

JÖKULHLAUPS IN ICELAND: SOURCES, RELEASE AND DRAINAGE

Helgi Björnsson
Institute of Earth Sciences, University of Iceland

Abstract

Jökulhlaups in Iceland may originate from marginal or subglacial sources of water melted by atmospheric processes, permanent geothermal heat or volcanic eruptions. Glacier-volcano interactions produce meltwater that either drains toward the glacier margin or accumulates in subglacial lakes. Accumulated meltwater drains periodically in jökulhlaups from the subglacial lakes and occasionally during volcanic eruptions. During the 20th century 15 subglacial volcanic eruptions (10 major and 5 minor events) took place, about one-third of all eruptions in Iceland during that century.

The release of meltwater from glacial lakes can take place as a result of two different conduit initiation mechanisms and the subsequent drainage from the lake occurs by two different modes. Drainage can begin at pressures lower than the ice overburden in conduits that expand slowly over days or weeks due to melting of the ice walls by frictional and sensible heat in the water. Alternatively, the lake level may rise until the glacier is lifted along the flowpath to make space for the water and water discharges rise linearly, peaking in a time interval of several hours to 1-2 days. In this case, discharge rises faster than can be accommodated by melting of the conduits. The rapidly-rising floods are often associated with large discharges and floods following rapid filling of subglacial lakes during subglacial eruptions or dumping of one marginal lake into another. Jökulhlaups during eruptions in steep ice and snow-covered stratovolcanoes are swift and dangerous and may become lahars and debris-laden floods. Normally jökulhlaups do not lead to glacier surges but eruptions in ice-capped stratovolcanoes have caused rapid and extensive glacier sliding.

Jökulhlaups have significant landscaping potential: they erode large canyons and transport and deposit enormous quantities of sediment and icebergs over vast outwash plains and sandur deltas. Jökulhlaups from subglacial lakes may transport on the order of 10^7 tons of sediment per event but during violent volcanic eruptions the sediment load has been 10^8 tons. Pleistocene glacial river canyons may have been formed in such catastrophic floods from subglacial lakes. Jökulhlaups have threatened human populations, farms and hydroelectric power plants on glacier-fed rivers. They have damaged cultivated and vegetation areas, disrupted roads on the outwash plains and have even generated flood waves in coastal waters.

Iceland is a unique and valuable study-site for glaciovolcanic interactions. This applies to the heat exchange between magma and the glacier, the dynamical response of the glacier to subglacial eruptions, the structure and growth sequence of hyaloclastite ridges and tuyas formed by subglacial eruptions, and jökulhlaups due to volcanic eruptions. The jökuhlaups can be seen as modern analogues of past megafloods on the Earth and their exploration may improve understanding of ice-volcano processes on other planets.

CHAP.8: Glacial Floods *in* - MOUNTAINS GEOMORPHOLOGY p.164-184. (eds. Philip Owens and Olav Slaymaker). Arnold Publishers. (2004)

GLACIAL LAKE OUTBURST FLOODS IN MOUNTAIN ENVIRONMENTS

Helgi Björnsson

1 Introduction

Floods can happen where glaciers dam lakes in mountainous areas. Occurring in both the temperate and subpolar regions of the Earth, such floods are called *débâcles* in the European Alps, *aluviones* in South America and *jökulhlaup*s in Iceland. A dam of ice or sediment blocks the water to form a lake, while drainage is initiated by an opening of the hydraulic seal, which can be broken either suddenly or gradually. The impounded water is released directly into river channels, and has a typical discharge that is orders of magnitude higher than when running as a direct result of intense ablation. In regions with active, ice-covered volcanoes, meltwater is repeatedly released in floods from lakes that collect at subglacial hydrothermal areas. Occasionally, these floods take place without any significant prior storage of water, since ice melts instantaneously in volcanic eruptions. During the largest glacial floods in history, discharges reached 106 m3 s_1. For comparison, the meltwater that was temporarily stored in lakes at the edges of downwasting Pleistocene ice sheets was released in bursts that were only one order of magnitude larger than this, even though the enormous volumes involved may have altered the circulation of deep water in the North Atlantic Ocean of the late Pleistocene era.
Glacial outbursts can have pronounced geomorphological impacts, since they scour river courses and inundate floodplains. Outbursts result in enormous erosion, for they carry huge loads of sediment and imprint the landscape, past and present, with deep canyons, channelled scabland, ridges standing parallel to the direction of flow, sediment deposited on outwash plains, coarse boulders strewn along riverbanks, kettleholes where massive ice blocks have become stranded and have melted, and breached terminal moraines. Some modern outbursts have produced flood waves in coastal waters (tsunamis). In the North Atlantic, outburst sediments dumped onto the continental shelf and slope have been transported great distances by turbid currents. Outburst floods wreak havoc along their paths, threatening people and livestock, destroying vegetated lowlands, devastating farms, disrupting infrastructure such as roads, bridges and power lines, and threatening hydroelectric plants on glacially fed rivers.

Knowledge of jökulhlaup behaviour is essential for recognizing potential or imminent hazards, predicting and warning of occurrences, enacting preventive measures, assessing consequences and responding for the purpose of civil defence. The goal of this chapter is to outline and describe the following:
(1) the location and geometry of glacial flood sources, including the properties of dams that impound the water; (2) the accumulation of water leading to outbursts and the conditions in which they begin; (3) the mechanisms and discharge characteristics of outbursts; and (4) case histories of floods, illustrating potential hazards.

2 Anatomy of glacial lakes and their outburst floods

2.1 Sources of glacial outbursts

Glacial lakes are found in various topographic settings. Meltwater may be impounded within the glacier (englacially and subglacially), on the surface of the glacier (supraglacially) or in lakes formed by dams at the glacier's margin (proglacially). The general characteristics, geometry and filling of glacial lakes can be described by the basic physics of hydrology. The movement of a thin film of water along the glacier base follows the gradient in the fluid potential

$$\phi_b = \rho_w g z_b + p_w, \qquad (1)$$

which is the sum of terms expressing the gravitational potential and the water pressure, *p*w, assuming the effects of kinetic energy to be negligible. The symbol w represents the density of water and equals 1000 kg m^3 , whereas *g* equals 9.81 ms^{-2} and represents the acceleration due to gravity, while z_b is the elevation of the glacier substrate above sea level (Figure 8.1). When describing the regional flow of basal water, it has proved useful to present a static approximation of water pressure, equal to the overburden pressure from the ice, where i equals 916 kg m^3 and represents the density of ice, *H* equals z_s-z_b and is the thickness of the glacier and z_s is the elevation of the ice surface in relation to sea level (Shreve, 1972). Thus the gradient driving the water is

$$\nabla\phi_b = (\rho_w - \rho_i)\, g\, \nabla z_b + g\, \rho_i \nabla z_s. \qquad (2)$$

This formula predicts that the surface slope of the glacier is some ten times more influential than the slope of its bed in determining the flow of basal water.Glacial lakes may be situated at points where water flows towards a minimum in the total fluid potential. Trapped in such a lake, water is surrounded by a hydraulic seal. As the overlying glacier floats in a state of static equilibrium, and the vertical force balance is reflected by the shape of the lake. The roof of a subglacial lake slopes approximately ten times more steeply than the surface of the ice, and in the opposite direction (Figure 8.2). While resembling a grounded ice shelf, the ice on the perimeter of the lake essentially comprises an ice dam. The state in which there is no gradient driving water inside the lake, $\nabla\phi_b = 0$, can be used to define the location and geometry of a subglacial reservoir. Hence describes the relationship of the slope in the ice/water outline of the lake to the slope at the upper surface of the glacier (note

that there might also be lakes with equal inflow and outflow which would not meet the condition of a zero gradient in relation to fluid potential). Given the glacier's surface and the bedrock geometry, it is possible to assess whether a water reservoir is likely to exist on the glacier bed.

$$\nabla z_b = -[\rho_i/(\rho_w - \rho_i)]\,\nabla z_s \qquad (3)$$

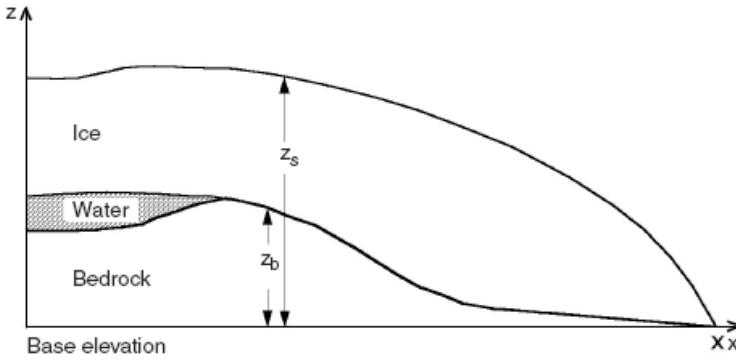

Figure 8.1 *Parameters for describing the principles of water flow in glaciers*

The general relationship in eq. (3) applies to all types of glacial lakes (Figure 8.2, Table 8.1). Water may gather in a bedrock hollow beneath a relatively flat or dome-shaped glacial surface, (Figure 8.2(a)) – in a type of reservoir which has been delineated beneath today's Antarctic Ice Sheet (Oswald and Robin, 1973; Ridley *et al*., 1993; Siegert *et al*., 2001) and was presumably widespread during the Quaternary glaciations. Another type of lake can form a cupola above the glacier bed, accompanied by a depression in the glacier's surface (Figure 8.2(b),(c)). Subglacial water reservoirs of this sort are common in Iceland, owing to volcanic and geothermal activity which causes the ice to melt and thereby creates depressions in the glacier surface (Björnsson, 1974, 1988). Meltwater flows along the bed and accumulates beneath the depression.

Subaerial glacial lakes (marginal or proglacial lakes) are confined by ice on one side and by topographic barriers on the other, for instance by the edges of ravines, riverbeds or main valleys (Figure 8.2(d)). The glacier's surface slopes toward the lake, which stores meltwater from the glacier along with runoff from the surrounding terrain. The lakes formed during the summer at the margins of subpolar glaciers may be sealed by an ice dam frozen to the bed (e.g., Maag, 1969).

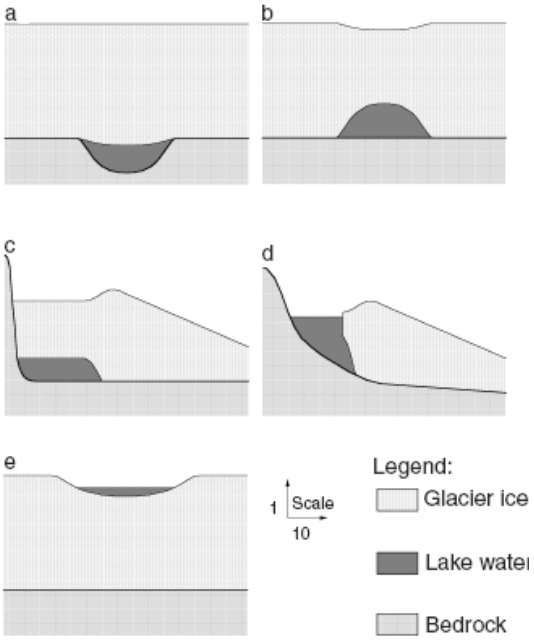

Figure 8.2 *Schematic diagram of the main types of glacial lake*

In other instances, a proglacial lake may lie in a depression behind moraine at the front of the glacier, which is typically retreating rapidly, while sediment is deposited too slowly to fill up the over-deepened bed. This happened in the case of the receding late Pleistocene ice sheets and applies to many shrinking twentieth century glaciers. Supraglacial lakes are isolated in depressions on the glacier surface (Figure 8.2(e)), hydrologically separated from the basal drainage system. A final addition to our list might be water stored in cavities located here and there inside the glacier (Kamb *et al*., 1985; Walder, 1986; Kamb, 1987).

2.2 Drainage of glacial lakes

In general, glacial lakes of every type can drain either continuously or in episodic bursts. Marginal and proglacial lakes sometimes drain constantly via subaerial spillways over the rock or sediment barrier that contains them. Such barriers might consist of moraine, volcanic material or landslides. Nevertheless, lakes held back by these materials may break forth abruptly if the dams fail. Floods released suddenly when sediment or ice

impoundments are breached rise almost linearly over a period of minutes or hours. They reach a high, sharp discharge peak and then fall along a steep recession limb (Figure 8.3(b)). Sediment dams can fail because of overtopping or accelerated fluvial erosion, which results in retrogressive incision enlarging the point of outflow. Moreover, a break in sediment dams can be caused by seepage and piping (progressive groundwater movement) within the sediment barrier, resulting in liquefied flows and embankment slips that weaken or disintegrate the dam. Tectonic activity and landslides are further threats to sediment dams, while breaching may also be triggered by flood water entering the lake or by heavy rain leading to a rapid rise in the lake level.

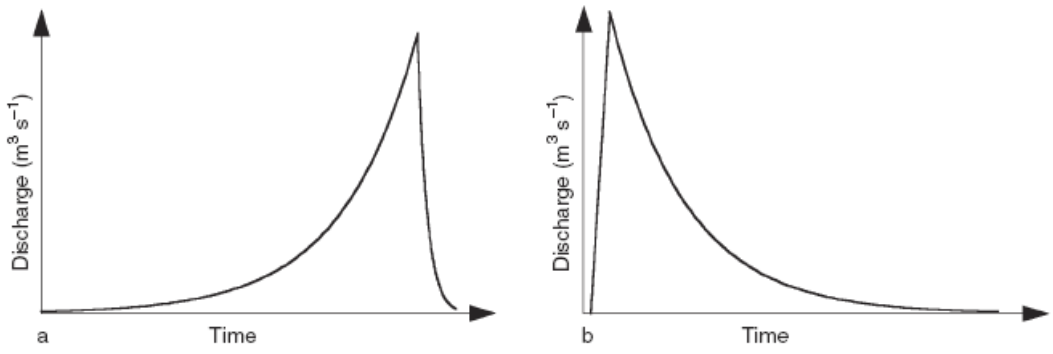

Figure 8.3 *Hypothetical graphs for two types of jökulhlaup. (a) Typical shape of the hydrograph when a single basal ice tunnel enlarges because of melting; (b) abruptly peaking curve not explained by the classical theory of outbursts*

Finally, dam failure can be generated by waves from landslides, rock falls, ice avalanches, calving icebergs or glacier surges into the lake. Providing the topographic barriers hold, on the other hand, proglacial lakes serve to dampen jökulhlaups from other areas. Any outburst that does occur may be a one-time event if it ruins the dam. Where the barrier is a wall of ice, it may break down mechanically, similarly to a sediment dam. Marginal lakes at subpolar glaciers, where the ice barricade is frozen
to the bed, are typically breached as lake water spills over the top of the dam into a supraglacial channel that melts into a bigger breach – commonly at the juxtaposition of the glacier and a rock wall (e.g., Schytt, 1956; Maag, 1969). The rate of ice melt, the level of the lake in relation to the outlet and the hypsometry of the water reservoir dictate the progress of lake drainage. As the lake surface falls, the breach may broaden and deepen, even undercutting the ice wall so as to cause calving. When subglacial lakes are situated in bedrock hollows under flat or dome-shaped glacial surfaces, they are not expected to expand and drain in sudden outbursts, except perhaps during rapid deglaciation which drastically alters glacier geometry and drainage (Goodwin, 1988). In contrast, when icedammed lakes, regardless of whether they are positioned subglacially or marginally, receive water inflow and are gradually made to expand, basal water pressure will increase and the overlying ice will be raised. Eventually, the hydraulic seal of the ice dam will be ruptured, so that water will begin to drain from the lake via a basal pathway. Seepage beginning beneath the ice blockage causes enlargement of the drainage system, initiating a flood under the surrounding ice. In a typical case, though for reasons not yet fully understood, leakage starts before the lake has reached the level which would cause flotation of the ice dam (Björnsson, 1975, 1988). After discharge has begun, pressure from the ice constricts the passageway, and water flow at an early stage in the jökulhlaup correlates primarily with enlargement of the ice tunnel owing to heat from friction against the flowing water and to thermal energy stored in the lake (Nye, 1976; Spring and Hutter, 1981, 1982; Clarke, 1982; Björnsson, 1992). Increasing as an approximate exponent of time over a matter of hours or days, the discharge falls quickly after peaking (Figure 8.3(a)). The recession stage of the hydrograph sets in when tunnel deformation begins to exceed enlargement by melting. The overlying ice may collapse abruptly into the tunnel and seal the lake again, sometimes before it is empty, with new water beginning to accumulate until another jökulhlaup occurs. The timing of bursts depends on what lake level will provide the subglacial water pressure necessary for breaking the hydraulic seal affected by the overburden pressure at the ice dam; therefore, if long-term records of lake levels are available, the elevation at which a jökulhlaup will begin can be predicted with some precision. Since the frequency of outbursts depends on the rate at which a lake is filled, marginal lakes often experience them at the end of the ablation season, when meltwater storage climaxes. Fluctuations in the thickness of the blocking ice, resulting from climatic variations or surges, may modify the outburst cycle or even stop bursts completely. Occasionally, jökulhlaups are triggered by flotation of the ice dam. Rather than initial drainage from the lake being localized in one narrow conduit, the water is suddenly released as a sheet flow, surging downhill and propagating a subglacial pressure wave, which exceeds the ice overburden and lifts the glacier in order to create space for the water. In this instance, discharge increases faster than can be explained by conduits expanding through melting (Björnsson, 1992, 1997, 2002; Björnsson *et al*., 2001; Jóhannesson, 2002). The resulting hydrograph (Figure 8.3(b)) presents a rapid rise to its peak, succeeded by a more gentle waning stage. While sheet flows may be followed by drainage through high-capacity conduits, swift floods may instead manage to cause hydrofracturing

and force their way englacially from the base of the glacier to its surface (Liestøl, 1977; Roberts *et al*., 2000; Russell *et al*., 2000; Roberts, 2002).

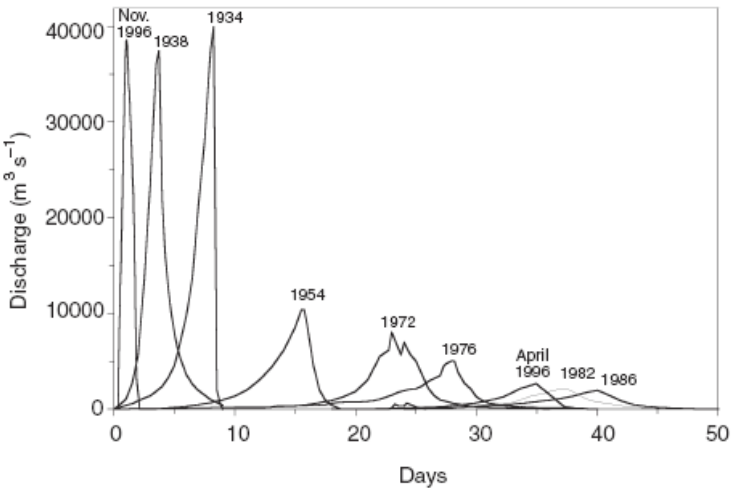

Figure 8.4 *Discharge hydrograph of various jökulhlaups from Grímsvötn, Iceland*

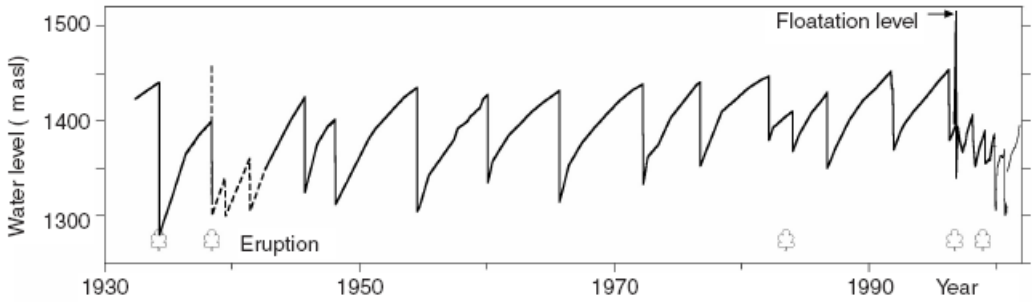

Figure 8.5 *The water level of lake Grímsvötn, 1930–2000.The crater level rises until a jökulhlaup takes place. In 1996 the lake rose to the level required for floatation of the ice dam*

Supraglacial lakes, on the other hand, are usually transient features (e.g., Björnsson, 1976), because they form englacial channels and drain down to the subglacial water system. Water that collects in lakes on polar ice masses frequently freezes and unites with the ice during the winter. Where glacial surges occur, floods may come about when a surge terminates and drainage of the water from subglacial cavities switches from a distributed system – conducting water slowly downglacier – to a quickly effective network of tunnels (Kamb *et al*., 1985; Kamb, 1987). While the outlets for these bodies of water are not fixed, they may be expected to empty into rivers running from the glacier before the surge. As a final case, there have been reports of frequent abrupt releases of water, lasting from minutes to some hours, from diminutive amounts of subglacial or englacial storage, but the nature of these releases is poorly described (Haeberli, 1983; Drieger and Fountain, 1989; Walder and Diedger, 1995).

2.3 Impacts of jökulhlaups

The impact of outbursts corresponds to their discharge rate, the peak and nature of the flow, sediment load, routeway topography and frequency. Depending on the concentration of sediment, jökulhlaups range across a continuum from water floods to hyperconcentrated flows and debris flows. Most jökulhlaups from lakes dammed by ice contain relatively small concentrations of sediment (<40% by weight and 20% by volume) and can be described adequately in terms of standard hydraulics in turbulent water flow (calculating flow by Manning's equation and sediment transport by Einstein's equation). In the most catastrophic floods, intense erosion may occur through cavitation; the enormous velocity of flow reduces absolute pressure, causing air bubbles to form, which collapse and generate shock waves. Conditions for this are favourable in constricted channels at low water depths, producing channelled scabland features, whereas more uniform flow produces a topography of subdued erosion.

Jökulhlaups triggered by the failure of a sediment dam or by volcanic eruptions may temporarily contain high concentrations of sediment. Hyperconcentrated jökulhlaups represent moderately turbulent to laminar flow of non-Newtonian fluids, with sediment concentrations varying between 40% and 70% by weight (20% and 47% by volume). Debris flows are laminar, containing a uniform sediment concentration ranging from 70% to 90% by weight and from 47% to 77% by volume (Costa, 1988). Hyperconcentrated flows produce crudely stratified, less finely sorted deposits than water floods, and the deposits from debris flows are composed of poorly sorted clasts.

River courses and landforms on outwash plains have adjusted to the magnitude of frequent or cyclic jökulhlaups, i.e., those occurring with annual regularity or at intervals of several years. During rare extensive floods, however, erosion, transportation and downstream deposition modify river courses extensively. During the aftermath, flood channels remain destabilized, which may lead to slumping and
debris flows.

3 Estimating the discharge of jökulhlaups

3.1 Measured and calculated discharge

Direct measurements of water current velocity and discharge are usually precluded in major jökulhlaups. Conventional stream-gauging stations are rarely set up for recording extreme floods, and even if the streams have been gauged no developed curves are available for comparing stage and streamflow. Large-scale floods overflow the normal riverbanks, distort river courses and damage or destroy instruments. Although a number of jökulhlaups have been gauged some distance downstream from glacier margins, the flood wave may have been significantly attenuated in the intervening interval by passing through such storage bodies as braided channels or lakes.

Indirect methods can be applied to estimate average stream velocity, using hydraulic calculations along with field evidence of channel geometry (including cross-sectional area, heights and dates of flood levels, and channel roughness). This approach employs Manning's equation, which was developed empirically for open, canalized waterways and which relates energy dissipation to the roughness of flood paths. In such an approximation, the surface slope at high water becomes the basis for determining the energy slope. Because of nonuniform flow, computations must take into account the conservation of mass and energy as the flood moves forward (Webb and Jarrett, 2002). The maximum flood stages are reconstructed by inspecting eroded channel margins, finding the highest flotation elevation of the largest boulders that were encased by ice and drifted downstream (ice-rafted erratics), and locating water divides where floodwater spilled over cols. The reconstruction of flood discharge obviously may be complicated when sedimentation at the end of the flood changes the area of the channel cross-section as well as the roughness of the flood course.

3.2 Prediction of discharge by theoretical and empirical methods

For the purpose of risk assessment, both empirical and theoretical methods can be relevant to predicting the probable rate of change of discharge, peak discharge and duration of jökulhlaups.

3.2.1 Subglacial drainage

Theoretical models of jökulhlaups discharging through water tunnels in the glacier base have been derived by Nye 1976), Spring and Hutter (1981) and Clarke (1982). These models are based on the physics of mass continuity, momentum, energy conservation and heat transfer, and they describe how water is driven by a fluid potential radient through a tunnel of given roughness. From his general model, Nye (1976) derived an analytical solution, which predicted discharge, *Q*, to rise asymptotically with time as *Q* (*t*)_*k* (1/*t*)4, if confinement by the overburden was neglected and expansion of the ice tunnel was solely attributed to the instantaneous transfer of frictional heat (i.e., the dissipation of potential energy) from the flowing water to the enclosing ice. Numerical models for simulating the entire hydrograph were derived by Spring and Hutter (1981), who included lake temperature, and Clarke (1982), who added lake geometry. Clarke (1982) successfully simulated jökulhlaups from Lake Hazard (the Yukon, Canada) and Summit Lake (British Columbia, Canada), which are dammed by marginal ice. Björnsson (1992) tested Clarke's (1982) modification of Nye's (1976) general model, applying it to Icelandic jökulhlaups and concluding that the amended model in some respects successfully simulated jökulhlaups from the subglacial lake Grímsvötn in Vatnajökull. In general, the ascending slopes simulated in the graph corresponded to the measured ones. The peak in the computed hydrographs, however, was not as sharp as the actual climaxes, rendering the simulation of the descending limbs unsatisfactory. This presumably happens because, in the model, the tunnel is assumed to be cylindrical. It was only possible to simulate the rapid rise of some outbursts in Iceland (from subglacial as well as marginal lakes) by assuming a lake temperature several degrees above the melting point, which may suggest that thermal energy stored in these bodies of water contributes to tunnel expansion and thereby affects the discharge rate. The values computed for lake temperatures, however, should not be taken seriously, as the theory of heat transfer is questionable. The simulation of such swift jökulhlaups completely failed to illustrate the closure of tunnels and the recession of discharge. An empirically based regression relation between the peak discharge *Q*max (in $m^3\ s^{-1}$) and the total volume *V*t (in $10^6\ m^3$) of water passing through subglacial tunnels in jökulhlaups was formulated by Clague and Mathews (1973):

$$Q_{max} = K\, V_t^{b}. \qquad (4)$$

For jökulhlaups emerging from ten marginal ice-dammed lakes, which ranged in volume from 10^6 to 10^9 m^3, Clague and Mathews obtained *K*=75/s $m^{-0.99}$ and the power coefficient *b*=0.67. A recent update for 26 marginal ice-dammed lakes throughout the world yielded *K*=46 s^{-1} $m^{-1.02}$ and *b*=0.66 (Walder and Costa, 1996). Referring to eleven jökulhlaups from the Icelandic lake Grímsvötn, Björnsson (1992) found *K*=4.15 10^3 /s $m^{-2.52}$ and the power coefficient *b*=1.84. Clarke (1982) derived theoretical relationships for predicting peak discharge, suggesting that *b* depended on the lake's contribution of stored thermal energy in proportion to the frictional energy dissipated in the jökulhlaup. The outcome of his calculations was that *b*=0.8 when the thermal energy originating in the lake was dominant in melting the tunnel and *b*=1.33 when its share was negligible. Ng and Björnsson (2003) point out that incomplete lake draining, a phenomenon contrasting with common behaviour in marginal lakes dammed by ice, may explain the deviation of Grímsvötn from statistically derived value.

Table 8.1 – Sources of glacial floods and characteristics of drainage[a]. p_w stands for water pressure and p_i for ice overburden pressure

Source/type of lake	Flood initiation and drainage routes				
	Subglacial drainage	Englacial drainage	Subaerial drainage (overtopping, downcutting, dam failure)		
Marginal lake[1]	Through ice tunnels at $p_w<p_i$ or in a sheet flow at $p_w=p_i$, propagating a flood wave at $p_w>p_i$	Upwards from the base, creating supraglacial outlets by hydrofracturing the ice and retrofeeding moulins at $p_w>p_i$	Drainage over a subaerial breach	Fluvial erosion of sediment dams; piping	Mechanical failure caused by tectonic activity; rockfalls; landslides
Subglacial eruption, often in the absence of significant storage[2]					
Subglacial lakes in hydrothermal areas[3]					
Supraglacial lakes in cauldrons and sink holes[4]		Downward to the base through englacial tunnels			
Englacial storage[5]					
Linked subglacial cavities[6]	Distributed drainage system switches to a tunnel system				

[a] Superscript numbers refer to publications as follows:

[1] Bretz (1925, 1969); Thorarinsson (1939); Liestøl (1956); Stone (1963); Maag (1969); Post and Mayo (1971); Clague and Mathews (1973); Björnsson (1976); Lliboutry *et al.* (1977); Haeberli (1983); Sturm and Benson (1985); Yamada (1998).

[2] Thorarinsson (1957, 1958); Sturm *et al.* (1986); Björnsson (1988); Thouret (1990); Pierson *et al.* (1990); Trabant and Meyer (1992); Guðmundsson *et al.* (1997).

[3] Björnsson (1974, 1988, 2002; Guðmundsson *et al.* (1995).

[4] Björnsson (1976); Russell (1993).

[5] Haeberli (1983); Driedger and Fountain (1989); Walder and Driedger (1995).

[6] Kamb *et al.* (1985); Kamb (1987); Björnsson (1998).

There is neither a theory nor sufficient empirical data yet available for describing how jökulhlaups drain subglacially at a faster rate than can be explained by the expansion of conduits through melting. This quicker drainage involves the ice overburden being exceeded by water pressure, which lifts the glacier and allows space for the water. Initially propagated as a pressure wave, the water then moves forward in a sheet flow, prior to draining through conduits (Björnsson, 1997, 2002; Björnsson *et al.*, 2001; Jóhannesson, 2002).

3.2.2 Subaerial drainage

A subaerial burst following the sudden breaching of an ice dam is typically over sooner than a flood exiting through a basal ice tunnel. Discharge in the former outburst may increase linearly with time and, for a given lake volume, peak discharges are significantly higher than for drainage through subglacial tunnels. The size of the outlet and the quantity of the impounded water body determine the peak discharge through the breach.

Physical models of drainage over a subaerial breach have been drawn up along similar lines to those for drainage through subglacial tunnels. Walder and Costa (1996) successfully simulated hydrographs for Lake George in Alaska. The widening of the opening is assumed to be controlled by melting, while the lake discharge spilling over the breach is dictated by the hydraulic conditions of critical flow through an open channel. Furthermore, an empirical power-law was derived in the form of eq. (4), with K=1100/s $m^{1.69}$ and b=0.44, i.e., similar figures to those for regression during known outbursts that breached man-made earthen dams, in which instances

K=1200/s $m^{-1.56}$ and *b*=0.48 (Costa, 1988). Raymond and Nolan (2000) made the first attempt to identify and describe by a physical model the processes controlling unstable drainage over a spillway with an ice floor; in other words, they formulated criteria for when discharge water would melt the spillway path down faster than the lake level dropped. Their work successfully explained observations of supraglacial drainage from Black Rapids Glacier, Alaska.

4 Case studies

4.1 Floods from sediment-dammed lakes

Floods in which lakes breach sediment dams carry large amounts of debris. Generally unpredictable, they are regarded as the most dangerous kind of outbursts, but have been successfully prevented at many hazardous locations by artificial drains through the sediment dams, which restrict lake depths. Advances and subsequent retreats of glaciers in the Little Ice Age created many unstable moraine dams, with examples reported from the European Alps, the Himalaya and Peru. An Austrian valley was flooded in 1874 when the terminal moraine of the Madatschferner glacier gave way and the lake escaped from in front of the retreating ice. The French Tête Rousse débâcle of 1892, released 2 $.10^5$ m^3 of water and 8.10^5 m^3 of sediment, killed 175 people (Lliboutry, 1971). In 1926 a flood released from the Himalayan Shyok glacier devastated a village and cultivated land 400 km from the source (Mason, 1929), while the Peruvian Jancarurish outburst of 1950 discharged 2 $.10^6$ m^3 of water and 3 10^6 m^3 of sediment (Lliboutry *et al*., 1977). In British Columbia, debris flows up to 20 m thick have travelled as far as 20 km downvalley after breaching terminal moraines (Evans and Clague, 1994). As still another example, an ice avalanche from the Langmoche glacier in Nepal broke a moraine dam in 1985, resulting in a flood that destroyed bridges, houses and a hydroelectric plant (Vuichard and Zimmermann, 1986, 1987)

4.2 Floods from marginal ice-dammed lakes

Jökulhlaups from ice-dammed lakes at glacial edges have posed a serious threat to roads, power lines and the human population in many countries of Europe, North and South America, Asia and New Zealand. In most countries, however, thinning of the ice dams by the warm climate of the twentieth century has led to smaller and more frequent outbursts from marginal lakes dammed by ice. Walder and Costa (1996) recently compiled a comprehensive review of outburst floods from glacially dammed lakes.

Some of the best-documented modern lakes blocked by ice are found in North America. Maag (1969) identified 125 lakes with ice dams on Axel Heiberg Island, Canada, and studies of several icedammed lakes in that country have been of major importance for the scientific understanding of jökulhlaups, for example, investigations of Tulsequah Lake, British Columbia (Marcus, 1960); Summit Lake, British Columbia (Mathews, 1965; Clarke, 1982; Mathews and Clague, 1993); Hazard Lake, Yukon Territory (Clarke, 1982); and Flood Lake, British Columbia (Clarke and Waldron, 1984).

Post and Mayo (1971) identified 750 lakes behind marginal ice dams in Alaska; of these, many have been thoroughly researched, such as Lake George (Stone, 1963; Hulsing, 1981; Lipscomb, 1989), Snow River (Chapman, 1981) and Strandline Lake (Sturm and Benson, 1985). The largest observed terrestrial flood from a breached impoundment took place on 8 October 1986, below the ice-dammed Lake Russell, Alaska. A surge had caused Hubbard Glacier, North America's largest tidewater glacier, to advance across the entrance of Russell Fjord, turning it into Lake Russell. A moraine was pushed up infront of the advancing glacier, raising inland water 25.5 m asl before the lake overflowed and cut the dam at the junction of the ice and the valley wall. The entire ice dam was removed within a few hours, with released water amounting to 5.4 10^9 m^3 and the peak discharge reaching 1.5 10^6 m^3 s^{-1} (Mayo, 1988, 1989). A similar event, though somewhat smaller, occurred in the summer of 2002.

In the Swiss Alps, damage from glacial floods occurs, on average, biennially; 60–70% of the outbursts originate in lakes at glacial margins and 30–40% in pockets of water within glaciers (Haeberli, 1983). Nowadays, about 15 ice-marginal lakes in Iceland drain by means of jökulhlaups (Thorarinsson, 1939; Björnsson, 1997) and frequently cause problems for bridges and other road structures. A pioneering thesis was written by Liestøl (1956) on glacially dammed lakes in Norway. Outburst floods have been scientifically described in Greenland (Schytt, 1956; Lister and Willie, 1957; Dawson, 1983; Russell, 1989), Argentina (Heinsheimer, 1954, 1958; Fernández *et al*., 1991), Pakistan (Gunn *et al*., 1930; Hewitt, 1982), and the former USSR (Glazyrin and Sokolov, 1976; Krenke and Kotlyakov, 1985; Konovalov, 1991).

The largest outbursts from ice-marginal lakes known through geological records occurred at the end of the last glaciation (Bretz, 1969; Baker, 1973, 1983; Teller and Clayton, 1983; Waitt, 1984; Clarke *et al*., 1984; Bond *et al*., 1992; Shaw, 1996, 2002). Jökulhlaups drained lakes that were dammed by margins of the Laurentide ice sheet in North America (Lake Agassiz and others) and by the Fennoscandinavian ice sheet (situated over the Baltic Sea). The Eurasian ice sheet had blocked off lakes, the outbursts of which emptied into northward-draining rivers in Siberia. Pulses of meltwater amassed in major proglacial lakes were released into the Mississippi and St Lawrence Rivers and the Arctic and Hudson Straits, eventually to enter the North Atlantic Ocean. These floods emitted enormous amounts of freshwater, which may have affected ocean circulation and deep-water production in the North Atlantic (Teller, 1990). Giant jökulhlaups from the Laurentide ice sheet during the last glacial cycle may have played a part in depositing the Heinrich layers in the North Atlantic (Heinrich, 1988; Alley and MacAyeal, 1994; Colman, 2002). Floods from glacial Lake Missoula at the border of the Laurentide ice sheet repeatedly transported around 2_1012 m3 (2000 km3) of water in less than four days, with flow velocities of up to 30 m s_1 and estimated peak discharges of 2_107 m3 s_1 (Baker, 1973; Baker and Bunker, 1985; O'Connor and Baker, 1992), so that they comprise the greatest discharges of freshwater known in geological history.

The Lake Missoula floods lasted approximately one week, and the magnitude of their peak discharge indicates

either supraglacial release or suddenly failing barriers, because such discharges cannot be explained by the gradual enlargement of basal ice tunnels. The floods from Lake Missoula produced the huge channelled scablands on the Columbia Plateau, Washington State.

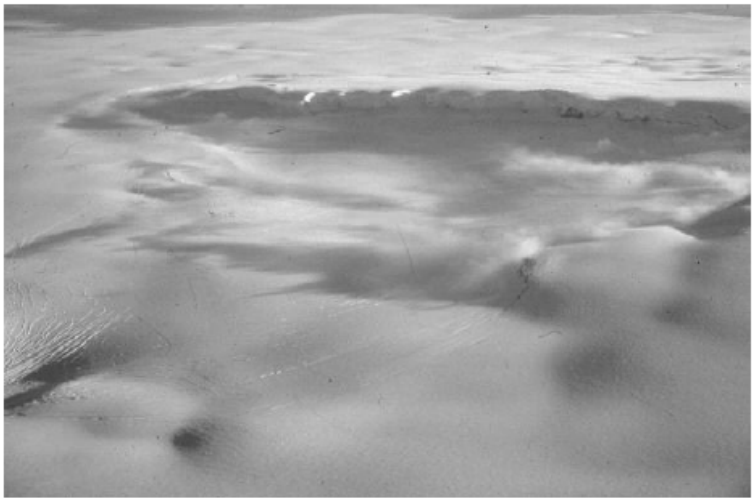

Figure 8.6 *A 10-km-wide depression formed by continuous melting at the subglacial hydrothermal area of Grímsvötn, Vatnajökull, Iceland. View towards the 400-m-high caldera rim, Mt Grímsfjall. Photo: H. Björnsson*

4.3 Floods from subglacial lakes

The best-documented floods from subglacial lakes occur in Iceland, where jökulhlaups regularly drain six lakes of this type. They are located in hydrothermal areas, where geothermal activity continuously melts ice on the glacier bed, creating a depression in the glacier surface, under which water accumulates until released in floods. The best-known jökulhlaups drain the lake Grímsvötn in Vatnajökull glacier (Björnsson, 1974, 1988; Thorarinsson, 1974) and occur at 1- to 10-year intervals. Their peak discharge ranges from 600 to 4–5_105 m3 s_1 at the outwash plain, their duration is two days to four weeks and their total volume at each event is 0.5–4.0_109 m3. The greatest floods have peaked in less than one week and subsided in two days, whereas the smaller ones peak in two to three weeks, after which they usually terminate in approximately one week (Figures 8.4, 8.5 and 8.6). Jökulhlaups from Grímsvötn flow a distance of some 50 km beneath the ice to the glacier terminus by the Skeiðarársandur outwash plain (Figure 8.7). The most violent Grímsvötn jökulhlaups have flooded this entire plain, measuring 1000 km2 (e.g., Björnsson, 1988). Typically, lake drainage begins at water pressures 6–7 bar lower than those exerted by the overburden at the ice dam. Conduits are enlarged in the course of several days or up to three weeks, so that the floods develop from small initial discharges which have been explained by classic jökulhlaup theories. Occasionally, nevertheless, the lake level rises until the ice dam floats; in this case, discharge increases faster than can be accommodated by the melting of conduits, and the glacier is lifted along the flow path as the water forces open space for itself. An outburst of this type took place in November 1996, when meltwater from the Gjálp eruption collected in Grímsvötn before flowing out in a disastrous flood: this is discussed below in connection with volcanism.

Other well-known jökulhlaups from subglacial Icelandic lakes originate at the Skaftá cauldrons (Figure 8.8), 10–15 km northwest of Grímsvötn, and result in floods of 50–350 10^6 m^3. They rise over one to three days to a peak discharge of 200–1500 $m^{3\ s-1}$, before receding slowly for one to two weeks. So far, the hydrographs of these outbursts have not been simulated theoretically. Although their speedy rise suggests a water temperature at the reservoir well above the melting point (10–20°C), this must not be considered definite, because the theory of heat transfer is debatable.

4.4 Floods related to subglacial volcanic eruptions

In active volcanic areas of Iceland and of North and South America, eruptions frequently trigger catastrophic glacial floods (Thorarinsson, 1957, 1958; Sturm *et al*., 1986; Björnsson, 1988; Trabant and eyer, 1992; Pierson, 1995; Gu_mundsson *et al*., 1997; Thouret, this volume). Lava erupts directly into water stored under the ice and the boiling water transfers heat readily. Meltwater created by subglacial eruptions may discharge instantly toward the glacier margins, depending on the rate of volcanic melting. The bursts may either travel subglacially in tunnels or spread out in a broad sheet, heaving up the ice. Moreover, the water may overtop the glacier, melt channels on its surface, and crack off giant blocks of ice. Alternatively, the meltwater forming beneath substantial ice masses may accumulate in subglacial lakes, eventually to exit from them in jökulhlaups. A recent example of such a flood occurred when meltwater from the 1996 Gjálp eruption gathered in the subglacial lake Grímsvötn, entering at a rate of up to 5 10^3 $m^{3\ s-1}$, before draining from the lake in a catastrophic flood, with discharge increasing almost linearly to a peak of 4 10^4 $m^{3\ s-1}$ in 16 hours. Within a period of 40 hours, 3.2 10^9 m^3 of water had left the lake. Even though the outburst had begun as a flood wave, so that the initial discharge was of the order of 5 10^3 to 5 10^4 $m^{3\ s-1}$, an exponential increase would have taken around two days to reach the estimated peak.

Figure 8.8 *A 3-km-wide and 150-m-deep cauldron after a jökulhlaup in Vatnajökull, Iceland. Photo: H. Björnsson*

Eruptions of snow-clad volcanoes may generate huge floods when pyroclastic, turbulent fluid melts the icy cover, producing slushy, debris-rich flows which speed down valley slopes. Thouret (this volume) describes how a relatively small eruption from the snow-capped volcano Nevado del Ruiz (5400 m high) in Colombia in 1985 caused disastrous lahars that killed more than 23 000 inhabitants of the town Armero, 72 km away. In 1966–68 an eruption at Mt Redoubt, Alaska, melted or washed away 6 10^7 m3 of glacial ice (Sturm *et al*., 1986) and in 1989–90 another eruption achieved double that amount (Trabant and Meyer, 1992).
A contemporary description of the outburst during the 1362 Öræfajökull eruption in Iceland provides an example of abrupt, destructive jökulhlaups from an ice-capped stratovolcano (Thorarinsson 1957, 1958). In less than one day, the flood may have reached its peak of at least 10^5 m^3/s (Thorarinsson, 1958). Water originating in the 2000 m high vicinity of the summit streamed subglacially down the slopes before bursting out to wash away several farmsteads and to leave dead ice, sediment and hummocks covering the lowlands at a depth of 2–4 m. Outwash plains appeared where sea depths had previously measured 50 m. A contemporary record (report by Rev. Jón Thorláksson, cited by Henderson (1818); Thorarinsson, 1958: p. 31) describes how "*several floods of water gushed out, the last of which was the greatest. When these floods were over, the glacier itself slid forwards over the plane ground, just like melted metal poured out of a crucible. The water now rushed down on the earth side without intermission, and destroyed what little of the pasture grounds remained . . . Things now assumed quite a different appearance. The glacier itself burst and many icebergs were run down [sic] quite to the sea, but the thickest remained on the plain at a short distance from the foot of the mountain . . . We could only proceed with the utmost danger, as there was no other way except between the ice-mountain and the glacier that had slid forwards over the plain, where the water was so hot that the horses almost got unmanageable".*

A less devastating eruption took place in AD 1727 (Thorarinsson, 1958). The swiftest, greatest outbursts of glacial meltwater noted in world history accompany volcanic eruptions in the Katla caldera, which rests under the Icelandic ice cap My´ rdalsjökull. Occurring on average twice per century, the outbursts have durations of 3–5 days, peak discharges estimated at 10^5–10^6 m^3/s, and total volumes of 1–8_109 m3 (Thorarinsson, 1957, 1975; Maizels, 1989, 1995; Tómasson, 1996; Larsen, 2000). Immense blocks of ice break off the glacial margins, and a mixture of water, ice, volcanic emissions and sediment surges over the outwash plain at velocities of 5–15 m /s. During a segment of the flow event, the water may consist of a hyperconcentrated fluid–sediment mixture. The amount of volcanic debris produced per event and carried away by the water has been estimated to range from 0.7 to 1.6_109 m3, or be of the order of 2_109 t (Tómasson, 1996; Larsen, 2000). During the last eruption in 1918, the neighbouring coastline advanced 3 km into the sea. Although many loose deposits have been washed away in succeeding years, the affected seashore remains 2.2–2.5 km further south than its position in 1660. Jökulhlaups have played a dominant role in building up the outwash plain, which like other such plains in Iceland is called a *sandur* – a term that has acquired international use. Marine sediments containing debris transported from the eruption site are found in the ocean several hundred kilometres to the south. Jökulhlaups from Katla have threatened local communities, damaged vegetation, ruptured roads on the alluvial flats surrounding the ice cap and even generated flood waves in coastal waters. On the northern side of My´ rdalsjökull, the outbursts have eroded deep canyons in the bedrock.

The largest, most catastrophic jökulhlaups in Iceland, with peak discharges of the order of 10^6 m^3 /s were caused by prehistoric eruptions in the voluminous, ice-filled calderas of Bárðarbunga and Kverkfjöll in the northern reaches of Vatnajökull (see Tómasson, 1973; Björnsson, 1988; Björnsson and Einarsson, 1991; Knudsen and Russell, 2002; Waitt, 2002). Floods sweeping down Jökulsá á Fjöllum carved a conspicuous scabland and a deep canyon Jökulsárgljúfur; Figure 8.9); erosion by cavitation is considered to have been a significant factor in their creation.

Figure 8.9 *A canyon eroded and carved by jökulhlaups (the 300-m-deep Jökulsárgljúfur, north of Vatnajökull, Iceland)*
Photo: Björn Rúriksson, reproduced with permission.

5 Concluding remarks and future prospects

This chapter has reviewed the current knowledge of glacial floods and their sources in impounded glacial meltwater, and on the dams holding back the water and dam failure. Also, I have described the characteristics of flood discharges, their impact in the proglacial zone, and their significance for society.

Despite some outburst sources lying hidden, field inspection or remote sensing can detect most of them. Potential jökulhlaup hazards can be recognized by examining the properties of reservoir dams and evaluating their stability. While the onset of outbursts cannot be timed exactly, those stemming from ice-dammed lakes may be predicted empirically – though no more precisely than to the nearest month, based on records of lake levels at the beginning of previous outbursts. The discharge rates of change and impacts of jökulhlaups depend on their release mechanisms, i.e., whether a sediment dam suddenly fails, an ice dam is abruptly lifted or overtopped, or the dam seal begins to leak through a subglacial tunnel at gradually increasing rates. The nature of the flood hazard depends on reservoirvolume and the temperature of the fluid, along with the character and content of the sediment that is entrained in the flow. Empirical and theoretical relations help to forecast the possible magnitude of jökulhlaups. Theoretical models of flood discharge may help to predict the slopes of the ascending limbs of the hydrograph if the drainage occurs through tunnels under an ice dam. However, formulating such models requires information on water temperature and bottom roughness, and these data are rarely available. At present, theoretical models are unreliable for predicting peak discharge, although empirical relationships may provide some estimate, given the total volume of the reservoir at the beginning of the outburst. Once the flood has started, the subsequent discharge rate may be predicted on the grounds of reservoir volume and of flow measured during the initial phase of the flood. No theory is yet available for subglacially draining jökulhlaups, which increase faster than can be explained by conduits widening through melting. Glacier lakes are ephemeral features, dependent on variable conditions such as the advance or recession of glacial termini. Continuous monitoring of impounded water and inflow rates is needed for assessing risks and delineating danger zones. Outbursts from lakes behind sediment dams at glacial margins can be prevented by installing drainage pipes to control water levels. Some englacial sources of floods may be difficult to detect, and subglacial volcanic eruptions are hard to predict, but maps of bedrock topography and the glacier surface can be used to identify potential hazard zones with regard to jökulhlaups. Field studies of landforms, sediments and other evidence of varying flow processes would improve understanding of the outburst mechanism. At present, both empirical and theoretical calculations suffer from inaccurate estimates of discharges and particularly of peak flows. Further studies are required on the physics of how jökulhlaups begin to enable more precise timing of their onset. Additionally, studies of supraglacial outbursts that melt gorges through ice dams and of subglacial bursts that lift the glacier to propagate a flood wave are still at an early stage.

Studies of the physics of modern glacial floods of every magnitude may fundamentally improve our understanding of palaeofloods in the late Pleistocene and early Holocene. They released enormous amounts of freshwater into the ocean, perhaps altering deep-water circulation and the global climate. In this respect, the glacial floods of today may become a key to the past.

References

Alley, R.B. and MacAyeal, D.R., 1994. Ice-rafted debris associated with binge/purge oscillations of the Laurentide Ice Sheet. *Paleooceanography*, **9**: 503–11.

Baker, V.R., 1973. *Paleohydrology and sedimentology of Lake Missoula flooding in Eastern Washington*. Geological Society of America Special Paper 144.

Baker, V.R., 1983. Large scale paleohydrology. In Gregory, K.J. (ed.), *Background to palaeohydrology*. Chichester: Wiley, 455–78.
Baker, V.R. and Bunker, R.C., 1985. Cataclysmic late Pleistocene flooding from glacial Lake Missoula: a review. *Quaternary Science Reviews*, **4**: 1–41.
Björnsson, H., 1974. Explanation of jökulhlaups from Grímsvötn, Vatnajökull, Iceland. *Jökull*, **24**: 1–26.
Björnsson, H., 1975. Subglacial water reservoirs, jökulhlaups and volcanic eruptions. *Jökull*, **25**: 1–14.
Björnsson, H., 1976. Marginal and supraglacial lakes in Iceland. *Jökull*, **26**: 40–51.
Björnsson, H., 1988. *Hydrology of ice caps in volcanic regions*. Reykjavík: Societas Scientarium Islandica, 45.
Björnsson, H., 1992. Jökulhlaups in Iceland: prediction, characteristics and simulation. *Annals of Glaciology*, **16**: 95–106.
Björnsson, H., 1997. Grímsvatnahlaup fyrr og nú. In Haraldsson, H. (ed.), *Vatnajökull. Gos og hlaup 1996*. Reykjavík, Iceland: Icelandic Public Roads Administration, 61–77.
Björnsson, H., 1998. Hydrological characteristics of the drainage system beneath a surging glacier. *Nature*, **395**: 771–74.
Björnsson, H., 2002. Subglacial lakes and jökulhlaups in Iceland. *Global and Planetary Change*, **35**: 255–71.
Björnsson, H. and Einarsson, P., 1991. Volcanoes beneath Vatnajökull, Iceland. Evidence from radio echosounding, earthquakes and jökulhlaups. *Jökull*, **40**: 147–68.
Björnsson, H., Pálsson, F., Gu_mundsson, M.T. and Flowers, G.E., 2001. The extraordinary 1996 jökulhlaup from Grímsvötn, Vatnajökull, Iceland. *Eos (Transactions, American Geophysical Union)*, **82**(47): F528.
Bond, G., Heinrich, H., Broecker, W., Labeyrie, L., McManus, J., Andrews, J., Huon, S., Jantschik, R., Clasen, S., Simet, C., Tedesco, K., Klas, M., Bonani, G. and Ivy, S., 1992. Evidence for massive discharges of icebergs into the North Atlantic Ocean during the last glacial period. *Nature*, **360**: 245–49.
Bretz, J.H., 1925. The Spokane flood beyond the Channeled Scablands. *Journal of Geology*, **33**: 97–115.
Bretz, J.H., 1969. The Lake Missoula floods and Channeled Scabland. *Journal of Geology*, **77**: 505–43.
Chapman, D.L., 1981. *Jökulhlaups on Snow River in southeastern Alaska: a compilation of recorded and inferred hydrographs and a forecast procedure*. National Oceanographic and Atmospheric Administration Technical
Memorandum NWS AR-31. Anchorage, Alaska: NOAA.
Clague, J.J. and Mathews, W.H., 1973. The magnitude of jökulhlaups. *Journal of Glaciology*, **12**: 501–504.
Clarke, G.K.C., 1982. Glacier outburst flood from "Hazard Lake", Yukon Territory, and the problem of flood magnitude prediction. *Journal of Glaciol*ogy, **28**: 3–21.
Clarke, G.K.C. and Waldron, D.A., 1984. Simulation of the August 1979 sudden discharge of glacier-dammed Flood Lake, British Columbia. *Canadian Journal of Earth Sciences*, **21**: 502–504.
Clarke, G.K.C., Mathews, W.H. and Pack, R.T., 1984. Outburst floods from glacial Lake Missoula. *Quaternary Research*, **22**: 289–99.
Colman, S.M., 2002. A fresh look at glacial floods. *Science*, **296**: 1251–52.
Costa, J.E., 1988. Rheologic, geomorphic, and sedimentologic differentiation of water floods, hyperconcentrated
flows, and debris flows. In Baker, V.R., Kochel, R.C. and Patton, P.C. (eds), *Flood geomorphology*. New York: Wiley, 113–22.
Dawson, A.G., 1983. Glacier-dammed lake investigations in the Hullet Lake area, South Greenland. *Meddelelser om Grönland*, *Geoscience*, **11**, 22 pp.
Driedger, C.L. and Fountain, A.G., 1989. Glacier outburst floods at Mount Rainier, Washington. *Annals of Glaciology*, **13**: 51–55.
Evans, S.G. and Clague, J.J., 1994. Recent climatic change and catastrophic geomorphologic processes in mountain environments. *Geomorphology*, **10**: 107–28.
Fernández, P.C., Fornero, L., Maza, J. and Yañez, H., 1991. Simulation of flood waves from outburst of glacierdammed lake. *Journal of Hydraulic Engineering*, **117**: 42–53.
Glazyrin, G.E. and Sokolov, L.N., 1976. Forecasting of flood characteristics caused by glacier lake outbursts. *Materialy Gliatsiologicheskikh Issledovanii*, **26**: 78–85.
Goodwin, L.D., 1988. The nature and origin of a jökulhlaup near Casey Station, Antarctica. *Journal of Glaciology*, **34**: 95–101.
Gu_mundsson, M.T., Björnsson, H. and Pálsson, F., 1995. Changes in jökulhlaup sizes in Grímsvötn, Vatnajökull, Iceland, 1934–1991, deduced from in situ measurements of subglacial lake volume. *Journal of Glaciology*, **41**: 263–72.
Gu_mundsson, M.T., Sigmundsson, F. and Björnsson, H., 1997. Ice–volcano interaction of the 1996 Gjálp subglacial eruption, Vatnajökull, Iceland. *Nature,* **389**: 954–57.
Gunn, J.P., Todd, H.J. and Mason, K., 1930. The Shyok flood, 1929. *Himalayan Journal*, **2**: 35–47.
Haeberli, W., 1983. Frequency and characteristics of glacier floods in the Swiss Alps. *Annals of Glaciology*, **4**: 85–90.
Heinrich, H., 1988. Origin and consequences of cyclic ice rafting in the northeast Atlantic Ocean during the past 130,000 years. *Quaternary Research*, **29**: 142–52.
Heinsheimer, G.J., 1954. Der Durchbruch des Morengletschers, Lago Argentino, Patagonien, 1953. *Zeitschrift für Gletscherkunde und Glaziologie*, **3**: 33–38.
Heinsheimer, G.J., 1958. Zur Hydrologie und Glaziologie des Lago Argentino und Ventisquero Moreno III. *Zeitschrift für Gletscherkunde und Glaziologie*, **4**: 61–72.
Henderson, E., 1818. *Iceland; or the journal of a residence in that island during the years 1814 and 1815, vol. I. Oliphant*. Edinburgh: Waugh and Innes.
Hewitt, K., 1982. Natural dams and outburst floods of the Karakoram Himalaya. In Glen, J.W. (ed.), *Hydrological aspects of alpine and high-mountain areas*. IAHS Publication 138. Wallingford: IAHS Press, 259–69.
Hulsing, H., 1981. *The breakout of Alaska's Lake George*. Popular publications of the U.S. Geological Survey. Reston, VA: USGS and Washington, DC: Government Printing Office.
Jóhannesson, T., 2002. Propagation of a subglacial flood wave during the initiation of jökulhlaup. *Hydrological Sciences Journal*, **47**: 417–34.
Kamb, B., 1987. Glacier surge mechanism based on linked cavity configuration of the basal water conduit system. *Journal of Geophysical Research*, **92**: 9083–100.
Kamb, B., Raymond, C.F., Harrison, W.D., Engelhardt, H., Echelmeyer, K.A., Humphrey, N., Burgman, M.M. and Pfeffer, T., 1985. Glacier surge mechanism: 1982–1983 surge of Variegated Glacier, Alaska. *Science*, **227**: 469–79.
Knudsen, Ó. and Russell, A.R., 2002. Jökulhlaup deposits at Ásbyrgi, northern Iceland: sedimentology and implications of flow type. In Snorrason, A., Finnsdóttir, H.P. and Moss, M.E. (eds), *The extremes of the extremes:extraordinary floods*. IAHS Publication 271. Wallingford: IAHS Press, 107–12.
Konovalov, V.G., 1991. Methods for computing the onset date and daily discharge hydrograph of the outburst from Mertzbacher Lake, Northern Inylchek Glacier, Tien Shan. In Kotlyakov, V.M., Ushakov, A. and Glazovsky, A. (eds), *Glaciers–ocean–atmosphere interactions*. IAHS Publication 208. Wallingford: IAHS Press, 359–66.

Krenke, A.N. and Kotlyakov, V.M., 1985. USSR case study: catastrophic floods. In: Young, G.J. (ed.), *Techniques for prediction of runoff from glacierized areas.* IAHS Publication 149. Wallingford: IAHS Press, 115–24.
Larsen, G., 2000. Holocene eruptions within the Katla volcanic system, Iceland: notes on characteristics and environmental impact. *Jökull*, **50**: 1–28.
Liestøl, O., 1956. Glacier dammed lakes in Norway. *Norsk Geografisk Tidsskrift*, **15**: 122–49.
Liestøl, O., 1977. Setevatnet, a glacier dammed lake in Spitsbergen. *Norsk Polarinstitutt Årbok*, **1975**: 31–35.
Lipscomb, S.W., 1989. *Flow and hydraulic characteristics of the Knik-Matanuska River estuary, Cook Inlet, southcentral Alaska.* U.S. Geological Survey Water Resources Investigations Report 89–4064. Denver, CO: USGS, Water Resources Division and Washington, DC: Government Printing Office.
Lister, H. and Wyllie, P.J., 1957. The geomorphology of Dronning Louise Land. *Meddelelser om Grönland*, **158** (1).
Lliboutry, L., 1971. Les Catastrophes glaciaires. *La Recherche*, **2**: 417–25.
Lliboutry, L., Arnao, B.M., Pautre, A. and Schneider, B., 1977. Glaciological problems set by the control of dangerous lakes in the Cordillera Blanca, Peru. I. Historical failures of morainic dams, their causes and prevention. *Journal of Glaciology*, **18**: 239–54.
Maag, H.U., 1969. *Ice dammed lakes and marginal glacial drainage on Axel Heiberg Island, Canadian Arctic Archipelago*. Axel Heiberg Osland Research Reports. Jacobsen-McGill Arctic Research Expedition 1959–1962. McGill University, Montreal.
Maizels, J.K., 1989. Sedimentology and paleohydrology of Holocene flood deposits in front of a jökulhlaup glacier, south Iceland. In Beven, K. and Carling, P. (eds), *Floods. Hydrological, sedimentological and geomorphological implications*. Chichester: Wiley, 239–52.
Maizels, J., 1995. Sediments and landforms of modern proglacial terrestrial environments. In Menzies, J. (ed.), *Modern glacial environments*. Oxford: Butterworth-Heinemann, 365–416.
Marcus, M.G., 1960. Periodic drainage of glacier-dammed Tukequant Lake, British Columbia. *GeographicalReview*, **50**: 89–106.
Mason, K., 1929. Indus floods and Shyok glaciers. *Himalayan Journal*, **1**: 10–29.
Mathews, W.H., 1965. Two self-dumping ice-dammed lakes in British Columbia. *Geographical Review*, **55**: 46–52.
Mathews, W.H. and Clague, J.J., 1993. The record of jökulhlaups from Summit Lake, northwestern British Columbia. *Canadian Journal of Earth Sciences*, **30**: 499–508.
Mayo, L.R., 1988. Hubbard Glacier near Yakutat, Alaska – the ice damming and breakout of Russel Fiord/Lake,1986. In Moody, D.W., *et al*. (compilers), *National water summary 1986; hydrologic events and ground-water quality*. U.S. Geological Survey Water-Supply Paper 2325. Reston, VA: USGS and Washington, DC: Government Printing Office, 42–49.
Mayo, L.R., 1989. Advances of Hubbard Glacier and 1986 outburst of Russel Fiord, Alaska, U. S. A. *Annals of Glaciology*, **13**: 189–94.
Ng, F. and Björnsson, H., 2003. On the Clague-Matthews relation for jökulhlaups. *Journal of Glaciology*, **49**.
Nye, J.F., 1976. Water flow in glaciers: jökulhlaups, tunnels and veins. *Journal of Glaciology*, **17**: 181–207.
O'Connor, J.E. and Baker, V.R., 1992. Magnitudes and implications of peak discharges from glacial Lake Missoula. *Geological Society of America Bulletin,* **104**: 267–79.
Oswald, G.K.A. and Robin, G. de Q., 1973. Lakes beneath the Antarctic Ice Sheet. *Nature*, **245**: 251–54.
Pierson, T.C., 1995. Flow characteristics of large eruption-triggered debris flows at snow-clad volcanoes. Constraints for debris-flow models. *Journal of Volcanology and Geothermal Research,* **66**: 283–94.
Pierson, T.C., Janda, R.J., Thouret, J.-C. and Borrero, C.A., 1990. Perturbation and melting of snow and ice by the 13 November 1985 eruption of Nevado del Ruiz, Colombia, and consequent mobilization, flow and deposition of lahars. *Journal of Volcanology and Geothermal Research*, **41**: 17–66.
Post, A. and Mayo, L.R., 1971. *Glacier dammed lakes and outburst floods in Alaska*. U.S. Geological Survey Hydraulic Investigations Atlas HA-455. Washington, DC: Government Printing Office.
Raymond, C.F. and Nolan, M., 2000. Drainage of a glacial lake through an ice spillway. In Nakawo, M. Raymond,C.F. and Fountain, A. (eds), *Debris-covered glaciers*. IAHS Publication 264. Wallingford: IAHS Press, 199–207.
Ridley, J.K., Cudlip, W. and Laxon, S.W., 1993. Identification of subglacial lakes using ERS-1 radar altimeter. *Journal of Glaciology*, **39**: 625–34.
Roberts, M.J., 2002. Controls on supraglacial outlet development during glacial outburst floods. Unpublished Ph.D. Thesis, Staffordshire University, UK.
Roberts, M.J., Russell, A.J., Tweed, F.S. and Knudsen, Ó., 2000. Ice fracturing during jökulhlaups: implications for englacial floodwater routing and outlet development. *Earth Surface Processes and Landforms*, **25**: 1–18.
Russell, A.J., 1989. A comparison of two recent jökulhlaups from an ice-dammed lake, Söndre Strömfjord, West Greenland. *Journal of Glaciology*, **35**: 157–62.
Russell, A.J., 1993. Supraglacial lake drainage near Söndre Strömfjord, Greenland. *Journal of Glaciology*, **39**: 431–33.
Russell, A.J., Tweed, F.S. and Knudsen, Ó., 2000. Flash flood at Sólheimajökull heralds the reawakening of an Icelandic subglacial volcano. *Geology Today*, **16**: 102–106.
Schytt, V., 1956. Lateral drainage channels along the northern side of the Moltke glacier, North-West Greenland. *Geografiska Annaler*, **38A**: 64–77.
Shaw, J., 1996. A meltwater model for Laurentide subglacial landscapes. In McCann, S.B. and Ford, D.C. (eds), *Geomorphology sans frontières*. Chichester: Wiley, 181–236.
Shaw, J., 2002. The meltwater hypothesis for subglacial landforms. *Quaternary International*, **90**: 5–22.
Shreve, R., 1972. Movement of water in glaciers. *Journal of Glaciology*, **62**: 205–14.
Siegert, M.J., Ellis-Evans, J.C., Tranter, M., Mayer, C., Petit, J.-R., Salamatin, A. and Priscu, J.C., 2001. Physical, chemical and biological processes in Lake Vostok and other Antarctic subglacial lakes. *Nature*, **414**: 603–609.
Spring, U. and Hutter, K., 1981. Numerical studies of jökulhlaups. *Cold Regions Science and Technology*, **4**: 221–44.
Spring, U. and Hutter, K., 1982. Conduit flow of a fluid through its solid phase and its application to interglacial channel flow. *International Journal of Engineering Science*, **20**: 327–63.
Stone, K.H., 1963. Alaskan ice-dammed lakes. *Annals of the Association of American Geographers*, **53**: 332–49.
Sturm, M. and Benson, C.S., 1985. A history of jökulhlaups from Strandline Lake, Alaska, U.S.A. *Journal of Glaciology*, **31**: 272–80.
Sturm, M., Benson, C.S. and MacKeith, P., 1986. Effects of the 1966–68 eruptions of Mount Redoubt on the flow of Drift Glacier, Alaska, U.S.A. *Journal of Glaciology*, **32**: 355–62.
Teller, J.T., 1990. Volume and routing of Late-Glacial runoff from the southern Laurentide ice sheet. *Quaternary Research*, **34**: 12–23.
Teller, J.T. and Clayton, L. (eds), 1983. *Glacial Lake Agassiz*. Canada: Geological Association of Canada Special Paper, 26.

Thorarinsson, S., 1939. The ice dammed lakes of Iceland with particular reference to their values as indicators of glacier oscillations. *Geografiska Annaler*, **21A**: 216–42.
Thorarinsson, S., 1957. The jökulhlaup from the Katla area in 1955 compared with other jökulhlaups in Iceland. *Jökull,* **7**: 21–25.
Thorarinsson, S., 1958. The Öræfajökull eruption of 1362. *Acta Naturalia Islandica*, 2.
Thorarinsson, S., 1974. *Vötnin stri_. Saga Skei_arárhlaups og Grímsvatnagosa*. Menningersjóður, Reykjavík, Iceland.
Thorarinsson, S., 1975. Kalta og Annáll Kötlugosa. *Árbók Fer_afélags Íslands*, **30**: 125–49.
Thouret, J.C. 1990. Effects of the November 13, 1985 eruption on the snow pack and ice cap of Nevado del Ruiz volcano, Colombia. *Journal of Volcanology and Geothermal Research*, **41**: 177–201.
Tómasson, H., 1973. Hamfarahlaup í Jökulsá á Fjöllum. *Náttúrufræ_ingurinn,* **43**: 12–34.
Tómasson, H., 1996. The jökulhlaup from Katla in 1918. *Annals of Glaciology*, **22**: 249–54.
Trabant, D.C. and Meyer, D.F., 1992. Flood generation and destruction of Drift Glacier by 1989–90 eruption of Redoubt Volcano, Alaska. *Annals of Glaciology*, **16**: 33–38.
Vuichard, D. and Zimmerman, M., 1986. The Langmoche flash-flood, Khumbu Himal, Nepal. *Mountain Research and Development*, **6**: 90–94.
Vuichard, D. and Zimmerman, M., 1987. The 1985 catastrophic drainage of a moraine-dammed lake. Khumbu Himal, Nepal: cause and consequences. *Mountain Research and Development*, **7**: 91–110.
Waitt, R.B., Jr, 1984. Prehistoric jökulhlaups from Pleistocene glacial Lake Missoula – new evidence from varved sediment in Northern Idaho and Washington. *Quaternary Research*, **22**: 46–58.
Waitt, R.B., Jr, 2002. Great Holocene floods along Jökulsá á Fjöllum, north Iceland. In Martini, I.P., Baker, V.R. and Garzón, G. (eds), *Floods and megaflood deposits. Recent and ancient examples*. International Association of Sedimentalogists Special Publication, 32. Malden MA: Blackwell 37–51.
Walder, J.S., 1986. Hydraulics of subglacial cavities. *Journal of Glaciology,* **32**: 439–45.
Walder, J.S. and Costa, J.E., 1996. Outburst floods from glacier-dammed lakes: the effect of mode of lake drainage on flood magnitude. *Earth Surface Processes and Landforms*, **21**: 701–23.
Walder J.S. and Driedger, C.L., 1995. Frequent outburst floods from South Tahoma Glacier, Mount Rainier,U.S.A.: relation to debris flows, meteorological origin and implications for subglacial hydrology. *Journal ofGlaciology*, **41**: 1–10.
Webb, R.H. and Jarrett, R.D., 2002. One-dimensional estimation techniques for discharges of paleofloods and historical floods. In House, P.K., Webb, R.H., Baker, V.R. and Levish, D.R. (eds), *Ancient floods, modern hazards. Principles and applications of paleoflood hydrology*. Washington, DC: American Geophysical Union, 111–25.
Yamada, T., 1998. *Glacier Lake and its outburst flood in the Nepal Himalaya*. Monograph No. 1. Tokyo: Data Center for Glacier Research, Japanese Society of Snow and Ice.

THE NORTH ATLANTIC OSCILLATION :

MECHANISMS AND SPATIO-TEMPORAL VARIABILITY

Christophe Cassou
Cerfacs-CNRS, 42 Av. G. Coriolis, 31057 Toulouse Cedex 1
Email: cassou@cerfacs.fr

Abstract

Over the middle and high latitudes of the northern hemisphere, the most prominent mode of atmospheric variability is the North Atlantic Oscillation (NAO). The spatio-temporal characteristics of the NAO variability are reviewed in this lecture. The general state of knowledge on the complex dynamical processes governing the NAO is described. Emphasis is laid on teleconnections and ocean signals known to modulate the temporal excitation of the NAO.

Introduction

The NAO commonly refers to swings in the atmospheric pressure difference between the Arctic and the subtropical Atlantic. The seesaw pattern is clearly pronounced during the boreal winter season and is associated with changes in the mean wind speed and direction as well as in the number of storms, their intensity, their preferred paths and their associated weather over the neighbouring continents. Significant anomalies in ocean surface temperature and heat content, ocean currents and related heat transport, ocean deep convection and sea ice cover in subarctic seas etc., are also linked to a great extent to the NAO.

The NAO across time scales

The NAO is one of the oldest known weather patterns as some of the earliest descriptions of it were from seafaring Scandinavians several centuries ago (Stephenson et al 2003). There is no single way to define the NAO. The simplest one often referred to as “NAO index” has been proposed by Walker and Bliss (1932) and recently updated by Rogers (1984) and Hurrell (1995) among others; it is calculated as the difference in normalized mean sea level pressure (SLP) between Azores (or Portugal) and Iceland thus capturing the north-south redistribution of atmospheric mass between the two main centres of action in the North Atlantic sector. Most studies of the NAO focus on the boreal winter, when the atmosphere is most active dynamically and perturbations grow to their largest amplitude. In the so-called positive phase, higher-than-normal surface pressures south of 55^{o}N combine with deeper Iceland Low to enhance the climatological meridional pressure gradient leading to stronger-than-average surface westerlies across the middle latitudes and enhanced penetration of the mild and moist oceanic influence towards most of Europe. During NAO+, northward shifted storm track leads to cooler and drier conditions over the Mediterranean basin.

A disadvantage of station-based indices is that they are fixed in space. They do not account for the seasonal migration of the NAO centres of action and they are polluted by transient meteorological phenomena not related to the NAO, especially in summertime and autumn. An alternative approach is Empirical Orthogonal Function (EOF) analysis (Hurrell et al 2003); the NAO is often identified as the leading eigenvector computed from the time variations of gridpoint values of SLP or some other climate variables (geopotentiel, zonal wind etc.). The associated principal component is used to evaluate the temporal evolution of the NAO. While EOFs clearly capture the spatial and large-scale coherence of the NAO pattern, a well known shortcoming stands however in the linear constraints of the method ; EOFs assumes preferred atmospheric circulation states come in pairs in which anomalies of opposite polarity have the same spatial structure. A solution among others to overcome this simplification is to use classification techniques or clustering, which seek for recurrent patterns of a specific amplitude and sign. Objective analyses based on these methods are often used to identify number, spatial structure and frequency of occurrence of recurrent anomalous circulations referred to as “weather regimes”. Travelling pressure systems or storms contribute to a significant fraction of the daily to interannual variability of the extratropical climate. Those are linked to the unstable nature of the upper-level westerly jet stream and interact with circulation patterns of large scale, or “weather regimes”, in which they are embedded. Those regimes can be interpreted as quasi-stationary atmospheric circulations during which the character of the synoptic storms is unusually persistent (Reinhold and Pierrehumbert 1982). They are recurrent, spatially well defined and limited in number and ideally correspond to statistical-dynamical equilibria in the climate phase space. Over the North Atlantic-European (NAE) domain when applied to daily atmospheric circulation fields, they traditionally

leads to four regimes (Vautard 1990). The two first regimes can be viewed as the negative and positive phases of the NAO (Fig.1). The third regime is named Atlantic Ridge and the fourth is often referred to as Scandinavian Blocking.

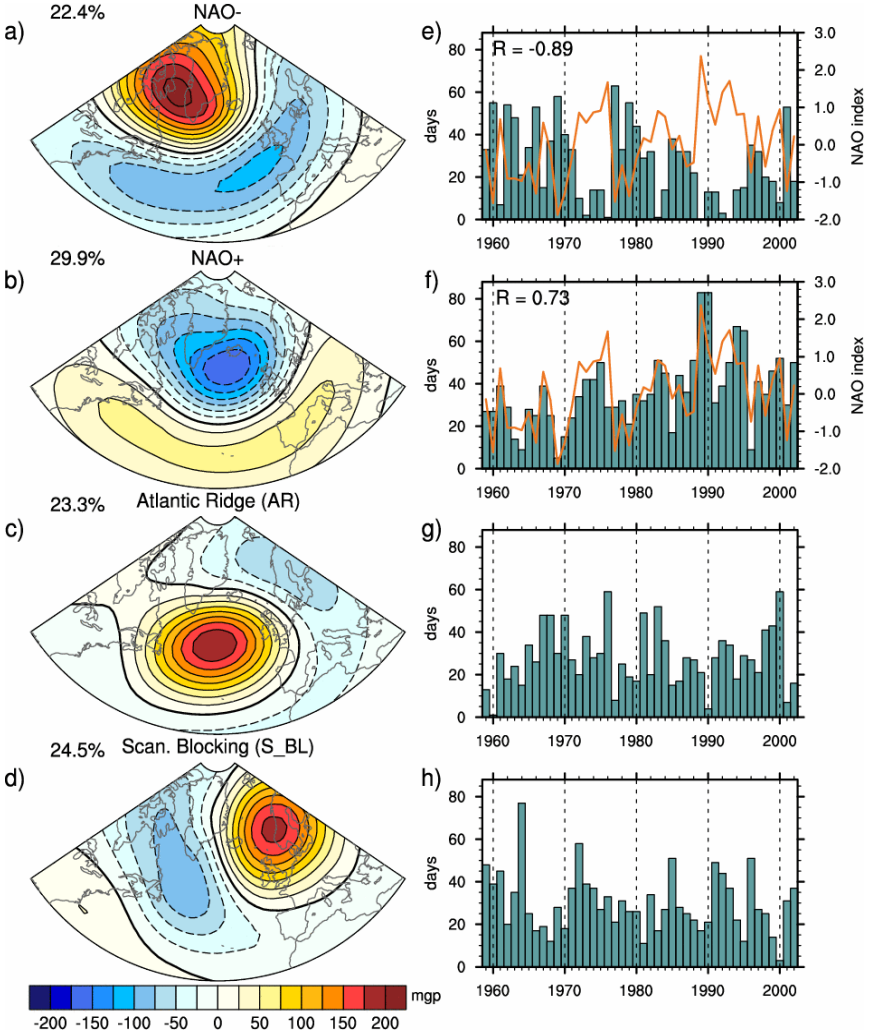

Figure 1: (a-d) Centroids of the four wintertime NAE Z500 weather regimes (m). Each percentage represents the mean frequency occurrence of the regime computed over 1958-2002 from 1 December to 31 March. Contour intervals are 25m. (e-h) Number of days of occurrence of each regime per winter from 1959 to 2002. The NAO index (orange curve) is superimposed on the upper two panels corresponding to the NAO regimes. Correlation (R) between the NAO index and the frequency of occurrence of the NAO regimes is provided. From Cassou et al. (2010).

The day-to-day meteorological fluctuations can be described in terms of temporal transition between regimes. The year-to-year (or longer timescale) climate fluctuations can be interpreted as changes in their frequency of occurrence provided the hypothesis of long term quasi-stationarity climate. This climate-oriented interpretation for weather regimes is shared with the so-called continuum paradigm elaborated for instance in Franske and Feldstein (2005) to better understand the low-frequency fluctuations of the northern hemisphere atmospheric teleconnections patterns. The NAO- and NAO+ regimes interannual occurrence (Fig.1ef) is strongly correlated to the traditional NAO index above discussed. Note however that spatial asymmetry between the two phases are clearly evidenced in winter by clustering techniques. Similar conclusions can de drawn for summertime.

Links between flow regimes and mean conditions over Europe have been documented from daily to decadal timescale as well as for weather (Cassou et al 2005) and climate extremes (Yiou et al 2007). 10-meter wind and air temperature composites derived from regime occurrence are also indicative of strong relationships between daily large-scale atmospheric circulation and ocean surface

over the entire Atlantic basin. Evidence has been provided that a large fraction of the low frequency trends in the Atlantic observed at the surface over the last 50 years in winter can be tracked back to changes in the occurrence of weather regimes and their tropical counterpart (Fig. 2, Cassou et al 2010).

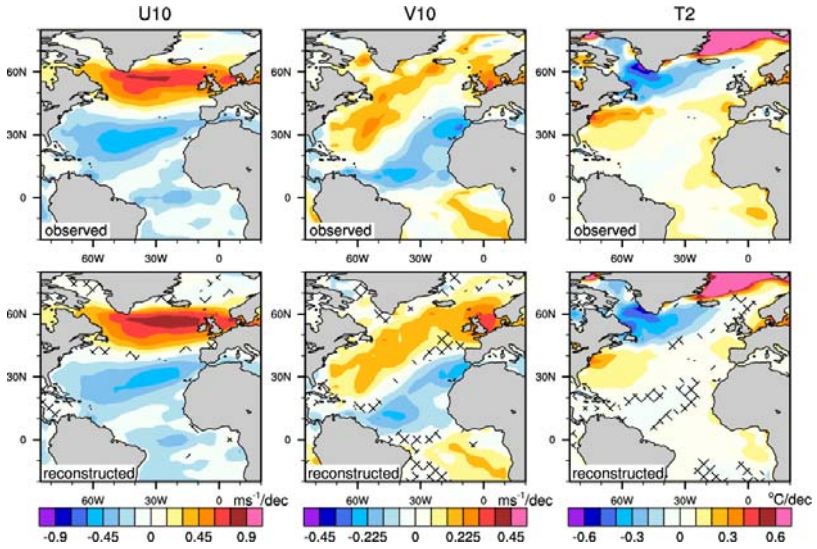

Figure 2: Linear trends computed over 1959-2002 for wintertime (a-c) ERA40 10-meter zonal (U10) and meridional (V10) wind and 2-meter temperature (T2) and for (d-f) reconstructed fields from multiple linear regression using NAE weather regime occurrences and tropical wind classes as predictors. Hashing stands for sign disagreement between observed and reconstructed trends. Contour intervals are 0.15 ms-1/decade, 0.075 ms^{-1}/decade for UV10 and V10 respectively, and 0.1^{o}C for T2. From Cassou et al. (2010).

Large-scale atmospheric circulation tendency are characterized by an intensification of the midlatitude westerlies and a concomitant strengthening of the Northeast trades. Northward displaced storm track is associated with prevalent southerlies north of 40^{o}N. The node for the wind trend corresponds to the mean position of the Azores High and is consistent with the positive trend in the NAO (Fig.1 and Hurrell et al 2003). Note that updated data until 2010 suggest though that the upward trend towards NAO+ enhanced occurrence is somehow reduced in the 2000's. The largest low-frequency changes for 2-meter temperature occur in the western part of the basin and strongly project on the North Atlantic tripole known to be forced by NAO dynamics (Deser and Timlin 1997).

The NAO governing processes

That the spatial pattern of the NAO remains largely the same throughout the year does not imply that it also tends to persist in the same phase for long. To the contrary, it is highly variable tending to change its phase from one week to the next, from one month to another, and its longer term behaviour clearly reflects the combined effect of residence time in any given phase and its amplitude therein. There is little evidence for the NAO to vary on any preferred time scale. The spectrum of the winter-mean NAO index reveals somewhat enhanced variance at quasi-biennial periods, a deficit of power at 3 to 6 year periods and slightly enhanced power in the 8-10 year band, but no significant peaks (Hurrell et al 2003). Note that those statistical characteristics are not stationary throughout the observed period.

It is now well recognized that the NAO type of variability arises from processes internal to the atmosphere in which various scales of motion interact with one another to produce quasi-random (and thus quasi unpredictable) variations. The variability of the extratropical flow can be divided into two broad classes: jet meandering, in which the latitude of the local zonal wind speed maximum in the upper troposphere exhibits pronounced north-south shifts; and jet pulsation, in which the local windspeed maximum exhibits marked strengthening and weakening without shifting latitude. Variability in the Atlantic zonal flow is characterized by both mechanisms because the subtropical jet is relatively weak and the baroclinic eddies tend to organize themselves in the poleward baroclinic zone ; the latter is particularly pronounced in the Atlantic due to the sharp meridional sea surface temperature (SST) gradient along the Gulf Stream/Labrador current, hence driving a purely eddy-driven jet. The NAO is thus associated with anomalous fluxes of zonal momentum of baroclinic waves across ~45^{o}N and

fluctuates on preferred timescales of ~10 days resembling a first-order Markov process (Feldstein 2000). Positive feedbacks between the zonal flow and the eddies, as well as interactions with the stationary waves, play a key role in setting the basin-wide shape of the NAO.

An emerging view for explaining the jet variation and its link to the NAO has been recently proposed based on wave-breaking theory (e.g. Benedict et al 2004, Woollings et al 2010). Synoptic wave-breaking on the equatorward side of the jet tends to be anticyclonic, following the ambient background shear. This leads to poleward eddy fluxes of zonal momentum that act to push the jet to the North and to set NAO+ regimes. Similarly, cyclonic wave-breaking dominates on the poleward side of the jet and the associated momentum fluxes push it to the south and tend to excite NAO- regimes.

Finally, the coupling between the lower stratosphere and the troposphere could also play an active role in setting the phase and persistence of the NAO. Large amplitude anomalies in the strength of the zonal flow along ~60^{o}N frequently seem to originate in the stratosphere and descend into the troposphere. The downward propagating stratospheric circulation anomalies appear to modulate relatively high frequency tropospheric variability for period up to ~60 days following the initiation of the stratospheric signal. A stronger stratospheric polar vortex more frequently leads to NAO+ like anomalies and vice-versa, thus exerting a downward control on surface climate. Even if controversial, the annular shape of the stratospheric mode supports the view that the NAO could be the regional expression of a larger scale hemispheric mode of variability known as the Arctic Oscillation (Thompson et al 2003).

The NAO modulation by external factors

Progress in understanding low frequency variability and predictability of the midlatitude atmospheric circulation relies on the identification of specific causes responsible for the favoured occurrence of the associated weather regimes, their persistence and/or transition. In other words, which factors external to pure atmospheric dynamics at the origin of the NAO could modulate its strength and phase?

At intraseasonal timescale, recent studies (e.g. Cassou 2008) suggest that the main climate oscillation in the tropics –the Madden-Julian Oscillation (MJO)- controls part of the distribution and sequences of the four NAE winter weather regimes (Fig.1). The NAO regimes are the most affected. NAO+ events mostly respond to a midlatitude low frequency wave train initiated by the MJO in the western-central Pacific and propagating eastward. Precursors for NAO- are found in the eastern tropical Pacific-western Atlantic leading to changes along the North Atlantic Storm-track. Wave breaking diagnostics tend to support the MJO preconditioning and the role of the transient eddies in setting the phase of the NAO. These findings reconcile the oscillatory paradigm of the MJO with the episodic view of the North Atlantic dynamics via the regime approach and open some perspectives in terms of medium range predictability.

From seasonal to decadal timescale, evidence is provided that the ocean plays an active role in determining the evolution of the NAO (e.g. Hurrell et al 2003 for a review). While intrinsic atmospheric variability exhibits temporal incoherence, the ocean tends to respond to it with marked persistence of heat content anomalies that feedback to the local atmosphere. The level of retroaction of the anomalous extratropical SST upon the NAO is however under debate and is likely very dependent on the time scale. Adding to the complexity of local ocean-atmosphere interaction is the possibility of remote forcing of the NAO from the tropical oceans; the latter influence appears to be more robust. Several studies have concluded that NAO variability is closely tied to SST variations over the tropical Atlantic. Those involve changes in the meridional SST gradient across the equator, which affect the strength and location of the tropical convection along the Inter Tropical Convergence Zone, and thus ultimately the North Atlantic midlatitude circulation via the excitation of Rossby waves propagating northeastward from the anomalous diabatic heating source. At decadal timescale, the warming of the Indo-Pacific warmpool from the mid-1970's onwards could be responsible for part of the positive trend of the NAO at the end of the XXth century. At interannual timescale, the impact of El Niño Southern Oscillation (ENSO) on the NAO remains open to debate. The correlation between the two indices is not significant and the relationships might be asymmetrical; La Niña events seems to favour NAO+ phases while El Niño events might not induce systematic remote responses. In addition, the ENSO-NAO link might be indirect via the ENSO impact on tropical North Atlantic SSTs or via the ENSO influence on the stratospheric vortex as suggested by the latest literature (e.g Bell et al 2009).

One of most urgent challenge is to advance our understanding of the interaction between greenhouse gases forcing and the NAO. The response might be felt as a change in the residence frequency of the NAO+ regimes with respect to NAO- ones, leading to a weak positive trend according to the most recent results. However, the locations of both regimes in the NAO phase space may be also altered in warmer climate, moving towards more positive values of the NAO index; in that context, the background change thus contributes to the trend.

References

Bell C.J., Gray L.J., Charlton-Perez A.J., Joshi M.M. and Scaife A.A. (2009): Stratospheric communication of ENSO teleconnections to European Winter, *J. Clim*., **22**, 4083-4096.

Benedict J.J., S. Lee and S.B. Feldstein (2004): Synoptic view of the North Atlantic Oscillation. *J. Atmos. Sci.*, **61**, 121-144.

Cassou, C. L. Terray and A.S. Phillips (2005): Tropical Atlantic influence on European heat waves. *J. Clim.* , **18**, 2805-2811.

Cassou C. (2008) : Intraseasonal interaction between the Madden and Julian Oscillation and the North Atlantic Oscillation. *Nature*, **455**, doi:10.1038/nature07286

Cassou, C., M. Minvielle, L. Terray and C. Périgaud (2010). A statistical-dynamical scheme for reconstructing ocean forcing in the Atlantic. Part I: weather regimes as predictors for ocean surface variables. *Clim. Dyn*, doi:10.1007/s00382-010-0781-7.

Deser C. and M.S. Timlin (1997) Atmosphere-ocean interaction on weekly timescales in the North Atlantic and Pacific. *J. Clim*., **22**, 396-413

Franske C. and S.B. Feldstein (2005): The continuum and dynamics of the northern hemisphere teleconnection patterns. *J. Atmos. Sci*., **62**, 3250-3267.

Feldstein S.B. (2000): The time-scale, power spectra and climate noise properties of teleconnections patterns. *J. Clim*., **13**, 4430-4440.

Hurrell W. J. (1995): Decadal trends in the North Atlantic Oscillation: regional temperatures and precipitation. *Science*, **269**, 676-679.

Hurrell W.J., Kushnir Y., Otterson G. and M. Visbeck (2003): An overview of the North Atlantic Oscillation. *AGU Geophys. Mono*, **134**, doi:10.1029/134GM01.

Reinhold B. and R. Pierrehumbert (1982):Dynamics of weather regimes: quasi-stationary waves and blocking. Mon. Wea. Rev., 110, 1105-1145.

Rogers J.C. (1984): The association between the North Atlantic Oscillation and the Southern Oscillation in the northern hemisphere. *Mon. Wea. Rev.*, **112**, 1999-2015.

Stephenson D.B., Wanner H., Brönnimann S. and J. Luterbacher (2003): The history of scientific research on the North Atlantic Oscillation. *AGU Geophys. Mono*, **134**, doi:10.1029/134GM02.

Thompson D.W, S. Lee and M.P. Baldwin (2003): Atmospheric processes governing the Northern Hemisphere Annular Mode/North Atlantic Oscillation. *AGU Geophys. Mono*, **134**, doi:10.1029/134GM05.

Vautard R. (1990): Multiple weather regimes over the North Atlantic analysis of precursors and processors. Mon. Wea. Rev., 118, 2056-2081.

Walker G.T. and E.W. Bliss (1932): World weather V, *Mem. Roy. Met. Soc*., **4**, 53-84.

Woollings T., A. Hannachi, B. Hoskins and A. Turner (2010): A regime view of the North Atlantic Oscillation and its response to anthropogenic forcing. *J. Clim*., **23**, doi:10.1175/2009JCLI3087.1

Yiou, P., R. Vautard, P. Naveau and C. Cassou (2007): Inconsistency between atmospheric dynamics and temperatures during the exceptional 2006-2007 fall/winter and recent warming in Europe. *Geophys. Res. Lett*., **34**, doi:10.1029/2007GL031981.

ENLARGEMENT OF THE ACTIVE RIFT DURING GLACIATIONS

O. Dauteuil [1] , O. Bourgeois [2], B. Van Vliet Lanoe [3]

1: University of Rennes 1, UMR-CNRS 6118, Géosciences Rennes, 35042 Rennes cedex, France – olivier.dauteuil@univ-rennes1.fr
2: Université de Nantes, CNRS, UMR 6112, Laboratoire de Planétologie et Géodynamique, , B. P. 92208, 44322 Nantes, France - olivier.bourgeois@univ-nantes.fr
3: Domaines Océaniques CNRS : UMR6538 – Université de Bretagne Occidentale IUEM Technopôle Brest-Iroise - 29280 Plouzané – France - Brigitte.Vanvlietlanoe@univ-brest.fr

Abstract

During the last glaciation, an ice sheet covered Iceland approximately 1000 m thick. A reconstruction of the ice flow lines shows that the ice sheet was partly drained through fast-flowing streams. The major drainage routes correlate with locations of geothermal anomalies, suggesting that ice stream activity was favoured by water produced in regions of high geothermal heat flux. A widening of active rift zone was also deduced revealing a coupling between deep and surface processes.

Introduction

By its location both on a hot spot and on the Mid-Atlantic Ridge, Iceland has a specific rheological structure (thin lithosphere with low viscosity at shallow depth), which controls the deformation processes on lithospheric scale. Furthermore, its position in the middle of the North Atlantic Ocean makes it highly sensitive to climate fluctuations due to oceanic and atmospheric circulations changes. Iceland is therefore subject to several deformation processes (magmatic, tectonic, and glacial) having their own wavelength and time response.

The dynamics of ice sheets depends on internal parameters, such as the mechanical and thermal properties of the ice, and on external boundary conditions. The external conditions are (1) the topography, (2) the nature of the bed, (3) the distribution of accumulation, ablation and temperature at the surface and (4) the géothermal heat flux at the base. When past and present ice sheets are studied or modelled, proper attention is given to the topography, to the nature of the bed and to the atmospheric conditions. In contrast, because the geothermal heat flux is measured with difficulty in glaciated regions, its effect on glacial flow is poorly known and is rarely taken into account. In tectonically and volcanically quiet regions, such as the Greenland and East Antarctica cratons, variations of geothermal heat flux in space and time are small and probably do not significantly affect glacial flow. However, there are major glaciated regions of the world that are also tectonically or volcanically active: tectonic control on glacier dynamics has been suggested in West Antarctica, East Antarctica, North America and South America. In Iceland, tectonics and volcanism, due to lithospheric spreading at the Mid-Atlantic Ridge, occurred during the last glaciation beneath an ice sheet approximately 1000 m thick. From a reconstruction of the flow patterns of this ice sheet, and from simple calculations, we illustrate how ice dynamics can be controlled by the geothermal heat flux associated with tectonic and volcanic activity.

Geological framework

Iceland is a young island, created by the interactions between the Mid-Atlantic Ridge and a mantle plume, 50 Ma ago. This specific context explains the anomalously thickness of the crust and the intense tectonic and magmatism of the island. The spreading rate of the Mid-Atlantic Ridge is about 2 cm/yr (DeMetz *et al.* 1994). Consequently, Iceland is crossed by a series of faults and volcanoes forming the Icelandic rift system at the junction between the Reykjanes Ridge at south and the Kolbeinsey Ridge at north. Three active zones composed of central volcanoes, rifts and fissure swarms accommodate the spreading and magmatism (Fig 1). The West Volcanic Zone (WVZ) in the southwest is linked to the East Volcanic Zone (EWZ) by transform fault systems, the South Iceland Seismic Zone (SISZ) and the Mid Iceland Belt (MIB). The North Volcanic Zone (NVZ) extends towards the north to the Tjörnes Fracture Zone (TFZ).

The Icelandic mantle plume enhances melt production under Iceland, generating an anomalously thick igneous crust. The crust is the thickest (40-41 km) above the centre of the plume, at the north-western part of the Vatnajökull icecap. It thins away from the plume centre and the thinnest crust (< 20 km) is found in the active rift zone such as the northern part of the NVZ and the southwest of the WVZ (Darbyshire *et al.*, 2000). Therefore the Icelandic lithosphere differs drastically by its thickness and its rheology from “classical” oceanic lithosphere.

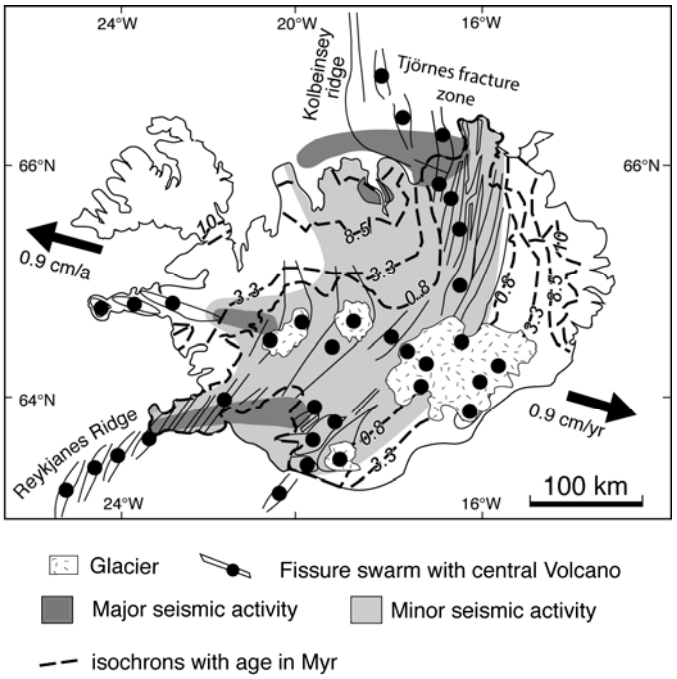

Figure 1 : Geological setting. Iceland lies at the junction between the Reykjanes Ridge to the southwest, and the Kolbeinsey Ridge to the north. Current tectono-volcanic activity occurs in the Neovolcanic Zone, composed of three main branches, the Northern (NVZ), Western (WVZ) and Eastern (EVZ) Volcanic Zones. The Saefellsnes peninsula, in western Iceland, is also active. Lithospheric spreading occurs in fissure swarms associated with central volcanoes (black dots). The dashed lines display the basalt ages. The light grey zone corresponds to the recent active while the dark grey one to the main seismic areas.

The location of Iceland in the middle of the North Atlantic Ocean makes the ice extents highly sensitive to climate changes and consequently to glacial stages. According to Einarsson & Albertsson (1988), 15-23 glaciations affected Iceland during the past three million years. The most recent glaciation, the Weichselian period, took place after the Eemian period, approximately between 120,000 and 10,000 yrs BP. The Last Glacial Maximum (LGM) in Iceland is estimated between 20,000 and 17,000 yrs BP (Van Vliet Lanöé *et al*., 2006) with an ice cap thickness up to 2000m in the centre of the island (Norddahl & Pétursson, 2005). The glacial extent during the LGM is still controversial. Some authors suggest an ice cap extent until the shelf break (Olafsdottir, 1975; Norddahl & Pétursson, 2005; Hubbard *et al.* 2007) and others authors (Van Vliet-Lanöé *et al*. 2006) suggest the ice cap was much less extended. Very abundant precipitation in the southern part of the island must have been responsible for the location in south Iceland of the thickest part of the ice sheet as it is nowadays (Bourgeois *et al*. 2000).

Flowing pattern of the ice cap

An ice cap flows both by internal creep and by sliding on its bed. After the ice cap has vanished, the sliding component is recorded in striaes, flutes and drumlins visible on the deglaciated bed. We used these geomorphic features to reconstruct the pattern of basal sliding of the Weichselian ice cap. Because the creep component has been neglected, the overall flow was probably slightly different from the proposed reconstruction. We used measured glacial striae described in the literature and observed in the field. These data have been combined with geomorphic features (glacial valleys, nunataks, flutes, drumlins, *roches moutonne´es*) observed in the field, on SPOT images, and on a digital elevation model. We assumed that all these features were Weichselian in age, i.e. that the last glaciation had obliterated older small-scale landforms. We also assumed that the landforms used in the reconstruction could be considered synchronous. This assumption is reasonable at our working scale. Indeed, the preserved moraines corresponding to the successive stages of déglaciation can be split into two consistent sets: successive end moraines at the front of the ice cap are concentric and nearly orthogonal to striae, whereas successive lateral moraines along the flanks of valleys formerly occupied by outlet glaciers are parallel to striae. This arrangement shows that no major changes in the ice flow lines occurred during the deglaciation.

First, the divides of the main ice cap were drawn from the directions of glacial striae in central Iceland. Second, a series of sliding lines were drawn at regular intervals from the ice divides towards the sea, following the directions of striae. These lines represent ice flow trajectories, but they do not reflect the amount of ice flowing at each place because the distribution of precipitation has not been taken into account in the reconstruction. In coastal areas, the ice cap was assumed to divide into outlet glaciers flowing between nunataks that behaved as emerging obstacles. We considered the flow of glaciers on the nunataks independently from the flow of the main ice cap: we assumed that valley

glaciers flowed radially away from nunatak summits, either up to the sea, or until they joined outlet glaciers of the main ice cap.

Results

This reconstruction outlines a four ice divides (Fig. 2): a first one extending from Reykjanes to Langjokull, a second one from Myrdalsjokull to Melrakkasletta, at North with and branch and a fourth one extending from Hofsjokull to Trollaskagi. Other ice divides were located on Vestfirdir and Snaefellsnes peninsulas. Between the ice divides, the flow was channelled into streams. Between ID1 and ID3, an ice Stream flowed southwestwards along the eastern flank of the WVZ. Between ID2 and ID4, two ice streams flowed northwards along the NVZ. Flow lines converging towards these ice streams show that they drained the major part of the ice cap and imply higher velocities relative to the surrounding ice.

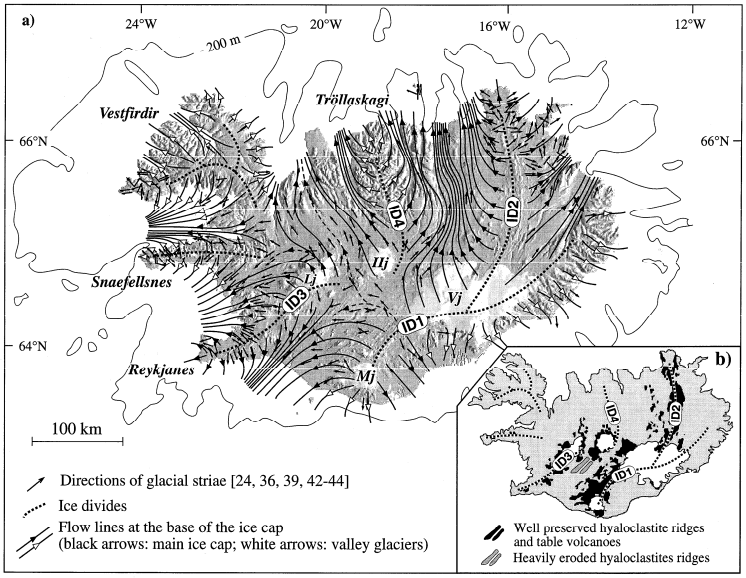

Figure 2: Reconstruction of the pattern of basal sliding of the ice cap. The main ice cap (black arrows) has been separated from the valley glaciers flowing through coastal mountains (white arrows). In addition to the two ice divides formerly recognised on the eastern flank of the Neovolcanic Zone (ID1 and ID2), two other ice divides lying on its western flank are shown (ID3 and ID4). Between the ice divides, the flow is channelled into streams. Two of them are located in the NVZ, another one is located on the eastern flank of the WVZ. (b) Comparison of the location of preserved subglacial volcanic edifices with the location of the ice divides in the reconstruction. Subglacial volcanic edifices have been preserved preferentially beneath ice divides. They are either nearly absent, or heavily eroded in areas occupied by ice streams.

There is a striking correlation, everywhere in Iceland, between the location of well preserved subglacial hyaloclastite ridges and the location of the ice divides in the reconstruction (Fig. 2). On the other hand, in areas occupied by ice streams in the reconstruction, hyaloclastite ridges are either nearly absent in north volcanic zone or heavily eroded (Hreppar area). Ice flows away from the ice divide, leavingat its base a wedge of stagnant ice. If a subglacial eruption occurs within this preserved area, its products will stay in situ and will pile up from one eruption to another. On the other hand, extensively fragmented and unconsolidated products erupted subglacially in a site far away from the ice divide will be easily dislocated, incorporated to the moving ice, and continuously removed in the time lap between eruptions.

Tectonic implications

Once the effect of glacial removal has been subtracted, the arrangement of subglacial volcanic edifices appears clearly. Similarly to post-glacial eruptive fissures, hyaloclastite ridges are gathered in swarms associated with central volcanoes located in the Neovolcanic Zone (Fig. 3). Because the North volcanic zone was occupied by an ice stream, subglacially erupted volcanics have been actively removed by fast ice flow. Few relics remain at the present time, except in table and central volcanoes where magmatic supply was sufficiently frequent to counteract removal by ice flow. Products of subglacial fissure eruptions have been preserved in the Fjallgardar Ridge, located beneath a former ice divide. The area where subglacial volcanic édifices have been preserved is 90 km wide, including table volcanoes of the NVZ and hyaloclastite ridges of the Fjallgardar Ridge. In contrast, the currently active NVZ in only 50 km wide (Fig. 3). In southern Iceland, present-day activity is restricted to the WVZ and EVZ, whereas hyaloclastite ridges give evidence of subglacial volcanic activity between them. Subglacial activity has been recorded in a 150 km wide zone, whereas the cumulative width of the WVZ and EVZ is only 100 km.

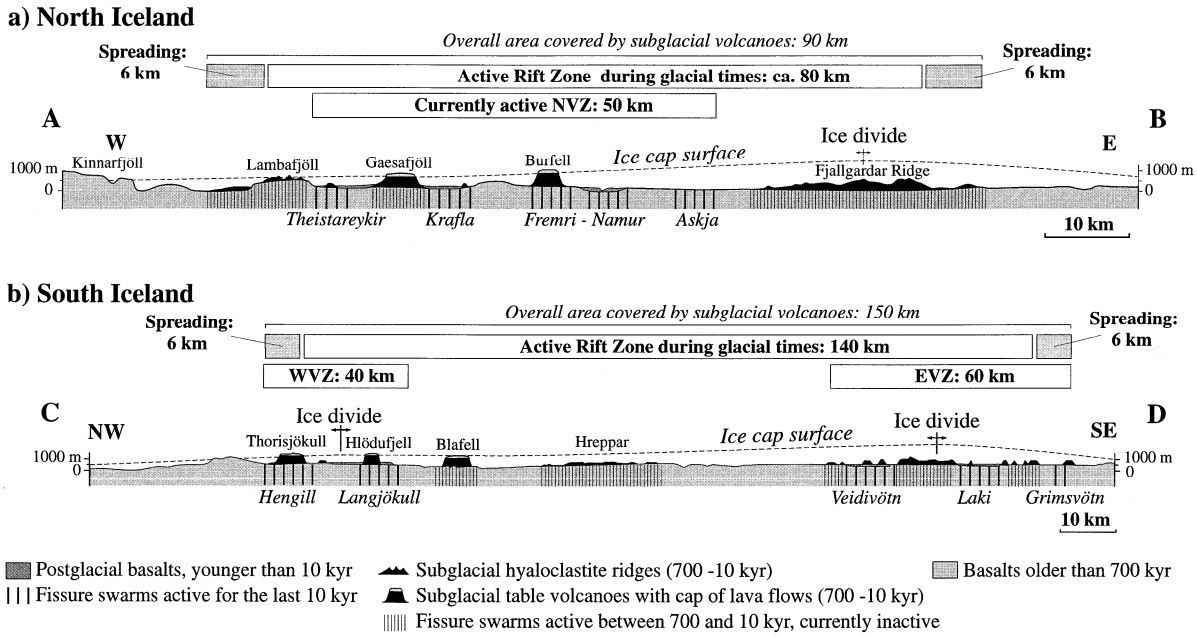

Figure 3: Cross-sections across the Neovolcanic Zone (Vertical exaggeration: 2). The surface of the former ice cap is drawn schematically. (a) Northern Iceland. Hyaloclastite ridges have been preserved beneath the Fjallgardar ice divide. Table volcanoes (Gaesafjoll, Burfell) have been preserved in the NVZ. Subglacial volcanic activity has been recorded in a 90 km wide region. The currently active fissure swarms (Theistareykir, Krafla, Fremri-Namur and Askja) affect a 50 km wide area only. (b) Southern Iceland. Subglacial volcanic edifices have been preserved beneath ice divides in the WVZ and EVZ. They have been eroded in the Hreppar area. Subglacial volcanic activity has been recorded in a 150 km wide area, whereas the cumulative width of the WVZ and EVZ is only 100km. Lithospheric spreading rate (1.8 cm=yr, full rate) can account for only 12 km of this width discrepancy. Either fissure swarms have wandered around their current location for 700 kyr, or the active rift zone has narrowed at the deglaciation.

DISCUSSION

External parameters controlling the direction and velocity of flow in an ice sheet are (1) the distribution of precipitation at the surface, (2) the bed topography, (3) the thermal conditions at the base and (4) the subglacial lithology. We now review these parameters in Iceland in order to determine how they can explain the reconstructed flow patterns and velocities.

Comparison of reconstructed ice flow lines with the map of geothermal heat flux shows that positions of main ice routes correlate with locations of geothermal anomalies (Fig. 4). The most probable ice streams (Skjalfandi, AxarfjoÈrdur and Hvita) were located in or close to the Neovolcanic Zone, where the geothermal heat flux reaches maximal values. A striking feature is the parallelism between the ice divides and the Neovolcanic Zone: ID1 and ID2 are on its eastern flank, ID3 and ID4 are on its western flank. This spatial correlation suggests that the dynamics of the ice sheet was partly controlled by the geothermal heat flux. Enhanced ice melting above geothermal anomalies probably involved intense water production at the base of the ice sheet, thus favouring lubrication of the bed and controlling the location of major ice routes and ice streams.

CONCLUSIONS

Flow lines of the Weichselian ice sheet in Iceland have been reconstructed on the basis of glacial directional features. The reconstruction reveals the existence of channels of preferential flow and of fast-flowing ice streams. Mega-scale lineations and pervasively deformed subglacial till have been well preserved on the bed of some ice streams. Both in northern and in southern Iceland, the extent of the hyaloclastite ridges is greater than the extent of the currently active fissure swarms. This discrepancy suggests either continuous wandering of the volcanic activity from fissure swarm to fissure swarm for the last 700 kyr, or narrowing of the active rift zone and=or decrease of the length of the active part of the fissure swarms at the end of the last glaciation.

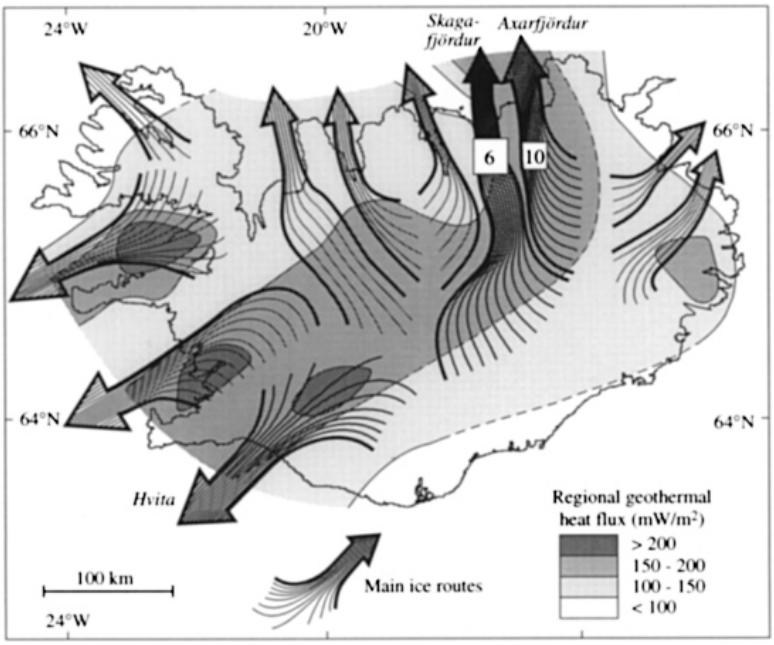

Figure 4: Correlation between flow patterns of ice sheet and geothermal heat flux. In order to avoid perturbations caused by circulation of warm water, the map of regional heat flux is based on values measured at carefully chosen sitesawayfrom hydrothermal areas (Flovenz and Saemundsson, 1993). The coincidence between location of main ice routes and location of thermal anomalies is striking.

References

Bourgeois, O., Dauteuil, O. & Van Vliet-Lanoët, B. 2000. Geothermal control on flow patterns in the Last Glacial Maximum ice sheet of Iceland. *Earth Surface Processes and Landforms* **25**, 59-76.

Bourgeois, O., Dauteuil, O. & Van Vliet-Lanoë, B. 1998. Subglacial volcanism in Iceland: tectonic implications. *Earth and Planetary Science Letters* **164**(1-2), 165-178.

Darbyshire, F. A., White, R. S. & Priestley, K. F. 2000. Structure of the crust and uppermost mantle of Iceland from a combined seismic and gravity study. *Earth and Planetary Science Letters* **181**(3), 409 - 428.

Dauteuil, O. & Bergerat, F. 2005. Interactions between Magmatism and Tectonics in Iceland: a review. **18/1**, 1-9.

Demets, C., Gordon, R. G., Argus, D. F. & Stein, S. 1994. Effect of recent revisions to the geomagnetic time scale on estimates of current plate motions. *Geophysical Research Letters* **21**, 2191-2194.

Einarsson, M. A. 1988. Precipitation in southwestern Iceland. *Jökull* **38**, 61-67.

Hubbard, A., S., S., Dugmore, A., Norddahl, H. & Pétursson, H. G. 2006. Quaternary Science Reviews. **25**(2283-2296).

Norddahl, H. & Petursson, H. G. 2005. Relative sea-level changes in Iceland: new aspects of the Weichselian deglaciation of Iceland. *Developments in Quaternary Science. Modern Processes and Past Environments.*(5), 25-78.

Olafsdottir, T. 1975. A moraine ridge on the Iceland shelf, west of Breidafjördur (in Icelandic with english summary). *Natturufraedingurinn* **45**, 31-36.

Van Vliet Lanoe, B., Gudmundsson, A., Guillou, H., Duncan, R. A., Genty, D., Ghaleb, B., Gouy, S., Récourt, P. & Scaillet, S. 2006. Limited glaciation and very early deglaciation in central Iceland. Implications for climate change. *Comptes Rendus Geoscience* **229**, 1-12.

LONG TERM AND RECENT CLIMATE CHANGES RECORDED IN NORTH ATLANTIC OCEANIC ARCHIVES AROUND ICELAND

Frédérique EYNAUD
Université Bordeaux I, Laboratoire EPOC , UMR CNRS 5805, Avenue des facultés , 33405 Talence cedex – France

Abstract

This contribution will compile paleoceanographic and paleoclimatic works which, over the last decades, provided major insights in our understanding of the Earth's climate natural variability and the underlying forcing mechanisms. A focus will be made on peri-icelandic marine records which document the climatic pace at different time-scales and are supported by multiproxy evidences. A special attention to the link in between the ocean and the cryosphere will be done.

1. Interest of the Icelandic sector

1.1. A "hot spot" for oceanographers!

The North Atlantic Ocean has always been the focus of extensive researches regarding modern and past oceanographic processes. This ocean is actually one of the world key areas to tackle the question of the thermohaline conveyor (THC) efficiency throughout time, as it houses important components of this major climatic artery (e.g. Broecker, 1997; Rahmstorf, 1997, Broecker, 1999). Iceland represents a topographic barrier at the confluence of the Greenland, Iceland and Norwegian seas (GIN seas, also called the Nordic seas), and major surface and deep gateways thus bracket this domain.

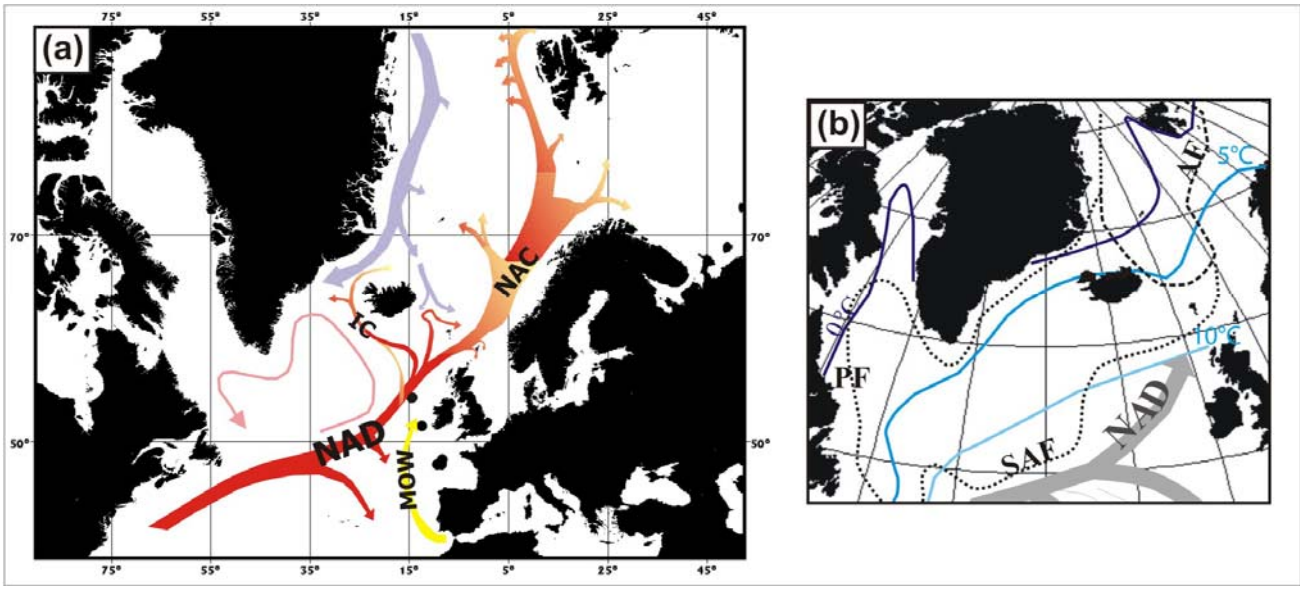

Figure 1 : (a) Schematic view (after Blindheim et al., 2000; McCartney and Mauritzen, 2001) of the North Atlantic major surface currents (NAD, North Atlantic Drift; NAC, Norwegian Atlantic Current; IC, Irminger Current) and the intermediate Mediterranean Outflow Water current (MOW). Source: Eynaud et al. (2007)
(b) Modern sea-surface hydrographic conditions of the North Atlantic Ocean. The SST isotherms are from Tchernia, 1978 (SST annual mean). Dotted lines locate the major hydrographic fronts: PF: Polar Front, AF: Arctic Front, SAF: Sub-Arctic Front, after Dickson et al. (1988). Source: Eynaud et al. (2009).

In the vicinity of Iceland, the duality of the cold currents originating from the Arctic basin versus the northward warm Atlantic inflow (Figure 1a) is plainly expressed at the surface and generates persistent hydrographic structures (Figure 1b) which constrain the distribution of the different water masses. This has direct repercussion on the planktonic living populations and, of course, on their fossil remains through sedimentary archives. Contrasted biological assemblages thus relay throughout time, from the seasonal time scale of the modern ocean, to the orbital scale of the Quaternary sediments.

Deep currents aliment the deposit of giant edifices along the complex bathymetry and physiography of this area (Figure 2). In the South Icelandic basin, especially, the Gardar Drift has

furnished high quality sedimentary sequences that helped to better constrain the long term and recent climatic changes of the north hemisphere. Sedimentary archives around Iceland furthermore benefit of invaluable chronostratigraphical indicators with the repetitive deposits of ash layers which constitute excellent age tie-points for paleoceanographers.

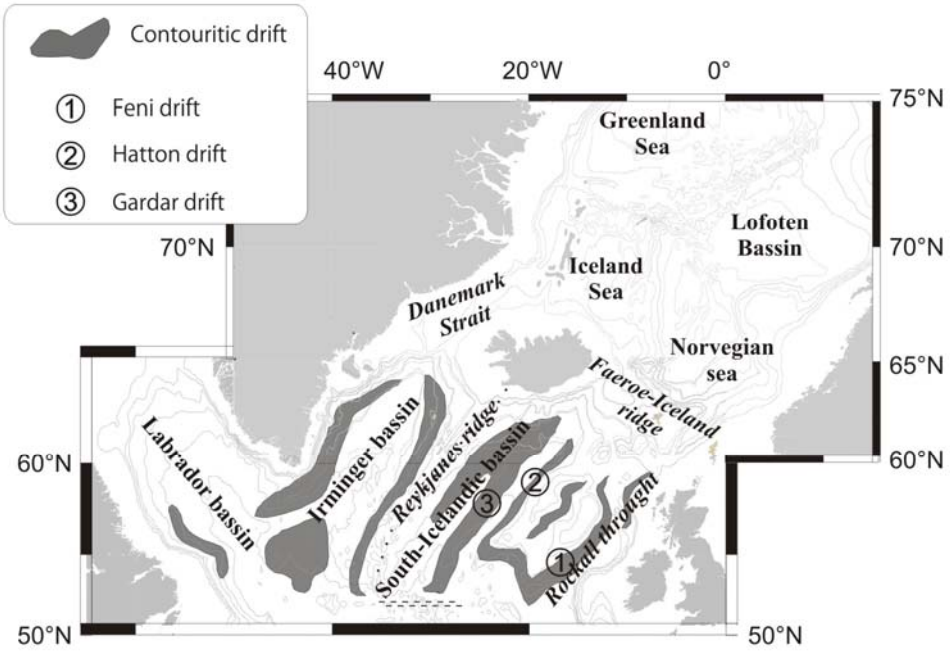

Figure 2 : Major physiographic provinces around Iceland (after Faugères et al., 1999).SOURCE : Eynaud PhD thesis 1999

1.2. A "hot spot" for paleoclimatologists!

One of the major finding in Paleoclimatology over the last decades has been revealed both in ice cores and in sediment cores with the evidence of large variations of air temperature over millennial and sub-millennial periods, coupled to major North-Atlantic hydrological changes (Dansgaard et al., 1993, Figure 3).

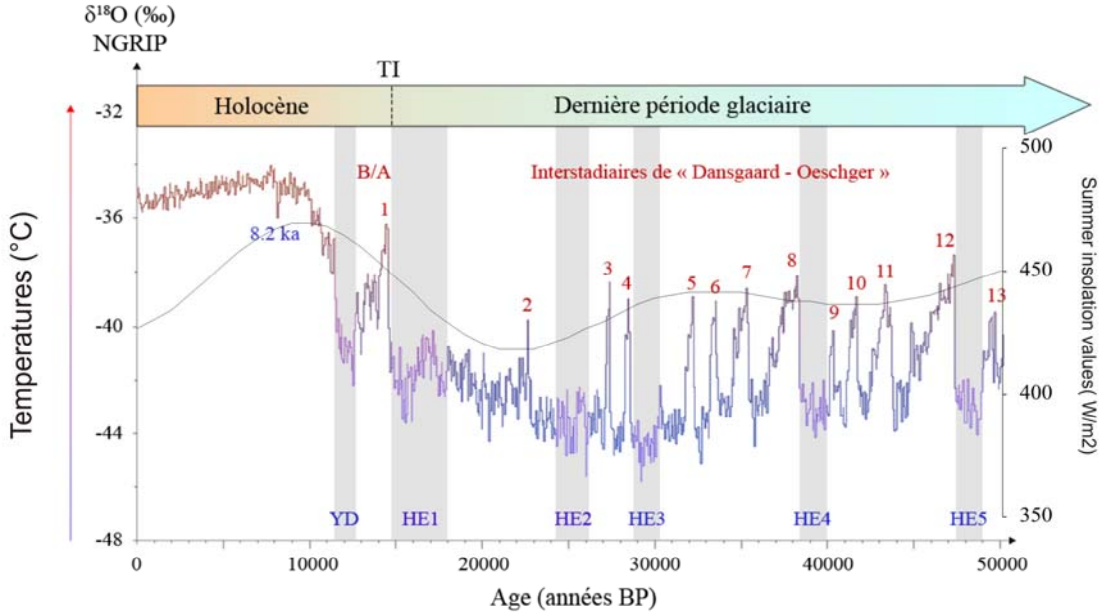

Figure 3 : Climatic evolution of the last 50 ka as depicted by the Greenland ice core record (^{18}O NGRIP) compared to the summer insolation values at 65°N. Numbers on the Figure identify the Dansgaard-Oeschger warm interstadials. HEs : Heinrich events, B/A = Bölling-Alleröd oscillation, YD = Younger Dryas oscillation, TI = Terminaison I. SOURCE : Penaud, A. PhD thesis 2009.

These rapid climatic oscillations, the so called Dansgaard–Oeschger (D–O) events, occur as cyclic but non-periodic phenomenon and represent abrupt and drastic flips of the climate system. They are major challenges regarding our comprehension of the Earth's climate variability and stability. The abrupt cold excursions, i.e. stadial events (Dansgaard et al., 1993) or Heinrich events (Heinrich, 1988), which occurred during the last glacial period (Figure 3), provide excellent archives of Pleistocene rapid climatic transitions. They, furthermore, raised major questions about the pace of the natural system.
The extreme Heinrich events result from a massive calving of icebergs in relation to the sudden collapse of the peri-arctic ice-sheets during the last glacial period (e.g. Heinrich, 1988; Bond et al., 1993, Hemming, 2004). They took place at the end of a saw-tooth shaped cooling cycle of 4 successive stadials/interstadials (e.g. Bond cycles: Bond et al., 1993). However, the triggering of these events is still a matter of debate, as they imply complex mechanisms linking ice-sheet, atmosphere and ocean dynamics. Their impact was recognized worldwide (e.g. Leuschner and Sirocko, 2000; Wang et al., 2001) and each of the Earth's surface reservoirs, i.e. the cryosphere, atmosphere, oceans, and biosphere, was affected. Some of the most severe Heinrich events impacted dramatically on the North Atlantic's overturning circulation (e.g. Zahn et al., 1997; Curry et al., 1999; Roche et al., 2004). These events potentially constitute catastrophic analogues of modern or near-future ice-sheet (Antarctic especially) collapses in the context of global warming.

Regarding its geographical position, the Icelandic sector appears as a strategic sector to study this kind of climatic variability. This is also true regarding long term timescales (Figure 4), as Iceland is surrounded by major gateways which have played a crucial role in the evolution of the climate of the last million years.

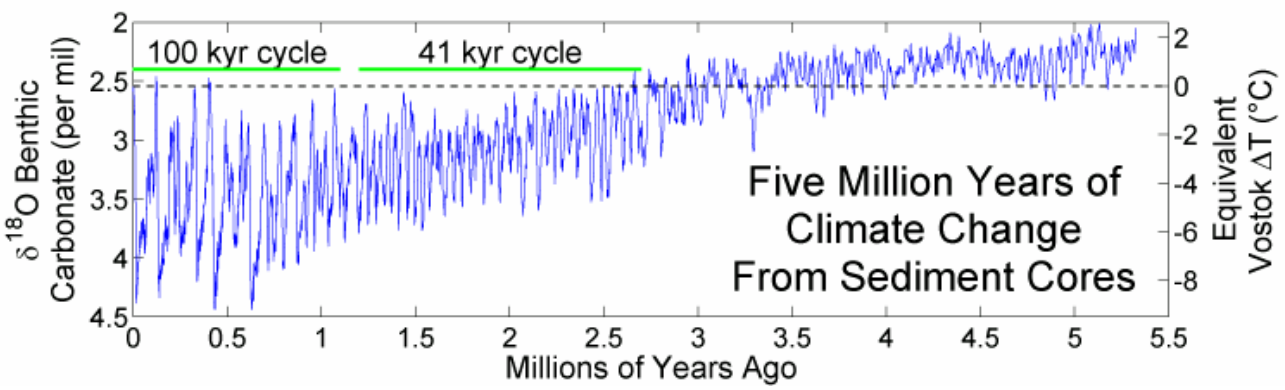

Figure 4 : Robert Rohde's Temperature Record Series over the last 5.5 millions years.

Several questions are raised on long term climate evolution, they are (1) the origin of the transition, approximately 4 million years ago, of Earth's climate into a state characterized by significant Northern Hemisphere (NH) continental glaciation; (2) the link in between the pace of Earth's climate and the orbital parameters (3) the shift at 900 ka from a 41-kyr obliquity cycle towards a 100 ka quasi-periodic cycle that has since dominated the Earth's climate history (e.g. Raymo, 1998). All these questions can be treated from an "Icelandic point of view"!

2. Some critical illustrations of the long term and recent climate changes around Iceland

2.1. About the THC variability

Thanks to the focus that has been put on giant contourite drifts, themselves built by the deep components of the THC, a significant number of sequences now exist in the south Icelandic basin, which furnish excellent documents of the THC variability throughout time. These sequences further served as supports of data compilation to better monitor paleoclimatic and paleoceanographic evolutions at the North Atlantic basin scale and thus represent excellent time –constrained records, tied to ice-core stratigraphies through regional climatic and ash layer tie-points and supported by traditional marine stratigraphic ($\delta^{18}O$) and dating techniques (^{14}C). This was the case, at suborbital time-scales, with the construction of the North Atlantic geomagnetic paleointensity stack (NAPIS, Laj et al., 2000; 2002; Stoner et al., 2002). In the same way, the "famous 'LR04'' stack of benthic $\delta^{18}O$ Pliocene-Pleistocene records, compiled by Lisiecki and Raymo (2005), also benefits for the North Atlantic sector from sequences retrieved in the south Icelandic basin.

These efforts contributed to the construction of a robust picture of the THC variability for the last

75 ka (Figure 5). Merged to the simulation works, they all showed its extreme sensitivity to freshwater inputs and challenged our understanding of abrupt climate changes, a major feature to prescribe its future evolution.

This is on this dynamic component that we will focus part of the discussion. The THC variability, as deduced from peri-Icelandic marine archives, will then be documented at different time-scales (from the sub-millennial one to the orbital one), furthermore using the largest set of paleoceanographic proxies yet available.

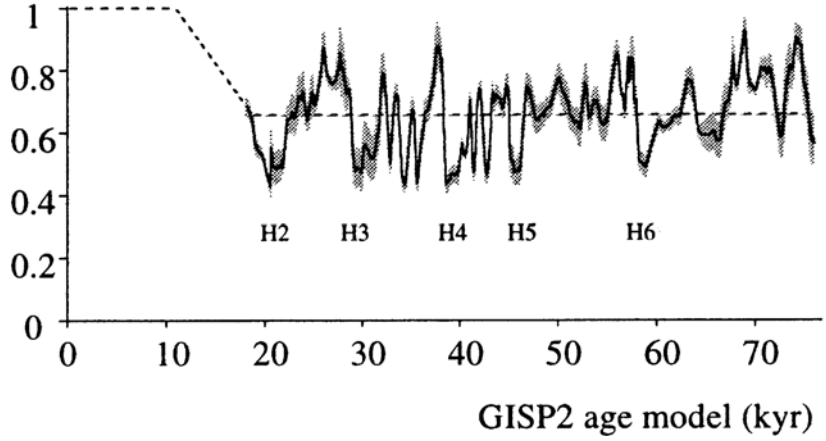

Figure 5 : Schematic profile of North Atlantic deep-water (NADW) changes in the past 75 kyr (normalized to unity for modern times) based on ARM (anhysteretic remanent Magnetization) results from North Atlantic cores. Laj et al. (2002).

2.2. Migration of the polar front and its relation to icebergs surges : from glacial to modern features

Intimely coupled to the dynamic of the THC is the evolution of the latitudinal position of the Polar Front (PF). At Present, the PF closely follows the Greenland and eastern Canadian continental margins (Figure 1b). In the ocean it is defined as a physical oceanographic structure with high temperature and salinity gradients, which separates two different surface-water masses: the relatively warm, high-salinity Atlantic Water, and the cold low-salinity modified Polar Water carried southwards by the East and West Greenland and Labrador currents (Holliday et al., 2007). This front constitutes a strong ecological barrier in the North Atlantic Ocean and also physically constrains sea-ice and iceberg drifting. The latitudinal migration of the Polar Front as south as 40°N during late Pleistocene cold events has been documented by numerous studies (e.g. McIntyre et al. 1976; Ruddiman and McIntyre, 1981; Duprat, 1983; Bard et al., 1987; Abrantes et al., 1998). We will build an inventory of its impact over Icelandic and peri-icelandic environments and paleoenvironments.

References

Abrantes, F., J. Baas, H. Haflidason, T. Rasmussen, D. Klitgaard, N. Loncaric, and L. Gaspar (1998), Sediment fluxes along the northeastern European Margin: Inferring hydrological changes between 20 and 8 kyr, Marine Geology, 152, 7-23.

Bard, E., M. Arnold, P. Maurice, J. Duprat, J. Moyes, and J.C. Duplessy (1987), Retreat velocity of the North Atlantic polar front during the last deglaciation determined by 14 C accelerator mass spectrometry, Nature, 328, 791–794.

Blindheim, J., V. Borokov, B. Hansen, S.A. Malmberg, W.R. Turrell, and S. Osterhus (2000), Upper layer cooling and freshening in the Norwegian Sea in relation to atmospheric forcing, Deep-Sea Research Part I, 47, 655-680.

Bond, G., W. Broecker, S. Johnsen, J. McManus, L. Labeyrie, G. Jouzel, and G. Bonani (1993), Correlations between climate records from North Atlantic sediments and Greenland ice, Nature, 365, 143-147.

Broecker, W. (1997). Thermohaline Circulation, the Achilles Heel of Our Climate System: Will Man-Made CO2 Upset the Current Balance? Science 278, 1582 -1588.

Broecker, W. (1999). What if the conveyor were to shut down? GSA Today 9, 1–6.

Curry, W. B., T. M. Marchitto, J. F. McManus, D. W. Oppo, and K. L. Laarkamp (1999), Millennial-scale changes in ventilation of the thermocline, intermediate, and deep waters of the Glacial North Atlantic, in Mechanisms of Global Climate Change at Millennial Time Scales, edited by P. U. Clark, R. S. Webb and L. D. Keigwin, AGU, Washington, D.C., pp. 59–76.

Dansgaard, W., S. J. Johnsen, H. B. Clausen, D. Dahl-Jengen, N. S. Gundestrup, C. U. Hammer, C. S. Hvidberg,

J. P. Steffensen, A. E. Sveinbjörnsdottir, J. Jouzel, and G. Bond (1993), Evidence for general instability of past climate from 250-kyr ice-core record, Nature, 364, 218-220.

Dickson, R. R., J. Meincke, S.-A. Malmberg and A. J. Lee (1988), The "Great Salinity Anomaly" in the Northern North Atlantic 1968-1982, Prog. Oceanog., 20, 103-151.

Duprat, J. (1983), Les foraminifères planctoniques du Quaternaire terminal d'un domaine péricontinental (Golfe de Gascogne, Cote Ouest Ibérique, Mer d'Alboran) Ecologie-Biostrat.., PhD Univ. Bordeaux I, 177 pp.

Faugères, J.-C., Stow, D.A.V., Imbert, P., Viana, A., 1999. Seismic features diagnostic of contourite drifts. Mar. Geol. 12, 1–38.

Eynaud, F. (1999), Kystes de Dinoflagellés et Evolution paléoclimatique et paléohydrologique de l'Atlantique Nord au cours du Dernier Cycle Climatique du Quaternaire, PhD thesis, 291 pp. University of Bordeaux 1

Eynaud, F., Zaragosi S., Scourse J., Mojtahid M., Bourillet J-F., Hall I. R., Penaud A., Locascio M., Reijonen A., 2007. Deglacial laminated facies on the NW European continental margin: the hydrographic significance of British-Irish Ice Sheet deglaciation and Fleuve Manche paleoriver discharges. G3, v. 8, DOI:10.1029/2006GC001496

Eynaud F., L. de Abreu, A. Voelker, J. Schönfeld, E. Salgueiro, J.-L. Turon, A. Penaud, S. Toucanne, F. Naughton, M.-F. Sanchez-Goñi, B. Malaizé, and I. Cacho: Position of the Polar Front along the western Iberian margin during key cold episodes of the last 45 ka, Geochem. Geophys. Geosyst., 10, Q07U05, doi:10.1029/2009GC002398. Highlight dans Nature Geoscience 2, (30 June 2009) doi:10.1038/ngeo575

Heinrich, H. (1988), Origin and Consequences of Cyclic Ice Rafting in the Northeast Atlantic Ocean during the Past 130,000 Year, Quaternary Research, 29, 142-152.

Hemming, S. R., (2004), Heinrich events: Massive late Pleistocene detritus layers of the North Atlantic and their global climate imprint, Reviews of Geophysics, 42, RG1005 1-43.

Holliday, N.P., Meyer, A., Bacon, S., Alderson, S.G. and B. de Cuevas (2007), Retroflection of part of the east Greenland current at Cape Farewell, Geophysical Research Letters, 34, 7, L07609

Laj, C., Kissel C., Mazaud A., Channell J.E.T., and J. Beer (2000), North Atlantic palaeointensity stack since 75 ka (NAPIS-75) and the duration of the Laschamp event, Philosophical Transactions of the Royal Society A: Mathematical, Physical and Engineering Sciences, 358 (1768), 1009-1025.

Laj, C., Kissel C., Mazaud A., Michel E., Muscheler R., and J. Beer (2002) Geomagnetic field intensity, North Atlantic Deep Water circulation and atmospheric Δ14C during the last 50 kyr, Earth and Planetary Science Letters 200: 177-190

Leuschner, D. C., and F. Sirocko (2000), The low-latitude monsoon climate during Dansgaard-Oeschger cycles and Heinrich Events, Quaternary Science Reviews, 19, 243-254.

Lisiecki, L. E., Raymo, M. E., 2005. A Pliocene-Pleistocene stack of 57 globally distributed benthic δ18O records. Paleoceanography 20, PA1003, doi:10.1029/2004PA001071.

McCartney, M. S., and C. Mauritzen (2001), On the origin of the warm inflow to the Nordic Seas, Progress in Oceanography, 51, 125-214.

McIntyre, A., N.G. Kipp, A.W.H. Be, T. Crowley, T. Kellogg, J.V. Gardner, W. Prell, and W.F. Ruddiman (1976), Glacial North Atlantic years ago: a CLIMAP reconstruction. In: Cline, R.M., Hays, J.D. (Eds.), Investigation of Late Quaternary Paleoceanography and Paleoclimatology, Mem. 145. Geol.Soc.Am, Boulder, pp. 43-76.

Penaud A. (2009), Interactions climatiques et hydrologiques du système Méditerranée/ Atlantique au Quaternaire, PhD thesis, 331 pp. University of Bordeaux 1

Raymo, M.E., 1998. Glacial puzzles. Science 281, 1467–1568.

Rahmstorf, S., 1997: Risk of sea-change in the Atlantic. Nature 388, 825-826.

Roche, D., D. Paillard, and E. Cortijo (2004), Constraints on the duration and freshwater release of Hein rich event 4 through isotope modelling, Nature, 432, 379-382.

Robert Rohde's Temperature Record.
http://www.globalwarmingart.com/wiki/Image:Short_Instrumental_Temperature_Record.png Ruddiman and McIntyre, 1981;

Stonner, J.S., C. Laj, J.E.T. Channell, C. Kissel, South Atlantic and North Atlantic geomagnetic Paleointensity Stacks (0-80ka): implications for inter-hemispheric correlation, Quaternary Sci. Reviews 21: 1141–1151

Tchernia, P. (1978), Océanographie Régionale, Description Physique des Océans and des Mers, In: Ecole Nationale Supérieure des Techniques Avancées, Paris, 257 pp.

Wang, Y. L., H. Cheng, R. L. Edwards, Z. S. An, J. Y. Wu, C.-C. Shen, and J. A. Dorale (2001), A High-Resolution absolute-dated Late Pleistocene monsoon records from Hulu Cave, China, Science, 294, 2345-2348.

Zahn, R., J. Schönfeld, H.-R. Kudrass, M.-H. Park, H. Erlenkeuser, and P. Grootes (1997), Thermohaline instability in the North Atlantic during meltwater events: stable isotope and ice-rafted detritus records from core SO75-26KL, Portuguese margin, Paleoceanography, 12, 696-710.

RECORD OF GLACIATIONS OFF THE EAST GREENLAND COAST OVER THE LAST 400 KYR: SM-ND ISOTOPIC SIGNATURE OF MARINE CLAYS

Nathalie Fagel[1]
in collaboration with Claude Hillaire-Marcel[2]

[1] AGEs, Argiles, Géochimie et Environnement sédimentaires
Department of Geology, University of Liège, B18, Allée du 6 Août, B-4000 Liège, Belgium. Tel. +32.4.366.2209; Fax. +32.4.366.2029; e-mail: nathalie.fagel@ulg.ac.be
[2] GEOTOP, UQAM, Montréal, Canada, chm@uqam.ca

Abstract

We use Nd isotope signature of the clay-size fractions of sediments from the Southern Greenland rise to track deep current changes over the last climate cycle. Fine particle supplies to the Labrador Sea by Western Boundary UnderCurrent (WBUC) were strongly controlled by proximal ice-margin erosion and thus echoed the glacial stage intensity. In contrast, distal WBUC-controlled inputs from NE Atlantic have been less variable, except for a marked increase in surface-sediments that suggests unique modern conditions

Introduction

The production of deep water in the North Atlantic is one of the puzzle in understanding the oceanic influence in climate changes. It is assumed that glacial to interglacial fluctuations in the exportation of North Atlantic Deep Water (NADW) to the Southern Ocean contributed to variations in atmospheric CO_2 concentrations during the Pleistocene. North Atlantic paleoceanography has been mainly investigated for the Last Glacial cycle, an interval may be not representative for the whole Pleistocene (Raymo et al., 2004). Most paleoceanographic reconstructions derived from biogenic proxies that are sensitive to ocean ventilation. Sedimentary abiotic components like magnetic properties (Kissel et al., 1997; Snowball and Moros, 2003), clay mineral assemblages (Bout-Roumazeilles, 1995; Fagel et al., 1997) or long period isotopic composition of clays (Bout-Roumazeilles et al., 1998; Frank et al., 2001; Fagel et al., 1999, 2004) were less investigated, even they bring indirect information on past circulation tracing the origin of the particles driven by the water masses. In this work, forty Sm-Nd isotope signatures were measured on the fine fraction of one sediment core (ODP Site 646) drilled in Labrador Sea, off Southern Greenland. Our aim is to record for the last four glacial/interglacial cycles (G-I) the relative contribution of fine particle supplies carried by the North Atlantic deep components into the Labrador Sea.

Material and method

Site 646 (58°12.56'N, 48° 22.15'W, water depth: 3460 m) was drilled in the Labrador Sea during Ocean Drilling Programme Leg 105 (Figure 1). Site 646 is located off Greenland on the upper northern flank of the Eirik Ridge sediment drift, below the high velocity axis of the WBUC. The WBUC drives NADW components overflowing the Denmark-Iceland-Faroe-Shetland sills (NSOW, ISOW) and the Denmark Strait Overflow Water (DSOW)] as well as a fraction of the Davis Strait Overflow, into a deep gyre in the Labrador Sea. The Labrador Sea Water (LSW) occupies the water column above NADW water masses. Surface waters are under the subpolar West Greenland Current (WGC) influence.

Sm-Nd isotopic signatures were determined in forty samples : we select 5 samples from each interglacial and glacial intervals. Sm-Nd concentrations and isotopic ratios were measured on the carbonate-free clay-size fraction. The < 2 μm fraction is the sedimentary faction that is the least affected by ice rafting and consequently more representative of the suspended particulate load of deep currents. The abundance of this clay-size fraction is slightly higher in glacials (mean = 6% ± 0.9) than in interglacials (mean = 3.7% ± 1.4). Sm-Nd data were measured using a VG-Thermal Ionisation Mass Spectrometer at GEOTOP.

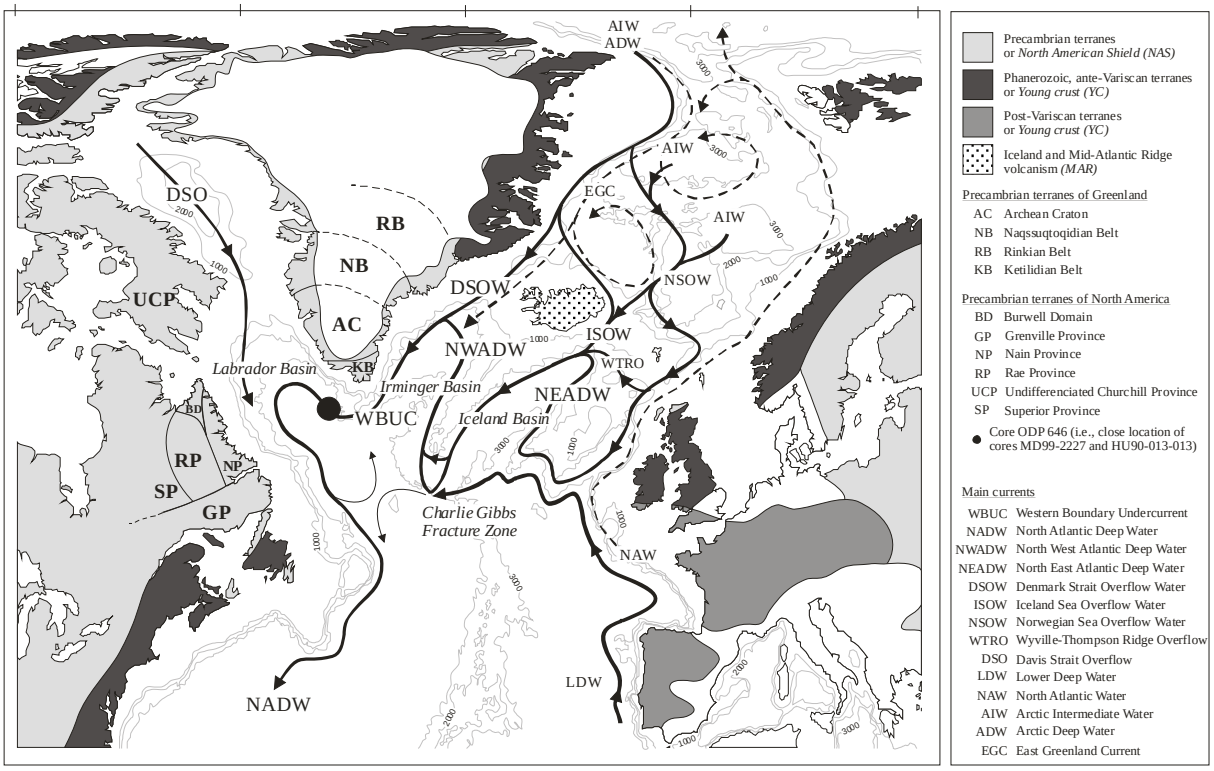

Figure 1 - Location of Site 646, Leg 105 ODP, Labrador Sea. The arrows indicate the pathways of deep or intermediate (plain line) and surface (broken line) currents. The structural terranes of the continental crust adjacent to the North Atlantic are indicated by grey levels and Iceland volcanism by dots (Fagel et al., 2004).

Radiogenic isotopic signature of marine clays: an indirect tracer for deep circulation

Goldstein and O'Nions (1981) showned that detrital clays in marine sediments retain their Nd isotopic signature throughout the sedimentary cycle, that is, from continental weathering, through sediment transport to diagenesis. The radiogenic isotopic signature of the detrital sedimentary fraction can therefore be used to trace sediment provenance. In marine sediments crustal–derived material, mainly carried by rivers and dispersed by oceanic currents, is mixed with volcanically-derived material from oceanic crusts. In order to constrain sedimentary mixing, we must identified and characterized the isotopic composition of the potential geological sources of particles to the North Atlantic basins. Based on literature compilation (Innocent et al., 1997 ; Fagel et al., 2004), three main sources contribute to sediment mixture at core location: an old Precambrian crustal material from Canada and Greenland (NAS) ; a Paleozoic or younger crustal material from East Greenland, Europa, and Scandinavia (YC) and ; a volcanic source from Iceland, Faeroe and Reykjanes Ridge (MAR) (Figure 1). Based on Sm-Nd signatures, the relative contribution of each source will be estimated in each clay fraction. Then evolution of sedimentary mixings will be used to reconstruct past deep circulation changes.

Results and interpretation

On average for the last 360 kyr, the clay fractions from the glacial stages are characterized by the lowest Nd ratios (i.e., unradiogenic composition with more negative mean ε Nd = –15.7) than the fine material from the interglacial stages (mean ε Nd –11.5) (Figure 2). We calculated a mixing grid based on different proportions of the three end members using a standard Sm-Nd mixing pattern (Faure 1986). The mean Sm/Nd signatures for glacial intervals OIS2, OIS6 and OIS10 lay along a mixing line that is parallel to the NAS-MAR axis. Supplies characterized by young crustal Sm/Nd signature remain more or less constant (~40%) between those three glacial intervals; whereas mean volcanic contribution increases, relatively to old craton material, from OIS 2 to OIS6 and, OIS6 to OIS10. The glacial OIS8 displays a mean Sm/Nd signature close to the interglacials OIS1, OIS5 and OIS9. As an exception, the mean OIS7 value plots along the YC-MAR axis. Its high YC contribution is peculiar but it contains ~30% MAR like the other interglacial means.

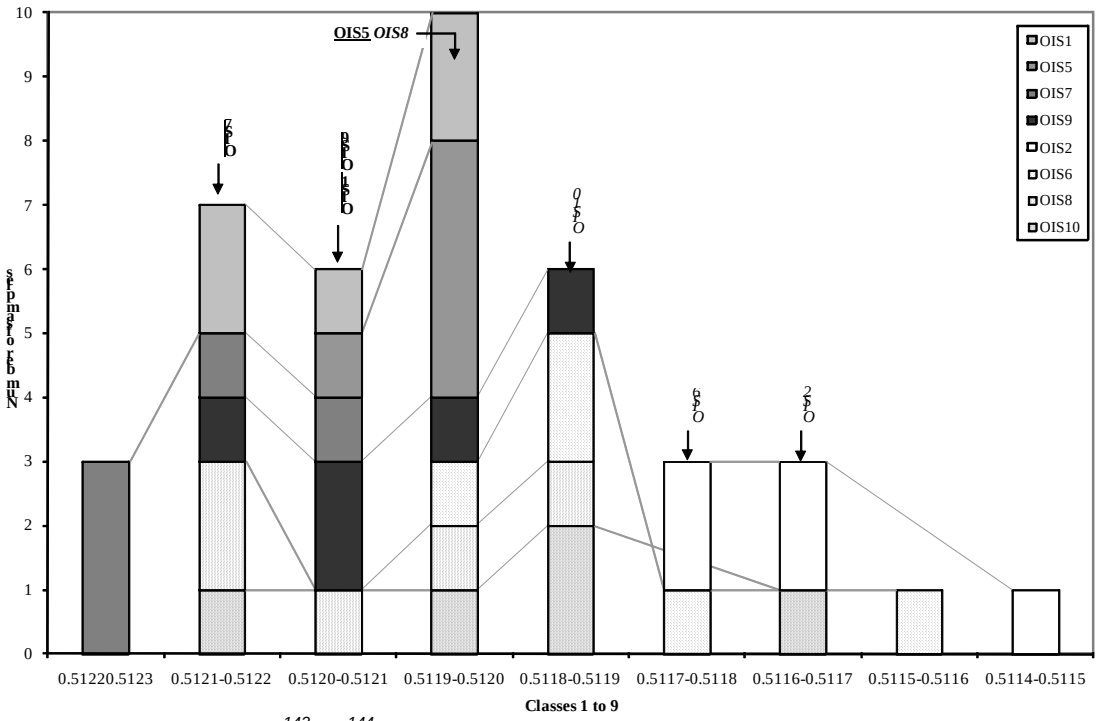

Figure 2 – Distribution of the $^{143}Nd/^{144}Nd$ ratios measured on the clay fraction. Nd data have been classed within 9 classes corresponding to a range of variation of 0.0001. Arrows indicate mean values.

In addition to internal variation within an OIS (probably underestimated by sampling resolution), the average contribution in NAS drops by a factor of 2 between a glacial interval and the adjacent younger interglacial. This evolution is mainly counterbalanced by higher mean MAR contribution within interglacials. Such evolution remains relative: any NAS drop could be due either to a decrease of NAS supplies or to higher supplies from the two others end-members (dilution process).

To decipher between higher supplies or dilution process, we estimate particle fluxes supplied by the end-members (Figure 3): NAS supplies are higher (relatively to the other end-members but also in absolute amount) during glacial intervals than during interglacials. The fine particle suppplies in Labrador Sea are therefore strongly controlled by proximal margin erosion: NAS supplies directly reflect the glacial stage intensity. MAR fluxes do not present significant G/I fluctuations for the last 360 kyr, except a marked increase in surface. The ODP646 Sm-Nd record confirms previous observations made from the study of nearby core MD99-2227: the late Holocene (i.e. < 3.1 kyr BP), characterized by an increase of MAR supplies, appear to be atypical with respect to the past 365 kyr. Peculiar recent conditions may be related to the unusual recent open sea ice conditions in Nordic seas favoring ocean convection, responsible for the observed anomalous large volumetric flux of NSOW today (Raymo et al., 2004) and/or the full appearance of the Labrador Sea Water mass.

Conclusion

The long-term evolution (i.e., over the last 365 kyr) of Sm-Nd ratios of fine particle fractions in deep Labador Sea sediments reflects changes in source provenance and deep-current paleointensity. Glacial Sm-Nd signatures are characterized by systematically lower $^{143}Nd/^{144}Nd$ and $^{147}Sm/^{144}Nd$ ratios than interglacials, reflecting enhanced proximal supplies related to continental margin erosion. *The sedimentary Sm-Nd glacial signature can be used as a fingerprint of the local or regional intensity of glacial erosion.*

In terms of long-distance transport, the flux of distal fine particles transported by deep water masses from the Iceland Basin-Reykjanes Ridge-Iceland areas did not change significantly between glacials and interglacials, although an overall long-term reduction seems probable.

Late Holocene conditions seems quite peculiar with respect to the past 365 kyr.

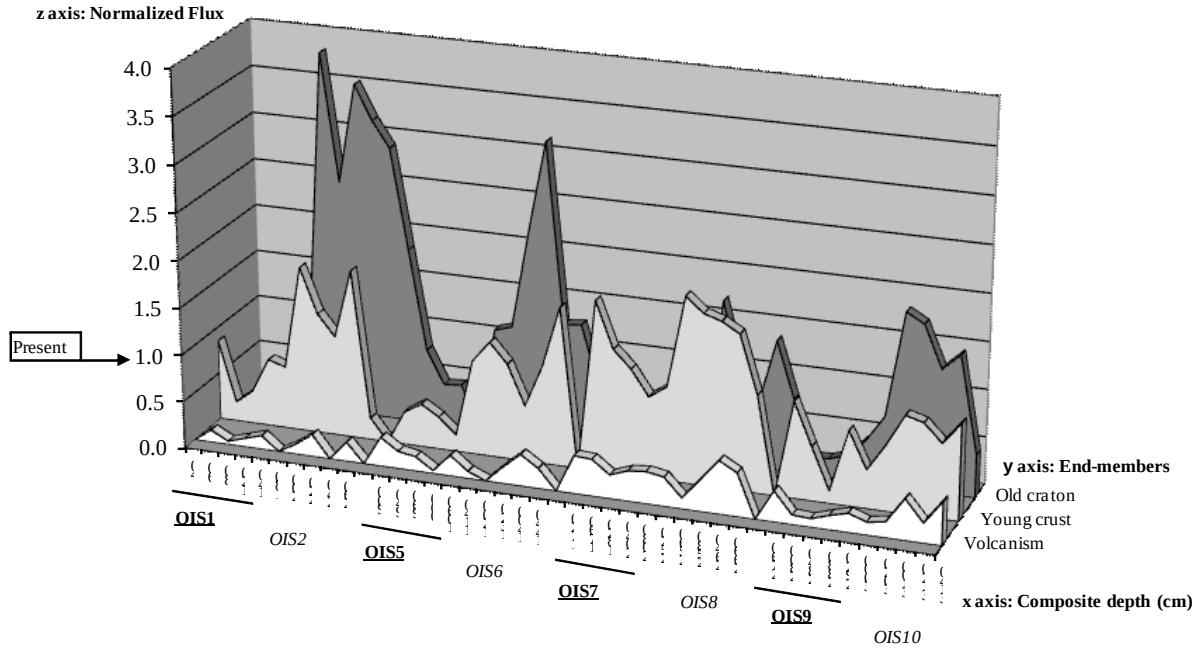

Figure 3 – Estimated contributions of the three identified end member NAS, YC, and MAR for the last four glacial/interglacial cycles. Each end member contribution has been normalized to surface representative sediment signature (vertical dashed line fixed at 1).

References

Bout-Roumazeilles V., 1995. Relations entre variabilités minéralogiques et climatiques enregistrées dans les sédiments de l'Atlantique Nord depuis les 8 derniers stades glaciaires-interglaciaires, Université de Lille I, unpubl., 180 p.

Bout-Roumazeilles V., Davies V.G. and Labeyrie L., 1998. Nd-Sr-Pb evidence of glacial-interglacial variations in clay provenance and transport in the North Atlantic Ocean, *Min. Mag.* 62A, 1443-1444.

Fagel N., Hillaire-Marcel C. and C. Robert, 1997. Changes in the Western Boundary Undercurrent outflow since the Last Glacial Maximum, from smectite/illite ratios in deep Labrador Sea sediments, *Paleoceanography* 12, 79-96, 1997.

Fagel N., Innocent C., Stevenson R.K. and Hillaire-Marcel C., 1999. Deep circulation changes in the Labrador Sea since the Last Glacial Maximum: new constraints from Sm-Nd data on sediments. *Paleoceanography* 14, 777-788.

Fagel N., Hillaire-Marcel C., Humblet M., Brasseur R., Weis D., and Stevenson R., 2004. Nd and Pb isotope signatures of the clay-size fraction of Labrador Sea sediments during the Holocene: Implications for the inception of the modern deep circulation pattern, *Paleoceanography* 19, doi 10.1029/2003PA000993.

Fagel N. (2007). Marine clay minerals, deep circulation and climate. In: C. Hillaire-Marcel & A. de Vernal. (Eds.), Paleoceanography of the Late Cenozoic, Volume 1: Methods, Elservier, Amsterdam, 139-184.

Frank M., Davies G.R., Claude-Ivanaj C. and Hofmann A.W., 2001. Radiogenic isotopes: New tools help treconstruct paleocean circulation and erosional input, EOS Trans. Am. Geophys. Union 82, 66 and 71.

Faure G. (1986) Principles of Isotope Geology. John Wiley and sons eds, New York, 589 pp.

Goldstein S.L. and O'Nions R.K. (1981) Nd and Sr isotopic relationships in pelagic clays and ferromanganese deposits, *Nature* 292, 324-327.

Innocent, C., Fagel N., Stevenson R. and Hillaire-Marcel C. (1997) Nd mixing models and sedimentary fluxes in the North Atlantic Ocean, *Earth and Planet. Sci. Lett.* 146, 607-625.

Kissel C., C. Laj A. Mazaud, and T. Dokken, 1997. Magnetic anisotropy and environmental changes in two sedimentary cores from the Norwegian Sea and the North Atlantic, *Earth and Planetary Sci. Lett.* 164, 617-626.

Raymo M. E., Oppo D. W., Flower B. P., Hodell D. A., McManus J. F., Venz K. A., Kleiven K. F. and McIntyre K., 2004. Stability of North Atlantic water masses in face of pronounced climate variability during the Pleistocene. *Paleoceanography* 19, doi 10.1029/2003PA000921.

Snowball I. and Moros M., 2003. Saw-tooth pattern of North Atlantic current speed during Dansgaard-Oeschger cycles revealed by the magnetic grain size of Reykjanes Ridge sediments at 59°N. *Paleoceanography* 18, doi 10.1029/2001PA000732.

HOLOCENE SUBPOLAR GYRE DYNAMIC AS VIEWED FROM GEOCHEMICAL TRACER RECORDS OF COLD-WATER CORALS

Norbert Frank
Laboratoire des Sciences du Climat et de l'Environnement – LSCE, CEA-CNRS-UVSQ
Norbert.Frank@cea.fr

Abstract

To reconstruct time series of oceanic patterns beyond the time covered by instrumental sea water measurements geochemical tracers recorded in cold-water corals provide a unique oceanic archive. Throughout this presentation it will be shown, which corals develop surrounding Iceland, which water masses influence and steer the growth of such corals and how the organisms incorporate information about the oceanic regime in which they develop.

Introduction

Deep water corals have come to light in the past decade as a new archive to study modern and past ocean circulation patterns (Adkins et al., 1998; Mangini et al., 1998; Montagna et al., 2006; Robinson et al., 2005; Robinson and van de Flierdt, 2009; Smith et al., 1997). Iceland being situated on the northern edge of the North Atlantic is known to be surrounded by a belt of frame work building and solitary deep water corals bathing in a complex oceanic regime driven by Atlantic and Arctic current systems operating at various depth and influenced by the support of matter and freshwater from Iceland's glaciers and volcanic aerosols. Many coral species construct aragonite skeletons to attach themselves in areas of strong bottom water currents. Through calcification trace elements and trace isotopes are incorporated into the skeletons that can be used to reconstruct oceanic parameters such as water mass origin, state of ventilation, temperature and even productivity. In addition, corals incorporate uranium from sea water and thus using uranium series disequilibrium methods the time of growth can be precisely determined (Cheng et al., 2000; Frank et al., 2004). Consequently time series of geochemical tracers can be established that allow reconstructing ocean dynamics and climate change in the past. The northern North Atlantic south of Iceland represents a part of the world ocean of great importance as warm waters are transported towards the north through the Irminger current that enter the supolar gyre and the Arctic Ocean. At depth intermediate depth waters originating in the Labrador Sea re-circulate along the topographic boundaries and at even deeper depth newly formed deep waters from the Norwegian and Greenland Seas enter the basin and mix with deep waters formed in the Labrador Sea to create the southward flowing North Atlantic Deep Water (NADW). Consequently Iceland is situated close to key areas of deep water production and northward flow of warm water. In addition, atmospheric circulation causes changes in the size and strength of the surface gyres that propagate to depth and that cause basin scale modifications of oceanic salt and temperature thus heat budgets. Through the use of "cold-water corals" as oceanic archive we may be able to reconstruct climate related change of the current systems and thus heat transport through time. Here, it will be briefly shown which coral species develop on the southern slopes of Iceland and how corals can be dated and how they can be used to determine the geochemical composition and physical parameters of sea water. The crucial location of Iceland in a highly dynamic environment between two main atmospheric circulation cells and its location at the interface of the oceanic polar front and the Atlantic gyre dynamic is well known since long, but cold-water corals and geochemical tracers to investigate such dynamic hydrological processes, the later operating on scales of years, decades and centuries, are just being developed. Consequently, this presentation will mainly focus on efforts undertaken during the past decades in various regions of the north Atlantic to demonstrate the potential of this new archive for future oceanic research south of Iceland.

Cold-water coral ecosystems

"Coral ecosystems evoke images of warm, tropical waters, not the deep, dark depths of the sea. Yet in the cold recesses of the ocean, there are coral ecosystems as biologically complex and diverse as their tropical counterparts. Cold-water corals are found worldwide and vary from reefs made by hard scleractinian corals to vast thickets of softer gorgonian corals. In the North Atlantic Ocean cold-water corals were first recorded in the 18th century but only in the last two decades have improved deep-ocean technologies allowed an exponential increase in scientific research on cold-water coral ecosystems. These studies have shown that cold-water corals support high biodiversity, are long-lived and slow-growing making them susceptible to physical disturbance by human activities (especially

bottom trawling). They have also highlighted the importance of cold-water corals as habitat for deep-water fishes, indicators of **past ocean climate regimes** and sources of novel bio-compounds. Finally, recent studies have shown that anthropogenic carbon dioxide is altering the chemistry of the seas and Atlantic corals may be among the most vulnerable marine ecosystems to this ocean 'acidification'" (cited from M. Roberts: TRACES - Prospectus: Trans-Atlantic Corals ecosystem study: www.lophelia.org). As mentioned by Murray Roberts such corals provide new and extraordinary ocean climate archives: as through their relatively slow growth rates (mm to cm/year) and intermediate to abyssal depth habitats (mostly 500 - 2000 depth), these species can record ocean changes in chemistry and circulation on many different time scales. Some species are constructional and form carbonate mounds, or bioherms while other species are ahermatypic occurring more sparsely throughout the world oceans (Figure **1** and **2**). Both constructional and ahermatypic corals mostly build up aragonite skeletons.

Figure 1: *Photos of living solitary and constructional coral species from Porcupine Seabight including a photo of the French remotely operated vehicle Victor 6000 and fish hiding in the coral frameworks (Images kindly provided by IFREMER - Caracole cruise, Porcupine Seabight). Lower left: destructed coral reef through deep trawling activity.*

Cold-water corals are cnidarians encompassing stony corals (Scleractinia), soft corals (Octocorallia, including ''precious'' corals, gorgonian sea fans, and bamboo corals), black corals (Antipatharia), and hydrocorals (Stylasteridae). They are azooxanthellate (i.e., lacking symbiotic dinoflagellates) and often form colonies supported by a common skeleton, providing structural habitat for other species. Here we focus on scleractinian reef framework– forming species and one specific solitary coral species. Species, habitats, and ecosystems discussed here are distinct from those of tropical coral reefs and are specifically associated with colder and deep offshore waters. Reefs and mounds tend to cluster in ''provinces,'' where specific hydrodynamic and food supply conditions favour coral growth. Some provinces are characterized by small mound features others by giant carbonate mounds where reefs have become repeatedly established since millions of years. Reef distribution, genesis, and development of cold-water corals are largely restricted to oceanic waters and temperatures between 4 and 12 C°. Approximately 800 species of reef-building scleractinians are described in shallow waters, yet fewer than 10 are known to make substantial deep-water reef frameworks. Of these, we have an incomplete view of their global distribution (Figure **2**), which remains skewed by the geographically varied levels of research activity and the bias of deep-water mapping initiatives to the developed world (Roberts et al., 2006). Further important aspects steering corals growth are high bottom water currents, hard substrates to which corals can attach too and important fluxes of labile organic matter and nutrients. Coral reef or mounds are build through the successive growth and decline of coral colonies on top of each other forming complex topographic structures on the seafloor with zones of active coral growth and sediment trapping and zones of dead coral rubbles and erosion (Figure **2b**). Sediment coring performed on such structures therefore provides a pile of fossil coral fragments and sediment representing the often discontinuous vertical development of reef framework forming coral. It is important to note that active coral growth leads to vertical extension rates of cm per year, while mound growth including degradation, compaction and erosion leads to far less vertical growth rates of several mm per year. To investigate solitary corals other than coring technologies need to be implied as corals cover the sea floor without creating significant vertical growth. Thus, either video grabs, dredges or ROV technologies are used to observe and recover such species. The lack of stratigraphic constrains on such complex and unique growth structures require that each individual investigated coral needs to be dated precisely.

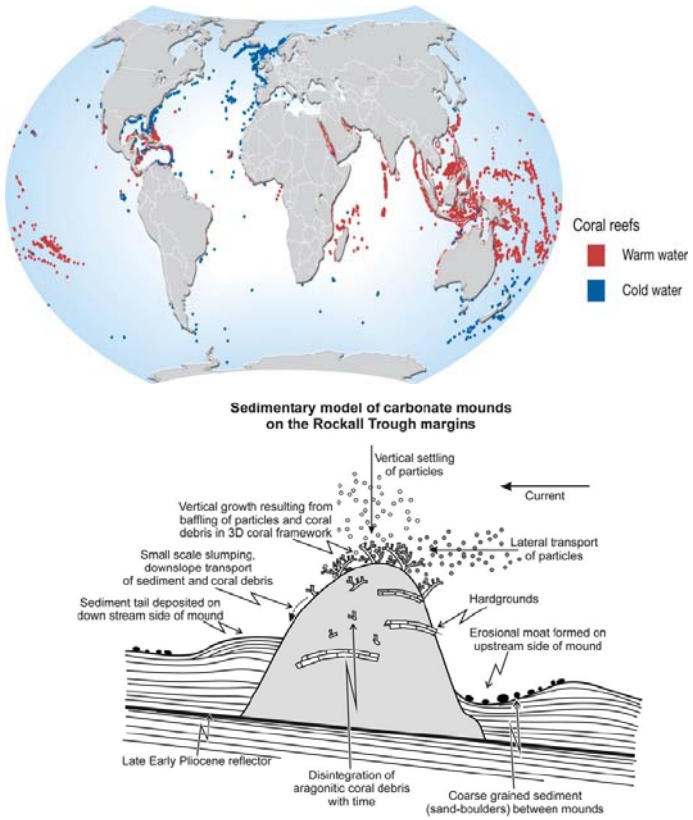

***Figure 2**: a) Present day known global distribution of cold water and tropical corals, largely biased for cold-water environments by the number of research activities. b) Sedimentary model of carbonate mounds at the Rockall Trough margins (extracted from (de Haas et al., 2009)).*

Coral dating

Corals incorporate into the skeleton uranium from sea water, but the radioactive daughter product ^{230}Th is not incorporated and thus a radioactive disequilibrium is created at the time of skeleton formation that provides an additional unique radioactive clock (Cheng et al., 2000; Douville et al., 2010). Through the precise and accurate measurement of Uranium-series isotopes (^{238}U, ^{234}U, ^{230}Th) one can precisely and accurately determine the "chronological" age of a fossil coral through the use of modern mass spectrometric technologies. This provides coral ages ranging from a few years of growth to several hundred thousand years of growth.

An example of coral dating using U-series methodologies is shown in figure **3** that here highlight the discontinuous character of coral reef development and demonstrates that corals provide oceanic archives capable to trace oceanic environmental changes over thousands of years.

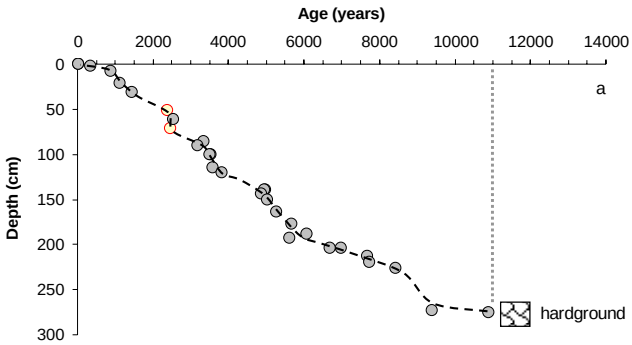

***Figure 3:** Coral growth on a carbonate mound determined by means of U-series dating of L. pertusa fragments (Frank et al., 2009). Between 11,000 years and present corals develop prosperously on the investigated site on Rockall Bank (MD01-2454G - 750m water depth). The coral age to sediment depth relationship yields the remaining speed of piling up dead coral fragments and is influenced by other processes such as compaction and erosion.*

Geochemical tracers and time series

Classically, the physical and chemical properties of water masses are reconstructed on time scales of several thousand years with "proxies" analyzed in carbonates such as foraminifera. Mg/Ca, Sr/Ca, U/Ca ratios are proxies for temperature. To investigate intermediate water properties through benthic foraminifera sequences of slope sediments need to be recovered allowing to reveal the vertical structure of the water column. Despite, those proxies do not reveal changes in air-sea gas exchange and cross thermocline exchange and generally provide no information on strength and direction of flow. Therefore, to better constrain changes in water mass mixing and advection through time other "tracers" are needed. ^{14}C is such a tracer derived from cosmogenic nuclide production that enters the largest carbon reservoir through air-sea gas exchange. It has been widely used to investigate modern ocean circulation as its distribution is strongly related to the state of ventilation in the surface ocean driven by vertical exchange of well and poorly ventilated water masses, sea ice cover and the strength of wind driven gas exchange (Broecker and Peng, 1982; Druffel, 1996; Guilderson et al., 1998; Nydal and Gislefoss, 1996; Östlund et al., 1974). Within the deep ocean ^{14}C participates in the advection and mixing of water masses and through radioactive decay the ^{14}C concentration is modified along the pathways of water mass (Broecker and Peng, 1982). As a consequence ^{14}C can serve to validate advection and gas exchange in coupled ocean circulation and carbon cycle models (Marchal et al., 2001; Rodgers et al., 2004). ^{14}C is incorporated in coral skeletons as part of the carbonate matrix and seawater ^{14}C contents can be reconstructed through combined U-series dating and ^{14}C dating (Adkins et al., 1998; Frank et al., 2004; Mangini et al., 1998). Consequently corals can be used to determine past ocean ^{14}C levels and therefore the temporal and vertical structure of ocean circulation and cross thermocline exchange (Robinson et al., 2005). The temporal variability of ^{14}C is well known in the atmosphere of the past 11,000 years (Figure **4**) as derived from measurements of ^{14}C in tree rings (Stuiver et al., 1998). As a consequence seawater ^{14}C can be reconstructed and interpretations of ocean circulation changes are feasible for this time span. For example, figure **4** shows the reconstruction of thermocline water ^{14}C on Rockall Bank and in cases for samples from South Iceland (kindly provided by J. Adkins, CALTECH) and the New England Seamounts and temperate Atlantic (Robinson et al., 2005). Without going into the detail of this record it is clear that on first order the early Holocene is marked by strong sub-surface water ^{14}C variability while the late Holocene (beyond 7000 years) tend to smoothly follow the atmospheric trend. Consequently, processes affecting the state of ventilation of thermocline water have been different during the early Holocene and seem to be similar to today during the late Holocene indicative of major changes in the water mass balance at upper intermediate depth.

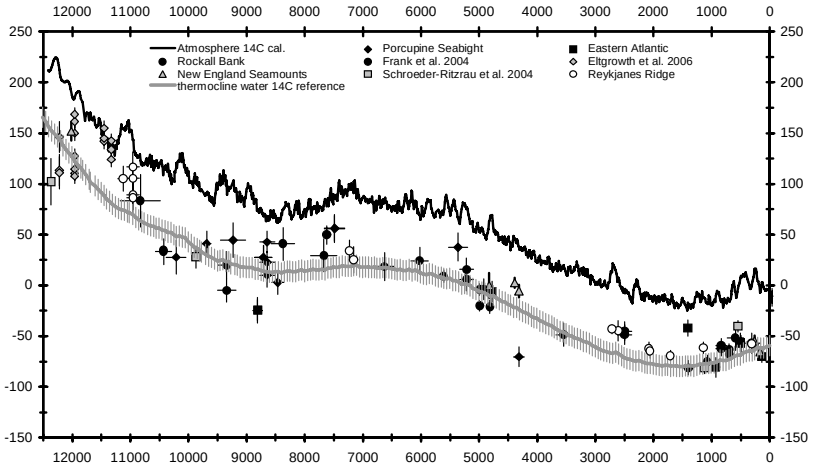

Figure 4: *Seawater radiocarbon in ‰ notation over the past 11000 years as reconstructed from cold-water corals in comparison to atmospheric radiocarbon and estimated intermediate water ^{14}C (using a constant reservoir effect of -65‰).*

Recently, also Nd-isotope ratios have been shown to be a very promising new tracer of the provenance of water mass and mixing and those have as ^{14}C the advantage to be independent of fractionation induced by biological processes in the water column. Nd is mainly in the dissolved form in seawater (90 to 95 %) with a concentration of about 10^{-12} g/g. Its residence time, recently re-assessed to about 500 - 1000 yr (Tachikawa et al., 2003), is shorter than the time for inter-ocean mixing. Consequently, through lithogenic inputs, water masses are characterized by different isotopic composition of Nd (continental fingerprint). The ε_{Nd} values of the North Atlantic Ocean are contrasted with low ε_{Nd} values in the Labrador Sea intermediate water and with much higher values in the eastern subtropical North Atlantic. Thus, ε_{Nd} values of the main surface and intermediate ocean currents which constitute the SPG and STG are highly sensitive to monitor present and past changes of water mass mixing between both. The only way to alter the isotopic composition of seawater despite of water mass mixing is to add Nd with a different isotopic composition through riverine and Aeolian inputs or by mixing with other water masses. But, away from direct riverine input and on short time scales (<500 years) ε_{Nd} can be considered a conservative tracer in the ocean. Cold-water corals provide excellent archives of seawater ε_{Nd}, allowing reconstruction of time-series of this water mass tracer at equal resolution as for ^{14}C. First results of this new technique are presented in figure **5** clearly identifying strong changes in water mass composition on Rockall Bank here over the past 10,000 years. In first order, ε_{Nd} values oscillate between modern SPG (ε_{Nd}~-11) and STG (ε_{Nd} ~-14) endmember values indicating long-term trends and secular short term oscillations of intermediate water provenance and water mass mixing at Rockall Bank.

Despite tracer used to “colour” oceanic transport and mixing, tracers of the physical and geochemical sea water composition have also been developed that will be briefly described to highlight the potential of corals as unique paleoceanographic archive. Based on the outlined geochronological tools and geochemical tracers it will be shown how those can be applied on cold-water corals from the South of Iceland to understand the temporal variability of the north Atlantic upper intermediate depth circulation from present to the past 10,000 years.

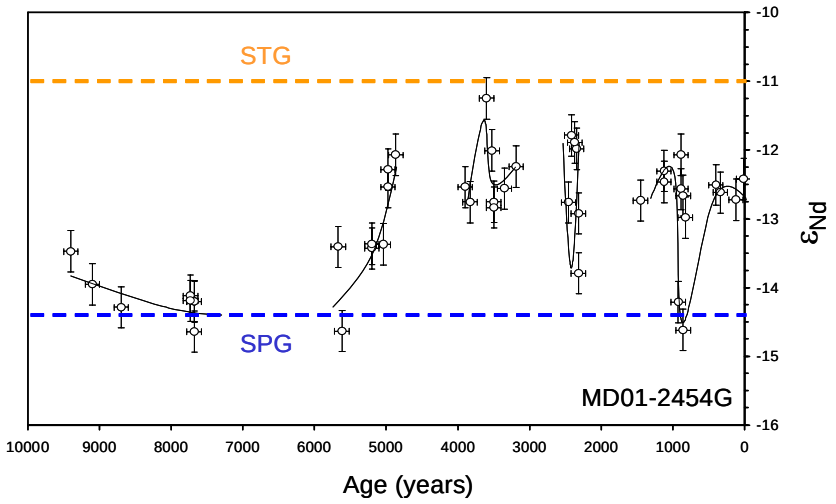

Figure 5: *Nd-isotopic variations (ε_{Nd}) against age [years] recorded over the past 10000 years by deep water corals from Rockall Bank (750m water depth) (Colin et al. accepted QSR).*

References

Adkins, J.F., Cheng, H., Boyle, E.A., Druffel, E.R.M. and Edwards, R.L., 1998. Deep-Sea coral evidence for rapid change in ventilation of the deep North Atlantic 15,400 years ago. Science, 280: 725-728.

Broecker, W.S. and Peng, T.-H., 1982. Tracers in the sea. Eldigio Press.

Cheng, H., Adkins, J.F., Edwards, R.L. and Boyle, E.A., 2000. U-Th dating of deep-sea corals. Geochimica et Cosmochimica Acta, 64: 2401-2416.

de Haas, H. et al., 2009. Morphology and sedimentology of (clustered) cold water coral mounds at the south Rockall Trough margins, NE Atlantic Ocean. Facies, 55: 1-26.

Douville, E. et al., 2010. Rapid and precise ^{230}Th/U dating of ancient carbonates using Inductively Coupled Plasma - Quadrupole Mass Spectrometry. Chemical Geology, 272: 1-11.

Druffel, E.R.M., 1996. Post-bomb radiocarbon records of surface corals from the tropical Atlantic ocean. Radiocarbon, 38(3): 563-572.

Frank, N. et al., 2004. Eastern North Atlantic deep-sea corals: Tracing upper intermediate water D^{14}C during the Holocene. Earth and Planetary Science Letters, 219: 297-309.

Guilderson, T., Schrag, D.P., Kashagarian, M. and Southon, J., 1998. Radiocarbon variability in the western equatorial Pacific inferred from a high-resolution coral record from Nauru Island. Journal of Geophysical Research, 103(C11): 24641-24650.

Mangini, A. et al., 1998. Coral provides way to age deep water. Nature, 392: 347.

Marchal, O., Stocker, T.F. and Muscheler, R., 2001. Atmospheric radiocarbon during the Younger Dryas: production, ventilation, or both? Earth and Planetary Science Letters, 185: 385-395.

Montagna, P., McCulloch, M., Taviani, M., Mazzoli, C. and Vendrell, B., 2006. Phosphorus in cold-water corals as a proxy for seawater nutrient chemistry. Science, 312: 1788.

Nydal, R. and Gislefoss, J.S., 1996. Further application of bomb ^{14}C as a tracer in the atmosphere and ocean. Radiocarbon, 38: 389-406.

Östlund, G.H., Dorsey, H.G. and Rooth, C.G.H., 1974. GEOSECS North Atlantic radiocarbon and tritium results. Earth and Planetary Science Letters, 23: 69-86.

Roberts, M., Wheeler, A.J. and Freiwald, A., 2006. Reefs of the Deep:The Biology and Geology of deep-water coral ecosystems. Science, 312: 543-547.

Robinson, L. et al., 2005. Radiocarbon variability in the western north Atlantic during the last deglaciation. Science, 310: 1469-1473.

Robinson, L. and van de Flierdt, T., 2009. Southern Ocean evidence for reduced export of North Atlantic Deep Water during Heinrich event 1. Geology, 37: 195-198.

Rodgers, K. et al., 2004. Radiocarbon as a thermocline proxy for the eastern Pacific. Geophysical Research Letters, 31(L14314): 1-4.

Smith, J.E., Risk, M.J., Schwarcz, H.P. and McConnaughey, T.A., 1997. Rapid climate change in the North Atlantic during the Younger Dryas recorded by deep-sea corals. Nature, 386: 818-820.

Stuiver, M. et al., 1998. Intcal98 radiocarbon age calibration: 24,000-0 cal BP. Radiocarbon, 40(3): 1041-1083.

Tachikawa, K., Athias, V. and Jeandel, C., 2003. Neodymium budget in the modern ocean and paleo-oceanographic implications. Journal of Geophysical Research, 108(3254, doi:10.1029/1999JC000285).

RIDGE JUMP PROCESS IN ICELAND

Sebastian GARCIA
Freie Universität Berlin – Department of Geologie, sgarcia@zedat.fu-berlin.de

Abstract

Eastward ridge jumps bring the volcanic zones of Iceland back to the centre of the hotspot in response to the absolute westward drift of the Mid-Atlantic Ridge. Mantellic pulses triggers these ridge jumps. One of them is occurring in Southern Iceland, whereas the exact conditions of the last ridge jump in Northern Iceland remain controversial. The diachronous evolution of these two parts of Iceland may be related to the asymmetric plume-ridge interaction when comparing Northern and Southern Iceland.

Introduction

Iceland is an emerged ridge that results from the interaction between the Mid-Atlantic Ridge (MAR) and the Icelandic hotspot. The apex of hot mantle upwelling is localized beneath the Vatnajökull ice cap (Fig.1) [Tryggvason et al., 1983]. Presently, accretion in Iceland occurs with a spreading rate of ~18 km/Myr [DeMets et al., 1990; DeMets et al., 1994]. It is localised along a curved ridge zone centred above the hotspot which includes two branches, the North and East Volcanic Zones (NVZ and EVZ, respectively). The Tjörnes Fracture Zone and the South Iceland Seismic Zone are transform fault zones that accommodate the eastward shift of the NVZ and of the EVZ relative to the Kolbeinsey Ridge and to the Reykjanes Ridge, respectively (Fig.1). In Southern Iceland, a third volcanic zone, the West Volcanic Zone (WVZ), accommodates part of the plate divergence. It corresponds to the inland continuation of the Reykjanes Ridge (Fig.1).

The North American-Eurasian plate boundary, marked by the MAR, migrates westward relative to the Icelandic hotspot [Burke et al., 1973]. Assuming a symmetrical accretion, the rate of the westward ridge migration varies from 3.7 km/Myr [Müller et al., 1993] to 11.5 km/Myr [Gripp and Gordon, 2002] along the N106°E divergence trend [De Mets et al., 1990; DeMets et al., 1994]. Because the westward ridge migration furthers off the active ridges from the hotspot, eastward ridge jumps are expected to bring the volcanic zones of Iceland back to the centre of the hotspot. Although the precise mechanism of ridge jump is still strongly discussed [e.g., Jurine et al., 2005; Kendall et al., 2005; Mittelstaedt and Ito, 2005], all models agree on the creation of a zone of weakness in the plate overriding the hotspot that triggers and localises the ridge jump.

A ridge jump implies the extinction of the formerly active ridge and the initiation of a new one. It has been documented on mid-oceanic ridges [e.g., d'Acremont et al., 2010], but generally remains difficult to analyze because the evidences for plume-ridge interaction are underwater. Iceland, as an emerged part of the MAR, offers the opportunity to study precisely such ridge jumps. Ward [1971] and Saemundsson [1974] first interpreted, in an eastward ridge jump context, the WVZ and its hypothetical extinct northern continuation as a paleo-ridge, and the EVZ and NVZ as the new ridges (Fig.1). This implies that a ridge jump is presently occurring in Southern Iceland, with the development of the EVZ at the expense of the WVZ [e.g., Aronson and Saemundsson, 1975; Perlt et al., 2008]. On the other hand, the exact timing of the last ridge jump in Northern Iceland, as the locus of the extinct paleoridge, remains controversial [e.g., Garcia, 2003; Saemundsson, 1974].

Ridge jump in Northern Iceland

In Northern Iceland, limits of the lava flows of the NVZ are easily recognisable as they unconformably overlie lava flows of the paleo-ridge (Fig.1). Lava flows of the NVZ dip 4-5°to the wes t on the eastern side of the NVZ and a few degrees to the east on the western side of the NVZ and then define a synform-like structure [Walker, 1964; Young et al., 1985]. This dip toward the ridge axis is a typical feature of the Icelandic volcanic systems [e.g., Palmason, 1980]. The ages of the lava increase away from the central part of the NVZ and reach 6-6.5 Myr in the vicinity of the eastern and the western unconformities [Jancin et al., 1985; McDougall et al., 1976a; McDougall and Wensink, 1966; Musset et al., 1980], the latest unconformity being named the Flateyjarskagi one.

A proposed location of the paleo-ridge axis, the Hunafloi-Skagi paleo-ridge, is similarly based on the

description of a synform-like structure (Fig.1) [Saemundsson, 1974]. This paleo-ridge would cease to accrete around 6-7 Ma [Everts et al., 1972]. All along its eastern flank, lava flows coming from the paleo-ridge are presumed to dip westward with increasing ages. It is the case along the eastern coast of Iceland where 12-14 Myr old lava flows [Bagdasaryan et al., 1976; McDougall et al., 1976b; Moorbath et al., 1968; Musset et al., 1980] dip 6-10°to the west. However, on the eastern side of the NVZ, paleo-ridge lava flows define a down-bending zone with westward dips as great as 15-18° [Walker, 1964]. This westerly increase in dip of the old lava pile may be due to excess loading from the capping NVZ lava pile. Considering the same deflection process, paleo-ridge lava flows close to the western side of the NVZ steeply dip eastward (20-25°E). Thus, they define a broad antiform between the Hunafloi-Skagi paleo-ridge axis and the western limit of the NVZ. This antiform structure, the Eyjafjördur antiform (Fig.1), strikes approximately NE-SW through the Flateyjarskagi and Tröllaskagi Peninsulas [Saemundsson et al., 1980; Young et al., 1985]. On both sides of the unconformities, the paleo-ridge lava flows are 9-10 Myr old [Bagdasaryan et al., 1976; Jancin et al., 1985; McDougall et al., 1976b; Moorbath et al., 1968; Musset et al., 1980].

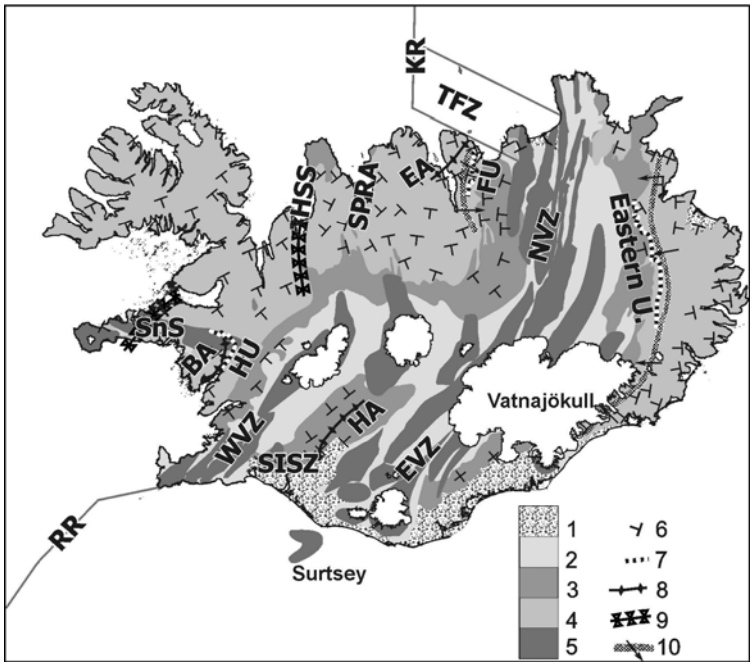

Figure 1: Structural map of Iceland: main active structures or resulting from rift jump process.
1: Holocene sediments; 2: Upper Pleistocene-Holocene lava flows (<0.8 Ma); 3: Plio-Pleistocene lava flows (<3.3 Ma and >0.8 Ma); 4: Tertiary lava flows (>3.3 Ma); 5: Active volcanic system; 6: Dip of lava flows; 7: Angular unconformity; 8: Axis of antiform-like structure; 9: Axis of synform-likestructure; 10: Flexure zone with sense of lava flows dip. BA: Borganes Antiform; EA: Eyjafjördur Antiform; EVZ: Eastern Volcanic Zone; FU: Flateyjarskagi Unconformity; HA: Hreppar Antiform; HSS: Húnaflói-Skagi Synform; HU: Hredavatn Unconformity; KR: Kolbeinsey Ridge; NVZ: Northern Volcanic Zone; RR: Reykjanes Ridge; SISZ: South Iceland Seismic Zone; SnS: Snaefellsnes; SPRA: Skagafjördur Paleo-Rift Axis; TFZ: Tjörnes Fracture Zone; U: Unconformity; WVZ: Western Volcanic Zone. Modified from Johannesson and Saemundsson [1998] and Kristjansson et al. [1992]

On the other hand, 7.5±0.5 Myr old dykes have been dated west of the Flateyjarskagi unconformity [Jancin et al., 1985]. As these dykes are attributed to the NVZ, their present sites imply retreat of the extent of the NVZ lava flows, probably due to glacial erosion. In addition, it implies that the exhumed, underlying paleo-ridge lava flows have been intruded at the earliest stage of the ridge jump by dykes injected by the NVZ. Garcia et al. [2003] also dated some dykes along a profile trending parallel to the plate divergence direction in Northern Iceland. They proposed a model for the ridge jump history in which the NVZ initiated at 8-8.5 Ma intruding 9-9.5 Myr old lava flows. They also localised the paleo-ridge approximately 60 km to the east of the Hunafloi-Skagi synform. This Skagafjordur paleo-ridge (Fig.1) has

been active until 3 Ma [Garcia et al., 2003]. In their model, the Hunafloi-Skagi synform simply result from the down-bending of Tertiary lavas under the weight of excess Plio-Pleistocene lavas emitted from the central part of Iceland (i.e., from the equivalent to the present Langjökull and Hofsjökull volcanic systems). The process that leads to the down-bending of paleo-ridge lava flows under the weight of the NVZ lavas would explain this down-bending of the Tertiary lavas [Garcia et al., 2008]. This would also explain the partial disappearing of the synform-like structure supposed to localise the Skagafjordur paleo-ridge.

Ridge jump in Southern Iceland

Two ridge jumps are usually considered in Southern Iceland. A major difference to Northern Iceland is that the last ridge jump still occurs there. This explains the simultaneous existence of two active ridges in Southern Iceland (i.e., the WVZ and the EVZ). The EVZ, which initiated following the last ridge jump, is presently propagating southward. While developing, the new rift propagates through older, chemically and mineralogically stratified crust, giving rise to alkaline volcanism at the leading tip, followed by FeTi basalts and later by tholeiitic rocks [Steinthorsson et al., 1985]. This temporal spectrum of composition is presently observed in the spatial distribution from tholeiitic basalts to Fe-Ti basalts up to alkali basalts when going southward from the EVZ to the island of Surtsey (Fig.1) [Sigmarsson et al., 1992]. At the same time, recent GPS data show a northward decrease of the divergence rate localised along the WVZ, concomitant with a northward increase of the divergence rate localised along the EVZ [Perlt et al., 2008]. This result fits with the southward propagation of the EVZ and the progressive transfer of the accretion process along this last volcanic zone at the expense of the WVZ.

The initiation of the EVZ dates from 2-3 Ma [Aronson and Saemundsson, 1975]. However, no unconformity underlying the contact between the lava flows erupted by the EVZ and those coming from the WVZ have been recognised in the field. Solely the Hreppar antiform (Fig.1) allow to distinguish lava flows dipping in direction of the WVZ from lava flows dipping in direction of the EVZ [Aronson and Saemundsson, 1975]. Moreover, the WVZ is active since ~7 Ma [Bagdasaryan et al., 1976; McDougall et al., 1977; Moorbath et al., 1968; Smith, 1967]. To the west, lava flows from the WVZ are separated along the unconformity of Hredavatn from lava flows as old as 9.4±0.7 Ma [Aronson and Saemundsson, 1975; Moorbath et al., 1968]. These latest flows have been erupted along a paleo-ridge whose axis is localised along the NE-SW trending Snaefellsnes synform. This paleo-ridge has been active until 6-7 Ma [Moorbath et al., 1968]. As in Northern Iceland, lava flows erupted by the Snaefellsnes paleo-ridge and close to the western side of the WVZ have been tilted eastward and thus define a broad antiform structure, the Borganes antiform (Fig.1).

Triggering mechanisms of ridge jump in the Icelandic context: a discussion

Assuming hotspots overlie sources of anomalously hot asthenosphere, there are several mechanisms that can promote ridge jumps including lithospheric tension induced by buoyant and convecting asthenosphere [Mittelstaedt and Ito, 2005], mechanical and thermal thinning of the lithosphere due to hot flowing asthenosphere [Jurine et al., 2005], and thermal weakening of the lithosphere due to the penetration of magma [Kendall et al., 2005]. Mittelstaedt et al. [2008] investigated the effect of the latter, in the specific Icelandic context. They demonstrate that, beyond a certain value of hotspot flux, the ridge can migrate away from the hotspot -or escape from it -, only if the migration rate of the ridge is equal or higher to the half-spreading rate. The exact timing of the ridge jump is then controlled by these two rates. If the velocity of migration is inferior to the halfspreading rate, then the ridge remains constantly above the hotspot. On the other hand, the described timing of ridge jumps in Iceland implies that escape of the ridge alternates with ridge being locked above the hotspot (the present-day situation in Northern Iceland since at least 7 Myr). A very convincing explanation for the observed alternation between these end-member situations can be a temporal variation in the hotspot flux. Temporal variations of temperature of the plume would be the source for these variations in the magmatic flux [e.g., Jones et al., 2002]. The related, enhanced melting events propagate along the MAR and have been imaged through the V-shaped ridges observed along the Kolbeinsey and Reykjanes Ridges [e.g., Appelgate, 1997; Smallwood et al., 1995]

In the model proposed first by Saemundsson [1974], the NVZ initiates at 6-6.5 Ma, through the 2.5-4 Myr older eastern flank of a paleo-ridge; the latter, the Hunafloi-Skagi paleo-ridge, stopped its activity simultaneously with the NVZ initiation. In their model, Garcia et al. [2003] suggest that the NVZ initiates at

8-8.5 Ma, intruding the 0.5-1.5 Myr older eastern flank of the Skagafjordur paleo-ridge; the two ridges being active simultaneously for 5-5.5 Myr. In Southern Iceland, following the model proposed first by Aronson and Saemundsson [1975], the actual ridge jump occurs since 2-3 Myr; whereas the previous ridge jump started at 7 Ma by intruding the 1.5-3 Myr older eastern flank of the Snaefellsnes paleo-ridge that may have been active for a maximum of 1 Myr more. Modelling of Mittelstaedt et al. [2008] tells us that a ridge jump in Iceland needs from 1 to 4 Myr to be completely achieved and that the intruded seafloor can not be older than 1.5 Myr. These boundary conditions fit with the available data for the rift jump process in Southern Iceland, but do not permit us to discriminate between the two available models for Northern Iceland. The melting anomalies that are behind the observed V-shaped ridges started to propagate from the Icelandic hotspot around 2.5, 7 and 9 Myr ago [Jones et al., 2002]. The times of these mantellic pulses, supposed to be the triggering factor of the ridge jumps, are compatible with both models of ridge jump in Northern Iceland as with the two described ridge jumps in Southern Iceland.

When considering the timing of the different ridge jumps that occurred in Iceland, a clear diachronism appears between the respective evolutions of Northern and Southern Iceland. In addition,
northward and southward profiles, from the Icelandic hotspot to the Kolbeinsey and the Reykjanes Ridges respectively, show that the topography, the bathymetry, and the crustal thickness are asymmetric [Hooft et al., 2006]. This is also the case when comparing the halo of mixing with an enriched source [Blichert-Toft et al., 2005; Graham, 2002; Mertz et al., 1991; Poreda et al., 1986; Schilling, 1999]; this interaction being more extended along the Reykjanes Ridge than along the Kolbeinsey Ridge. All these data suggest an asymmetric plume-ridge interaction. One can then hypothesise that the diachronous evolution of Northern Iceland relative to Southern Iceland is somehow related to this asymmetric plume-ridge interaction.

References

Appelgate, B., Modes of axial reorganisation on a slow-spreading ridge: the structural evolution of Kolbeinsey Ridge since 10 Ma, *Geology, 25*, 431-434, 1997. Aronson, J.L., and K. Saemundsson, Relatively old basalts from structurally high areas in central Iceland, *Earth Planet. Sci. Lett., 28*, 83-97, 1975. Bagdasaryan, G.P., V.I. Gerasimovkiy, A.I. Polyakov, and R.K. Gukaysan, New data on the absolute age of Icelandic volcanic rocks, *Geokhimiya, 9*, 1333-1339, 1976.

Blichert-Toft, J., A. Agranier, M. Andres, R. Kingsley, J. Schilling, and F. Albarède, Geochemical segmentation of the Mid-Atlantic Ridge north of Iceland and ridge–hot spot interaction in the North Atlantic, *Geochemistry Geophysics Geosystems, 6*, Q01E19, doi:10.1029/2004GC000788, 2005.

Burke, K., W.S.F. Kidd, and J.T. Wilson, Plumes and Concentric Plume Traces of the Eurasian Plate, *Nature, 241*, 128-129, 1973.

d'Acremont, E., S. Leroy, M. Marcia, P. Gente, and J. Autin, Volcanism, jump and propagation on the Sheba ridge, eastern Gulf of Aden: segmentation evolution and implications for oceanic accretion processes, *Geophys. J. Int., 180*, 535–551, doi: 10.1111/j.1365-246X.2009.04448.x, 2010.

DeMets, C., R.G. Gordon, D.F. Argus, and S. Stein, Current plate motion, *Geophys. J. Int., 101*, 425478, 1990.

DeMets, C., R.G. Gordon, D.F. Argus, and S. Stein, Effect of recent revisions to the geomagnetic reversal time scale on estimates of current plate motions, *Geophys. Res. Lett., 21*, 2191-2194, 1994.

Everts, P., L.E. Koerfer, and M. Schwarzbach, Neue K/Ar datierungen isländischer basalte, *Neues Jahrbuch Geologie und Paläontologie Monasthefte, 5*, 280-284, 1972.

Garcia, S., Implications d'un saut de rift et du fonctionnement d'une zone transformante sur les déformations du Nord de l'Islande. Approches structurales, sismotectoniques et radiochronologiques, Ph.D. thesis, 287 pp., University Pierre et Marie Curie, Paris, 2003.

Garcia, S., J. Angelier, F. Bergerat, C. Homberg, and O. Dauteuil, Influence of rift jump and excess loading on the structural evolution of Northern Iceland, *Tectonics, 27*, TC1006, doi:10.1029/2006TC002029, 2008.

Garcia, S., N.O. Arnaud, J. Angelier, F. Bergerat, and C. Homberg, Rift jump process in Northern Iceland since 10 Ma from ^{40}Ar/^{39}Ar geochronology, *Earth Planet. Sci. Lett., 214*, 529-544, 2003.

Graham, D.W., Noble gas isotope geochemistry of mid-ocean ridge and ocean island basalts: Characterization of mantle source reservoirs, in *Noble Gases in Geochemistry and Cosmochemistry*, vol. 47, edited by D. Porcelli, R. Wieler and C. Ballentine, pp. 247–318, Rev. Mineral. Geochem., Mineral. Soc. Am., Washington, D. C., 2002.

Gripp, A.E., and R.G. Gordon, Young tracks of hotspots and current plate velocities, *Geophys. J. Int., 150*, 321-361, 2002.

Hooft, E.E.E., B. Brandsdottir, R. Mjelde, H. Shimamura, and Y. Murai, Asymmetric plume-ridge interaction around Iceland: The Kolbeinsey Ridge Iceland Seismic Experiment, *Geochemistry Geophysics Geosystems, 7, Q05015, doi:10.1029/2005GC001123*, 2006.

Jancin, M., K.D. Young, and B. Voight, Stratigraphy and K/Ar ages across the west flank of the Northeast Iceland axial rift zone, in relation to the 7 Ma volcano-tectonic reorganisation of Iceland, J. Geophys. Res., 90, 9961-9985, 1985

Johannesson, H., and K. Saemundsson, Geological map of Iceland, Icelandic Institute of Natural History, Reykjavik, 1998.

Jones, S.M., N. White, and J. Maclennan, V-shaped ridges around Iceland: Implications for spatial and temporal patterns of mantle convection, *Geochemistry Geophysics Geosystems, 3*, 1059, doi:10.1029/2002GC000361, 2002.

Jurine, D., C. Jaupart, G. Brandeis, and P.J. Tackley, Penetration of mantle plumes through depleted lithosphere, *J. Geophys. Res., 110*, doi:10.1029/2005JB003751, 2005. Kendall, J.M., G.W. Stuart, C.J. Ebinger, I.D. Bastow, and D. Keir, Magma-assisted rifting in Ethiopia, *Nature, 433*, 2005.

Kristjansson, L., H. Johannesson, and I. McDougall, Stratigraphy, age and paleomagnetism of Langidalur, Northern Iceland, *Jökull, 42*, 31-44, 1992.

McDougall, I., K. Saemundsson, H. Johannesson, N.D. Watkins, and L. Kristjansson, Extension of the geomagnetic polarity time scale to 6.5 m.y.: K-Ar dating, geological and paleomagnetic study of a 3,500-m lava succession in western Iceland, *Geol. Soc. Am. Bull., 88*, 1-15, 1977.

McDougall, I., N.D. Watkins, and L. Kristjansson, Geochronology and paleomagnetism of a Miocene-Pliocene lava sequence at Bessastadaa, eastern Iceland, *Am. J. Sci, 276*, 1078-1095, 1976a.

McDougall, I., N.D. Watkins, G.P.L. Walker, and L. Kristjansson, Potassium-argon and paleomagnetic analysis of Icelandic lava flows: limits on the age of anomaly 5, *J. Geophys. Res., 81*, 1505-1512, 1976b.

McDougall, I., and H. Wensink, Paleomagnetism and geochronology of the Pliocene-Pleistocene lavas in Iceland, *Earth Planet. Sci. Lett., 1*, 232-236, 1966.

Mertz, D.F., C.W. Devey, W. Todt, P. Stoffers, and A.W. Hoffman, Sr-Nd-Pb isotope evidence against plume-asthenosphere mixing north of Iceland, *Earth Planet. Sci. Lett., 25*, 411–414, 1991.

Mittelstaedt, E., and G. Ito, Plume-ridge interaction, lithospheric stresses, and the origin of near-ridge volcanic lineaments, *Geochemistry Geophysics Geosystems, 6*, Q06002, doi:10.1029/2004GC000860, 2005.

Mittelstaedt, E., G. Ito, and M.D. Behn, Mid-ocean ridge jumps associated with hotspot magmatism, *Earth Planet. Sci. Lett., 266*, 256–270, 2008.

Moorbath, S., H. Sigurdsson, and R. Goodwin, K-Ar ages of the oldest exposed rocks in Iceland, *Earth Planet. Sci. Lett., 4*, 197-205, 1968.

Müller, R.D., J.-Y. Royer, and L.A. Lawver, Revised plate motions relative to the hotspots from combined Atlantic and Indian Ocean hotspot tracks, *Geology, 21*, 275-278, 1993.

Musset, A.E., J.G. Ross, and I.L. Gibson, $^{40}Ar/^{39}Ar$ dates of eastern Iceland lavas, *Royal Astron. Soc. Geophys. Jour., 60*, 37-52, 1980.

Palmason, G., A continuum model of crustal generation in Iceland; kinematic aspects, *J. Geophys., 47*, 7-18, 1980.

Perlt, J., M. Heinert, and W. Niemeier, The continental margin in Iceland — A snapshot derived from combined GPS networks, *Tectonophysics, 447*, 155–166, 2008.

Poreda, R.J., J.-G. Schilling, and H. Craig, Helium and hydrogen isotopes in ocean-ridge basalts north and south of Iceland, *Earth Planet. Sci. Lett., 113*, 129–144, 1986.

Saemundsson, K., Evolution of the axial rifting zone in northern Iceland and the Tjörnes fracture zone, *Geol. Soc. Am. Bull., 85*, 495-504, 1974.

Saemundsson, K., L. Krisjansson, I. McDougall, and N.D. Watkins, K-Ar dating, geological and paleomagnetic study of a 5-km lava succession in northern Iceland, *J. Geophys. Res., 85*, 36283646, 1980.

Schilling, J.-G., Dispersion of the Jan Mayen and Iceland mantle plumes in the Arctic: A He-Pb-Nd-Sr isotope tracer study of basalts from the Kolbeinsey, Mohns, and Knipovich Ridges, *J. Geophys. Res., 104*, 10,543–10,569, 1999.

Sigmarsson, O., M. Condomines, and S. Fourcade, Mantle and crustal contribution in the genesis of recent basalts from off-rift zones in Iceland: Constraints from Th, Sr and O isotopes, *Earth Planet. Sci. Lett., 110*, 149-162, 1992.

Smallwood, J.R., R.S. White, and T.A. Minshull, Sea-floor spreading in the presence of the Iceland plume: the structure of the Reykjanes Ridge at 61°4 0'N, *Journal of the Geological Society of London., 152*, 1995.

Smith, P.J., The intensity of the Tertiary geomagnetic field, *Geophys. J. R. Astron. Soc., 12*, 239-258, 1967.

Steinthorsson, S., N. Oskarsson, and G.E. Sigvaldason, Origin of alkali basalts in Iceland: a plate tectonic model, *J. Geophys. Res., 90*, 10027-10042, 1985.

Tryggvason, K., E.S. Husebye, and R. Stefansson, Seismic image of the hypothesized Icelandic hot spot, *Tectonophyics, 100*, 97-118, 1983.

Walker, G.P.L., Geological investigations in eastern Iceland, *Bull. Volcanol., 27*, 351-363, 1964.

Ward, P.L., New interpretation of the geology of Iceland, *Geol. Soc. Am. Bull., 82*, 2991-3012, 1971.

Young, K.D., B. Jancin, and N.I. Orkan, Transform deformation of tertiary rocks along the Tjörnes Fracture Zone, North Central Iceland, *J. Geophys. Res., 90*, 9986-10010, 1985.

THE NE-ATLANTIC SYSTEM

Laurent Geoffroy[1], and Laurent Gernigon[2]

1: UFR Sciences et Techniques, Université du Maine, UMR 6112 « Planétologie et Géodynamique »
2: Geological Survey of Norway (NGU), Leiv Eirikssons vei 39, Trondheim, Norway

The NE-Atlantic system represents the northward propagation of the Atlantic Ocean north of the Charly Gibbs Fracture Zone (Fig. 1). This region includes both continental and oceanic domains and experienced a long and complex tectonic evolution since the Caledonian orogen.

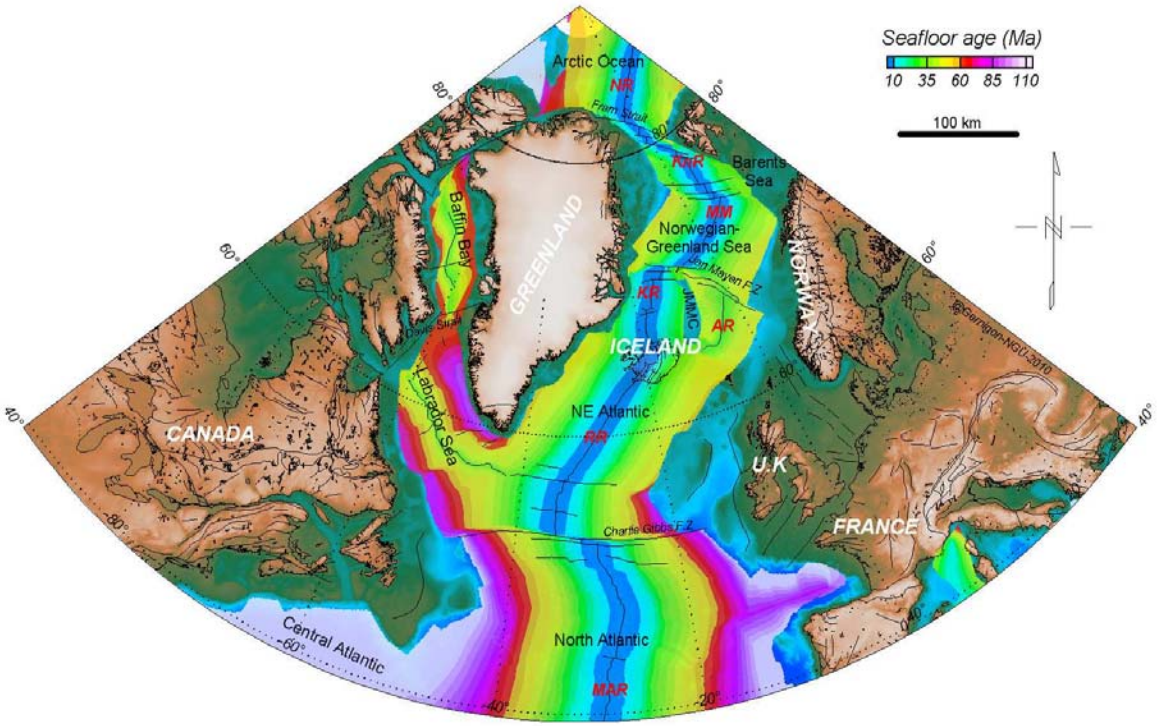

Figure 1: Main features of the NE Atlantic region. Seafloor ages after Müller et al. (2008), elevation grid after Sandwell and Smith (1997). AR: Aegir Ridge, JMMC: Jan Mayen microcontinent, KR: Kolbeinsey Ridge, KnR: Knipovich Ridge, MAR: Mid. Atlantic Ridge, MR: Mohn´s Ridge, NR: Nansen Ridge, RR: Reykjanes Ridge.

During the Lower Palaeozoic, the Laurentia and Baltica continents progressively became a single continent (Laurussia) through subduction of the Iapetus oceanic lithosphere. The consecutive orogen formed the Caledonian fold belt extending from N-America to N-Europe by the end of the Silurian (Fig. 1). The Pangaea supercontinent was subsequently affected by the Variscan Carboniferous collision between Laurussia and Gondwana. These two orogens set the structural grain for later tectonic episodes and reactivation.

During the Devonian, the Caledonian belt collapsed under its own weight and initiated the earliest stages of a very long period of lithosphere extension between Greenland and Europe. This extension spanned, although episodically, until continental breakup in the Early Tertiary (Fig. 2).

Although it is unclear if the control is crustal or mantellic, crustal extension and the resulting formation of rift basins between Norway and Greenland attempted to fragment Pangaea along a weakness zone sub-parallel to the ancient Iapetus Ocean (Ziegler, 1999; Torsvik et al., 2002; Lundin and Doré, 2005, Faleide et al., 2008).

In the NE Atlantic, rift developed sporadically during the Late Permian and continued into the Early Triassic (Fig. 2). During Early and Middle Jurassic times, the rift axis propagated progressively northwards concomitantly with the formation of the Central Atlantic Ocean. Following the intense rift tectonics of the

Permian and Triassic, areas between Scandinavia and East Greenland were, however, subject only to a period of reduced tectonic activity during this period.

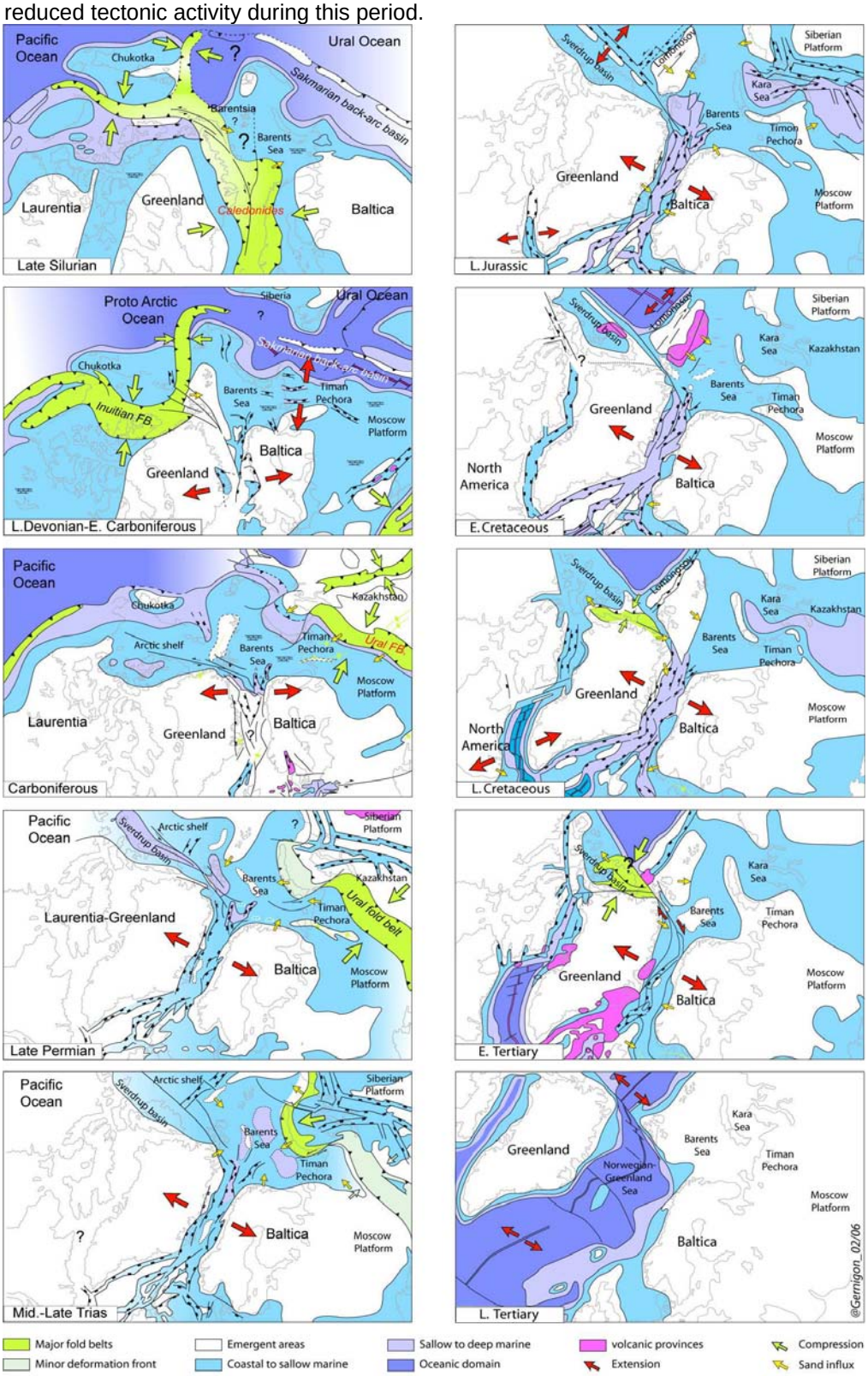

Figure 2: Schematic cartoon of the geodynamic evolution of the North Atlantic and Arctic Region (modified after Ziegler et al. 1999, Smelror et al., 2009)

The late Jurassic-Early Cretaceous period probably represents the most important rift episode in terms of lithospheric stretching and thinning. A new extensional axis propagated northward between Greenland and Canada and was superimposed on the older rift structure. Breakup and early oceanic accretion occurred along this axis in the Labrador Sea at Chron 33 or Chron 27 (a debated issue) whereas continental extension propagated in the Baffin Bay (Geoffroy et al., 2001). In the NE-Atlantic this period clearly individualized a hyper-extended rift axis from Rockall Trough to the south to the Lofoten to the north (Fig. 2). Nowhere did true oceanic crust formed between Greenland and Europe but serpentinized peridotites are thought to nearly floor part of the major rift basins (e.g Rockall Trough, Møre Basin ?).

Regional extension continued during Cretaceous but the last rift climax developed in the very Late Cretaceous (Campanian)-Paleocene before the onset of a major regional uplift observed from West-Greenland to Europe in latest Maastrichtian-Early Paleocene (Gernigon et al., 2004). This uplift was followed in Late Paleocene-Early Eocene by a significant volcanic event leading to the formation of the so-called “North Atlantic Large Igneous Province”. The averaged rate of magma extrusion was in the range of 1-2 cubic kilometres a year at that time. This transient magmatic episode has long-time been interpreted as reflecting the impact and spreading of the Icelandic "mantle plume" head beneath the thinned NE-Atlantic lithosphere (White and McKenzie, 1989). It should however be noticed that other interpretations challenge this hypothesis now (Lundin and Doré, 2005; Meyer et al., 2007).

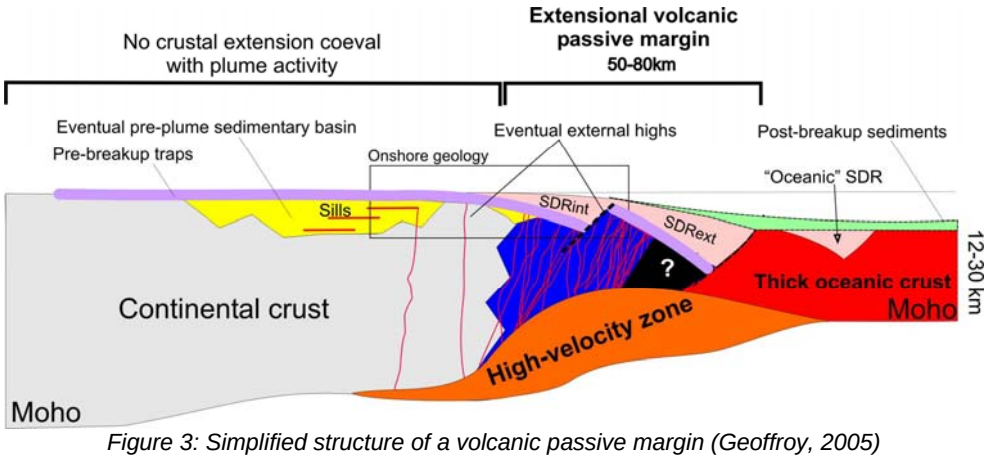

Figure 3: Simplified structure of a volcanic passive margin (Geoffroy, 2005)

A very important event, associated with the North Atlantic Large Igneous Province is the breakup of the continental lithosphere and the onset of oceanic accretion in the NE-Atlantic Ocean and Baffin Bay, respectively. The first magnetic chron in the NE-Atlantic is recorded at 24n (Early Eocene age ~-53 Ma). In these regions, the lithospheric rupture was accompanied by punctual mantle melting and consecutive increase in melting rates along the proto-breakup axis. Association between huge mantle melting and fast-rate lithosphere extension gave birth to a particular type of passive margins. The so-called volcanic passive margins are mostly characterised by magma emplaced in the crust as intrusions (underplated mafic bodies, dyke swarms, sills) and important lava flows forming the Seaward Dipping Reflectors (SDRs) developed along the proto-breakup axis (Fig. 2).

Volcanic margins are specifically located immediately north of the Davis Strait in the Labrador-Baffin system and from the Charly Gibbs Fracture Zone to the Lofoten Margin in the NE-Atlantic (Fig. 1). It must also be noticed that the Arctic oceanic rift (Fig. 1) formed at the same time but no major magmatism occurred there during the breakup. From C24 to C13, the Reykjanes, Aegir and Nansen Ridges were active together but locally dislocated by major transform (e.g. Jan Mayen Fracture Zone) or megashear regions (e.g. Fram Strait) accommodating the Greenland-Europe divergence in the ~NW-SE trend (Engen et al., 2008; Gernigon et al., 2009; Gaina et al., 2009) (Fig. 2). The coeval functioning of two divergent axes from apart Greenland during the Early Palaeogene was associated with the northward drift of the new Greenland Plate to the N-NW leading to the formation of the Eurakan intraplate transpressional to collisional foldbelt NW of Greenland (notably in the Ellesmere, Axel Heiberg and Spitzbergen areas) (Fig.

4). North-East of Greenland, this northward displacement was guided by the pre-existing Fram Strait configuration (Fig. 4).

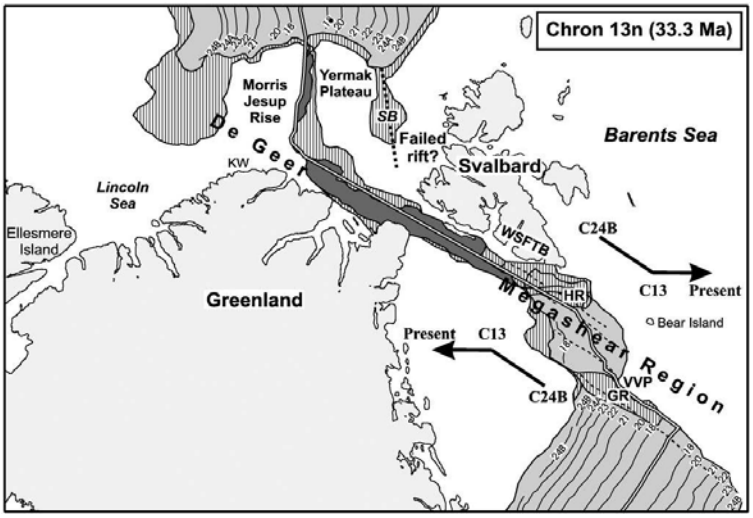

Figure 4: Plate tectonic reconstruction of the Fram Strait region to Chron 13 times (earliest Oligocene), when relative plate motion between Greenland and Eurasia changed from right-lateral shear to oblique divergence (arrows). Figure after Engen et al. (2008)

Major plate reorganization occurred during the earliest Oligocene (~C13, 33,3 Ma). Extinction of the Labrador-Baffin spreading axis was coeval with a major kinematic change within the NE-Atlantic (Skogseid et al., 2000; Gaina et al., 2009). The Aegir axis died and the creation of a new spreading axis east of Greenland along the Kolbeinsey Ridge, led to the insulation of the Jan Mayen microcontinent (Fig. 1). This was associated with a major change of the kinematic vector between North-America (including Greenland) and Eurasia. From C13, Greenland was no more a plate and no more compression acted in the Eurekan area and a transtensional oceanic opening progressively initiated within the Fram Strait (Engen et al., 2008; Døssing et al., 2010). Assuming that the onset of deep-water exchange depended on the formation of a narrow, oceanic corridor, the Fram Strait gateway between the Artic and NE-Atlantic oceans probably formed during early Miocene times (20–15 Ma) (Engen et al., 2008).

Since the Eocene, mantle melting is locally in excess beneath the NE-Atlantic Reykjanes spreading axis as outlined by thicker-than-normal oceanic crust observed along the transverse Greenland-Iceland-Faeroe aseismic ridge (Fig. 2), where crust thickness is locally as high as 35-40 km. This ridge was long-time emerged (like the present-day Iceland) and displays similar tectonic features with the adjacent volcanic margins (such like oceanic SDRs, cf. Fig. 3). Like Iceland the high melting rates beneath the ridge is interpreted as accretion over the residual tail of the Thulean mantle plume but its apparent symmetry is still problematic (Lundin and Doré, 2005; Meyer et al., 2007).

To conclude, the topography and bathymetry of the NE-Atlantic domain is strongly controlled by its past evolution and, notably, by abnormal mantle melting in the area since the Palaeocene. Because the crust is often thicker than normal (at both passive margins and in the oceanic domain), the lithosphere is lighter. This isostatic effect depends on the finite amount of past mantle melting. Because melting was heterogeneous (rate and/or duration), the bathymetry of the NE-Atlantic and the Labrador-Baffin is highly contrasted (Fig. 1). These lithospheric controls of the bathymetry are possibly combined with dynamical mantle uplift and low density of a hotter-than-normal asthenosphere, creating the net and large positive geoid anomaly over the area.

References

Døssing, A., Stemmerik, L., Dahl-Jensen, T. & Schlindwein, V. 2010: Segmentation of the eastern North Greenland oblique-shear margin — Regional plate tectonic implications. *Earth and Planetary Science Letters* 292, 239-253. Engen, O., Faleide, J.I. & Dyreng, T.K. 2008: Opening of the Fram Strait gateway: A review of plate

tectonic constraints. *Tectonophysics* 450(1-4), 51-69. Faleide, J.I., Tsikalas, F., Breivik, A.J., Mjelde, R., Ritzmann, O., Engen, Ø., Wilson, J. & Eldholm, O. 2008: Structure and evolution of the continental margin off Norway and the Barents Sea. *Episodes* 31(1), 82-101.

Gaina, C., Gernigon, L. & Ball, P. 2009: Paleocene-Recent plate boundaries in the NE Atlantic and the formation of the Jan Mayen microcontinent. *Journal of the Geological Society, London* 166, 1-16. Geoffroy, L., Callot, J.P., Scaillet, S., Skuce, A., Gelard, J.P., Ravilly, M., Angelier, J., Bonin, B., Cayet, C., Perrot, K. & Lepvrier, C. 2001: Southeast Baffin volcanic margin and the North American-Greenland plate separation. *Tectonics* 20(4), 566-584.

Geoffroy, L. 2005: Volcanic passive margins. *Comptes Rendus Geoscience* 337(16), 1395-1408. Gernigon, L., Ringenbach, J.C., Planke, S. & Le Gall, B. 2004: Deep structures and breakup along volcanic rifted margins: Insights from integrated studies along the outer Vøring Basin (Norway). *Marine and Petroleum Geology* 21(3), 363-372.

Gernigon, L., Olesen, O., Ebbing, J., Wienecke, S., Gaina, C., Mogaard, J.O., Sand, M. & Myklebust, R. 2009: Geophysical insights and early spreading history in the vicinity of the Jan Mayen Fracture Zone, Norwegian-Greenland Sea. *Tectonophysics* 468(1-4), 185 -205.

Lundin, E. & Doré, A.G. 2005: NE Atlantic break-up: a re-examination of the Iceland mantle plume model and the Atlantic-Arctic linkage. *In* Doré, A. G. & Vining, B. A. (eds.) *Petroleum geology: North-West Europe and Global perspectives-Proceedings of the 6th Petroleum Geology Conference*. Geological Society of London, 739-754.

Meyer, R., van Wijk, J. & Gernigon, L. 2007: The North Atlantic Igneous Province: a review of models for its formation. *In* Foulger, G. R. & Jurdy, D. M. (eds.) *Plates, plumes and Planeary processes*. Geological Society of America Special paper 430, 525-552. Müller, R.D., Sdrolias, M., Gaina, C. & Roest, W.R. 2008: Age, spreading rates, and spreading asymmetry of the world's ocean crust. *Geochemistry Geophysics Geosystems* 9, Q04006, doi:10.1029/2007GC001743.

Sandwell, D.T. & Smith, W.H.F. 1997: Marine gravity anomaly from Geosat and ERS1 satellite altimetry. *Journal of Geophysical Research* 102(B5), 10039-10054.

Skogseid, J., Planke, S., Faleide, J.I., Pedersen, T., Eldholm, O. & Neverdal, F. 2000: NE Atlantic continental rifting and volcanic margin formation. *In* Nøttvedt, A. (eds.) *Dynamics of the Norwegian margin*. Geological Society Special Publications 167, 295-326 Smelror, M., Petrov, O., Larssen, G.B. & Werner, S.C. 2009: *ATLAS: Geological History of the Barents Sea*. Norges geologiske undersøkelse (Geological Survey of Norway, NGU), 135 pp.

Torsvik, T.H., Carlos, D., Mosar, J., Cocks, R.M. & Malme, T.N. 2002: Global reconstructions and North Atlantic paleogeography 440 Ma to Recent. *In* Eide, E. & Coord. (eds.) *BATLAS: Mid Norway plate reconstructions atlas with global and Atlantic perspectives:*. Geological Surevy of Norway, 18-39.

White, R.S. & McKenzie, D. 1989: Magmatism at rift zones: the generation of volcanic continental margins and flood basalts. *Journal of Geophysical Research* 94, 7685-7729. Ziegler, P.A. 1989: Evolution of the North Atlantic-An Overview. *In* Tankard, A. J. & Balkwill, H. R. (eds.) *Extensional Tectonics and Stratigraphy of the North Atlantic Margins.* American Association of Petroleum Geologists, 111-129.

THE HOLOCENE CLIMATIC HISTORY OF THE CIRCUM-ICELANDIC OCEANIC REALMS

Jacques GIRAUDEAU
Université de Bordeaux, CNRS, UMR 5805 EPOC, Avenue des Facultés, 33405 Talence cedex, France,
j.giraudeau@epoc.u-bordeaux1.fr

Abstract

One of the achievements of the IPY was to foster an unprecedented amount of research initiatives aiming at studying recent (Holocene) changes in ocean circulation and climate in the subarctic and arctic domains. Paleo-investigations offer invaluable information on natural environmental changes at decadal to millennial scale, as well as on the processes driving them. We hereby present some recent results based on proxy records from circum Icelandic areas.

Introduction

The northern North Atlantic and its subarctic and arctic seas have shown in recent decades unprecedented changes in physical and chemical conditions, which directly influence the ecosystem structure and processes. This region is extremely sensitive to the changes related to the human-induced global warming (IPCC 2007) since there is an intricate connection of cryospheric (ice-sheets and sea-ice), atmospheric (winds related to strong gradients in sea-level pressures) and oceanic (through the opposition of northward flowing Atlantic water and southward flowing polar waters) processes. In particular, satellite observations have revealed a considerable decline in sea ice cover, mostly for the seasonal sea ice which constitutes approximately 50% of total ice coverage for the Arctic and the Antarctic (Serreze et al., 2007). The decline in seasonal ice extent is of particular concern since sea ice not only plays a central role in polar ecosystems but also has a great influence onto the Earth climate system itself. The sensibility of the marine biosphere to changes in local physico-chemical characteristics of the northern North Atlantic has been evidenced in the last decades by in-situ observations of biogeographical shifts of plankton biodiversity (e.g. Beaugrand et al., 2002) or satellite observations showing drastic modifications in phytoplankton community (e.g. coccolithophore blooms in the Iceland Sea and the Barents Sea). Theses changes are thought to reflect modifications in the stratification and temperature of the water column linked with freshening of the northern ocean induced by sea-ice melting (Curry and Maulitzen, 2005) and increased surficial temperature due to increased northward inflow of Atlantic water (Hatun et al., 2005).

The instrumental record is far too short to document the full range of natural variability. In order to produce more reliable predictions of future change, data on longer time scales than the instrumental records, are needed. The climatic history of the past 2000 years with a succession of warm (Roman, Mediaeval) and cold (Little Ice Age) periods shows that rapid climate changes have occurred repeatedly in the recent past with major implications for human settlement throughout the Nordic seas (i.e. Inuit and Viking cultures). In addition, new evidences for optimal thermal conditions during the early part of the present interglacial (Holocene) suggest that the Arctic might have been seasonally ice-free around 9000 yrs before present (Fisher et al., 2006) to an extent which might only be reached by the mid-21st century (Johannessen et al. 2004). However, discrepancies between observed and simulated sea ice distribution raises a need for improving our understanding of the sensitivity of the high latitude feedbacks. There is a crucial need to gain detailed information on the amplitude, the regional patterns, and the mechanisms of past environmental changes observed during the Holocene in order to predict the scale of current climate change. This information can be obtained using two complementary approaches, namely proxy records from marine sedimentary archives and paleoclimate modelling experiments. Proxy records are ideal to document regional ecosystem changes and to assess the physical-chemical processes which drove these ecological shifts.

The aim of this presentation is to question the view of a climatically stable Holocene period, and to provide, based on new proxy-based data, some tips on the regional complexity of both long and short-

term (millennial to centennial) climate and ocean circulation changes in the circum-Icelandic oceanic realms.

Oceanographic setting

The Iceland shelf and nearby oceanic realms bear essential components of the present surface, intermediate and deep circulation of the northern North Atlantic (Hopkins, 2001; Fig. 1). It is located close to the Arctic front which separates Arctic/Polar water masses carried by the southeastward East Iceland Current from Atlantic waters (AW). Atlantic waters bathing the western and north-central Iceland shelf originate from the North Iceland Irminger Current, a branch of the Irminger Current; whereas the eastern and north-eastern shelf are fed with warm waters from the main corridor of Atlantic waters toward the Nordic Seas (the North Atlantic Drift and Norwegian Atlantic Current).

Iceland separates an eastern (Iceland-Scotland) strait from a western (Denmark) strait, the passageways of surface Atlantic water inflow to the Nordic Seas and Arctic Ocean, and surface and bottom outflow to the mid-latitudes of the Atlantic Ocean. In terms of volume, the AW inflow to the Nordic Seas has been assessed through year-long instrumental measurements within both straits as ca. 8 Sv, most of this inflow being compensated by outflow from the bottom as ca. 6 Sv (surface outflow carried by the East Greenland Current being assessed at about 1.3 Sv (Blindheim, 2004).

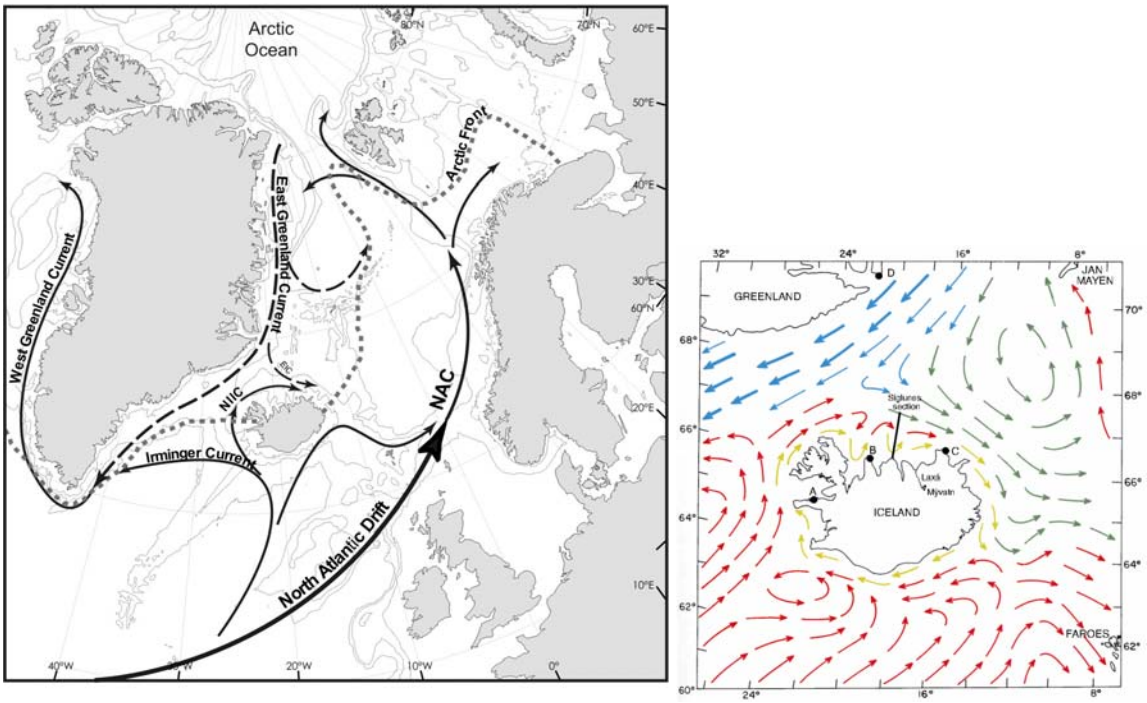

Fig. 1: Main component of the surface circulation. Left: Solid and dashed arrows represent warm and cold currents, respectively (NAC-North Atlantic Current, NIIC-North Iceland Irminger Current). The dotted line refers to the present position of the Arctic Front (after Giraudeau et al., 2010). Right: surface circulation around Iceland (red to dark blue colors refer to the SST gradient from warm Atlantic to cold Polar waters).

Together with the contour drifts moulded by the Norwegian Sea Overflow Water, and distributed along the eastern flank of the Reikjanes Ridge south of Iceland, the North Iceland Shelf stands as one the favourite play-ground for the late Quaternary/Holocene paleoceanographers. It owes it mainly because of the vertical distribution of key-elements of the surface and intermediate water masses of the Nordic Seas within a spatially restricted area.

Holocene long-term trends

A zonal diachronism in long-term Holocene sea-surface temperature (SST) trends in the mid/high latitudes of the North Atlantic, equivalent to a ca. 3.5 kyr delay between the eastern and western North Atlantic has been documented from sediment cores in the Labrador, Irminger and Iceland Seas (as summarized by Solignac et al., 2006) and the Norwegian Sea (as summarized by Jansen et al., 2008).

This zonal SST delay across the northern North Atlantic (Fig. 2; after Kaufman et al., 2004) corresponds to a similar zonal diachronism in long-term Holocene pattern of AW flow between the Denmark Strait and the Iceland-Scotland Strait (Giraudeau et al., 2010).

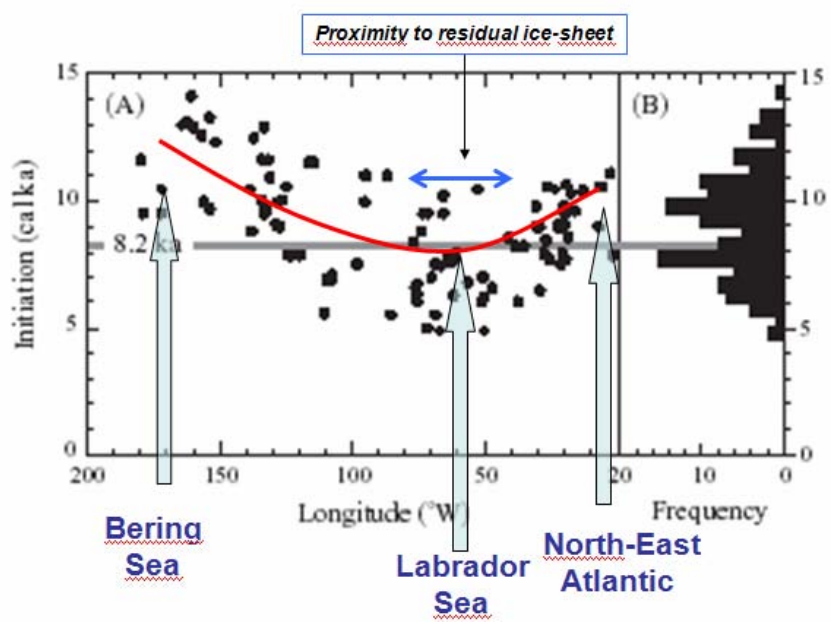

Fig. 2: Proxy-based timing of the initiation of the Holocene altithermal across a longitudinal transect from the North-East Atlantic to the Barents sea (after Kaufman et al., 2004). The horizontal blue arrow points to the area close to the remnant Laurentide ice-sheet, where the maximum delays are recorded.

As suggested by Marchal et al. (2002), this delayed recovery of the circulation pattern close to Greenland might be related to the relative inertia of the remnant Laurentide ice sheet compared to the Fennoscandian following the last deglaciation. Surface circulation off north-west Iceland seems to follow this western Atlantic pattern, some biotic proxy-records indicating peak penetration of Irminger Current Water (in the form of Intermediate waters) between 3.5 and 5.5 cal kyr BP (Fig. 3; Giraudeau et al., 2004). A potential influence of the more proximal Greenland ice cap as shown by Jennings et al. (2006) for the last glaciations might also partly explain this diachronism, although the volume of fresh water released by this ice cap was much smaller than that from the Laurentide Ice Sheet. Foraminiferal-based SST estimates in the nearby Irminger Sea also provide evidence for maximum thermocline temperature centred at 4-5 cal kyr BP (Came et al., 2007), hereby confirming the circulation trend reconstructed off NW Iceland.

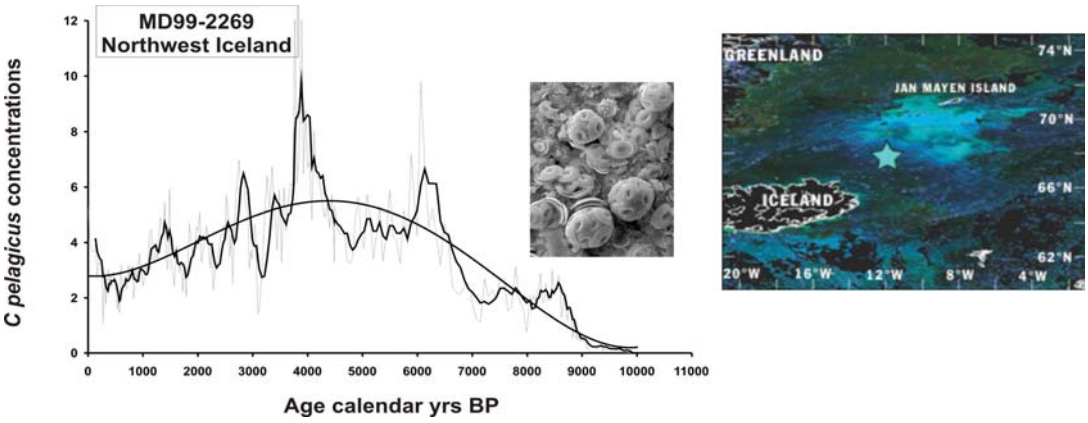

Fig. 3: The overwhelming contributor to carbonate production and sedimentation off Iceland is the coccolithophore species C. pelagicus (central picture) who might occasionally bloom in arctic waters (right picture). Carbonate

production off Iceland is tightly linked with input of nutrient-rich Irminger waters. The Holocene record of C. pelagicus concentration off NW Iceland suggest maximum input of Atlantic/Irminger water between 3.5 and 4.5 cal kyr BP (Giraudeau et al., 2004).

A special point should however be raised on differences in reconstructed SSTs and circulation trends between the northwestern and the north central-eastern Icelandic shelf, this last area showing an Holocene climatic optimum 2 to 3000 years before its western counterpart. Such local disagreements might be explained by differences in environmental signature of the various proxies, and/or the influence of the local topography on circulation features.

Millenial-scale variability

Terrestrial and ice-core data from circum-North Atlantic locations point to millennial-scale anomalies of Holocene climate in relation with changes in the modes of atmospheric and oceanic circulation and transport of heat to high latitudes (e.g. Denton and Karlen, 1973; Magny, 2004; Dahl and Nesje, 1996). Although hardly temporarily consistent and reproducible, geochemical (Came et al., 2007; Oppo et al, 2003) and sedimentological (Andrews 2009; Bianchi and McCave, 1999; Bond et al., 1997; Hall et al., 2004, Rousse et al., 2006) records from the subpolar and polar North Atlantic, support the implication of the surface and deep ocean circulation patterns in the amplification of these recurrent recent climate anomalies and their transmission to distant areas. A major pitfall in this last assumption on Holocene times is the lack of firm, direct evidences for recurrent millennial-scale changes in the dynamics of the North Atlantic Drift (NAD) component of the meridional overturning circulation. While suggesting the existence of centennial to millennial-scale modulations of the surface circulation in the Nordic seas (Risebrobakken et al., 2003; Andersen et al., 2004) and the subpolar gyre (Giraudeau et al., 2000; Came et al., 2007), biotic proxy-records available so-far often suffer from either subdued amplitude of changes or limited temporal resolution, and are therefore hardly conclusive.

Still, the most undisputable evidences for pervasive millennial-scale changes in Holocene climate are provided by terrestrial and ice-core records which all highlight recurrent changes in the modes of atmospheric circulation in the boreal Atlantic.
The time series of sea-salt sodium (ssNa) flux in the Greenland Ice Sheet Project Two (GISP2) core (O'Brien et al., 1995), believed to be an indicator of winter storminess and sea spray in the atmosphere of the high-latitude North Atlantic, strikingly exhibits peaks at times similar to the Holmsa loess record of windy, winter-like conditions over southern Iceland compiled by Jackson et al. (2005). The mean grain size of the loess from Holmsa, in turn shows a succession of peaks coeval with higher than average winter precipitation in the maritime climate-influenced southern Norway (Bjune et al., 2005).

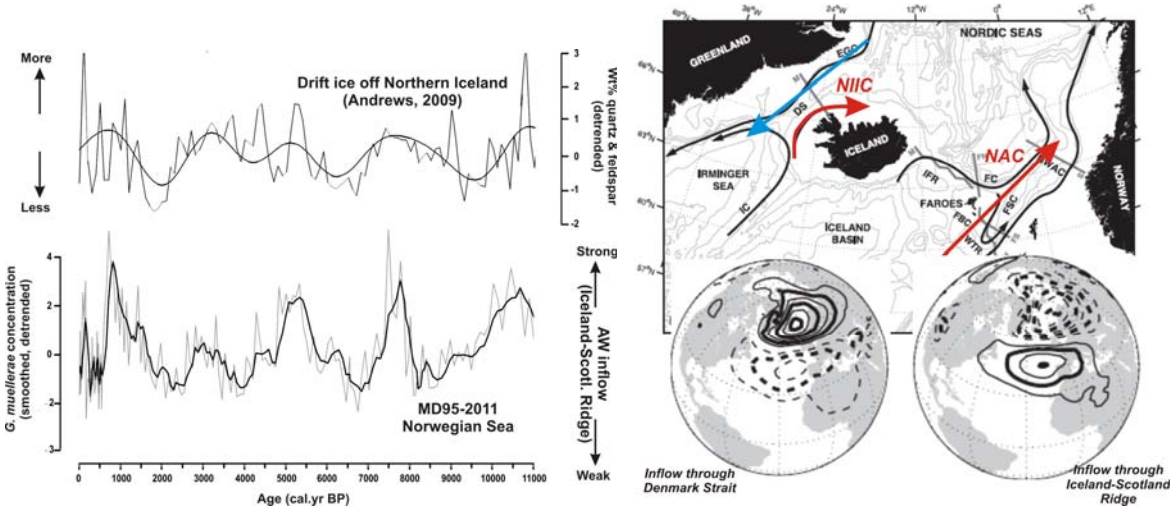

Figure 4: Left - Detrended and smotthed biotic record of AW flow into the Norwegian Sea (Giraudeau et al., 2010) compared with the detrended stacked record of IRD-based drift ice off Northern Iceland (Andrews, 2009). Right – Winter mean sea level pressure regressed on standardized simulated inflows of Atlantic waters into the Nordic Seas. Isolines are drawn at 0.5 mb intervals, negative values with dashed lines (from Nilsen et al., 2003).

Recent marine proxy-records (Fig. 4 left) such as drift ice abundances off Northern Iceland (Andrews, 2009) or the Holocene paleodynamics of AW flow through the Denmark and Iceland-Scotland Straits (Giraudeau, 2010) suggest that the intensity of the southward polar and arctic water outflow carried by the East Greenland Current varied according to a millennial pacing, and in phase with the inflow of the North Atlantic Current to the Norwegian Sea. Such a pattern is consistent with dynamical considerations which relate the present tight link between the AW inflow in the Iceland Scotland Ridge and the polar outflow to the Denmark Strait to the winter-average cyclonic conditions over the Greenland, Iceland and Irminger seas (Fig. 4 right; Blindheim et al., 2000; Nilsen et al., 2003).

References

Andersen C., Koç N., Moros M., 2004, A highly unstable Holocene climate in the subpolar North Atlantic: evidence from diatoms. *QSR*, 23, 2155-2166.

Andrews J.T., 2009, Seeking a Holocene drift ice proxy: non clay mineral variations from the SW to N-central Iceland shelf: trends, regime shifts, and periodicities. *JQS*, 24, 664-676.

Beaugrand, G., Reid, P.C., Ibanez, F., Lindley, A.L., Edwards, M., 2002, Reorganization of North Atlantic marine copepod biodiversity and climate. *Science,* 296, 1692-1694.

Bianchi G.G., McCave I.N., 1999, Holocene periodicity in North Atlantic climate and deep-ocean flow south of Iceland. *Nature,* 397, 515-517.

Bjune A.E., Bakke J., Nesje A., Birks H.J.B., 2005, Holocene mean July temperature and winter precipitation in western Norway inferred from palynological and glaciological lake sediment proxies. *The Holocene*, 15, 177-189.

Blindheim J., Borovkov V., Hansen B., Malmberg S.-A., Turrell W.R., Osterhus S., 2000, Upper layer cooling and freshening in the Norwegian Sea in relation to atmospheric forcing. *DSR I*, 47, 655-680.

Blindheim J., 2004, Oceanography and climate. In: Skjoldal H.E. (Ed.), *The Norwegian Sea Ecosystem*. Tapir Academic Press, Trondheim, pp. 65-95.

Bond G., Showers W., Cheseby M., Lotti R., Almasi P., de Menocal P., Priore P., Cullen H., Hajdas I., Bonani G., 1997, A pervasive millenial-scale cycle in North Atlantic Holocene and Glacial Climates. *Science*, 278, 1257-1266.

Came R.E., Oppo D.W., McManus J.F., 2007, Amplitude and timing of temperature and salinity variability in the subpolar North Atlantic over the past 10 k.y.. *Geology*, 35, 315-318.

Curry R., and Mauritzen C., 2005, Dilution of northern North Atlantic ocean in recent decades. *Science,* 308, 1772-1774.

Dahl S.O., Nesje A., 1996, A new approach to calculating Holocene winter precipitation by combining glacier equilibrium-line altitudes and pine-tree limits: a case study from Hardangerjøkulen, central southern Norway. *The Holocene*, 6, 381-398.

Denton G.H., Karlen W., 1973, Holocene climatic variations – Their pattern and possible cause, *QR*, 3, 155-205.

Fisher D., Dyke A., Koerner R., Bourgeois J., Kinnard C., Zdanowicz, C., et al. 2006, Natural variability of arctic sea-ice cover over the Holocene. *EOS Transactions of the AGU*, 87, 273-275.

Giraudeau J., Cremer M., Manthé S., Labeyrie L., Bond G., 2000, Coccolith evidence for instabilities in surface circulation south of Iceland during Holocene times. *EPSL*, 179, 257-268.

Giraudeau J., Jennings A.E., Andrews J.T., 2004, Timing and mechanisms of surface and intermediate water circulation changes in the Nordic Seas over the last 10 000 cal. Years : A view from the North Iceland shelf. *QSR*, 23, 2127-2139.

Giraudeau J., Grelaud M., Solignac S., Andrews J.T., Moros M., Jansen E., 2010, Millenial-scale variability in Atlantic water advection to the Nordic Seas derived from Holocene coccolith concentration records. *QSR*, 29, 1276-1287.

Hatun H., Sandu A.B., Drange H., Hansen B. Valdimarsson H., 2005, Influence of the Atlantic subpolar gyre on the thermohaline circulation. *Science*, 309, 1841-1844.

Hopkins T.S., 1991, The GIN Sea – a synthesis of its physical oceanography and literature review 1972-1985. *ESR*, 30, 175-318.

Jackson M.G., Oskarsson N., Trønnes R.G., McManus J.F., Oppo D.W., Grönvold K., Hart S.R., Sachs J.P., 2005. Holocene loess deposition in Iceland: Evidence for millennial-scale atmosphere-ocean coupling, in the North Atlantic. *Geology*, 33, 509-512.

Jansen E., Andersson C., Moros M., Nisancioglu K.H., Nyland B.F.,Telford R.J., 2008, The early to mid-

Holocene thermal optimum in the North Atlantic. In: Battarbee, R.W., Binney, H.A., *Natural Climate Variability and Global Warming - A Holocene Perspective*. Wiley-Blackwell, 123-137.

Jennings A.E., Hald M., Smith M., and Andrews J.T., 2006, Freshwater forcing from the Greenland Ice Sheet during the Younger Dryas: Evidence from southeastern Greenland shelf cores. *QSR*, 25, 282–298.

Johannessen O. M. et al., 2004, Arctic climate change: observed and modelled temperature and sea-ice variability. *Tellus* 56A, 328-341.

Kaufman D.S., et al., 2004, Holocene thermal maximum in the western Arctic (0-180°W). *QSR*, 23, 529-560.

Magny M., 2004, Holocene climatic variability as reflected by mid-European lake-level fluctuations, and its probable impact on prehistoric human settlements. *QI*, 113, 65-80.

Marchal O., Cacho I., Stocker T.F., Grimalt J.O., Calvo E., Martrat B., et al., 2002, Apparent cooling of the sea surface in the northeast Atlantic and Mediterranean during the Holocene. *QSR*, 21, 455-483.

Nilsen J.E.O., Gao Y., Drange H., Furevik T., Bentsen M., 2003, Simulated North Atlantic – Nordic Seas water mass exchanges in an isopycnic coordinate OGCM. *GRL*, 30, 1536.

O'Brien S.R., Mayewski P.A., Meeker L.D., Meese D.A., Twickler M.S., Whitlow S.I., 1995, Complexity of Holocene climate reconstructed from a Greenland ice core. *Science*, 270, 1692-1694.

Oppo D.W., McManus J.F., Cullen J.L., 2003, Deepwater variability in the Holocene epoch. *Nature*, 422, 277-278.

Risebrobakken B., Jansen E., Andersson C., Mjelde E., Hevroy K., 2003, A high-resolution study of Holocene paleoclimatic and paleoceanographical changes in the Nordic Seas. *Paleoceanography*, 18, 1017.

Rousse S., Kissel C., Laj C., Eiríksson J., Knudsen K.L., 2006, Holocene centennial to millennial-scale climatic variability: evidence from high-resolution magnetic analyses of the last 10 cal kyrs off North Iceland (core MD99-2275). *EPSL*, 242, 390–405.

Serreze M.C., Holland M.M., Stroele J., 2007, Perpsectives on the Arctic's shrinking sea-ice cover. *Science*, 315, 1533-1536.

Solignac S., Giraudeau J., de Vernal A., 2006, Holocene sea surface conditions in the western North Atlantic: Spatial and temporal heterogeneities. *Paleoceanography* 21, PA2004.

ROCK GLACIERS AND RELICT DEBRIS BODIES IN CENTRAL NORTH ICELAND

Gudmundsson Agust

Jarðfræðistofan (GEOICE Geological Services) Reykjavik Iceland. email. jardis@geoice.net

Abstract

Active rock glaciers exist in the mountains of north and east Iceland and are also found very scattered in the south and west Iceland. They are normally found below N and NE facing cirques at altitudes higher than 800m but are occasionally detected at elevation down to 600m. In the mountainous costal areas of west, north west, north and east Iceland exist numerous debris bodies fulfilling all criteria requested for relict rock glaciers. In some cases we have continuous sequence from active rock glaciers at the top, changing over to relict debris bodies at lower altitudes. Spatial distribution of these debris formations in central north Iceland has been analysed and are discussed.

Introduction

Rock glaciers (RG) are tongue shaped bodies or lobate features generally composed of angular boulders. Their form resembles usually the form of a small outlet glaciers, in active state often with steep 20-40m high fronts and normally showing well defined surface relief. Rock glaciers are normally devised into three stages of activity; active, inactive and relict. Active RG are considered to show the most expressive indication of permafrost in alpine topography and relict RG are considered to show expression of former cooler climate (permafrost). Rock glaciers are found at various cool climate conditions, both in dry continental mountains as well as in maritime regions. At the present, they are frequently found in mountains or costal areas adjacent to present glaciers (Humlum 1996). Definition and mapping of rock glaciers has not been extensive in Iceland as well as (until recently) in other Nordic countries (Svenson 1989).

Topography and bedrock

Tröllaskagi is a mountainous peninsula between the glacially eroded fjords, Skagafjörður and Eyjafjörður in central north Iceland, see figures 3 and 10. The bedrock of Tröllaskagi is what remains of an old plateau where mountain-tops rise frequently above 1200-1300m peaking up to 1536m in the highest mountain Kerling. The bedrock consists of late tertiary (8-13 M.y.) basalt lavas, frequently 5-15m thick, intercalated with scattered relatively thin sediments. Several relict central volcanoes exist buried in the basalt plateau, consisting of various volcanic and sedimentary rock types and tectonic structures, resulting in higher susceptibility to rock weathering than the "average" plateau basalt.

Present climatic conditions in the Tröllaskagi peninsula show annual mean temperature of 3-4 °C at sea level and precipitation of 1500-1700 mm in the upper part of the mountains. The Tröllaskagi has been more or less ice-free during at least the last 10 ka (or even longer), as supported by dated shell remains, (11,2 ka C^{14} BP uncorrected) in costal sediments at the Sauðárkrókur town in Skagafjörður and 12,7 ka (C^{14} BP uncorrected) in Héðinsfjörður and 42 ka at Almenningar west from Siglufjörður).

Figure 1. Composite talus derived and glacial derived rock glaciers near Holar in Tröllaskagi.

Mapping, definition and distribution

Rock glaciers in the mountains of Tröllaskagi, have been mapped discontinuously by the present author during the last 25 years, both in the field and by interpretation of aerial photos. The definition criteria used for active, inactive and relict rock glaciers has been described in various papers (e.g.: Warhaftig and Cox 1959; Corte 1987; Barsch, 1996, Humlum; 1998.

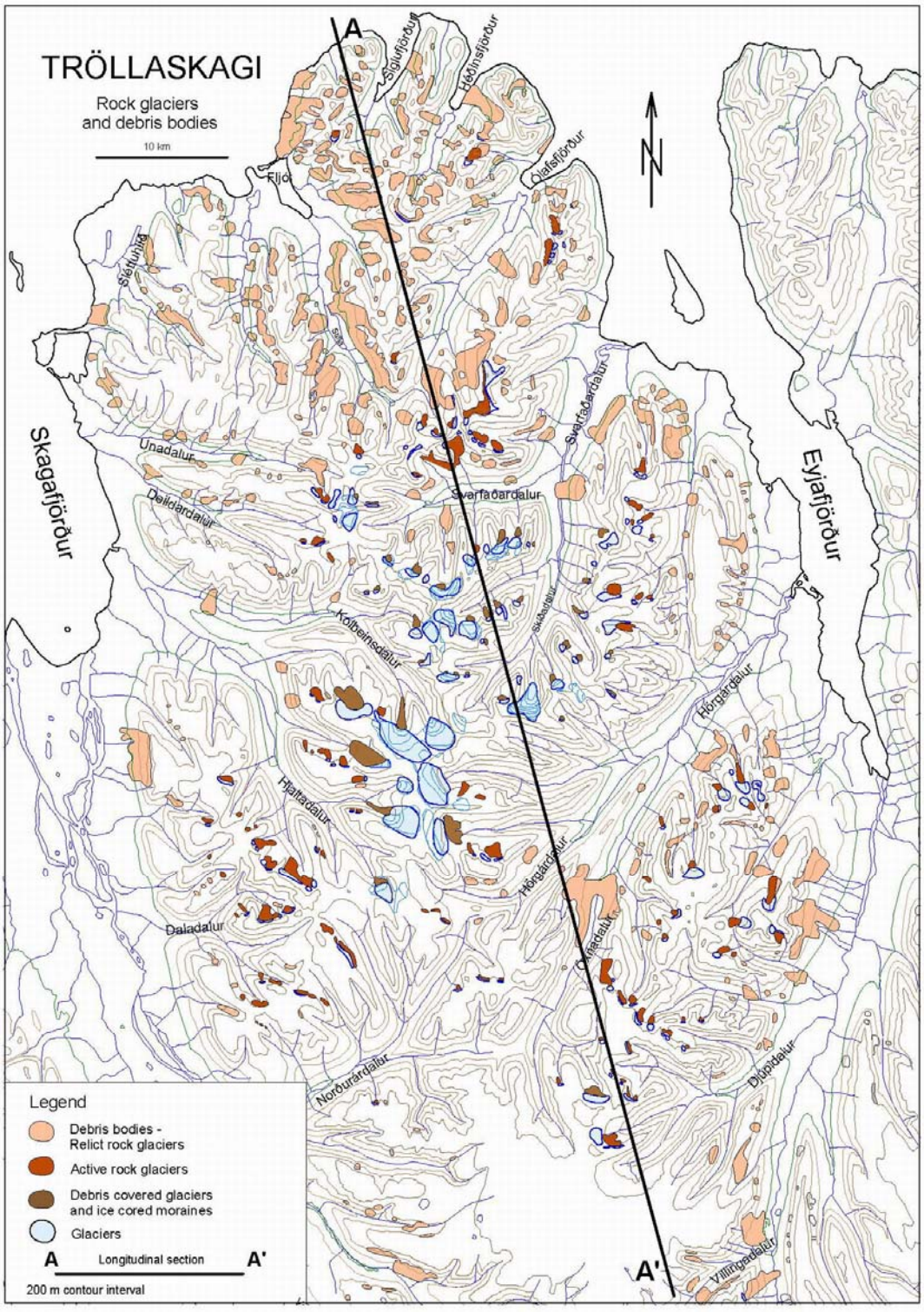

Figure 2. Map of the Tröllaskagi peninsula showing distribution of rock glaciers / debris covered glaciers

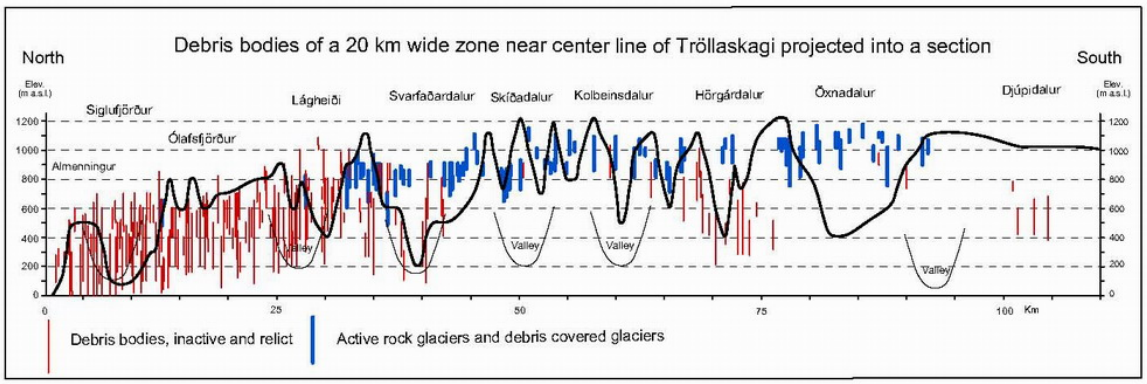

Figure 3. Section along Tröllaskagi showing active and relict rock glaciers of a 40 km wide zone, projected into section A-A'. In the central area of Tröllaskagi, only active RG exist at high altitude, probably indicating existence of glaciers there, during the formation period of relict RG in peripheral area of Tröllaskagi.

Activity and spatial distribution

All activity stages of rock glaciers are found in the Tröllaskagi mountains, active, inactive and relict. The active RG are considered to have formed during the Holocene, and the inactive RG are possibly also mainly from the Holocene time (some of them could possibly be older). Approx 570 rock glaciers have been defined, but the number might increase considerably, depending on how to define composed small lobate RG and various composite bodies of relict RG. Of the rock glaciers 165 (approx 30%) are defined active and 402 (approx. 70%) inactive and relict (most of them relict). A similar ratio of activity has been described in the Disco area W-Greenland (Humlum 1998, and in Alaska and middle west USA (Wahrhaftig and Cox 1959).

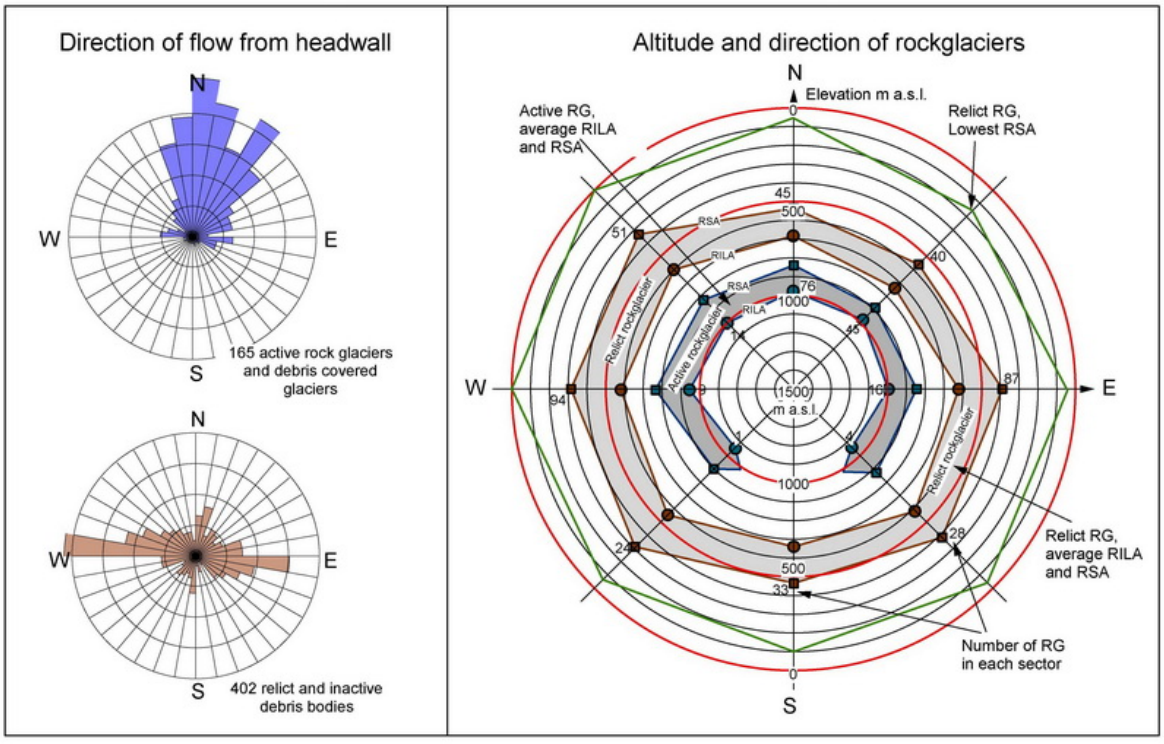

Figure 4a. Rose diagram showing directional trend of active rock glaciers and relict debris bodies defined as relict rock glaciers. Figure 4b. Diagram showing average elevation and direction of RILA and RSA for active rock glaciers and relict debris bodies defined as relict rock glaciers.

Active rock glaciers

Most of the active rock glaciers are glacially derived, showing ice on the surface in the upper part (Corte 1987). The lobate rock glaciers are normally talus derived, much smaller or especially shorter and relatively thicker (thickness/length) than the others. these are often located side by side under steep walls or in north heading cirques (see figure 1). Both the glacial- and talus derived genetic types of rock glaciers occur in composite various stages where one tongue is overridden by a younger one sometimes forming layered pile of ice cored debris bodies consisting of up to 4-5 layers (see figure 1). The average size of active rock glaciers in Tröllaskagi peninsula is approx. 0.5 km^2 forming a total area of almost 82 km^2.

Highest frequency of the active debris bodies is heading towards N and NNE with the average inclination of 17°. The average altitude of RILA (rock glacier initiation altitude (see definitions by Humlum 1988 for explanations of RILA, RAL, RSA) is 986 m a.s.l. and average RSA (rock glacier snout altitude) is at 853 m a.s.l., thus covering an average altitude difference of 133 m. The glacially derived rock glaciers extend over considerably greater altitude difference compared to the talus derived. The creep rate of several active RG has been measured as 0,2-1m / year.

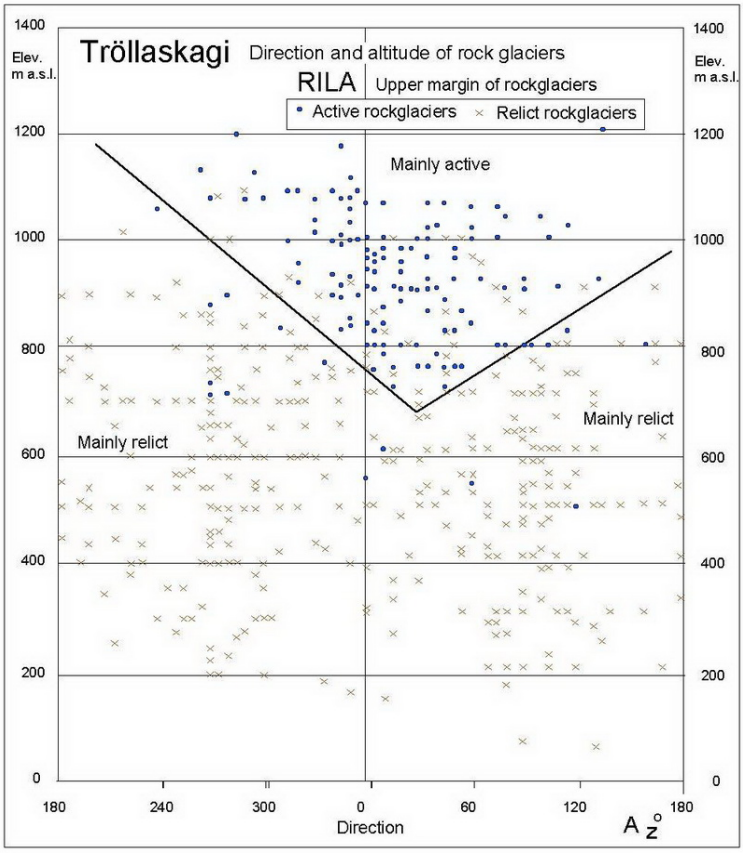

Figure 5.: Direction and elevation of individual active rock glaciers and relict debris bodies.

Relict and inactive rock glaciers

Over 400 debris bodies in the Tröllaskagi area. have been defined as relict or inactive rock glaciers. The definition criteria for relict RG and the recognition of individual bodies is mainly based on surface appearance and relief (frequently defined by using aerial photos as well as in the field). The definition is also based on internal structure, layering and on grain size distribution, compared to grain sizes of other kind of sedimentations. The material and grain size distribution resembles the internal character of active

rock glaciers, described in such literature (e.g. Evin 1987) and often also have grain distribution like Icelandic glacial moraines.

The average size of the debris bodies in the area, defined relict rock glaciers is approx. 0.8 km^2 forming a total area of 320 km^2. Highest frequency of the inactive and relict debris bodies are facing towards N-NNW and less frequency is facing E-SES. The average inclination of these bodies is 13°. Less frequently the relict rock glaciers is facing north and south. The average altitude of RILA is 629 m a.s.l. and average RSA 403 m a.s.l., thus covering a height difference of 226 m.

The RILA of both the active and relict rock glaciers is generally about 200 m lower altitude in the northern part of the peninsula compared to the southern part. Also there is a great increase in number and average size of debris bodies towards north, with high frequency of relict RG and lower ratio of the active ones. On the other hand, the relict debris bodies almost disappear in the innermost part of the deep walleyes in the middle part of the Tröllaskagi but increase in number and size towards the costal mountains of Skagafjörður and Eyjafjörður (fig. 1). On the other hand the greatest number of the active rock glaciers is found in the central part of the Tröllaskagi peninsula. The creep rate of several debris bodies or relict RG has been measured as 0,1-0,6m / year.

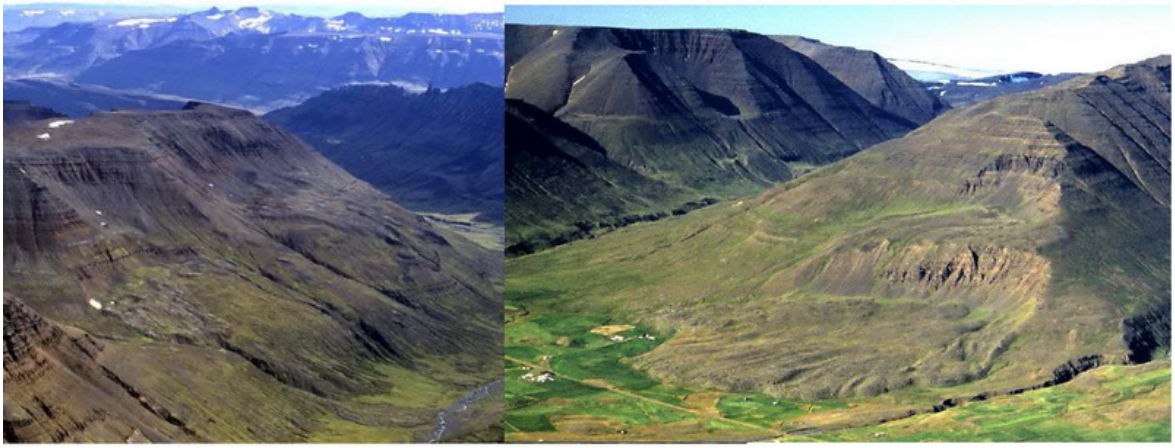

Figure 6.: Debris bodies most probably of relict rockglaciers in Eyjafjörður.

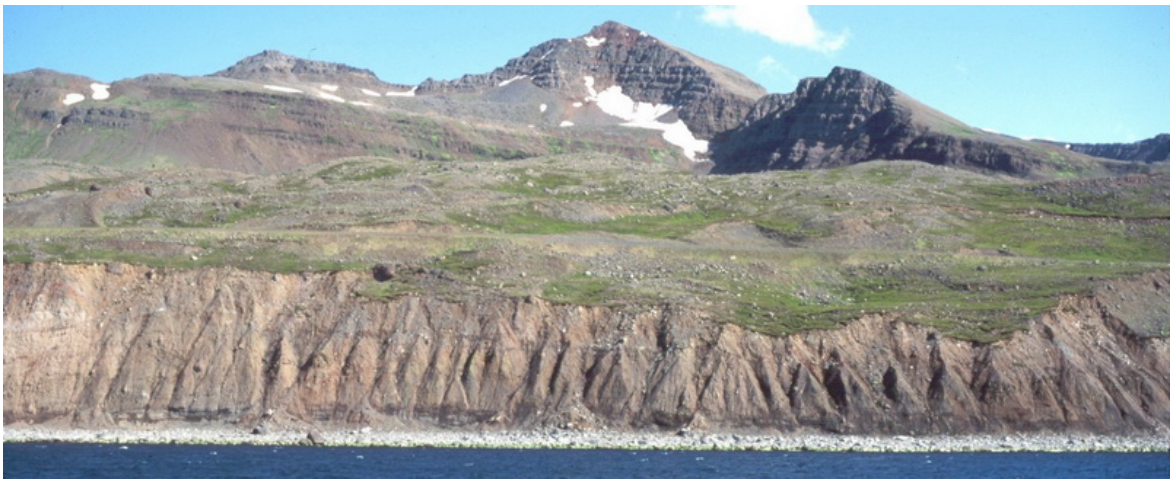

Figure 7.: Debris bodies of relict/inactive stratified rockglaciers at the sea shore west of Siglufjörður. The debris bodies are resting on stratified gravel containing shell remains C^{14} 42 ky. old.

Figure 8.: Stratified debris bodies at the sea shore west of Siglufjörður. Layers of very coarse grained subangular and angular rock fragments inbetween more fine grained and silty sediments

Traditionally these debris bodies in the Tröllaskagi area as well as elsewhere in Iceland have previously been described as sedimentations formed by bergsturz (Jónsson 1976, Sigurðsson 1990, Hjartarson 1982 and 1998), and this seems to be consistent to what is widely cited or referred to as misinterpretation in papers on rock glaciers (Barsch 1996, Giardino, Shroder and Vitek 1987).

Rock glaciers in other areas of Iceland

Although active RG and ice cored moraines are most frequent and best developed in the Tröllaskagi area, central north Iceland, such RG features also exist, almost up to the same degree in the peninsula east of Eyjafjörður as well in the mountains south of Vopnafjörður and in the mountains of east Iceland south from Héraðsflói. Scattered active RG and ice cored moraines exist in the highest mountains of east Iceland. Additionally scattered active RG are found in the surrounding mountains of Vatnajökull and a few near Langjökull, see figure 9 for brief locations..

Debris bodies classified as relict rock glaciers (and formerly ice cored moraines and debris covered glaciers) are very frequent in the peripheral range of the Vestfirðir (north west peninsula). They exist in the Snæfellsnes peninsula and in the alpine mountains of Faxaflói (Esja - Skarðsheiði). In northern Iceland the debris bodies are frequent in the high- and costal mountains of Húnaflói and Skagafjörður area, culminating around Eyjafjörður (both sides). In east Iceland the relict debris bodies are frequent in the mountains south of Héraðsflói, gradually decreasing south to the Djúpivogur area. From there (Djúpivogur) such relict debris bodies are very rare in south Iceland, along the inland and the south coast to Faxaflói.

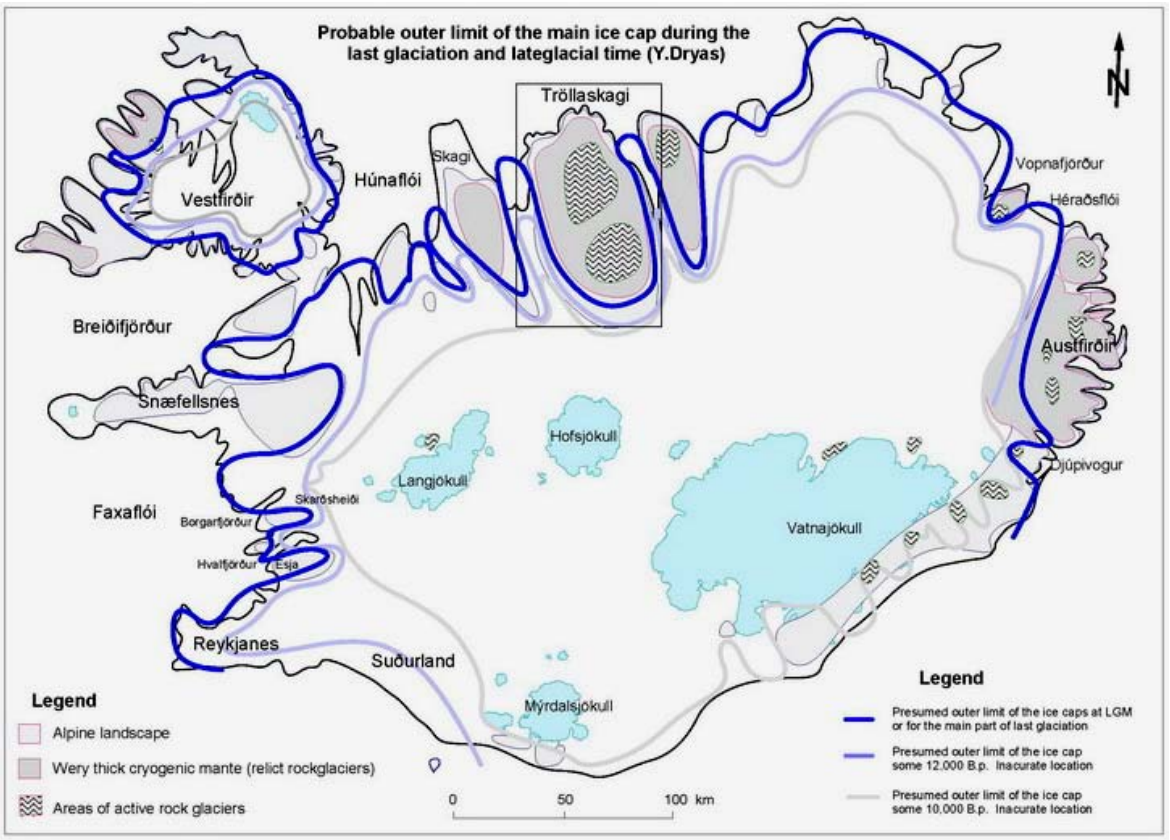

Figure 9. Iceland, distribution of rock glaciers areas and possible outer limits of the ice cap during considerable part of last glaciation.

Conclusion

Rock glaciers of all stages of activity (active, inactive and relict) exist in the mountains of Tröllaskagi middle north Iceland. The active RG are formed during the Holocene time with some periods of varying production activity resulting in layered or stratified rock glaciers.

The formation of relict rock glaciers probably took place during the Weichselian glaciation and late glacial time. At the northernmost coast of Tröllaskagi, sea shore sediments are encountered, containing shell remains expressing with dated carbon figures of over 42 ka (conventional ^{14}C BP). Directly on the top of these sea shore sediment exist relict debris bodies of relict RG presently creeping slowly towards the cost (Figs. 7 and 8). Numerous debris bodies, defined as relict rock glaciers, designate no major glaciers in the northern part of Tröllaskagi area during last glaciation.

Glacial moraines in the Skagafjörður district in addition to dated shell remains from the town Sauðárkrókur and Héðinsfjörður, indicate limited glaciers and no major glaciers in the Tröllaskagi area in lateglacial time. Distribution of debris bodies defined as relict rock glaciers in the peripheral range of the peninsula, and the low frequencies of these in the middle part of Tröllaskagi indicate valley glaciers of limited extent in the area at least during and since late glacial time.

Dated shell remains from the Reykjanes peninsula (SW Iceland) show measured dating figures in the range of 20-35 thousand years and dated volcanic rock formed over 40 thousand years ago from the same area, indicate limited glaciers in SW Iceland during the later part of last glaciation. (No dated shells have been found in Iceland from the period 13-20 thousand years ago, probably as a result of relatively low sea level during that period. The dated shell remains and rock from the Reykjanes-Faxaflói area support limited extent of the inland ice cap during Weichselian glaciation, making possibilities for growth of rockglaciers in the peripheral mountains of Iceland.

References

Hjartarson Á. 1982. Berghlaup á Íslandi. Týli 12 (1): 1-6.

Barsch, D. 1996. Rockglaciers. Indicators for the Present and Former Geoeceology in High Mountain Environments. Springer-Verlag, Heidelberg, Germany, 331 p.

Bergthorsson, Páll 1969: An Estimate of Drift Ice and Temperature in Iceland in 1000 years. Jökull 19. p. 94-101.

Capps, S. R 1910, Rock glaciers in Alaska, Jour. Geol., v. 18, pp359-375.

Corte, A. E. 1987a. Rock glacier taxonomy, in *Rock glaciers, edited by Giardino, J. R, Shroder, J. F. Jr. and Vitek, J. D., Allen and Unwin* Boston. 27-39.

Evin, M. 1987. Lithology and fracturing control of rock glaciers in southwestern Alps of France, in *Rock glaciers, edited by Giardino, J. R, Shroder, J. F. Jr. and Vitek, J. D., Allen and Unwin* Boston. 83-106.

Giardino, J.R, Shroder, J. F. and Vitek, J. D. 1987. Rock Glaciers, *Allen and Unwin Inc.* Boston. 335 pp.

Giardino, J.R. and Vick, S. G. 1987. Geological engineering aspects of Rock Glaciers, in *Rock glaciers, edited by Giardino, J. R, Shroder, J. F. Jr. and Vitek, J. D., Allen and Unwin* Boston. 265-287.

Björnsson H. 1978. The surface area of glaciers in Iceland. Jökull 28. ár, bls 31.

Björnsson H. 1991. Jöklar á Tröllaskaga. *Árbók Ferðafélags Íslands* 1991. 21-37.

Humlum O. 1998. The climatic significance of rockglaciers. Permafrost and periglac. process. 9: 375-395.

Humlum O. 1988. Rock glacier appearance level and rock glacier initiation line altitude: A methodological approach to the study of rockglaciers. Artic and Alpine research, vol. 20, No. 2, 1988, pp. 160-178.

Sæmundsson K. et al. 1980. K-Ar dating, geological and palaeomagnetic study of a 5-km lava succession in Northern Iceland. Journ. of Geophysical Res., 85, 3628-3646.

Jónsson Ó. 1976. Berghlaup. *Ræktunarfélag Norðurlands,* Akureyri, 623 bls.

Sigurðsson O. 1990. Möðrufellshraun, berghlaup eða Jökulruðningur?. Náttúrufræðingurinn 60, p 107-112.

Summerfield, M. A. 1991. Global Geomorphology. Longman Scientific and Technical. Essex England, 535 p.

Svenson, H. 1989. The Rock Glacier, A New Feature in Scandinavian Geomorphology. Geografiske Annaler, 71A (1989). p. 95-98.

Tatenhove, F.v. and Dikau, R. 1990. Past and present permafrost distribution in the Turtmantal, Wallis, Swiss Alps. *Arctic and Alpine Research,* 21. 302-316.

Wahrhaftig, C. and Cox, A. 1959. Rock glaciers in the Alaska Range. *Geol. Soc. Am. Bull.*, 70. 383-436.

FLUID TRANSPORT IN VOLCANOES

Agust Gudmundsson

Department of Earth Sciences, Queen's Building, Royal Holloway University of London, Egham, UK
(a.gudmundsson@es.rhul.ac.uk)

Abstract

Fluids play a vital role in the formation, behaviour, and evolution of volcanoes. Not only are all volcanic eruptions in essence fluid (magma) transport to the surface, but earthquakes, landslides, and volcano instability are also related to the transport and storage of fluids inside volcanoes. The effects of increasing pore-fluid pressure on the probability of shear failure, such as during landslides and earthquakes, are well known. Here, however, the focus is on fluid transport in volcanoes through magma-driven fractures, hydrofractures. All rock fractures driven open by fluid overpressure (driving pressure) are extension fractures, the well-known examples in volcanoes being dykes, inclined sheets, and sills For such fractures to reach the surface, to supply magma to volcanic fissures, they must propagate through numerous layers and contacts. Most dykes become arrested on their paths, commonly at contacts between mechanically dissimilar layers. When a hydrofracture meets a contact between layers, or other types of discontinuities, the fracture may (a) become arrested, (b) deflect into the contact to form a sill-like structure, or (c) penetrate the contact. Scenarios (a) and (b) are more likely where the layers on either side of the contact are mechanically dissimilar, whereas (c) is more likely when the layers are mechanically similar. Similar layers are much more common in basaltic edifices than in stratovolcanoes, which may be one reason why dyke-fed eruptions are so much more common in basaltic edifices, composed primarily of mechanically similar basaltic layers, than in stratovolcanoes, composed largely of mechanically dissimilar pyroclastics, sedimentary layers, and lava flows. Once the hydrofracture, a dyke or a sheet, reaches the surface, the volumetric flow rate (the volume of magma per unit time) depends on the length of the fissure, but primarily on its opening or aperture. Thus, even if a volcanic fissure becomes somewhat longer during the early stage of an eruption, or shorter during the later stages, the length variations have much less effects on the volumetric flow rate than the aperture variations during the eruption. Two other factors that affect the volumetric flow rate are the dip of the feeder-dyke (feeder-sheet) and the density of the magma in relation to that of the host rock.

Introduction

Fluid transport in the crust is primarily through fractures. This applies in particular to the transport of high-viscosity fluids such as magma. The flow of groundwater and geothermal water is partly through porous media, particularly in sediments and sedimentary rocks, but in most solid rocks the primary mechanism of fluid transport is through fractures. Fluids transported through volcanoes include groundwater, geothermal water, and magma. The porous-media aspects of fluid transport, in volcanoes and elsewhere, are now well established and will not be reviewed here. Many aspects of fluid transport in fractures, in volcanoes and elsewhere, are still poorly understood and subject to intensive research. In this paper, the focus is on fluid transport in fractures, primarily magma transport. The main aims of this paper are to explain briefly some aspects of dyke and sheet propagation in volcanoes and their volumetric flow rates once a volcanic fissure has formed.

Dykes

Most dykes and sheets (and sills) injected from a magma chamber never reach the surface to supply magma to volcanic fissures. Instead, the dykes/sheets become arrested, commonly at contacts between dissimilar layers. Thus, most potential dyke-fed eruptions are prevented by the layering and local stresses in the volcano (Gudmundsson and Philipp, 2006; Gudmundsson, 2009).

There are three related processes by which dykes become arrested (Fig. 1; Gudmundsson, 2009): (i) Cook-Gordon debounding (delamination), (ii) stress barriers, and (iii) unfavourable material-toughness ratios due to elastic mismatch (difference in Young's moduli or stiffnesses between layers in contact). In the Cook-Gordon mechanism, a weak contact or another type of discontinuity (a fault, a fracture, for

example) opens up as a result of dyke-induced tensile stress. A stress barrier is a layer where the local
str
up
te
lay
lay

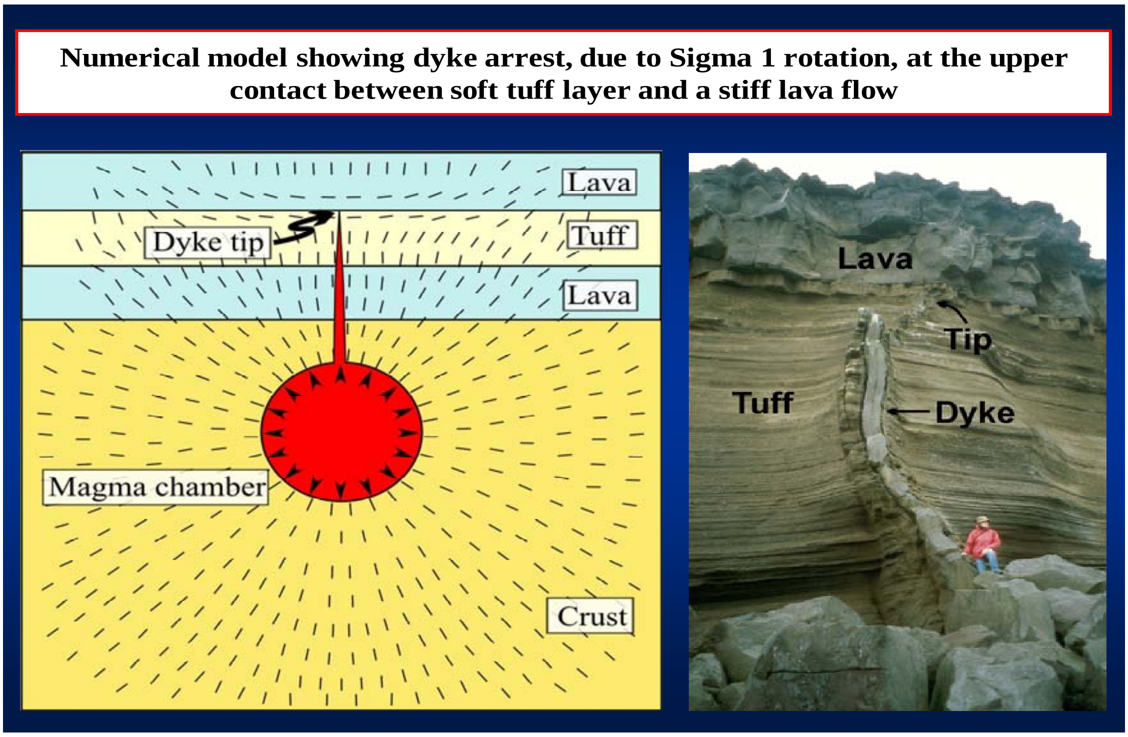

Fig. 1. A numerical model (left) and a field photograph (right) of an arrested dyke in SW Iceland.

Field results suggest that all these mechanisms may cause dyke to become arrested or deflected at a contact. Since stratovolcanoes are largely composed of alternating soft and stiff layers, the proportion of dykes that become arrested is much higher in stratovolcanoes than in basaltic edifices, thereby partly explaining why dyke-fed eruptions are much more common in basaltic edifices than stratovolcanoes. Some dykes, however, reach the surface and become feeder dykes. These have special structures that differ from those of non-feeders (Geshi et al., 2010).

Feeder-dykes

Those dykes that reach the surface generate volcanic fissures (Fig. 2). The fissure can range in lengths from a few tens of metres to many tens of kilometres or more. The shortest volcanic fissures in Iceland have only one crater, whereas the longest (about 65 km) have tens of crater cones. In fact, the Laki Fissure has more than hundred crater cones (Fig. 2).

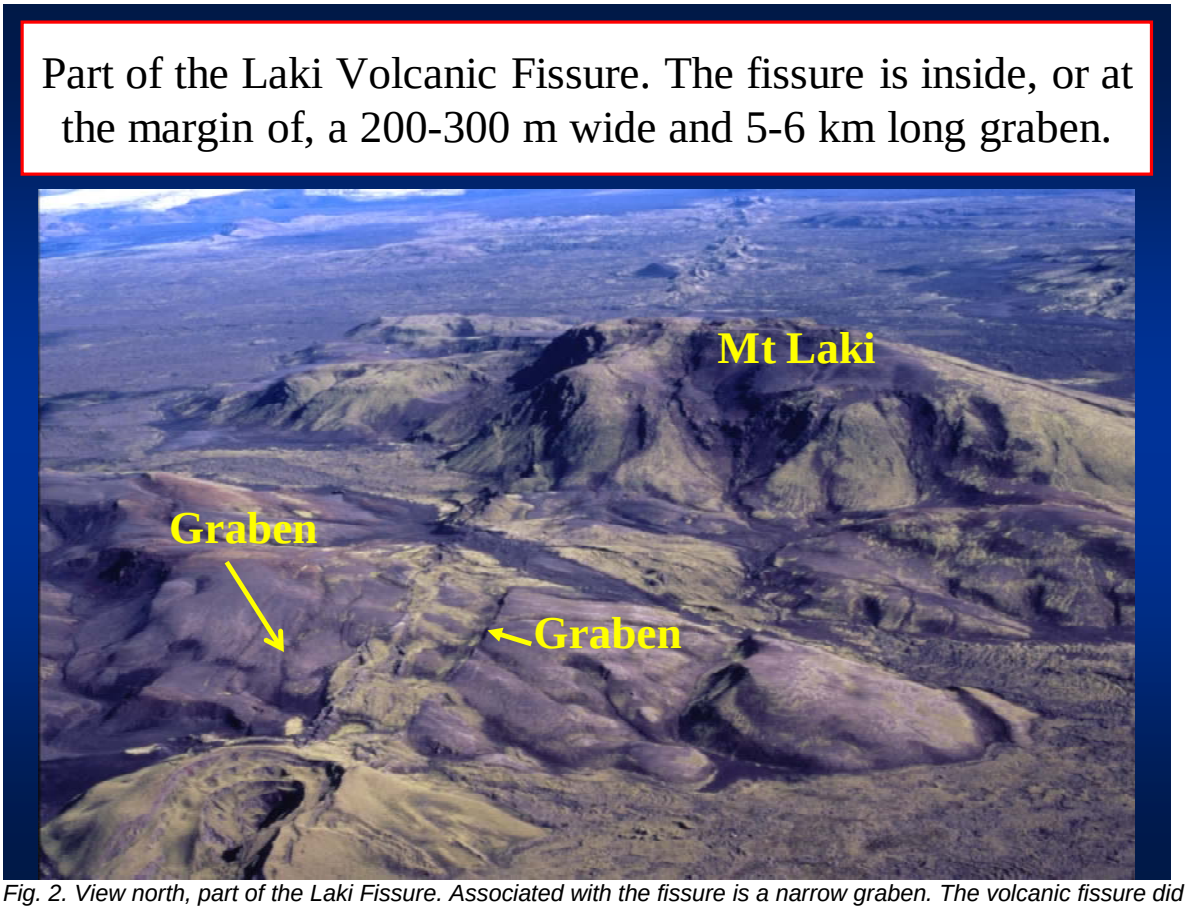

Fig. 2. View north, part of the Laki Fissure. Associated with the fissure is a narrow graben. The volcanic fissure did not reach the top of the hyaloclastite (basaltic-breccia) mountain Laki.

Volcanic fissures are always segmented; only part of a fissure is active at any one time. In addition, recent studies show that there is a very significant difference between shape or geometry of feeder dykes, supplying magma to fissures, and non-feeders (Geshi et al., 2010). The feeders are thickest at the surface and rapidly decrease in thickness over a vertical distance of a few tens of metres, below which they maintain an essentially constant thickness to depths of several hundred metres. By contrast, non-feeders are, necessarily, with a zero thickness at their vertical upper end, that is, the point where they are arrested, then increase rapidly in thickness to a maximum a few tens of metres below the vertical upper end, and then decrease gradually in thickness for the next several hundred metres. While these results are from a specific volcano in Japan, they are probably rather general and thus likely to apply to dykes in Iceland.

Volumetric flow rates

When a feeder reaches the surface, its volumetric flow rate, that is, the volume of magma or lava issued per unit time from the volcanic fissure, depends on several factors. These factors are best summarised through the following equation (Gudmundsson and Brenner, 2005):

$$Q = \frac{\Delta u^3 W}{12\mu_f}\left[(\rho_r - \rho_f)g\sin\alpha - \frac{\partial p_e}{\partial L}\right] \qquad (1)$$

where Q is the volumetric flow rate in the vertical direction L (up the dip dimension of the dyke), Δu is the opening or aperture of the feeder dyke (the volcanic fissure) at the surface, W its width in a direction that is perpendicular to the magma-flow direction (so that the fracture cross-sectional area perpendicular to the flow is $A = \Delta u W$ and it is assumed that $W >> \Delta u$), μ_f is the dynamic (absolute) viscosity and ρ_f the density of the magma (assumed constant), ρ_r is the average density of the host rock, g is the acceleration

due to gravity, α is the dip of the feeder dyke or sheet, and *L* is the linear distance from the point of rupture at the magma chamber and sheet initiation, at the boundary of the magma chamber, to the surface (Fig. 3). The excess magma pressure in the chamber at the time of rupture is p_e so that the pressure gradient from the chamber to the surface is $\partial p_e / \partial L$ (and negative in the direction of the flow).

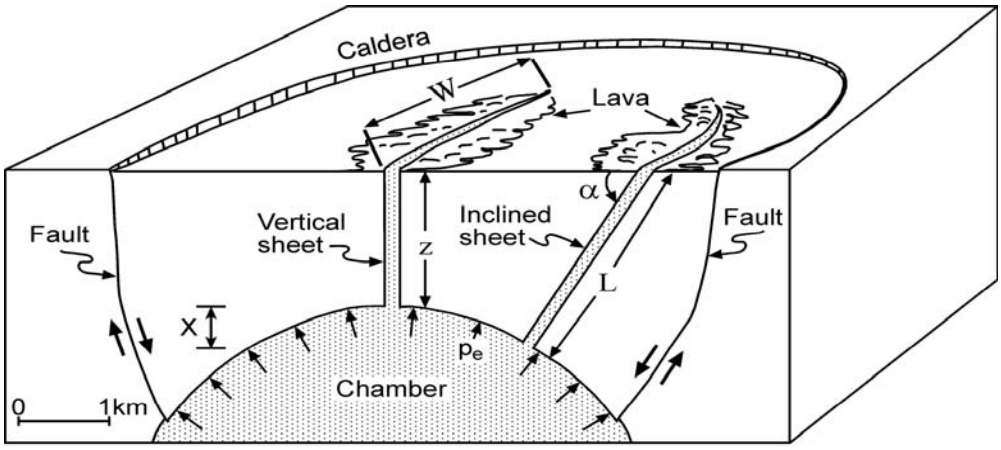

inclined sheet
ion z which is
at the time of
rupture and dyke/sheet injection is p_e, and the difference in depth between the point of initiation of inclined sheet and vertical sheet is x (modified from Gudmundsson and Brenner, 2005).

As an example of application of Eq. (1), consider the 1991 eruption of the volcano Hekla in South Iceland. The maximum volumetric flow rate during the first hours of the eruption reached 800 m^3 s^{-1} (Gudmundsson et al., 1992). During these early stages of the eruption, the active volcanic fissure was about 2 km long. The depth of the magma reservoir supplying magma to Hekla eruptions is estimated at 10 km, the average crustal density being about 2800 kg m^{-3}. For a basaltic magma we may take the density as 2650 kg m^{-3} and the viscosity as 100 Pa s, and the excess pressure in the reservoir before rupture and dyke emplacement as 3 MPa. Using these data and Eq. (1), the aperture of the feeder-dyke during the beginning stage of the Hekla eruption is estimated at 0.6 m. This is a very reasonable figure and fits with the average thickness of dykes in many central volcanoes in Iceland. The Hekla dyke was vertical: if however, it had been an inclined sheet, then Eq. (1) indicates that the volumetric flow rate would have been smaller, other things being equal. This means that, to produce equal volumetric flow rate, an inclined sheet normally has to have a larger opening and/or surface fissure length than a vertical dyke.

Conclusions

In conclusion, most injected dykes and sheets never reach the surface but rather become arrested. Those that reach the surface become feeders to fissure eruptions. Feeders have different geometric shapes from those of non-feeders. The volumetric flow rate of a feeder and its volcanic fissure depends on the density contrast between the host rock and the magma, and the length and aperture of the fissure. Rough calculations indicate that for a typical eruption in a central volcano in Iceland, such as in the Hekla Volcano in South Iceland, the feeder dyke would have an aperture of about 0.6 m. This estimate is in excellent agreement with field studies of dykes and sheets in central in volcanoes in Iceland.

References

Geshi, N., Kusumoto, S., Gudmundsson, A., 2010. Geometric difference between non-feeder and feeder dikes. Geology, 38, 195-198.

Gudmundsson, A., 2009. Deflection of dykes into sills and magma-chamber formation. Tectonophysics (on line October 2009).

Gudmundsson, A., Brenner, S.L., 2005. On the conditions of sheet injections and eruptions in stratovolcanoes. Bulletin of Volcanology, 67, 768-782.

Gudmundsson, A., Philipp, S.L., 2006. How local stresses prevent volcanic eruptions. Journal of Volcanology and Geothermal Research, 158, 257-268.

Gudmundsson, A., Oskarsson, N., Grönvold, K., Saemundsson, K.,Sigurdsson, O., Stefansson, R., Gislason, S.R., Einarsson, P., Brandsdottir, B., Larsen, G., Johannesson, H. and Thordarson, Th., 1992. The 1991 eruption of Hekla, Iceland. Bull. Volcanol. 54, 238-246

NEW UNSPIKED K-AR AGES OF QUATERNARY SUB-GLACIAL AND SUB-AERIAL VOLCANIC ACTIVITY IN ICELAND

Hervé Guillou[(1)], Brigitte Van Vliet-Lanoë[(2)], Agust Guðmundsson[(3)] and Sébastien Nomade[(1)]

(1) : LSCE/IPSL, Laboratoire CEA-CNRS-UVSQ, Domaine du CNRS , Bât. 12, Avenue de la Terrasse, 91198 Gif sur Yvette, France

(2) : UMR 6538 CNRS Domaines Océaniques,IUEM, Place N.Copernic, 29480 Plouzané, France

(3) : JFS ,Geological Services Raudagerdi 31, 108 Reykjavik, Iceland

Introduction

Application of volcanic proxies to paleoenvironmental studies in Iceland has generally lagged behind the improvements of undisputable geochronologies. This is particularly frustrating because a link between volcanism and deglaciation in Iceland is an appealing hypothesis and questions about the extent of the ice cap during Icelandic glaciations remain pending (Einarsson et al., 1988; Geirsdttir et al., 1997; Ingolfsson et al., 1997; Hoppe, 1982).

The postglacial eruptive history of Iceland after the last deglaciation is now well documented (Licciardi et al., 2007; Sinton et al., 2005, Saemundsson, 1991). One of its main characteristics is an increase in the volcanic eruption rate, which coincides with the end of the last ice age (11 ka BP; Slater et al., 1998; Maclennan et al., 2002; Sigvaldason et al., 1992; Hardarson et al., 1991; Jull et al., 1996). However, the pattern of volcanism for more evolved rocks, such as rhyolites, comprising 10-12% of outcrop on Iceland, is less well established. In fact, the opposite trend may be apparent, or at least sub-glacial rhyolite eruptions are frequent during interglacial periods (Flude et al., 2008).

This relationship between deglaciation and volcanism has been convincingly demonstrated in Iceland only for the last deglaciation (Maclennan et al., 2004; Sinton et al., 2005; Licciardi et al., 2007, McGarvie et al., 2006, McGarvie et al., 2007). Therefore, we consider that it is important to explore this relationship through older periods.

The purpose of this study is then to evaluate the potential of the unspiked K-Ar dating method in dating Quaternary Icelandic volcanics to contribute to this debate.

The unspiked K-Ar technique applied here is perfectly adapted to these purposes because it is an accurate and precise dating tool which has proven to be efficient and suitable to date young Quaternary lavas. To test the relevance of our approach, we collected and dated sub-aerial lavas contemporaneous with warm periods; hyaloclastites and lavas formed in sub-glacial environments.

Geological setting of the dated samples

Volcanism in Iceland, initiated about 12 Ma ago and is still active, occurring during both glacial and interglacial periods. Two types of sub-glacial volcanic bodies are distinguished: Table Mountains also known as Móbergs or Tuyas and Hyaloclastite ridges.

Table mountain volcanoes which result from central vent eruptions are the sub-glacial equivalent of sub-aerial shield volcanoes (Werner et al., 1996). They are produced when volcanoes erupt beneath a pre-existing ice-sheet. Their shape is roughly circular with steep flanks and characterized by a flat top. At their base, their diameters vary from several hundred meters to a few kilometers. Their height usually ranges between 200 and 1000m. From the base to the top, they consist of a thick pile of pillow-lavas and hyaloclastites surrounded by volcanic breccias. This succession reflects a decrease in external pressure as the volcano grows higher toward the ice cap surface, during its evolution. When the magmatic activity was strong and sufficiently long-lasting, flat-lying sub-aerial lava flows capped these volcanoes. Thus, the height of these table mountains may be a good indicator of ice thickness at the time of their emplacement (Bourgeois et al., 1998; Werner et al., 1999; Smellie, 2000).

Hyaloclastite ridges can be as long as 40 km, 2-4 km wide and several hundred meters high. They are the sub-glacial equivalent of aerial eruptive fissures and they are aligned within the general tectonic trend. They are made up of fragmented pillow-lavas and hyaloclastites. It is generally accepted that the volumes of lava emitted during sub-glacial fissural eruptions are lower than those that produced the table mountain volcanoes (Guðmundsson, 1986).

During warmer periods, sub-aerial eruptions dominate. In comparison with sub-glacial eruptions which produced high topographic bodies of restricted lateral extent, sub-aerial eruptions tend to drape and smooth the topography. During these eruptions, very large lava flows flowing from eruptive fissures or shields can be generated. Volumes can occasionally exceed 20 km^3 (Lakí lava flows field) and can be both of pahoehoe and aa types. The Gerduberg basalt columns are a spectacular example of sub-aerial volcanic activity.

Twenty-three samples were selected for this geochronological study. 12 samples are from Móbergs or hyaloclastite ridges and are considered to be emplaced in sub-glacial environments. The other 11 samples were collected from sub-aerial lava flows emplaced in an ice-free environment.

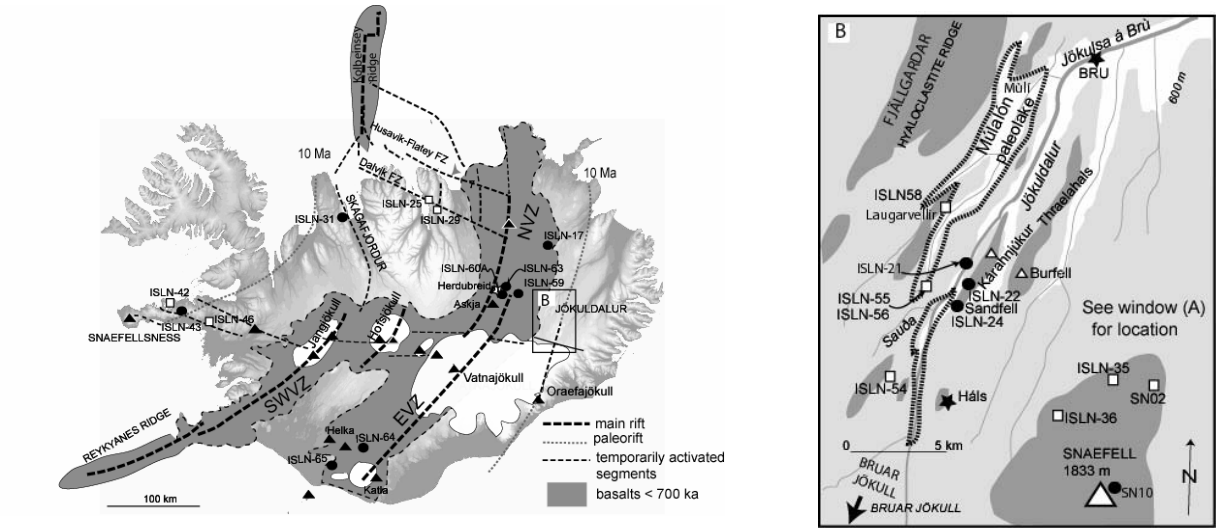

Figure1 - Location map of the dated samples. a: general map. b: details of the north volcanic zone. Grey stars refer to major volcanic centers. WVZ : west volcanic zone; EVZ: east volcanic zone, NVZ: north volcanic zone, SWZ: southwest volcanic zone. Black dots : Sub-glacial samples. Empty squares : Sub-aerial samples.

Figure 2 -Examples of sub-glacial and sub-aerial lavas. ISLN-65, Móberg Þórósfell, details on the cube jointed part of the hyaloclastite unit. ISLN-59, massive rounded block from the Upptyppingar hyaloclastite ridge. ISLN-43, intrusion within the hyaloclastite formation of Móberg Vatnafell. ISLN-46, sub-aerial columnar jointed lava of Gerduberg. ISLN-56, upper part of a partially dismantled sub-aerial lava close to Mülalön.

Results and discussion

Analytical reproducibility, at the 2s level on the ages, is observed for all samples including the very young samples (i.e. ages lower than 150 ka). The precision is between 10 and 15% for the two youngest

samples (ISLN-17 and ISLN-59). Age precisions of samples dated between 150 and 400 ka with K contents between 0.5 and 1% range between 2.5 and 6%. Precision as good as 5% is obtained for 100 ka old samples with K contents around 1% (ISLN-46 and ISLN-42). The ages of the sub-glacial samples vary between 1007 ± 25 (sample ISLN-31) and 48 ± 7 ka (sample ISLN-59). Two samples, ISLN-63 and ISLN-65, respectively from Móberg Herðubreid and Móberg Þórósfell, gave a zero age. Sub-aerial lavas are dated between 759 ± 27 (ISLN-58) and 93 ± 5 ka (ISLN-42).

We can evaluate whether these new ages are good indicators of the crystallisation ages by comparing some of them to previous $^{40}Ar/^{39}Ar$ published ages. Two of our samples from the Snaefell volcanic center and two others from the Kárahnjúkar volcanic formation were previously dated by the $^{40}Ar/^{39}Ar$ method (Helgason et al., 2003; Helgason et al., 2005). Reported $^{40}Ar/^{39}Ar$ ages are consistent with the K-Ar ages, but much less accurate. The K-Ar ages of these samples are not affected by systematic errors due to excess ^{40}Ar and can be regarded as reliable crystallization ages and this validates our experimental procedures.

We can evaluate our new ages by comparing them to the stacked $d^{18}O$ record of benthic foraminifera from Lisieki and Raymo (2005). Following the same approach as Licciardi et al. (2007), we plotted the mean ages of the sub-glacial and sub-aerial dated samples combined with the $d^{18}O$ proxy record of sea level (Lisieki and Raymo, 2005). This allows a direct comparison of eruption ages with a global paleoclimatic record. Fluctuations of the ice cover in Iceland are representative of the variation in the global ice volume as illustrated by the Lisieki and Raymo record. Nevertheless, at present, 11% of Iceland is covered in glaciers, so sub-glacial volcanism can occur during interglacials. As a consequence, sub-glacial volcanic products can have radiometric ages corresponding to both glacial and interglacial periods. More probably, sub-aerial volcanics should have radiometric ages coherent with interglacials (warm periods).

In addition, numerous studies about Icelandic volcanism focus on the link between glacial unloading and enhanced volcanism (Maclennan et al., 2002, Sinton et al., 2005, Licciardi et al., 2007).

Our limited dataset combined with the large uncertainties on some of the dated samples and the lack of volume estimates do not allow us to produce a statistical study such as those proposed by Sinton et al. (2005) and Licciardi et al. (2007) but it can be observed that in the studied areas:

1-Six of the sub-glacial samples were emplaced during a warm to cold MIS transition (ISLN-64, ISLN-17, and ISLN-59) or at a cold maxima (ISLN-21, ISLN-24, SN-10). Two of them (ISLN-43, ISLN-22) were emplaced during or briefly after deglaciation.

2- Five of the nine reliably dated sub-aerial lavas (ISLN-58, ISLN-56, ISLN-36, ISLN-25, and ISLN-42) were emplaced during a warm to cold MIS transition.

3-Three other sub-aerial lavas were emplaced at the end (ISLN-46) or briefly (SN-02, ISLN-55) after deglaciation.

4-Only one sub-aerial sample (ISLN-29) emplaced at a cold maxima.

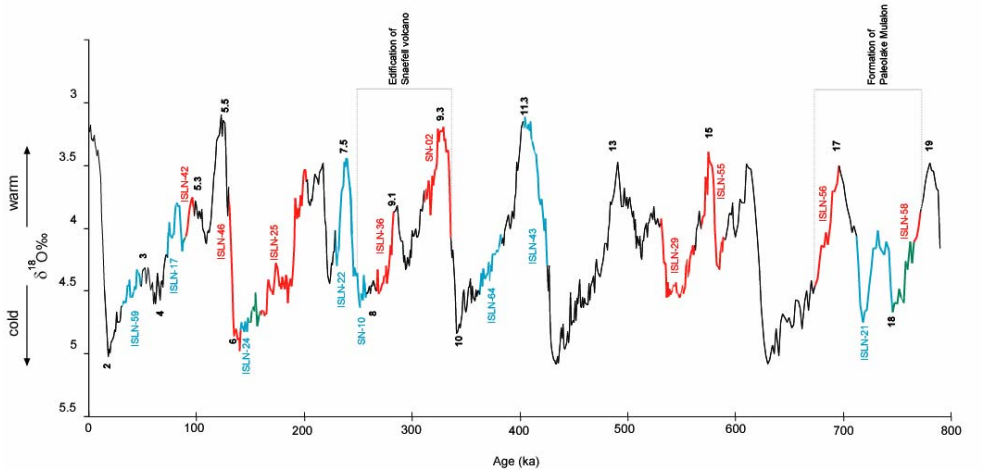

Figure 3 – Representation on the stacked $\delta^{18}O$ record of benthic foraminifera of the eruption time intervals established from the radiometric ages. In red: sub-aerial eruptions, in blue: sub-glacial eruption, in green: intersection zones

between sub-aerial and sub-glacial ages. In this graphic, ages are reported with an error at two sigma error on the ages except for sub-aerial samples older than 500 ka which are reported at the one sigma level. The width of the red and blue sectors cover the age uncertainties.

Conclusions

We have successfully established the potential of the unspiked K-Ar dating method to date Quaternary Icelandic volcanics because direct comparisons between the $^{40}Ar/^{39}Ar$ and the unspiked K-Ar methods demonstrate that recent Quaternary (i.e., younger than 500 ka) basalts from Iceland can be reliably dated using the K-Ar clock in general and the unspiked K-Ar method in particular. Nevertheless, despite the good accuracies obtained for most of our K-Ar ages, we are not able at this time to establish a clear correlation between climate and volcanism and to demonstrate a clear link between deglaciation and enhanced volcanism. But, based on this promising work, a further step is now the extensive dating of Quaternary Móbergs to check whether we reach the same conclusions as Licciardi et al. (2007), who proposed that most of the recent Móberg edifications coincide or shortly follow important warming events.

References :

Bourgeois, O., Dauteuil, O., Van Vliet-Lanoë, B., 1998. Pleistocene sub-glacial volcanism in Iceland : tectonic implications. Earth and Planetary Science Letters 164, 165-178.

Einarsson, T., Albertsson, K.J., 1988. The glacial history of Iceland during the past three million years, Philos. Trans. R. Soc. Lond. 318, 637–644.

Flude, S., Burgess, R., McGarvie, D.W., 2008. Silicic volcanism at Ljosufjöll, Iceland : Insights into evolution and eruptive history from Ar-Ar dating. Journal of Volcanology and Geothermal Research 169, 154-175.Smellie, J.L., 2000. Sub-glacial eruptions. In: Geirsdttir, A., Hardardottir, J., Eirıksson, J., 1997. The depositional history of the Younger Dryas-Preboreal Budi moraines in southcentral Iceland. Arctic Alpine Research 29, 13–23.

Gudmundsson, A., 1986. Mechanical aspects of postglacial volcanism and tectonics of the Reykjanes peninsula, southwest Iceland. Journal of Geophysical Research 91, 12711-12721.

Helgason, J., Duncan, R.A., 2001. Glacial-interglacial history of the Skaftafell region, southeast Iceland, 0-5 Ma. Geology 29, 179-182.

Helgason, J., Duncan, R.A., 2003. Ar-Ar age dating of the Kárahnjúkar volcanic formation. Ekra Geological Consulting, Report on the Kárahnjúkar Hydroelectric Project made for Landsvirkjun (Iceland power company), August 2003. LV-2003/090, 38 pp.

Hardarson, B.S., Fitton, J.G., 1991. Increased mantle melting beneath Snaefellsjökull volcano during late Pleistocene deglaciation. Nature 353, 62-64.

Hoppe, G., 1982. The extent of the last Iceland ice sheet, Jökull 33, 3–11.

Ingolfsson, O., Björck, S., Haflidason, H., Rundgren, M., 1997. Glacial and climatic events in Iceland reflecting regional North Atlantic shift during the Pleistocene–Holocene transition. Quat. Sci.Rev.16, 1135–1144.

Jull, M., McKenzie, D., 1996. The effect of deglaciation on mantle melting beneath Iceland. Jour. of Geophysical Research 101, 21815-21828.

Licciardi, J.M., Kurz, M.D., Curtice, J.M., 2007. Glacial and volcanic history of Icelandic table mountains from cosmogenic ^{3}He exposure ages. Quaternary Sciences Review 26, 1529-1546.

Lisieki, L.E., Raymo, M.E., 2005. A Pliocene-Pleistocene stack of 57 globally distributed benthic $d^{18}O$ records. Paleoceanography 20, doi: 1029/2004PA001071.

Maclennan, J., Jull, M., McKenzie, D., Slater, D., Grönvold, K., 2002. The link between volcanism and deglaciation in Iceland. Geochemistry Geophysics Geosystems 3, 1062, doi :10.129/2001GC000282.

McGarvie, D.W., Burgess, R., Tindle, A.G., Tuffen, H., Stevenson, J.A., 2006. Pleistocene rhyolitic volcanism at the Torfajokull central volcano, Iceland: eruption ages, glaciovolcanism, and geochemical evolution. Jökull 56, 57-75.

McGarvie, D.W., Stevenson, J.A., Burgess, R., Tindle, A.G., 2007. Volcano-ice interactions at Prestahnúkur, Iceland: rhyolite eruption during the last interglacial-glacial transition. Annals of Glaciology, 45 38-47.

Saemundsson, K., 1991. Jardfraedi Kröflukerfisins, in Nattura Mytvatns, edited by A. Gardarsson and A. Einarsson, 24-95, Hid islenska natturufraedifelg, Reykjavik

Sigurdsson, H., (Ed.), Encyclopedia of Volcanoes. Academic Press, San Diego, 403-418.

Sigvaldason, G.E., Annertz, K., Nilsson, M., 1992. Effect of glacier loading/deloading on volcanism: Postglacial volcanic production rate of the Dyngjufjöll area, central Iceland. Bulletin of Volcanology 54, 385-392.

Sinton, J., Grönvold, K., Saemundsson, K., 2005. Postglacial eruptive history of the western volcanic zone, Iceland. Geochemistry Geophysics Geosystems 6, Q12009, doi :10.1029/2005GC001021.

Slater, L., Jull, M., McKenzie, D., Grönvold, K., 1998. Deglaciation effects on mantle melting under Iceland : Results from the northern volcanic zone. Earth and Planetary Science Letters 164, 151-154.

Werner, R., Schminke, H-U., 1999. Englacial vs lacustrine origin of volcanic table mountains: evidence from Iceland. Bulletin of Volcanology 60, 335-354.

L'ISLANDE, UN POINT CHAUD PARTICULIER

Christophe Hémond
UMR 6538 UBO-CNRS Domaines océaniques, IUEM, Place Copernic, 29280 Plouzané, chhemond@univ-brest.fr

Abstract

Le point chaud islandais est particulier en ce qu'il interagit avec la dorsale médio-atlantique et que nous possédons 15 Ma d'enregistrement continu de son activité. La persistance et les variations de l'abondance du magmatisme ont permis d'évaluer pour la première fois les échanges et interactions entre zones de fusion et le régime de la fusion partielle. La genèse d'une épaisse croûte et son rôle dans le magmatisme différencié ont aussi été expliqués.

Introduction

Le point chaud islandais est le cas particulier d'un panache situé sous une dorsale, la ride médio-atlantique nord. Il a été l'objet d'études très nombreuses parce qu'il est une partie émergée de la dorsale et de ce fait, très accessible. Il résulte des observations que l'Islande offre 15Ma d'années d'activité et d'interactions à l'affleurement, cas unique sur Terre. Son activité a fait l'objet d'études spatiales décrivant les effets de l'interaction ou la variabilité de composition dans l'espace comme d'études temporelles par l 'analyse de longues coupes de l'activité passée entre 15 et 2Ma dans les régions du nord-ouest ou de l'est.

Le point chaud

Le premier résultat de l'activité du point chaud islandais est la construction d'un vaste plateau océanique induit la production d'une croûte océanique anormalement épaisse. L'épaisseur totale des roches volcaniques (de 8 à 16km) est beaucoup plus grande que celle d'une croûte océanique normale (6km en moyenne) et reflète certainement l'influence de l'anomalie thermique résultant de la présence du point chaud. L'existence de picrites, des tholéiites très magnésiennes, corrobore cette observation. De façon générale, les laves islandaises sont chimiquement anormales comparées à des MORBs. Des concentrations plus élevées en éléments en traces incompatibles et les compositions isotopiques en Sr et Nd hétérogènes ont été signalées dans de nombreux travaux.

Deux types de modèles ont été rapidement proposés pour expliquer les données chimiques. Le premier nécessite l'existence d'hétérogénéités dans le manteau : les laves enrichies provenant d'une source enrichie dans le panache, les laves appauvries d'un autre composant du panache ou du manteau supérieur, source des MORBs appauvris de l'Atlantique nord. Le deuxième considère un manteau source homogène dont sont issus les magmas qui interagissent lors de leur remontée vers la surface avec la croûte islandaise ancienne et hydrothermalement altérée. La justification pour ce deuxième type venait essentiellement de l'existence de valeurs inhabituellement basses des compositions isotopiques d'oxygène. La seule source d'oxygène pauvre en isotope léger réside dans les eaux météoriques qui circulent abondamment dans la croûte entraînant son altération. Notons aussi que la croûte islandaise est chimiquement enrichie du fait de l'abondance des produits différenciés émis par les stratovolcans centraux en Islande. Ce modèle permettait d'éliminer la nécessité d'un composant enrichi dans le manteau. L'origine des roches différenciées et de leur abondance en Islande a fait l'objet de plusieurs études dont certaines par les déséquilibres radioactifs sur les volcans dits centraux (Hekla, Askja, Krafla) et il en ressort que les processus AFC (Assimilation-Fractional Crystallization) dominent cette production (Nicholson et al. 1991; Sigmarsson et al. 1991).

Les co-variations des compositions isotopiques de Sr, Nd et Pb observées ont mené à proposer un modèle de manteau hétérogène sous l'Islande, contenant un composant géochimiquement appauvri et un autre, enrichi. Il restait à déterminer l'origine de ces composants et s'il semblait admis que le composant enrichi dérivait directement du panache de manteau profond, la source du composant appauvri n'était pas claire bien qu'on ait suggéré une origine dans le manteau supérieur. Il se posait néanmoins le problème de l'absence de corrélation entre les données isotopiques d'hélium et des gaz rares en général et celles des isotopes de Sr et Nd. Les données acquises sur des échantillons provenant des deux dorsales

s'éloignant de l'Islande, ride de Reykjanes au sud-ouest et de Kolbeinsey au nord montraient un gradient de compositions isotopiques qui semblait indiquer que même le composant appauvri en Islande n'était pas identique à celui reconnu dans l'Atlantique nord, ou bien qu'il était contaminé par le point chaud. De nouvelles données de plomb et d'éléments en traces sur des échantillons auparavant déjà très bien documentés, ont mené à proposer que le volcanisme islandais est essentiellement dominé par le magmatisme du point chaud, lui-même issu d'un panache hétérogène. Il contiendrait lui-même les deux composants, enrichi et appauvri dont l'origine est à rechercher dans le recyclage d'une section complète de croûte océanique. Cette croûte recyclée qui se trouve aujourd'hui dans le faciès éclogite, domine largement le bilan des éléments en traces incompatibles et des compositions isotopiques. La partie basaltique influencerait les laves à affinité alcaline, plus radiogéniques, alors que l'influence des gabbros serait visible dans les picrites et tholéiites à olivine à anomalie positive en Sr. Le magmatisme interagit avec celui des dorsales voisines représenté par un MORB moyen de l'Atlantique Nord mais les « trends » de mélange sont distincts car c'est le composant islandais, celui issu du panache, qui est différent dans les deux cas : il est plus appauvri au nord près de la ride de Kolbeinsey qu'au sud-ouest près de celle de Reykjanes.

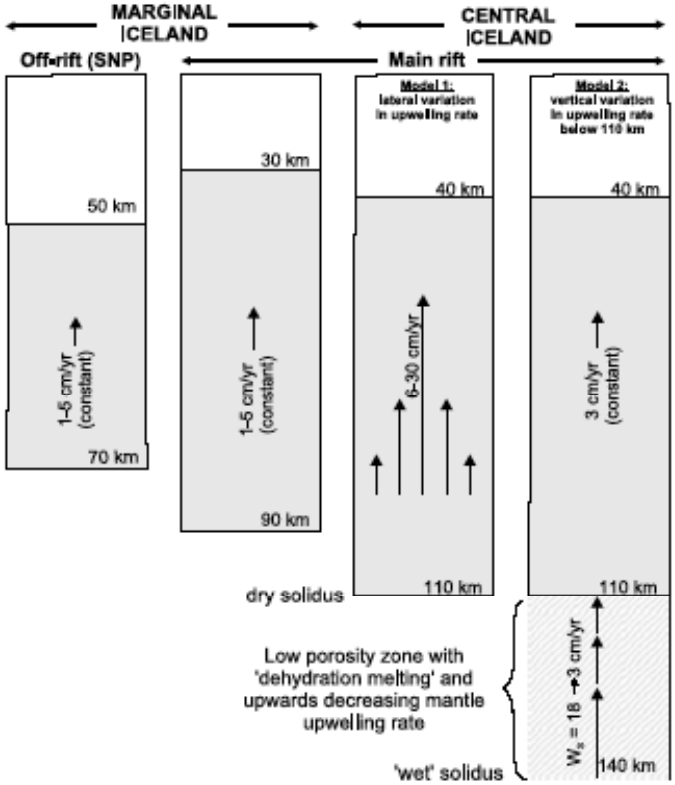

Fig.1: Longueur de la colonne de fusion et vitesse de remontée du manteau dans le modèle de fusion dynamique sous les zones magmatiques actives centrale et périphérique d'Islande d'après Kokfelt et al. (2003)

De nouvelles mesures isotopiques de Th à l'échelle de l'Islande (Kokfelt et al. 2003, après les travaux de Hémond et al. 1988) montrent que les excès de ^{230}Th sont moins forts à proximité de la zone centrale d'influence du panache. Ils sont interprétés en termes de vitesse de remontée du manteau solide (mantle upwelling) sous cette région : le matériel plus chaud au centre du panache et donc plus léger remonte plus rapidement que dans la périphérie du panache. Ce dernier réside alors moins longtemps dans une colonne de fusion montante. Il en résulte un temps de percolation entre liquide et solide moins que dans les zones périphériques. Cette rapidité d'ascension permet aux liquides de subir des fractionnements entre Th et U plus faibles puisque la colonne et la durée de percolation sont plus courtes. On peut en déduire que les fractionnements les plus faibles sont visibles au centre du point chaud plutôt qu'à la périphérie et qu'une vitesse de remontée rapide limite leur intensité. Ceci est confirmé par ailleurs, par la faiblesse des fractionnements ^{230}Th-^{238}U dans les laves d'Hawaii, le point chaud le plus chaud à la vitesse de remontée la plus rapide.

Parallèlement, Hanan et Schilling (1997), Fitton et al. 2002) et Kitagawa et al. (2008) ont étudié l'activité du point chaud islandais au cours des 15 derniers millions d'années grâce à l'analyse d'éléments en traces ou à des mesures précises des compositions isotopiques du Pb et au développement des mesures de compositions isotopiques du Hf. Ils ont mis en évidence une variation d'activité du point chaud avec un maximum de magmatisme vers 13-12 et 8-7 millions d'années. La notion de point chaud variable au cours du temps s'est ainsi trouvée confirmée. Il ressort des analyses de traces et isotopiques que le magmatisme plus abondant est lié à une contribution plus grande du composant enrichi du panache qui , cependant, diffère légèrement entre les deux épisodes (Kitagawa et al. 2008). Fitton et al. (2002) soulignent que la contribution relative des différents composants du manteau est liée à la position de ce magmatisme par rapport à la dorsale, à l'axe ou hors axe et donc au degré de fusion partielle. Ainsi des magmas issus de faibles taux de fusion hors axe dériveront d'abord des composants enrichis et plus fusibles du manteau alors qu'une fusion plus intense sous l'axe produit des magmas plus proches en composition de la composition globale du panache. Les coulées de faible volume et appauvries représentent des liquides qui dérivent préférentiellement un composant appauvri et plus réfractaire du panache. L'existence de ce composant appauvri spécifique fait débat encore de nos jours. Hanan et Schilling (1997) contestent son existence et considèrent le manteau supérieur ambiant source des MORB comme tel. A la suite de Hémond et al. (1993), Thirlwall (1995) grâce à des données isotopiques de Pb, Kerr et al. (1995); Fitton et al. (1997) soutiennent la nécessité d'un composant appauvri intrinsèque distinct du manteau supérieur source des MORB. Hanan et al. (2000) ont tenté de réfuter le modèle de composant appauvri spécifique en se basant sur de nouvelles analyses de Hf et de traces. Ces conclusions ont été contredites par Fitton et al. (2002). Kitagawa et al. (2008) soulignent à leur tour dans leur étude du magmatisme des derniers 15 Ma qu'entre les périodes de forte activité, c'est le composant appauvri islandais qui alimente un magmatisme moins intense.

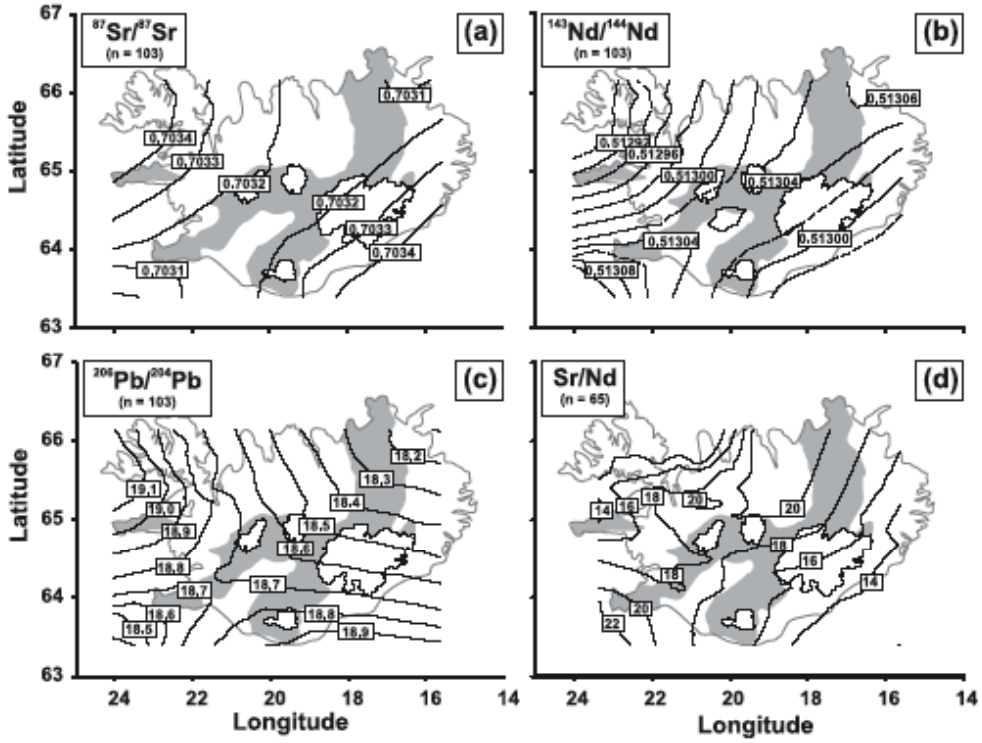

Fig.2: Cartographie isotopique du point chaud islandais d'après Kokfekt et al. (2006)

L'augmentation sensible du nombre d'analyses de qualité depuis une dizaine d'années a permis des analyses en composantes principales (Hanan et al. 1997, Malfère et al. 2002, et Kitagawa et al. 2008). Hanan et Schilling (1997) suggèrent un modèle à trois composants. Le premier est enrichi et contenu dans le panache, le deuxième est appauvri et peut être celui présent de façon régionale dans l'Atlantique nord. Le troisième est plus inhabituel car de composition type EM1, il serait de la lithosphère sous-

continentale entraînée dans le manteau. Comme mentionné plus haut, cela est fortement contesté par Fitton et al. (2002). Les données isotopiques les plus récentes en traces et en isotope des Sr, Pb, Nd et Hf (Malfère et al. 2002) sur 120 laves islandaises de moins de 700ka constituent le travail le plus abouti. Le grand nombre d'analyses sur des laves récentes permet une véritable étude statistique des différents composants présents dans le manteau source. Ils ont montré que les processus magmatiques de types cristallisation fractionnée et contamination crustale étaient marginaux sur les laves produites par des éruptions fissurales. Les hétérogénéités du panache islandais sont la source première de la variabilité des compositions et différents mélanges créent la diversité isotopique observée.

Les constituants sont de type manteau enrichi EM1 et EM2 et C plus les basaltes et les gabbros d'une section de croûte recyclée. Plus que la présence du manteau supérieur de type MORB dans la source sous l'Islande, c'est plutôt le panache islandais qui envahit la source des dorsales voisines comme suggéré par Chauvel et Hémond (2000). Comme mentionné aussi par Kokfelt et al (2006), l'analyse en composantes principales des six rift zones révèle que le panache est hétérogène géographiquement : Le composant EM1 est plutôt bien identifiable dans le nord est, la signature EM2 dans le sud-est et centre-est et le composant C mélangé à la signature des basaltes recyclés dans les basaltes alcalins du sud de la rift zone sud-est. L'influence des gabbros recyclés est visible dans la zone nord est de Theistareykir mais aussi , de façon moindre dans les basaltes du centre et du sud ouest. Les âges U-Th-Pb et Sm-Nd indiquent une origine archéenne pour le matériel océanique recyclé.

Les processus crustaux ne sont en revanche pas négligeables sous les stratovolcans. Ceux ci possèdent des chambres magmatiques complexes installées dans la croûte dans lesquelles les processus de contamination ou de type AFC surviennent. De nombreuses études ont eu lieu dont celle réalisées par Sigmarsson et al. (1991) sur des laves primaires et différenciées des volcans centraux Hekla (sud) et Askja (centre-est) ou Nicholson et al. (1991) sur le Krafla (nord-est). Cette étude a permis de répondre à la question en combinant les isotopes du Th, sensibles à la durée des processus, de l'oxygène sensibles aux interactions de basse température avec les eaux météoriques et de Sr et Nd, systèmes nous apportant l'information de type manteau. Bien que les compositions isotopiques de Sr et de Nd fussent quasi identiques pour tous les échantillons d'Hekla, les compositions de Th variaient et démontraient que les roches acides ne pouvaient dériver de magmas primitifs simplement par cristallisation fractionnée. Des résultats comparables furent obtenus sur les deux autres volcans où les compositions d'O sont beaucoup plus basses dans les magmas siliceux que dans les magmas basiques. Ces données suggéraient donc un modèle dans lequel de grands volumes de roches différenciées sont produits sous les volcans centraux des zones néovolcaniques d'Islande par refusion partielle de la croûte sous-jacente préalablement altérée par les eaux météoriques. Nicholson et al. (1991) ont confirmé ce modèle par un étude exhaustive du volcan Krafla.

References

Chauvel C. and Ch. Hémond, 2000, Melting of a complete section of recycled oceanic crust: Trace element and Pb isotopic evidence from Iceland, G^3 ,1.

Fitton J. G., A. D., Saunders, P. D. Kempton, & B. S. Hardason, 2003, Does depleted mantle form an intrinsic part of the Iceland plume? G^3, 4, 2002GC000424.

Fitton J.G., A.D. Saunders, M.J. Norry, B.S. Hardarson, R.N. Taylor, 1997,Thermal and chemical structure of the Iceland plume, Earth Planet. Sci. Lett. 153, 197-208.

Hanan B.B. & J.-G. Schilling, 1997, The dynamic evolution of Iceland mantle plume: the lead isotope perspective. Earth Planet. Sci. Lett. 151, 43–60.

Hanan B.B., J. Blichert-Toft, R. Kingsley & J._G. Schilling, 2000, Depleted Iceland mantle plume geochemical signature: artifact or multicomponent mixing? G^3, 1, 1999GC000009.

Hards V. L., P. D. Kempton and R. N. Thompson,1995, The heterogeneous Iceland plume: new insights from the alkaline basalts of the Snaefell volcanic centre, *J. Geol. Soc. London* 1995; v. 152; p. 1003-1009

Hémond Ch., M. Condomines, S. Fourcade, C.J. Allègre, N. Oskarsson and M. Javoy, 1988, Thorium, Strontium and oxygen isotopic geochemistry in recent tholeiites from Iceland: crustal influence on mantle-derived magmas, Earth Planet. Sci. Lett., 87, 273-285.

Hémond Ch., N.T. Arndt, U. Lichtenstein, A.W. Hofmann, N. Oskarsson and S. Steinthorsson, 1993, The Heterogeneous Iceland Plume: Nd-Sr-O Isotopes and Trace element constraints, J.Geophys.Res. 98-B9, 15833-15850.

Kempton P.D.,J.G. Fitton, A.D. Saunders, G.M. Nowell, R.N. Taylor, B.S. Hardason & G. Pearson, 2000, The Iceland plume in space and time: a Sr–Nd–Pb-Hf study of the North Atlantic rifted margin. Earth Planet.Sci. Lett. 177, 255–271.

Kerr A.C.,A.D. Saunders, J. Tarney. & N.H. Berry,1995, Depleted mantle-plume geochemical signatures: no paradox for plume theories. Geology 23, 843–846.

Kitagaw H.a, K. Kobayashi, A. M.& E. Nakamura, 2008, Multiple Pulses of the Mantle Plume:Evidence fromTertiary Icelandic Lavas, Journal of the Geological Society 1995; v. 152; p. 1003-1009

Kokfelt T. F., K. Hoernle, F. Hauff, J. Fiebig, R. Werner, D. Garbe-Schoenberg,2006, Combined trace element and Pb-Sr-Nd-O isotope evidence for recycled oceanic (upper and lower) crust in the Icelandic plume, J. Petrol. 47-9, 1705-1749.

Kokfelt T.F., K. Hoernle & F. Hauff, 2003, Upwelling and melting of the Iceland plume from radial variation of ^{238}U–^{230}Th disequilibria in postglacial volcanic rocks. Earth Planet. Sci. Lett. 213, 167–186.

Malfere J.-L. 2002 Etude des variations géochimiques le long des zones néovolcaniques de l'Islande. Thèse de l'université deGenève.

Nicholson H., M. Condomines, J.G. Fitton, A.E. Fallick, K. Grönvold & G. Rogers, 1991, Geochemical and isotopic evidence for crustal assimilation beneath Krafla, Iceland. J. Petrol. 32, 1005–1020.

Sigmarsson S., Ch. Hémond, M. Condomines, S. Fourcade and N. Oskarsson, 1991, Origin of silicic magma in Iceland revealed by Th isotopes, Geology, 19, 621-624.

Thirlwall, M.F. 1994, Generation of the Pb isotopic characteristics of the Iceland plume, J. Geol. Soc. London 152, 991-996.

FORAMINIFERA ISOTOPIC RECORDS... WITH SPECIAL ATTENTION TO HIGH NORTHERN LATITUDES AND THE IMPACT OF SEA-ICE DISTILLATION PROCESSES

Claude Hillaire-Marcel, GEOTOP-UQAM

Abstract

Since the reassessment of oxygen isotope paleotemperatures by N. Shackleton in the late 60s, most papers using isotopic records from planktic or benthic foraminifers imply a direct relationship between oxygen isotopes in seawater and the ice/ocean volume, thus some linkage with salinity, sea level, etc. Such assumptions are also made when incorporating "isotopic modules" in coupled models. Here, we will further examine the linkages between salinity and oxygen isotope ratios of sea-water recorded by foraminifers, and their potential temporal and spatial variability, especially in the northern North Atlantic and the Arctic oceans. If temporal and spatial changes in the isotopic composition of precipitations and ice meltwaters tune the isotopic properties of the fresh water end-member that dilutes the ocean, rates of sea-ice formation and evaporation at the ocean surface play a further role on the salt and oxygen isotope contents of water masses. Thus, the oxygen 18-salinity relationship carries a specific isotopic signature for any given water mass. At the ocean scale, residence time and mixing of these water masses, as well as the time dependent-achievement of proxy-tracer equilibrium, will also result in variable recordings of mass transfers into the hydrosphere, notable between ice-sheets and ocean. Since these records in water mass may vary in both amplitude and time, direct correlations of isotopic records will potentially be misleading. Implications of such issues on the interpretation of oxygen isotope records from the sub-arctic seas will be discussed, as well as the inherent flaws of such records due to sedimentological and or ecological parameters.

Introduction

It is not the intention here to review the literature about stable oxygen and carbon isotopes in the ocean and their recording by biogenic carbonates such as foraminifers. Review papers exist (e.g., Ravelo and Hillaire-Marcel, 2007). We presume that some knowledge of such proxies that constitute the basics of paleoceanography is now secured in the geoscience community. The present summary will thus address departures from basic principles, with special attention to processes of particular importance in the northern North Atlantic and the Arctic Ocean. Foraminiferal isotopic records have intrinsic limitations linked to foraminifer ecological properties and/or sedimentological processes. Such limitations are of concern everywhere, however high latitude recordsare also impacted by the effect of sea-ice production rates on the ^{18}O-salinity properties of water masses. In addition, the Atlantic Meridional Overturning Circulation (AMOC) has been strongly impacted by freshwater pulses from the growth and decay of the large continental ice-sheets of the northern hemisphere. Such events have left characteristic imprints in oxygen isotope records that may deserve further examination to be properly interpreted in terms of hydrographical changes in the North Atlantic. These are the few aspects we will examine below in more detail.

From oxygen isotopes in calcite to water mass properties

The so-called paleotemperature equation most currently used (Shackleton, 1974) is as follows:

$$t\,(°C) = 16.9 - 4.38\,(\delta c - A) + 0.10\,(\delta c - A)^2$$

with $A = (\delta w - 0.27)$, δc and δw standing for the oxygen isotope composition in δ-values against VPDB and VSMOW (see Coplen, 1983), and the 0.27‰ correction standing for the offset, on the VPDB scale, between the CO2 equilibrated with VSMOW at 25°C and that extracted from the VPDB, at the same temperature.

The task of the paleoceanographer has been to use this equation with the two unknowns: the temperature and the isotopic composition of the ambient water at the time of carbonate growth, assuming that isotopic equilibrium was indeed achieved during precipitation. Fortunately, many foraminifers currently

used in paleoceanographic reconstructions seem to form their calcite under such conditions. Noticeable exceptions exist, such as *Cibicidoïdes wuellerstorfi*. It nonetheless follows other benthic foraminiferal records with a quite constant 0.64‰ offset (Shackleton and Opdyke, 1973), still not fully explained.

In the near future, we hope to see instrumental capabilities for the analysis of rare isotopic combinations, such as ^{13}C-^{18}O (e.g., mass 47 in the CO2 extracted from calcite), to be analyzed from very small samples. This would provide a quantitative assessment of the temperature during carbonate precipitation (cf. "clumpted isotope temperatures"; e.g., Eiler, 2007). Currently, paleotemperatures extracted from elemental ratios such as Mg/Ca from foraminifer shells remain the best way to provide the above equation with a reliable temperature value (see Barker et al., 2005, for a review).

Assuming that the growth temperature of the foraminiferal calcite analyzed is known, one then faces the challenge of correctly interpreting the δw value calculated from the paleotemperature equation. Since Shackleton's papers in the late 1960s, direct linkages between the isotopic composition of seawater and its salinity have been postulated. Indeed, the growth of continental ice sheets represents a distillation process where isotopically light fresh water is removed from the ocean, only to produce opposite trends when returned as melt water. Some departure from this "ideal" budget of mass-transfers within the hydrosphere has been highlighted by Waelbroeck and others (2002). As a matter of fact, the temporal and spatial variability of the isotopic composition of ice meltwater and freshwater,, and the oceanic distribution of water masses with specific properties are likely to result in local isotopic records. These records may show significant departures from any stacked record, whatever the "representativity" of this record may be (e.g., Lisiecki and Raymo, 2005). Site-specific interpretations of such isotopic offsets in terms of changes in salinity are similarly questionable. Distillation processes produced by sea-ice formation at high latitudes, and evaporative processes at low latitudes, result in salt-isotope properties of water masses. These processes produce isotopic values that deviate from any simple linear relationship between local freshwaters and standard mean ocean water. In this overview, we will further examine the processes linked to sea-ice growth.

Isotopic imprint of the distillation of sea-water through sea-ice formation

As illustrated below in Figure 1, the linkage between salinity and isotopic composition of water masses from the North Atlantic is more complicated than a simple mixing system between freshwater and seawater.

.

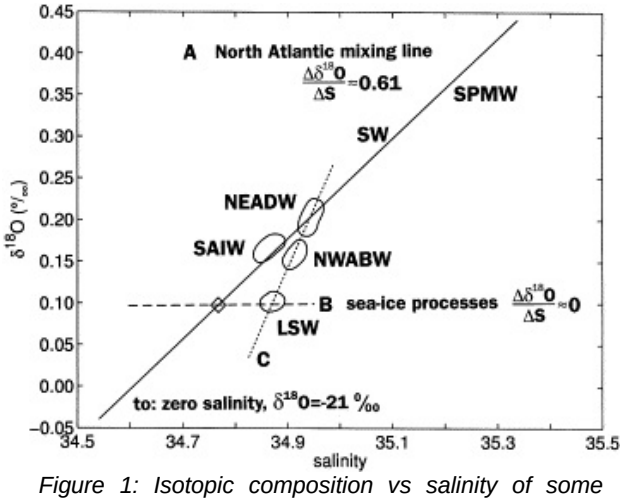

Figure 1: Isotopic composition vs salinity of some major North Atlantic Water masses (Frew et al., 2000).

SPMW: Sub-Polar Mode Water (~ surface water -SW- of the NW Atlantic); NEADW: North-East Atlantic Deep Water (~Iceland-Faroe-Scotland overflow); NWABW: North-West Atlantic Bottom Water (~Denmark Strait overflow water); LSW: Labrador Sea Water; SAIW: Sub-Arctic Intermediate Water. Note that the surface water line, with its -21‰ y-intercept, does not correspond to a mixing line between Standard Mean Ocean Water and any surface water from high latitudes, where the mean isotopic composition of Arctic rivers is of about -17‰. Thus, even this recirculated water mass shows a $\delta^{18}O$-salinity relationship significantly modified by distillation processes resulting in unconservative properties.

At low latitudes, the deviations are caused by kinetic effects linked to evaporation, affecting the $\delta^{18}O$-salinity properties of surface waters such as those of the Gulf Stream. However at high latitudes, distillation of sea-ice from the low salinity, low $\delta^{18}O$ surface water layer notably of the Arctic Ocean, results in the production of isotopically light brines as illustrated in figures 2 and 3 below.

The distillation of sea-ice thus releases brines even slightly more depleted in heavy isotopes than the surface water mass itself due to the slight ^{18}O-enrichment of ice vs water which sink in the water column. When melting, sea-ice contributes to the low salinity of the surface water layer while enriching it with

heavy isotopes. These processes are illustrated in the figure below.

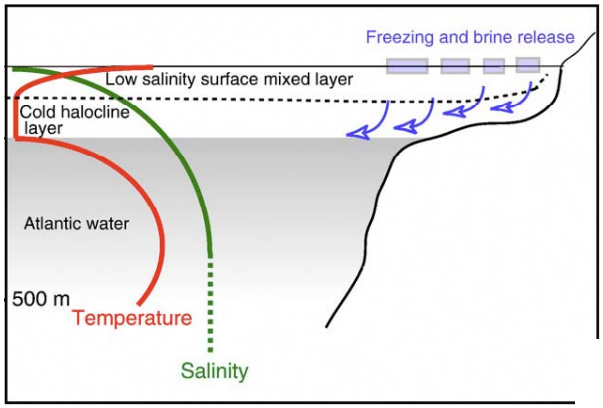

Figure 2: Sketch (modified from Aagaard, 1981) illustrating sea-ice production (with subsequent release of brines sinking in the water column) in the low-salinity (low $\delta^{18}O$) surface water layer of the Arctic Ocean.

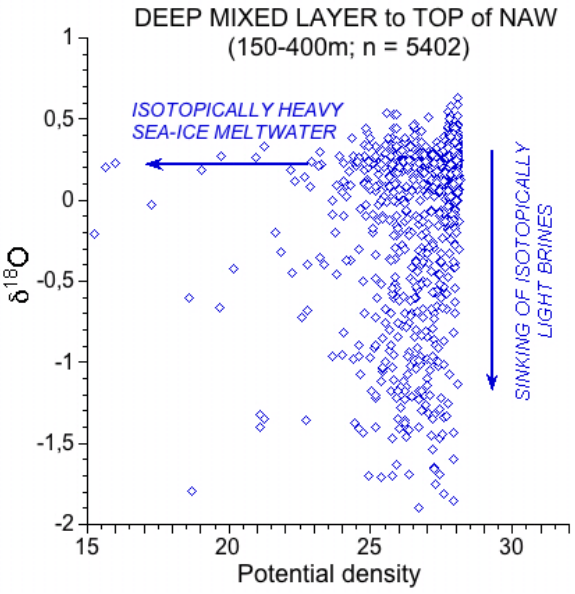

Figure 3: Isotopic composition vs potential density of the subsurface water mass of the Arctic Ocean (on top of the "warm" and saline North Atlantic Water mass, where asymbiotic planktic foraminifers may find a suitable habitat). Data from Schmidt et al., 1999).

Neogloboquadrina pachyderma is the only species of planktic foraminifera present in the Arctic. It has also been abundant throughout glacial intervals in North Atlantic records. This planktic species, as well as benthic foraminifers living under areas of sea-ice production, capture these salinity related isotopic offsets. This is illustrated below using isotopic measurements of core-top assemblages of *N. pachyderma* in the Arctic Ocean.

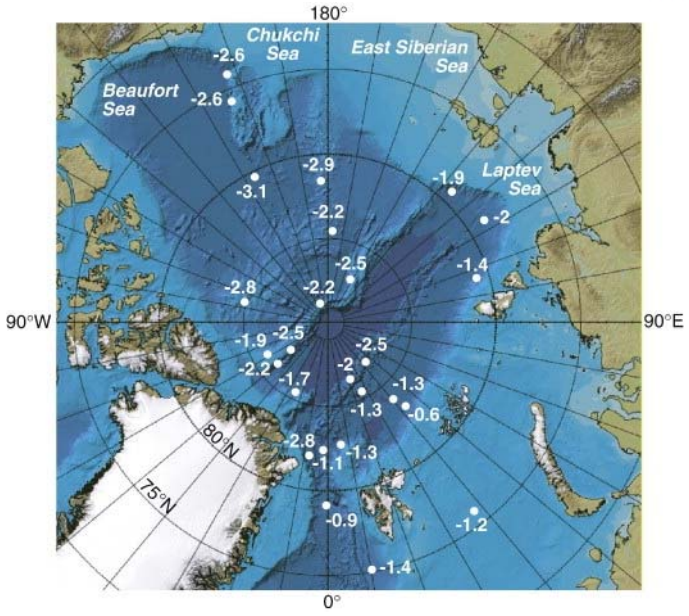

Figure 4: Sketch-map of the distribution of isotopic offsets in Neogloboquadrina pachyderma vs equilibrium conditions for a calcite precipitated at mid-depth along the pycnocline between the cold and dilute surface water layer of the Arctic Ocean and the underlying North Atlantic Water mass. These isotopic offsets have been tentatively linked to the rate of production of isotopically light brines linked to sea ice formation (from Hillaire-Marcel and de Vernal, 2008; The Arctic topography map is from the International Bathymetric Chart of the Arctic Ocean IBCAO).

Based on these observations, one must thus question the forcing process behind the large isotopic excursions recorded by planktic foraminifers in the past, specifically during Heinrich events (Hillaire-Marcel and de Vernal, 2008). Although freshwater pulses such as the final drainage of Lake Agassiz into the NW North Atlantic approximately 8.4 ka ago have practically left no isotopic imprint on planktic foraminiferal records (Hillaire-Marcel et al., 2007 and 2008), episodes of sea-ice formation that occurred in the North Atlantic during Heirich events resulted in characteristic "light" isotope shifts (e.g., Hillaire-Marcel and de Vernal, 2008).

In the example below, from Jennings et al. (2006), several records from the Denmark Strait area depict such large amplitude light ^{18}O-peaks in both planktic and benthic foraminifers during the Younger Dryas cold spell. N. pachyderma in fact reach values as low as 1.6‰. On one hand, the release of huge amounts of fresh water during this interval seems improbable, but on another hand, such a high dilution of the surface water would be incompatible with salinity requirements of *N. pachyderma* (> 34; cf. Hilbrecht, 1997). Thus, the most likely explanation here is that these fossil assemblages recorded pulses in sea-ice growth with significant addition of ^{18}O-depleted brines to *N. pachyderma* habitat, deeper in the water column or in brine-rich micro-habitat in the ice itself.

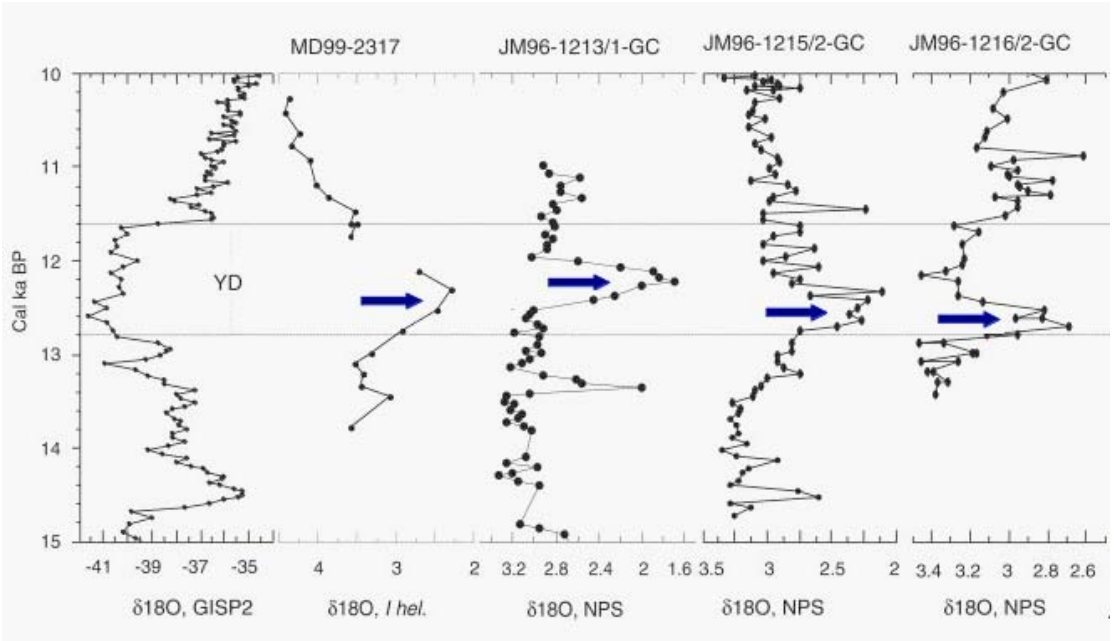

Figure 5. Records spanning the Younger Dryas interval from the Greenland Shelf, east of Denmark Strait (from Jennings et al., 2006), with reference to the GISP2 ice record (Grootes et al., 1993). Note the large light isotopic excursions (blue arrows), which might indicate episodes of enhanced sea-ice formation

A subsequent concern is the dispersal pattern of an isotopic/salinity event in the ocean and thus, the correlation and interpretation of isotopic records in general. Firstly, it has been shown that "major gradients exist, laterally, between the abyssal North Atlantic and North Pacific, and vertically over much of the ocean, persisting for periods longer than 2000 years and with magnitudes bearing little or no relation to radiocarbon ages" (Wunch and Heimbach, 2008). Furthermore, both the glacial and interglacial oceans cannot be seen in an equilibrium state: transient states seem to characterize even relatively long interglacial stages (e.g., de Vernal and Hillaire-Marcel, 2008). Thus, linkages between calculated δ^{18}Ow-values from foraminiferal records, with specific source-events from glaciers, continents and ocean reorganization cannot be made without care. They might be valid near the sources, but questionable in distal sites.

Inherent limitation in foraminiferal and sedimentological records

Several other properties of isotopic and sedimentological records must be kept in mind when using such records as proxy for paleohydrographical conditions, regardless of the latitude of the study site and basin. They are briefly evoked here. A more exhaustive examination of such intrinsic limitations of paleoceanographical records can be found in Ravelo and Hillaire-Marcel (2007) and Huygens (2007).

Among major parameters, with respect to records from planktic foraminifers: the seasonality and the interannual/interdecadal variability in their production is particularly important at high latitudes, where they often live near boundaries of their optimal habitat. Similarly,, their ecological affinities and depth habitat are quite critical. Most asymbiotic species depict some isopycnal distribution where T and S may varywhile preserving a mean density. With respect to benthic foraminifers, special attention should also be paid to their specific micro-habitat from sediment surface to a few centimeters below. Then, linked to benthic life in general, the mixing of sediment occurs with a depth-pattern and intensity which are linked to several parameters (organic carbon content, oxygen availability, bathymetry, benthic ecological structure, turbidity, grain size...), thus varying strongly in time and space. This process results in a redistribution of proxy-indicators in the sediment, along with some smoothing and transformation of records, which are further accentuated by variable fluxes of carrier organisms and particles.

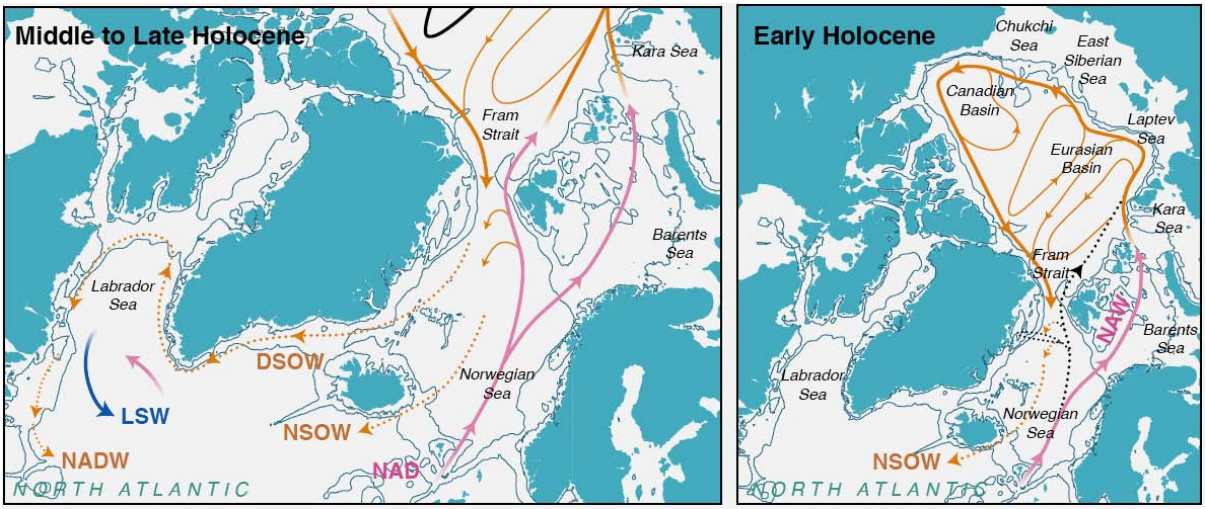

Figure 6. The behavior of the AMOC during the Middle and Late Holocene (left) and the Early Holocene (right), from Weaver and Hillaire-Marcel (2004). Intermediate or deep water masses are orange; the incoming North Atlantic warm and saline water mass (North Atlantic Drift (NAD) then North Atlantic Water (NAW)) is red. Cold and dilute surface currents evacuating Arctic fresh waters westward are not shown. Note the strong opposition between a high-salinity northeast North Atlantic and a low-salinity northwest North Atlantic. Maximum outflow of Norwegian Sea Overflow Water (NSOW) occurred during the early Holocene, whereas Denmark Strait Overflow Water (DSOW) peaked during the mid-Holocene and Labrador Sea Water (LSW) formation reached a maximum during the late Holocene. This east-west temporal shift is linked to increasing density of surface waters westward. Under the condition of increasing freshwater fluxes from the Arctic, the most sensitive sector of deep-intermediate formation would thus be the Labrador Sea, as also indicated by recent modeling experiments.

For example, stable isotope data combined with radiogenic and U-series isotope studies have yielded some large features with respect to the Holocene inception of the modern AMOC pattern as illustrated in Figure 6.

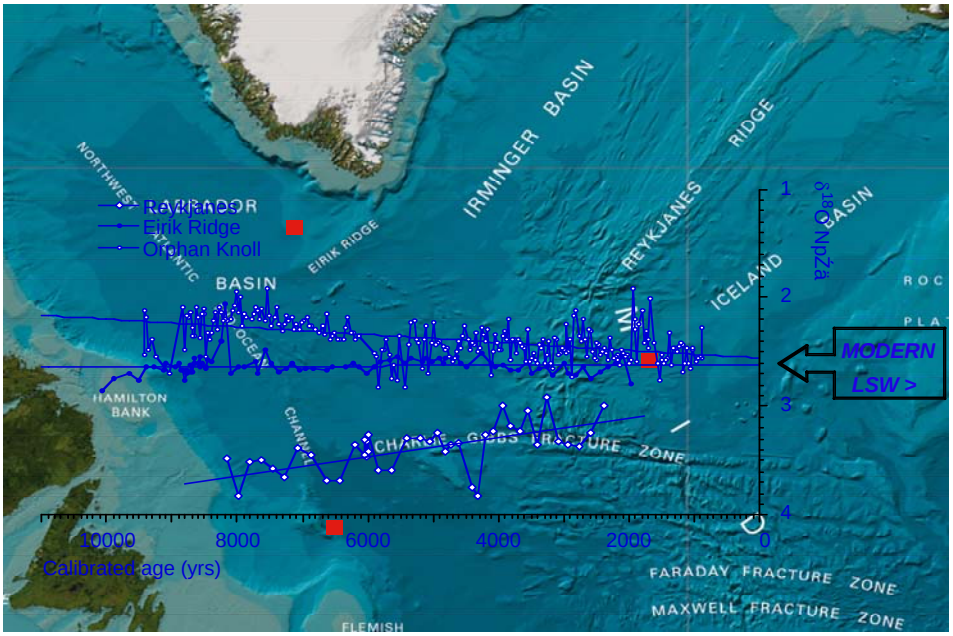

Figure 7: Isotopic composition of N. pachyderma in three sites of the North Atlantic suggesting a trend for homogenization of isotopic compositions on top of the LSW mass (N. pachyderma's habitat) (data from de Vernal and Hillaire-Marcel, 2006).

For a given water-mass, at a basin scale, it is also possible to derive some information about the evolution of this water mass, as in the example of the Labrador Sea Water illustrated in Figure 8. Due to temperature requirement, *N. pachyderma* occupies the lower pycnocline of the Holocene North Atlantic, on top of the Labrador Sea Water (LSW) since its inception approximately 7 to 8 ka ago (see de Vernal and Hillaire-Marcel, 2006, and references therein). The trends of oxygen isotope

compositions from records illustrating several sectors of the North Atlantic converge to a "modern" value of about 2.6‰, suggesting that the complete homogenization of the LSW required a few thousand years, as suggested by Wunch and Heimbach's experiments (2008).

The examples above provide arguments to continue documenting isotopic compositions in foraminiferal assemblages, especially at basin to sub-basin scales. The caveat, in terms of extrapolation of interpretative lines at a larger scale, is even more critical when looking at nearshore records. In the example of Iceland, the presence and temporal and spatial variability of several water masses around the island may result in "isotopic" ambiguities, where any isotopic signal could indeed respond to some excursion of a nearby water mass or to changes in the properties of a given water mass. In this case, multiproxy approaches will be essential.

References

Aagaard, K., 1981. On the deep circulation of the Arctic Ocean. *Deep Sea Research 28*: 251–268.

Coplen, T., 1994. Reporting of stable hydrogen, carbon, and oxygen isotopic abundances. Pure and Applied Chemistry 66: 273-276.

de Vernal, A., Hillaire-Marcel, C., 2008. Natural Variability of Greenland Climate, Vegetation and Ice Volume during the Last Million Years. *Science* 320: 1622-1625.

de Vernal, A., Hillaire-Marcel, C. 2006. Provincialism in trends and high frequency changes in the northwest North Atlantic during the Holocene. *Global Planetary Cycles* 54: 263-290.

Eiler, 2007. "Clumped-isotope" geochemistry-The study of naturally-occurring, multiply-substituted isotopologues. Earth and Planetary Science Letters 262: 309-327.

Frew, R.D., Dennis, P.F., Heywood, K.J., Meredith, M.P., Boswell, S.M., 2000. The oxygen isotope composition of water masses in the northern North Atlantic. Deep Sea Research 47: 2265-2286.

Grootes, P.M., Stuiver, M., White, J.W.C., Johnsen, S., Jouzel, J., 1993. Comparison of oxygen isotope record from the GISP2 and GRIP Greenland ice cores. Nature 366: 552–554.

Hilbrecht, H., 1997. Morphologic gradation and ecology in Neogloboquadrina pachyderma and N. dutertrei (planktic foraminifera) from core top sediments. Marine Micropaleontology 31: 31-43.

Hillaire-Marcel, C., de Vernal, A., 2008. Stable isotope clue to episodic sea ice formation in the glacial North Atlantic. *Earth and Planetary Science Letters* 268: 43-150.

Hillaire-Marcel, C., Hélie, J.-F., McKay, J., de Vernal, A., 2008. Elusive isotopic properties of deglacial meltwater spikes into the North Atlantic: Example of the final drainage of Lake Agassiz. *Canadian Journal of Earth Science* 45: 1235-1242.

Hillaire-Marcel, C., de Vernal, A., Piper, D. J W., 2007. Lake Agassiz Final drainage event in the northwest North Atlantic. *Geophysical Research Lett*ers 34, L15601, doi:10.1029/2007GL030396.

Huygens, K.A., 2007. Radiocarbon dating of deep-sea sediments. In *Methods in Late Cenozoic Paleoceanography. Elsevier*, Hillaire-Marcel and de Vernal, eds., Elsevier, Amsterdam (NL), pp. 193-218.

Jennings, A.E., Hald, M., Smith, M., Andrews, J.T., 2006. Freshwater forcing from the Greenland Ice Sheet during the Younger Dryas: Evidence from southeastern Greenland shelf cores. Quaternary Science Reviews 25: 282-298.

Lisiecki, L.E., Raymo, M.E., 2005. A Pliocene-Pleistocene stack of 57 globally distributed benthic $\delta^{18}O$ records. Paleoceanography 20, PA1003, doi:10.1029/2004PA001071.

Ravelo, C., Hillaire-Marcel, C., 2007: The Use of Oxygen and Carbon Isotopes of Foraminifera in Paleoceanography. In *Methods in Late Cenozoic Paleoceanography. Elsevier*, Hillaire-Marcel and de Vernal, eds., Elsevier, Amsterdam (NL), pp. 735-764.

Schmidt, G. A., Bigg, G. R., Rohling, E. J., 1999. Global seawater oxygen-18 database, http://data.giss.nasa.gov/o18data/.

Shackleton, N.J., 1974. Attainment of isotopic equilibrium between ocean water and the benthonic foraminifera genus Uvigerina: isotopic changes in the ocean during the last glacial, in *Les méthodes quantitatives d'étude des variations du climat au cours du Pléistocène*, J. Labeyrie, ed., Centre National de la Recherche Scientifique (CNRS), Paris, pp. 203-209.

Shackleton, N.J., 1967. Oxygen isotope analyses and Pleistocene temperatures reassessed. Nature 215, 15–17.

Shackleton, N.J., Opdyke, N.D., 1973. Oxygen isotope and palaeomagnetic stratigraphy of Equatorial Pacific core V28-238: Oxygen isotope temperatures and ice volumes on a 10^5 year and 10^6 year scale. Quaternary Research 3: 39-55.

Waelbroeck, C., Labeyrie, L., Michel, E., Duplessy, J.C., McManus, J.F., Lambeck, K., Balbon, E., Labracherie, M., 2002. Sea-level and deep water temperature changes derived from benthic foraminifera isotopic records. Quaternary Science Reviews 21: 295–305.

Wunch, C., Heimbach, P., 2008. How long to oceanic tracer and proxy equilibrium? Quaternary Science Reviews 27: 637-651.

Weaver, A.J., Hillaire-Marcel, C., 2004. Global warming and the next ice-age. *Science* 304: 400-402.

RECENT CHANGES IN THE NORTH ATLANTIC CIRCULATION

Thierry Huck
<thuck@univ-brest.fr>
Laboratoire de Physique des Océans (UMR6523 CNRS IFREMER IRD UBO)
UBO-UFR Sciences F308, 6 avenue Le Gorgeu, CS 93837, 29238 Brest Cedex 3, FRANCE

Abstract

The three-dimensional ocean circulation is hardly observable but its quantification has greatly improved over the last two decades, due to moored array observations, deep float trajectories and satellite altimetry. Historical temperature and salinity data reveal changes on various periods in the North Atlantic: a global warming trend of the upper layers, quasi-decadal and multidecadal oscillations. The associated changes in the circulation are not yet clearly determined, but some hints from observations and models are presented.

Introduction

The large-scale ocean circulation is driven by the winds and exchanges of heat and freshwater with the atmosphere at the surface. It plays a role equivalent to the atmosphere in the Earth climate system and contributes to 1/3 of the poleward heat transport, reducing the temperature gradient at the Earth surface. The North Atlantic and Arctic Oceans are the very unique places where most of the transformation of warm surface waters into cold deep waters occurs and feed the global conveyor belt or thermohaline circulation, although this may not have always been the case in the past. In fact the intensity of this transformation through convection has varied over the last decades, in response to changes in the atmospheric conditions. Reciprocally, deep water formation releases a large amount of heat to the atmosphere that is brought to Europe by the predominant westerlies in the midlatitudes, modulating temperature and precipitations. The observed freshening of the North Atlantic, reducing the seawater density hence its ability to convect, analyses of repeated hydrographic sections, and coupled climate models results, have raised uncertainty in the maintenance of the thermohaline circulation within the ongoing global warming.

Unfortunately, the large-scale ocean circulation is difficult to measure directly: historical currentmeter data are often short, very localized and polluted by very energetic high-frequency signals due to tides and mesoscale eddies; recent Acoustic Doppler Current Profiler data allow continuous monitoring on moored arrays or along ship tracks, but suffer otherwise the same limitations. Hence currents are often deduced from hydrology, namely temperature and salinity, that have been measured accurately since the 1950's, continuously on the vertical through CTD (conductivity-temperature-depth) deployments from ships since the 1970's, and now on autonomous profilers as in the Argo program. The combination of the equations of movements (the geostrophic equilibrium between pressure gradient and Coriolis force, and the hydrostatic balance) leads to the thermal wind balance, that provides the vertical derivative of the horizontal velocity given the density field (computed from temperature and salinity). One finally needs some additional information or hypothesis for the absolute velocity at a given depth (the famous level of no motion) to compute the absolute velocity field.

Fortunately, the development of satellite altimetry has provided continuous almost-global observations of sealevel since late 1992 that proves the most complete oceanographic dataset nowadays. Surface geostrophic currents can be computed at 1/2° resolution from 70°S to 70°N on a weekly basis in near real time. Associated with the deployment of the Argo array of profiling floats since 2003 (the target 3000 floats spread worldwide was reached in 2009), providing vertical profiles of temperature and salinity down to 2000m every 10 days as well as trajectories at their usual parking depth of 1000m, the global observing system of the ocean has never been so dense, maybe at the expense of reduced funding for measurements below 2000m...

Given these landmarks in the evolution of the observing system of the ocean and the associated uncertainties to estimate the ocean currents, we will successively describe the North Atlantic general circulation and its reported variations during the last decades.

The ocean general circulation in the North Atlantic

The surface circulation of the North Atlantic Ocean is composed of the anticyclonic subtropical gyre, between 5°N and 45°N, and the cyclonic subpolar gyre, between 45°N and the sills around 65°N between Greenland, Iceland, Faroe and Scotland. The intense western boundary current of the subtropical gyre, the famous Gulf Stream, follows the eastern coast of the USA from Florida to Cape Hatteras, where it detaches from the coast and heads eastward as the North Atlantic Current. Part of it

recirculates southward in the subtropical gyre, the other part heading northward in the subpolar gyre and ultimately crossing the sills into the nordic seas. This upper circulation is estimated through surface drifters data for instance, and its variations can be monitored through satellite altimetry. The deep circulation is far more difficult to monitor: from the north, it is composed of the overflows from the sills, that find their way along the complex bathymetry as Western Boundary Currents. The Iceland-Scotland Overflow Water follows first the eastern slope of Reykjanes Ridge, than the western slope into the Irminger Sea, where it joins the Denmark Strait Overflow Water along the east coast of Greenland, around Cape Farewell, than flows cyclonically in the Labrador Sea, and exits as the Deep Western Boundary Current along the Grand Banks of Newfoundland. More details for the subpolar gyre surface and deep currents and transports are shown in Figure 1.

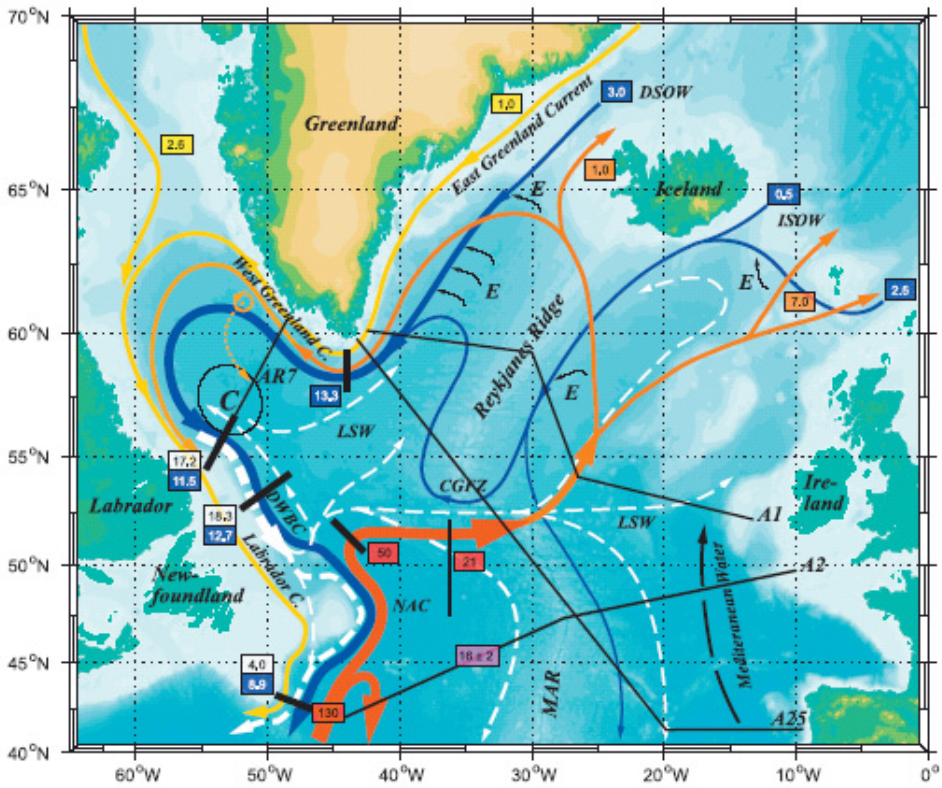

Figure 1: Schematic circulation of the subpolar North Atlantic with topographic features and different current branches identified (CGFZ Charlie Gibbs Fracture Zone, MAR Mid-Atlantic Ridge; DWBC Deep Western Boundary Current, NAC North Atlantic Current, DSOW and ISOW Denmark-Strait and Iceland-Scotland Overflow Water, LSW Labrador Sea Water; C Convection, E Entrainment). Locations of moored current-meter arrays of quoted transports (Sv = 10^6 m^3/s) are marked by heavy black bars. Also shown are the WOCE Hydrographic Program lines A1, A2 and A25 (Ovide) across the Atlantic and AR7 across the Labrador Sea (thin black). Transports are marked for the mean DWBC (LSW layer in white box, deeper layers in blue box), for the NAC (red box) and extensions (orange box) as well as for the shallow Arctic inflow (yellow box); MOC Meridional Overturning Circulation across A2 (magenta box) as obtained from inverse models (after Schott and Brandt 2007).

The transformation of warm surface waters into cold deep waters occurs through convection in regions of intense surface cooling, in the Nordic, Irminger and Labrador Seas. The associated large-scale circulation, named the thermohaline circulation or also conveyor belt, originates from temperature and salinity - hence density - contrasts that drives gravity currents. Its complexity results from multiscale interaction of dynamical and thermodynamical processes: the global balance of deep water formation and consumption remains relatively unclear since the processes controlling diapycnal (vertical on first order) mixing are not yet known, the overflows interaction with bottom topography induces entrainment and mixing difficult to quantify, convective chimneys are intermittent and their size is of order of kilometers, surface water densification is intensified by brine rejection through sea ice formation...

The Meridional Overturning Circulation, the two-dimensional latitude-depth view of these currents, results from the northward flow in the upper layers (NAC) and the southward flow at depth (DWBC). Estimates for the intensity of the Atlantic MOC are obtained from inverse model calculations, along

hydrographic sections or for regional configurations, and yields values from 13 to 18 Sv at 48°N (1 Sverdrup is about the cumulated flow of all the world rivers). The associated poleward heat transport, resulting from the northward transport of *warm* upper waters in the North Atlantic Current and the southward return flow of *cold* waters within the Deep Western Boundary Current, is estimated at 0.61±0.07 PW (1 PW = 10^{15} W is 100 times the global energy production of electricity and heat).

Decadal and interdecadal changes in North Atlantic circulation

While hydrographic data have been collected for more than 60 years in the North Atlantic, such a historical dataset is not available for direct measurements of currents. In order to determine the evolution of ocean currents over the last decades, one needs to rely on theoretical links between hydrography and currents. The overflows from the nordic seas and the deep convection in the Labrador (and probably Irminger) Sea lie at the source of the Atlantic overturning. The recent monitoring of the overflows does not show significant variability but may be too short to address decadal and longer periods. The availability of hydrographic data collected in the Labrador Sea since 1948 reveals long term changes of temperature and salinity: cooling and freshening from 1966 to 1992 (Dickson et al. 2002), associated with atmospheric circulation shift from strongly negative to strongly positive values of the North Atlantic Oscillation index.

Analyses of surface data (for which we have the longest historical record) through various statistical techniques (EOF Empiral Orthogonal Fonctions, MSSA Multichannel Singular Spectrum Analysis) usually identify different signals in the North Atlantic: a quasi decadal signal which characteristic SST pattern is tripolar (Alvarez-Garcia et al. 2008); a multidecadal signal named Atlantic Multidecadal Oscillation (AMO, Kerr 2000), which index is defined as the averaged North Atlantic Sea Surface Temperature (SST) from 0 to 70°N (detrended); and a global warming signal, often nonlinear. Distinguishing the two latter may be challenging and an original method based on coupled model ensemble simulations has been proposed (Knight 2009). Although the cold (1905-1925, 1970-2000) and warm (1925-1970, 2000 onward) phases of the AMO appear respectively associated with reduced and strengthened thermohaline circulation and North Atlantic Current (Knight et al. 2005, Álvarez-García et al. 2008), the mechanism sustaining this oscillation is still unclear. A coupled model simulation reproducing AMO-like centennial variability suggest a coupled mechanism involving northward shift of the ITCZ position with strong MOC, increased freshwater input into the tropical North Atlantic Ocean hence generation of negative salinity anomaly that propagates slowly northward and modify after several decades the overturning (Vellinga and Wu 2004).

The analysis of the now 17 year long record of sea surface height (SSH) from satellite altimetry show a remarkable signal in the North Atlantic (Figure 2). The mean surface geostrophic currents flow cyclonically (anticyclonically) around the low (high) values of SSH in the subpolar (subtropical) gyre, in analogy with the surface winds around the icelandic low (Azores high) pressure in the atmosphere. Almost continuously from 1994 to 2004, the lowest SSH in the center of the subpolar gyre have been rising, reducing the intensity of the subpolar gyre surface currents by almost 20% (Häkkinen and Rhines 2004). As the the subpolar gyre shrinks, warmer and saltier waters from the North Atlantic Drift make their way to the Nordic Seas (Häkkinen and Rhines 2009). However the relationship between this upper ocean horizontal subpolar circulation and the vertical Atlantic meridional overturning circulation is still unclear, although some numerical models suggest strong linkages between subpolar gyre circulation, Labrador Sea Water production and the Atlantic MOC. (now associated with ADCP current measurements). A few of these sections have been repeated in the North Atlantic around 24°N, 48°N, and between Greenland and Portugal (Fourex, Ovide). They provide a very instantaneous view of the circulation and contain very energetic mesoscale signals that may be difficult to separate from the lower frequency signal one is looking for. The early results from the repeated hydrographic section along 24°N (Bryden et al. 2005) may be in doubt given the large high-frequency variability observed in the transport (Cunningham et al. 2007). Inversions across 48°N for 5 sections from 1993 to 2000 show no decadal trend (Lumpkin et al. 2008). On the other hand, the ongoing Ovide program of repeated hydraphic sections between Greenland and Portugal, close to the A25 line sampled in 1997 (Fourex), suggest a possible decline of the overturning from 18.5 Sv in 1997, 16.4 Sv in 2002 and 2004, to 11.4 sv in 2006 (in density coordinates, Gourcuff 2008), although the latter value may be unusually low due to high frequency variability.

Results from numerical models, with or without data assimilation, do not help much in sorting out these results: we observe a large dispersion for the mean values of the MOC as well as its variability, although many suggest a declining trend since 1995. Sustained monitoring is required in order to better understand what is going on. Direct measurements of the overturning requires coast to coast

hydrographic sections

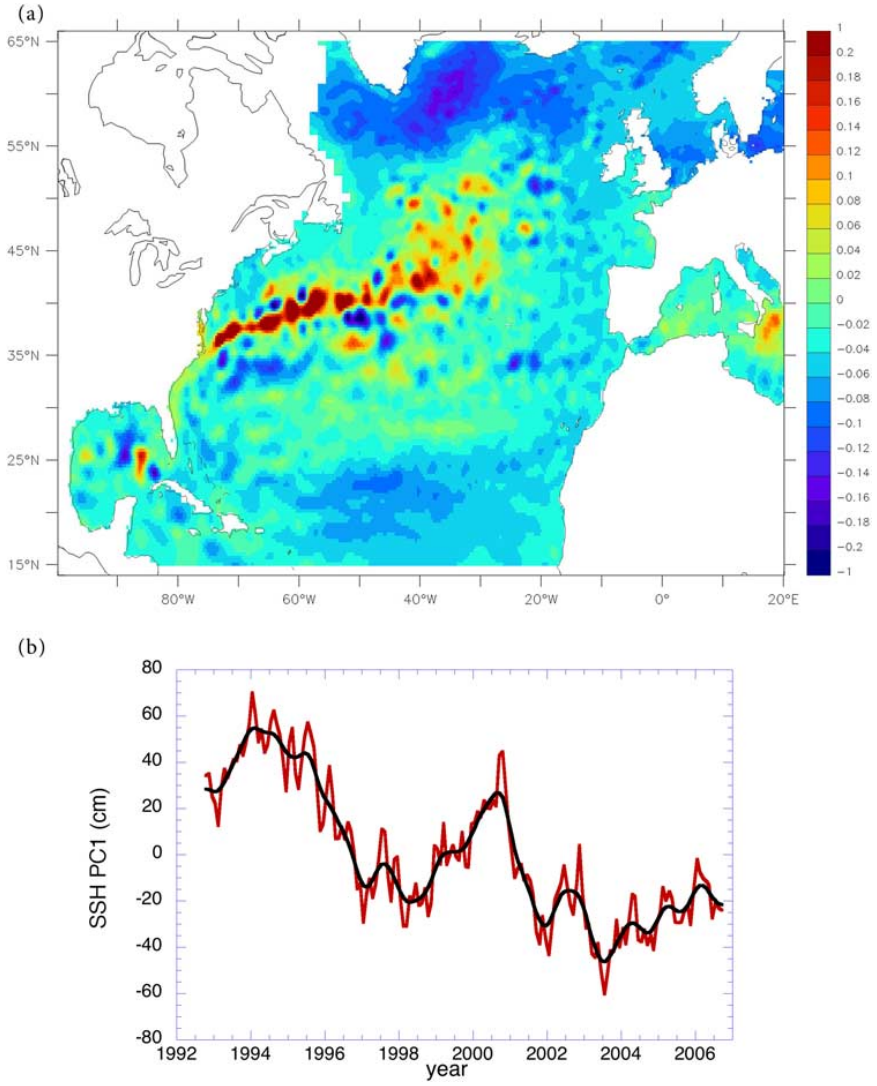

Figure 2: (top) The spatial pattern of the first empirical orthogonal function and (bottom) associated time series for the sea surface height from AVISO altimeter data. The spatial pattern is dimensionless, the time series have units of centimeters (after Häkkinen and Rhines 2009).

References

Álvarez-García F., Latif M., Biastoch A., 2008, On Multidecadal and Quasi-Decadal North Atlantic Variability. *J. Clim.*, 21, 3433-3452.

Bryden H. L., Longworth H. R., Cunningham S. A., 2005, Has the Atlantic overturning circulation slowed? *Nature,* 438, 655-657.

Cunningham S. A., Kanzow T., Rayner D., Baringer M. O., Johns W. E., Marotzke J., Longworth H. R., Grant E. M., Hirschi J.-M., Beal L. M., Meinen C. S., Bryden H. L., 2007, Temporal Variability of the Atlantic Meridional Overturning Circulation at 26.5°N. *Science,* 317, 935-938.

Dickson B., Yashayaev I., Meincke J., Turrell B., Dye S., Holfort J., 2002, Rapid freshening of the deep North Atlantic Ocean over the past four decades. *Nature*, 416, 832-837.

Flatau M. K., Talley L., Niiler P. P., 2003, The North Atlantic Oscillation, surface current velocities, and SST changes in the subpolar North Atlantic. *J. Clim.*, 16, 2355-2369.

Gourcuff C., 2008, Etude de la variabilité de la circulation du gyre subpolaire de l'Atlantique Nord à l'aide des données Ovide et des mesures satellitaires. PhD manuscript, Université de Bretagne Occidentale, Brest, France.

Häkkinen S., Rhines P. B., 2004, Decline of subpolar North Atlantic circulation during the 1990s. *Science*, 304, 555-559.

Häkkinen S., Rhines P. B., 2009, Shifting surface currents in the northern North Atlantic Ocean. *JGR*, 114, C4, C04005, doi:10.1029/2008JC004883 .

Kerr R. A., 2000, A North Atlantic climate pacemaker for the centuries. *Science,* 288, 1984-1986.

Knight J. R., Allan R. J., Folland C. K., Vellinga M., Mann M. E., 2005, A signature of persistent natural thermohaline circulation cycles in observed climate. *GRL*, 32, 20, L20708, doi:10.1029/2005GL024233 .

Knight J. R., 2009, The Atlantic Multidecadal Oscillation inferred from the forced climate response in coupled general circulation models. *J. Clim.*, 22, 1610-1625.

Lumpkin R., Speer K., Koltermann K. P., 2008, Transport across 48°N in the North Atlantic Ocean. *JPO,* 38, 733-752.

Parker D., Folland C., Scaife A., Knight J., Colman A., Baines P., Dong B., 2007, Decadal to multidecadal variability and the climate change background. *JGR,* 112, D18, doi: 10.1029/2007JD008411 .

Schott F. A., Brandt P., 2007, Circulation and Deep Water Export of the Subpolar North Atlantic During the 1990's. In: Ocean Circulation: Mechanisms and Impacts, Geophysical Monograph Series 173, American Geophysical Union, 91-117, doi: 10.1029/173GM08.

Vellinga M., Wu P., 2004, Low-Latitude Freshwater Influence on Centennial Variability of the Atlantic Thermohaline Circulation. *J. Clim.*, 17, 4498-4511, doi: 10.1175/3219.1.

TEPHROCHRONOLOGICAL DATING OF HOLOCENE MORAINES AT ICELANDIC GLACIERS, AND CLIMATIC INTERPRETATIONS.

Martin Kirkbride
School of Social and Environmental Sciences
University of Dundee
Dundee DD1 4HN

Abstract

Fluctuations of Icelandic glaciers reveal the impact of regional climate change on the cryosphere, filtered by the different response characteristics of individual glaciers. Frequent tephra deposition upon steadily aggrading aeolian soils provides a useful dating environment, in which basal tephras often provide close minimum ages on underlying tills and outwash deposits in areas where the local tephrostratigraphy is well constrained. We have dated moraines at glaciers across Iceland to improve the Holocene glacial chronology in terms of its temporal extent and resolution. Tephrochronology also provides a test of lichenometric dating, an area for further research. At least five groups of regionally-synchronous advances occurred between c. AD 1700 and 1930 during the "Little Ice Age". The maximum extent of "Little Ice Age" glaciers varies by up to 200 years across Iceland, due more to the response chraracteristics of individual glaciers than to regional climatic variation. At Gígjökull, two glacier advances occurred before the 3rd century AD, with others in the 9th and 12th centuries AD bracketing the Medieval Warm Period. In central and northern Iceland, earlier glacier advances are dated to c. 4.5-5.0, c.3.0-3.5 ka BP, c. 2.0-2.5 ka BP. This classic "Neoglacial" sequence is comparable to other parts of Europe and Scandinavia, but is discernible only at smaller mountain glaciers. In contrast, the 19th-Century advance of large ice caps censored evidence of earlier fluctuations from the moraine record, and preservation potential is preconditioned by glacier type. In general, the forefields of steep, fast-responding glaciers contain more complete archives of Holocene climatic changes than do the margins of the large icefields. Glacier advances appear to be favoured by a weakening of zonal circulation (the negative mode of the North Atlantic Oscillation) associated with cooler, drier winters and cooler, wetter summers.

References

Kirkbride, M.P. and Dugmore, A.J. (2008) Two millennia of glacier advances in southern Iceland dated by tephrochronology. *Quaternary Research* 70, 398-411.

Kirkbride, M.P. and Dugmore, A.J. (2006). Responses of mountain ice caps in central Iceland to Holocene climate change. *Quaternary Science Reviews* 25, 1692-1707.

Kirkbride, M.P. (2002). Icelandic climate and glacier fluctuations through the terminus of the "Little Ice Age". *Polar Geography* **26**, 116-133.

Kirkbride, M.P. and Dugmore, A.J. (2001a) Can lichenometry be used to date the "Little Ice Age" glacial maximum in Iceland? *Climatic Change* **48**, 151-167.

Kirkbride, M.P. and Dugmore, A.J. (2001b) Timing and significance of mid-Holocene glacier advances in northern and central Iceland. *Journal of Quaternary Science* **16**, 145-153.

ARCTIC SEA ICE: HIGH RESOLUTION RECONSTRUCTIONS

Guillaume Massé[1], Simon Belt[2], Marie-Alexandrine Sicre[3]
[1] LOCEAN, UMR7159 CNRS, UPMC,IRD,MNHN, guillaume.masse@upmc.fr
[2] LSCE, UMR8212 CNRS, CEA, UVSQ
[3] SOGEES, University of Plymouth, UK

Abstract

Sea ice is an essential component of the Earth climate. In the current context of global climate change, it is therefore essential to obtain a clear and detailed account of its historical variations. The recent development of IP_{25}, a novel sea ice proxy based on the preservation in marine sediments of a unique chemical fossil produced by sea ice algae has allowed for the a series high resolution accounts of Arctic sea ice over the last few millennia to be constructed.

Introduction

Given the current debate regarding climate change on Earth and, in particular, the relative contributions of natural processes and anthropogenic inputs, it is crucial to obtain a clear and detailed account of past climatic variations and the factors controlling these (Jones et al., 2001). Over the past few years, considerable attention has been given to the seasonal sea ice coverage of the Earth's Polar Regions. Advanced satellite data has revealed a considerable decline in ice cover, particularly for the seasonal sea ice which constitutes approximately 50% of total ice coverage for the Arctic and the Antarctic (Serreze *et al*., 2007, 2003; Stroeve *et al.*, 2005). The decline in seasonal ice extent is of particular concern since sea ice plays such a major role in contributing to the dominant oceanic processes and the reflection of incoming solar radiation via the so-called 'albedo' effect (Holland et al., 2001). Although satellite data exists for recent decades, there is a paucity of sea ice data prior to the 1970's and data that does exist is only available at low temporal and spatial resolution. Since predictive climate models rely so heavily on historical datasets, there is a widely accepted urgent need for high resolution accounts of past sea ice coverage (Jones *et al*., 2001). In the absence of direct observational records, acquisition of such datasets is achieved using so-called proxy methods.

Proxy methods for palaeo sea ice reconstruction exist through examination of ice cores and sediments (e.g. Gersonde *et al*., 2005), though many of such methods suffer substantial drawbacks and are usually extremely time-consuming, preventing high resolution studies to be achieved routinely. As such, there are currently relatively few detailed sea ice accounts. It is therefore imperative to develop new proxy methods which will permit rapid acquisition of high resolution sea ice data.

Artic Sea Ice extent

Recently, we have been developing the use of a new sea ice proxy which offers major advantages over traditional methods. The basis of the proxy is a lipid biomarker (IP_{25}) which is synthesised specifically by a number of sea ice associated diatoms (Belt et al., 2007). When detected in sediments below sea ice, this biomarker chemical can be readily distinguished from chemicals derived from marine or terrestrial sources. IP_{25} can be detected in extremely small sediment samples and has been detected in sediments dated >9000 years. As such, quantification of IP_{25} can be achieved at high resolution and over significant timescales (the Holocene, at least) thus allowing for high resolution reconstructions of past sea ice variations.

This lecture will focus on a detailed analysis of a series of sediment cores collected across the Arctic with a particular emphasis on those collected from the Nordic seas area. Using the variations in IP_{25} abundances in the sediments, historical sources documenting past sea ice occurrences (e.g. Koch, 1945; Bergthórsson, 1969; Ogilvie, 1992; Ogilvie and Jonsson, 2001) and several other well established proxies, we have been able to produce high resolution accounts of sea ice for the last few millennia showing evidence for abrupt changes to sea ice and/or climate conditions during that period. For example; Figures 1 & 2 show a continuous record of the relative abundance of IP_{25} for the top (ca. 300 cm) of the MD99-2275 sediment core (collected from the North Icelandic Shelf). These results, when compared with climatic data from previous studies (Ogilvie, 1992; Crowley and Lowery, 2000; Jones et al., 2001; Ogilvie and Jónsson, 2001; Knudsen et al., 2004; Eiriksson et al., 2006; Jiang et al., 2006) show a series of excellent correlations throughout the entire period (Figs. 1 & 2). On an centennial scale, abundances of IP_{25} are entirely consistent with previous estimations of the Little Ice Age (LIA), the Mediaeval Warm Period (MWP) and relative centennial temperatures (Jones et al.,

2001; Ogilvie and Jónsson, 2001). At a higher temporal resolution, 1690-1700 is considered to be the coldest decade for the 17th century in the northern hemisphere (Jones et al., 1998; Crowley and Lowery, 2000) including Iceland (Ogilvie and Jónsson, 2001), and this is reflected by the highest abundance of the IP_{25} biomarker in the MD99-2275 sediment core over the past 1000 years. IP_{25} is also abundant in sediments dated 1776, 1638, 1364, 1331 and 1309 corresponding to decades where large amounts of sea ice have been reported around Iceland (Ogilvie and Jónsson, 2001). In addition, these dates correspond to cold decades as shown by both the diatom-based sea surface temperatures (Fig. 1, Jiang et al., 2005) and the mean northern hemisphere temperatures (Fig. 2; Crowley and Lowery, 2000).

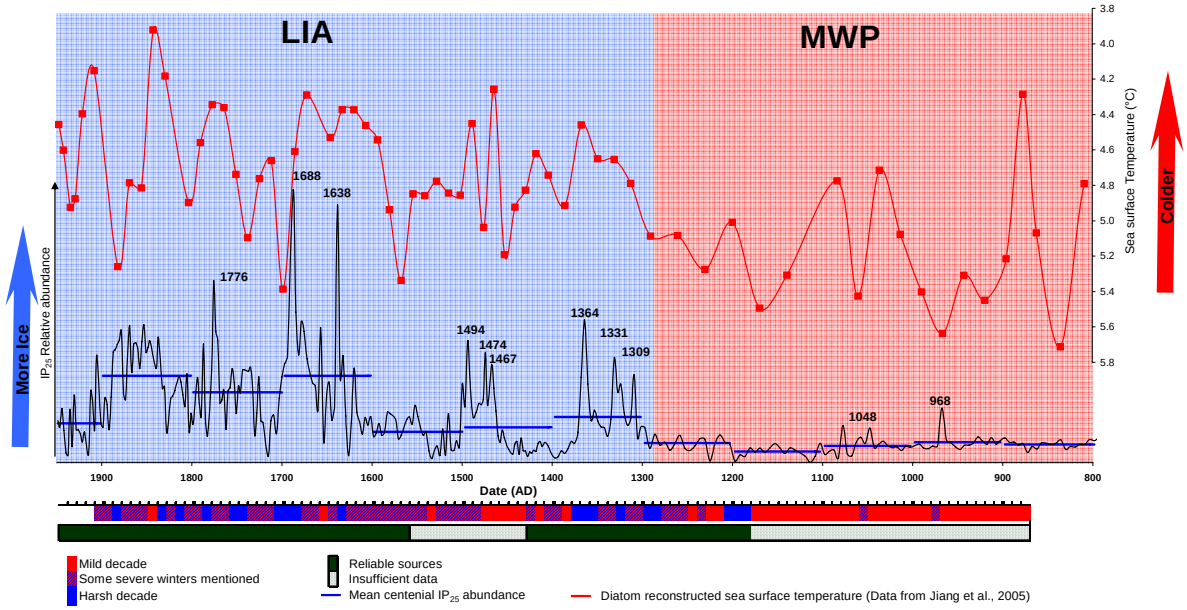

Figure 1 Relative concentrations of IP_{25} found in the core MD99-2275 for the period 800-1950 AD plotted against historical records of Icelandic sea ice interpreted from Ogilvie (1992) and Ogilvie and Jónsson (2001) (bottom scales) and diatom-based reconstructed sea surface temperature (Jiang, 2005).

The current IP_{25} data also provide additional sea ice information for periods where the historical sources are limited or unreliable. For example, very little data about Icelandic climate is available for periods corresponding to the earliest days of Iceland colonisation (ca. 870) to the end of the 13th century and from 1430 to 1560 (Ogilvie and Jónsson, 2001). The epoch immediately following the first colonisation period corresponds to the end of the MWP and therefore little or no sea ice might be predicted for this time. Consistent with this hypothesis and also in agreement with diatom-based sea surface temperature reconstructions and northern hemisphere temperature profiles, IP_{25} abundances are low with mean values for 800-1300 lower than the subsequent 700 years (Fig. 1). However, our data shows dramatic differences for the mid-late 15th century, where there are abrupt increases in the abundance of IP_{25} (particularly 1494, 1474 and 1467), reflecting enhanced sea ice occurrences due to more severe conditions during this period, with the centennial mean close to that of the preceding 14th century, for which reliable historical records suggest several severe decades (Ogilvie and Jónsson, 2001). Thus, despite a paucity of historical climate records for the 1430-1560 era, we provide compelling evidence for substantial changes in climate during this time including a 40-50 year period of extensive sea ice cover. Interestingly, these rapid and dramatic changes in the abundance of IP_{25} during the mid-late 15th century are also consistent with substantial oscillations observed in the diatom-based temperature record (Fig.1). Additional abrupt and coincident changes in both the IP_{25} abundances and sea surface temperatures are observed during the 14th, 17th and 18th centuries (e.g. 1364, 1638, 1688 and 1776) confirming that a number of substantial climate changes occurred in Iceland during the LIA.

As such, the high resolution and continuous dataset achieved in this study has enabled several abrupt changes to sea ice conditions to be determined for which there have been little or no precedent from previous decadal (or longer timescale) determinations (Fig. 1). Similar datasets were produced for various locations across the Arctic showing that such abrupt changes to sea ice conditions have occurred during the past few millennia and provided essential insights into the role of sea ice onto the earth climate system. Finally, not only will such data enhance the quality of climate prediction models but, for locations where there is the additional impact on past human populations, a more accurate

account of climate-induced control over human activity should become achievable.

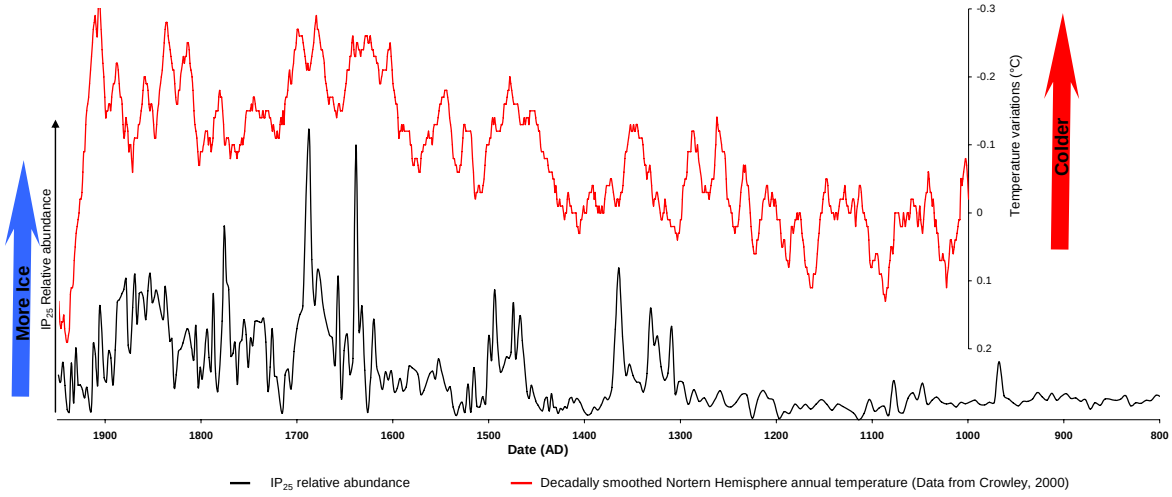

Figure 2 Relative concentrations of IP25 found in the core MD99-2275 for the period 800-1950 AD plotted against reconstructed Northern Hemisphere annual temperatures (Crowley, 2000).

References

Belt, S. T., Massé, G., Poulin, M., LeBlanc, B., Michel, C., Rowland, S., 2007 A novel chemical fossil of palaeo sea ice: IP25. Org. Geochem. 38, 16-27.

Bergthórsson, P., 1969. An estimate of drift ice and temperature in Iceland in 1000 Years. Jökull. 19, 94-101.

Crowley, T.J., Lowery, T.S., 2000. Northern Hemisphere temperature reconstruction. Ambio. 29, 51-54.

Eiriksson, J., Larsen, G., Knudsen, K. L., Heinemeier, J., Simonarson, L.A., 2004. Marine reservoir age variability and water mass distribution in the Iceland sea. Quat. Sci. Rev. 23, 2247-2268.

Eiriksson, J., Bartels-Jonsdottir, H.B., Cage, A. G., Gudmundsdottir, E.R., Klitgaard-Kistensen, D., Marret, F., Rodrigues, T., Abrantes, F., Austin, W.E.N., Jiang, H., Knudsen, K.L., Sejrup, H.P., 2006. Variability of the North Atlantic current during the last 2000 years based on shelf bottom water and sea surface temperatures along an open ocean/shallow marine transect in western Europe. The Holocene. 16, 1017-1019.

Gersonde, R., Crosta, X., Abelmann, A., Armand, L. (2005) Sea-surface temperature and sea lee distribution of the Southern Ocean at the EPILOG Last Glacial Maximum - A circum-Antarctic view based on siliceous microfossil records. Quaternary Science Reviews 24, 869-896.

Holland, M.M., Bitz, C.M., Eby, M, Weaver, AJ (2001). The role of ice-ocean interactions in the variability of the North Atlantic thermohaline circulation. Journal of Climate 14, 656-675.

Jiang, H., Eiriksson, J., Schultz, M., Knudsen, K.L., Seidenkrantz M.S., 2005. Evidence for solar forcing of sea surface temperature on the North Icelandic Shelf during the late Holocene. Geology. 33, 73-76.

Jones, P.D., Briffa, K.R., Barnett, T.P., Tett, S.F.B., 1998. High-resolution palaeoclimatic records for the last millennium: interpretation, integration and comparison with General Circulation Model control-run temperatures. The Holocene. 8, 455-471.

Jones, P. D., Osborn, T. J., Briffa, K. R., 2001. The evolution of the climate over the last millennium. Science. 292, 662-667.

Knudsen, K.L., Eiriksson, J., 2002. Application of tephrochronolgy to the timing and correlation of palaeocanographic events recorded in Holocene and late Glacial shelf sediments off North Iceland. Mar. Geol. 191, 165-188.

Koch, L., 1945. The East Greenland ice, in: Komissionen for videnskabelige Undersøgelser i Grønland (Ed.), Meddelelser om Grønland, Copenhagen.

Ogilvie, A. E. J., 1992. “Documentary evidence for changes in the climate of Iceland AD 1500 to 1800, in: Bradley, R.S. and Jones, P.D. (Eds.), Climate since AD 1500, London & New York, pp 92-117.

Ogilvie, A. E., Jónsson, T., 2001. Little ice Age research: A perspective from Iceland. Climatic Change. 48, 9-52.

Serreze, M.C., Holland, M. M. & Stroeve, J. (2007). Perspectives on the Arctic's shrinking sea-ice cover. Science 315, 1533-1536.

Serreze, M.C., Maslanik, J.A., Scambos, T.A., Fetterer, F., Stroeve, J., Knowles, K., Fowler, C., Drobot, S., Barry, R.G., Haran, T.M. (2003). A record minimum arctic sea ice extent and area in 2002. Geophysical Research Letters 30, Art. No. 1110.

Stroeve, J.C., Serreze, M.C., Fetterer, F., Arbetter, T., Meier, W., Maslanik, J., Knowles, K. (2005) Tracking the Arctic's shrinking ice cover: Another extreme September minimum in 2004. Geophysical Research Letters 32, Art. No. L04501.

ICELANDIC TEPHROCHRONOLOGY MATCHING THE PROVENANCE OF PROXIMAL AND DISTAL VOLCANIC GLASSES USING LA-ICPMS TRACE ELEMENT DATA

Martin Menzies[1], Emma Tomlinson[1], Wolfgang Muller[1], Thor Thordarson[2], Christine Lane[3], Vicky Smith[3], Simon Blockley[4] and the RESET Consortium[5]

[1]Earth Sciences, Royal Holloway University of London, Egham
[2]School of GeoSciences, University of Edinburgh, Edinburgh
[3]Research Laboratory for Archaeology & the History of Art, Oxford
[4]Department of Geography, Royal Holloway University of London, Egham
[5] RESET WWW site : http://c14.arch.ox.ac.uk/reset/

Abstract

Thorarinsson (1944) pioneered the use of tephrochronology and its application in NW Europe. The basis of this chronological tool is the use of time-parallel marker tephra (i.e., ash <2mm) horizons to correlate proximal volcanic deposits with distal tephras found in marine-lacustrine-ice cores and terrestrial sequences. The trace element geochemistry of volcanic glasses [determined by LA-ICPMS] offers an improved diagnostic tool for matching the juvenile components of proximal and distal tephras and has considerable potential for assigning provenance to cryptotephras (<100 microns) provided they are of sufficient size and thickness.

Introduction

In the context of the last 100ka western Europe offers a unique opportunity to use recurrent explosive volcanic activity and widespread tephra dispersal as a basis for evaluating the temporal and spatial relationships between the migration of ancient modern humans (AMH) and abrupt environmental transitions (AETs). Tephras in (a) archaeological sites hold the key to AMH migration patterns and (b) lacustrine, marine and ice core constrain AETs. Juvenile (magmatic glass) compositions are forthcoming from (a) pumice or scoria clasts in pyroclastic fall deposits (b) pumice or fiamme in proximal pyroclastic flow deposits, (c) glass adhering to entrained xenoliths, and (d) cryptotephras at distal sites (i.e., < 100 microns). EMPA & LA-ICPMS techniques (e.g., Tomlinson et al 2010a) are applied to all proximal and distal juvenile class with SIMS utilized where particles are too small/thin. The provenance of these distal tephras is paramount and is defined by matching the geochemistry of distal juvenile clasts with the RESET geochemical database for proximal European tephras. Once diagnostic chemistries are matched, $^{40}Ar/^{39}Ar$ ages (K-rich phenocrysts) from proximal sites link the continental-lacustrine-marine archives. This time lattiice is refined with the addition of temporal detail from varve counting (lacustrine), ^{14}C, U-Th dating (archaeological sites), & biostratigraphy (marine).

Katla & the Vedde ash (*ca.* 11ka) : proximal-distal correlation

The Vedde Ash has been reported from distal terrestrial, marine and ice cores across Northern Europe and forms an important stratigraphic marker for palaeoclimatic reconstructions across the North Atlantic (e.g., Mangerud et al. 1984; Lowe and Turney, 1997; Wastegård et al., 2000; Davies et al., 2005). The Vedde ash has been dated close to its type site in Western Norway, giving a ^{14}C age of 10,310 ± 50 ^{14}C years or 11,841 to 12,383 cal years BP (Birks et al., 1996). The Vedde Ash is a bimodal rhyolitic (clear shards) and basaltic (brown shards) tephra layer believed to have been erupted from the Katla volcano in Southern Iceland (Lacasse et al., 1995). However, distal tephra correlations are soley based on somewhat equivocal data including glass shard morphology and major element EMPA chemistry indicating a basalt-rhyolite magmatic lineage. Lacasse et al (1995) identified the Sólheimar ignimbrite, erupted from Katla, as the likely source of the Ash Zone 1 tephra again on the basis of total alkali-silica (TAS) classification and feldspar compositions. These may not be diagnostic in the context of Icelandic magmatism and the potential exists for confusion between distal basalt-rhyolite cryptotephra and the many basalt-rhyolite centres on Iceland that have erupted over the last 100ka. Tomlinson et al (2010b) undertook trace (LA-ICP-MS) element analysis of volcanic glasses from a proximal volcano-stratigraphic section of the Sólheimar ignimbrite and distal glasses from the type Vedde site at Ålesund in Western Norway (Mangerud et al., 1984). The rhyolitic (SiO_2>68%) Sólheimar pumice and obsidian and the distal Vedde clear glass shards have restricted and overlapping

trace element compositions that demonstrate a close correlation between the Sólheimer ignimbrite and the Vedde Ash. Importantly Tomlinson et al (2010b) highlighted key differences between the Sólheimar rhyolite and other rhyolites from the Icelandic Southern Transition Zone such that provenance can assigned with greater confidence. *They conclude that the proximal rhyolitic component of the Sólheimar ignimbrite is compositionally identical to the distal rhyolitic clasts from the classic Vedde fall locality in terms of both major and trace element geochemistry*. Magmatic variability exists along 1500 km of the tephra dispersal axis between Katla and Vedde with greater magmatic representation in the distal Vedde tephra (i.e. fall deposit) than at the proximal "bimodal" site at Sólheimer which is dominantly basaltic-andesite fall and rhyolititc flows deposits. Similar along-axis variability over 3000km was reported from continental-marine correlations between Afro-Arabia and the Indian Ocean (Ukstins-Peate et al 2003, 2008). Along axis differences appear to be characterised by (a) the most evolved magmas being located at distal sites, and (b) bimodality being restricted to proximal sites.

Thorsmork & Ash Zone 2 (*ca.* 57ka) – continental-marine correlation

Ash zone 2, an alkali rhyolite tephra layer found in north Atlantic and Arctic marine cores (Lacasse & Garbe-Schoonberg 2001) and the GISP2 Greenland ice core (Ram et al 1996), has been correlated with the Thorsmork ignimbrite. This provenance match is based on a combination of major element data and tephra stratigraphy. Tindfjallajokull, the source of the Thorsmork ignimbrite, is a bimodal basalt-rhyolite volcano in the Eastern Volcanic Zone Iceland, represented by a series of pyroclastic flow deposits. The homogenous rhyolite pumice dominates the deposit, which also contains subordinate basalt scoria (Jörgensen 1980). These two compositional components are also represented in the fiamme but there is no textural evidence for mixing or mingling between the basalt and rhyolite components. The Thorsmork ignimbrite has been the focus of $^{40}Ar/^{39}Ar$ dating (Sigurdsson et al 1998, Storey and Stecher 2009) with a robust age of 57ka (W. McIntosh 2010 pers comm). Tomlinson et al (2010a) report LA-ICP-MS and AES data for the Thorsmork rhyolite and its juvenile component. They argue that the bimodal Thorsmork ignimbrite is the product of physical mixing of basaltic and rhyolitic magmas. Furthermore Tomlinson et al (2010a) compare other potential volcanic sources from the Icelandic Southern Transition Zone (Hekla, Torfajökull, Oaerfajökull, Tindfjallajökull). Rhyolite glass from the Thorsmork Ignimbrite can be distinguished from these other Icelandic rhyolites, because the major differences between the Icelandic rhyolites are driven by high-level processes in the magma chamber, principally phenocryst fractionation. Tomlinson et al (2010a) compare the Thorsmork glass chemistry with published trace element data for ash zone 2 tephra (SU9029) from the Irminger Basin, North Atlantic (Lacasse & Garbe-Schoonberg 2001). They conclude that ash zone 2 is indistinguishable from the proximal Thorsmork juvenile clasts and that Ash Zone 2 is likely to be a distal sample of the Thorsmork Ignimbrite.

Summary

Volcanic glass geochemistry offers a robust basis for matching proximal juvenile clasts, from primary fall & flow deposits, with distal tephras and cryptotephras [<100microns]. Glass chemistries from two Icelandic volcanoes have been used to demonstrate : (a) proximal-distal correlations over 1500km with Katla confirmed as the source of the "Vedde Ash" in Norway (11ka), and (b) continental-marine correlations with Thorsmork (57ka Tindfjallajokull) shown to be the source of Ash Zone 2 found in the North Atlantic marine cores.

Acknowledgements

The RESET Consortium (2008-2012) is funded by the NERC (UK) and the CNRS supported attendance at the Ecole Thématique CNRS Summer School "Iceland and the Northern Atlantic" in Plouzané France 2010.

References

Birks, H.H., Gulliksen, S., Haflidason, H., Mangerud, J., and Possnert, G., 1996, New radiocarbon dates for the Vedde ash and the Saksunarvatn ash from western Norway: *Quaternary Research*, **45**, 119-127.

Davies, S.M., Hoek, W.Z., Bohncke, S.J.P., Lowe, J.J., O'Donnell, S.P., and Turney, C.S.M., 2005, Detection of Lateglacial distal tephra layers in the Netherlands: *Boreas*, **34**, 123-135.

Jörgensen, K., 1980. The Thorsmork Ignimbrite - an unusual comenditic pyroclastic flow in southern Iceland. *Journal of Volcanology and Geothermal Research*, **8**, 7-22.

Lacasse, C. and Garbe-Schoonberg, C.-D., 2001. Explosive silicic volcanism in Iceland and the Jan Mayen area during the last 6 Ma: sources and timing of major eruptions. *Journal of Volcanology and Geothermal Research*, **107**,113-147

Lacasse, C., Sigurdsson, H., Johannesson, H., Paterne, M., and Carey, S., 1995, Source of Ash-Zone-1 in the North-Atlantic: *Bulletin of Volcanology*, **57**, 18-32

Lowe, J.J., and Turney, C.S.M., 1997, Vedde ash layer discovered in a small lake basin on the Scottish mainland: *Journal of the Geological Society*, v. 1**54**, 605-612.

Mangerud, J., Lie, S.E., Furnes, H., Kristiansen, I.L., and Lømo, L., 1984, A Younger Dryas Ash Bed in western Norway, and its possible correlations with tephra in cores from the Norwegian Sea and the North Atlantic: *Quaternary Research*, **21**, 85-104.

Ram M., Donarummo J. and Sheridan M., 1996. Volcanic ash from Icelandic similar to 57,300 yr BP eruption found in GISP2 (Greenland) ice core. *Geophysical Research Letters*, **23**, 3167-3169697

Sigurdsson, H., McIntosh, W.C., Dunbar, N., and Lacasse, S.N. (1998) Thorsmork Ignimbrite in Iceland: possible source of North Atlantic ash. EOS *Transactions AGU*.

Storey, M. and Stecher, O. (2009) 40Ar/39Ar Age of the Thorsmörk ignimbrite, Iceland and correlation with North Atlantic Z2 ash: Cross-calibration of ~60,000 counted annual layers in the Greenland ice cores. EOS *Transactions AGU*.

Thorarinsson, S. (1944) Tefrokronologiska studier på Island. *Geografiska Annaler*, **26**, 1-217.

Tomlinson, E., Thordarson, T., Lane, C., Blockley, S., Muller, W., and Menzies, M.A, (2010a) Micro-analysis of tephra by LA-ICP-MS. *Chemical Geology* (in review)

Tomlinson, E., Thordarson, T., Lane, C., Blockley, S., Muller, W., and Menzies, M.A, (2010b) The Solheimer ignimbrite (Katla, southern Iceland) and the source of the "Vedde Ash" stratigraphic marker tephra. *Geology* (in preparation)

Ukstins Peate, I. et al., 2003. Correlation of Indian Ocean tephra to individual Oligocene silicic eruptions from Afro-Arabian flood volcanism. *Earth and Planetary Science Letters*, **211,** 311-327.

Ukstins Peate, I., Kent, A.J.R., Baker, J.A. and Menzies, M.A., 2008. Extreme geochemical heterogeneity in Afro-Arabian Oligocene tephras: Preserving fractional crystallization and mafic recharge processes in silicic magma chambers. *Litho*s, 1**02**, 260-278.

Wastegård, S., Wohlfarth, B., Subetto, D.A., and Sapelko, T.V., 2000, Extending the known distribution of the Younger Dryas Vedde Ash into northwestern Russia: *Journal of Quaternary Science*, **15**, 581-586.

RESET Response of Humans to Abrupt Environmental Transition

JÖKULHLAUPS AND CLIMATE

Jean-Luc Schneider
Université Bordeaux 1, Observatoire Aquitain des Sciences de l'Univers,
CNRS-UMR 5805 « EPOC », Avenue des Facultés, F-33405 Talence cedex,
jl.schneider@epoc.u-bordeaux1.fr

Abstract

Jökulhlaups are large-volume and short duration glacial lake outbursts with peak discharges up to 10^7 $m^3.s^{-1}$. They have a strong erosive impact on the proglacial fluvial systems. The transported sediments spread on large outwash plains (sandar), and can feed distal submarine gravity flows (turbidites). The largest jökulhlaups draining large glacial-dammed lakes (e.g. former Missoula and Agassiz lakes) occur during deglaciation periods. The related input of large volumes of freshwater into the ocean can induce global climatic changes (e.g. the Younger Dryas). Smaller-scale jökulhlaups result of subglacial volcanic eruptions (Iceland) or are related to glacier melting and retreat during warmer climatic periods, and ice dam formation and failure during glacial surges.

Introduction

Jökulhlaups (from Icelandic *jökull* = glacier and *hlaup* = outburst), also called *glacial lake outburst floods* (GLOFs), are the largest floods known on Earth (O'Connor *et al.*, 2002). In the present-day conditions, the large volumes of water involved have a high hazard potential and are increasingly threatening people, property and infrastructure in mountainous areas worldwide. The glacial outburst floods originate by sudden release of large volumes of meltwater from glacial or ice-dammed lakes. They are short events that occur over a period of minutes to several weeks, with high peak discharges (Roberts, 2005). They are part of a wider spectrum of similar large floods generated by the failure of natural dams (landslides, moraines; Costa and Schuster, 1988). Jökulhlaups occur around englaciated areas in mountainous regions (Alaska, Canadian Rocky Mountains, Western Alps…; Korup and Clague, 2009), and also in Iceland where they are related to subglacial volcanic eruptions. In comparison to classical fluvial floods of hydrometeorological origin, jökulhlaups display discharges that can reach 10 to 100 times their magnitude, with peak discharges up to 10^7 $m^3.s^{-1}$. The largest known glacial outbursts are dated of the end of the Pleistocene, and were related to the retreat of large ice sheets, mainly in North America, northern Europe, and Siberia (Baker and Bunker, 1985; Baker *et al.*, 1993; Teller *et al.*, 2002). The aim of the present work is to present the main characteristics of the hydrodynamic characteristics and erosion and sedimentation processes related to jökulhlaups. The climatic forcing on outburst triggering and the potential effects of major GLOFs on the climate itself are also presented.

Floods origins and characteristics

Jökulhlaups result of the rapid outflow of a large volume of meltwater from a glacial lake (fig. 1) that develop at the glacier's front (proglacial lake), surface (supraglacial lake), base (subglacial lake) or along its edges (ice-marginal lake). Moreover, glacial impounded lakes (Tweed and Russell, 1999) develop within fluvial valleys upstream of (1) ice dams that develop during surge phases or (2) moraine dams left by retreating glaciers. Various situations can induce ice melting, and to the development of glacial lakes. Warm climatic condition is the most common context (exogenous forcing; Walder and Costa 1996; Tweed and Russell, 1999). High geothermal heat flow and subglacial volcanic eruptions (Björnsson, 2002) also melt the glacier soles to form subglacial lakes (endogenous forcing).

Outburst occurs when the glacial lake has risen to a critical level and when the water pressure allows the failure or floatation of the fragile and low-density ice dam, or structurally weak and unstable moraine dam breaching. During subglacial volcanic eruptions, it occurs when the hydrostatic overpressure related to the presence of the melt water reservoir favors the uplift of the ice by floatation and subsequent rupture of the peripheral dam (Björnsson, 1992, 2002). Usually, glacial outbursts are sudden and short duration events (hours to weeks) of water release, the magnitude of which depends on the volume of drainable meltwater, and size and shape of the outlet(s) at the source and of the outwash stream channel. During glacial outbursts, multiple outlets can be simultaneously active along the glacier front.

The resulting flash floods (fig. 2) are always characterized by short (~hours to weeks) and large peak discharges (10^3 to 10^7 $m^3.s^{-1}$), and display hydrodynamic similarities with natural dam breakage floods (Costa et Schuster, 1988). Discharged water volumes can reach 10^{12} m^3 (e.g. Lake Missoula) for the largest glacial outbursts during the Quaternary. For ancient glacial outburst floods, peak discharges are estimated from the location of the slackwater deposits and from the elevation of

recognized water surface elevations (Baker, 2008). Flow speeds are variable with a torrential or less fast flowing. Depths of the floods can exceed 100 m.

Jökulhlaups have the capacity to transport large amounts of sediment in suspension. Ordinary jökulhlaups issued from subglacial lakes may transport about 10^7 tons of sediment, but sediment loads up to 10^8 tons have been estimated during the most violent subglacial volcanic eruptions. Thus, floods correspond from hyperconcentrated to debris flows, depending on their sediment concentration. Their hydrodynamic behavior vary from subcritical to supercritical, giving them a strong erosive capacity. Studies of the composition of the transported sediments indicate that an important amount of sediment is eroded from the bottom and edges of the channel, and picked-up into the flow (Maria *et al.*, 2000). Jökulhlaups also transport large amounts of ice blocks (up to decametric sizes), and have the capacity to transport plurimetric-scale rock blocks.

The largest recognized GLOFs occurred at the end of the Pleistocene. They were always related with the drainage of huge lakes that developed around retreating ice caps, like the Laurentide ice sheet in North America (Missoula and Agassiz lakes; Baker and Bunker, 1985; Teller *et al.*, 2002) and the Fennoscandian ice sheet in northern Europe (Smith, 1985; Russell and Marren, 1998; Gupta *et al.*, 2007), or from ice-dammed lakes that developed within the glacial complex of the Altai mountains in southern Siberia (Baker *et al.*, 1993; Rudoy, 2002).

Morphological effects and deposits

From their outlets, jökulhlaups flow downstream along a transit fluvial system to the proglacial outwash fan and, in some cases, up to the sea. The main effects of jökulhlaups are *erosion* along the outwash stream system and *sedimentation* on the distal outwash fan. They can feed submarine gravity flows by the discharge of water into the sea from the fluvial system, but also by direct input when ice caps line the shoreline.

Erosion structures

Along the outwash fluvial system, jökulhlaups are highly erosive because of their high peak discharges. Consequently, they play a major geomorphic role on the fluvial valley landform evolution (fig. 1), and can deepen the valley floors. Recognition of these erosion structures is crucial to reconstruct paleo-jökulhlaup pathways. Erosion efficiently affects the sedimentary cover of the valleys floor and flanks (depending on the thickness of the flood wave), but also the bedrock (Carriwick *et al.*, 2004). Dissection can be major along the constrictions of the valleys, where the outburst has a supercritical hydrodynamic behavior. Narrow and deep gorges (outburst gorges; Rudoy, 2002) and bedrock benches can be incised into the substratum during runoff phases, and plunge basins (dry cascades) can be formed by outburst water cascading down topographic scarps (Teller *et al.*, 2002). Typical spillway erosion structures are large-scale elongated scours around eroded mesas, with long axes parallel to the flow direction. They mimics a large-scale braided fluvial network. These large-scale landforms related to erosion by cataclysmic jökulhlaups have been first recognized in the Columbia River basin (U.S.A.); they correspond to the so-called *Channeled Scablands* (Bretz, 1923, 1969) related to the discharges from former Lake Missoula, Montana (*cf.* below). The preservation potential of these erosion structures is good, at least since the Pleistocene.

Similar landforms were observed in the Altai Mountains, southern Siberia (Baker *et al.*, 1993; Rudoy 2002) and along the spillway valleys around former Lake Agassiz, Canada (*cf.* below; Teller *et al.*, 2002). Moreover, the origin of the 400 km-long eroded network of large ancient valleys in English channel has been interpreted to have formed very likely by megafloods erosion (Smith, 1985; Gupta *et al.*, 2007). During the Fennoscandian ice sheet retreat, the North Sea lake that developed along its southern edge cataclysmically overflowed through the Calais strait, eroding the former barrier of the Weald-Artois anticline during a low-stand period. The event very likely occurred during the Eemian/Ipswichian stage (MIS 5e; Gupta *et al.*, 2007).

Jökulhlaup sedimentation

Sediments from jökulhlaups can be emplaced along the spillway valleys. Deposits are mainly present on terraces (slackwater benches) and within pounded zones in tributary backwater areas. The slackwater deposits can correspond to rhythmic superimposed layers resulting of recurrent flood events. The deposits correspond to polymictic coarse bedded sediments with well-washed gravel, with break-stones and debris, interfingered with sand lenses. Large blocks, sometimes stacked and imbricated, are also present, but usually concentrate within the stream channels. Along wider channels of the transit zone, large gravel dune and giant current ripple fields can develop (Baker, 1973; Rudoy,

2002). Dune heights can reach up to 30 m with wavelengths up to 200 m. Foresets are underlined by washed open framework gravel layers. The giant current ripples are up to 3 m high with wavelengths of 70 m. The formation of these structures seems to be related to changes of both the slope and width of the channel and the water depth of the flow (Baker, 1973), but generally occur on wide surfaces. Large-scale antidunes can develop during supercritical stages of the flows. Delta bars covered by large dunes can be formed by floodwaters spilling from main stream channels.

The main part of the sediments transported in suspension are accumulated as outwash deposits on a fan called *sandur* (pl. *sandar*; fig. 1) located at the front of the glacier (small-scale outbursts) or at the distal mouth of the runoff valley from the glacier-dammed lakes (large-scale outbursts). The architecture of the sandar displays a complex interstratification of sand and gravel bars emplaced during multiple jökulhlaup events. This geometry denotes deposition by sheetflows that spread within a complex braided channel system (Maizels, 1997; Zielinski and van Loon, 2002; Kjær *et al.*, 2004). Mean grain size of the sediments decreases from proximal to distal parts of the sandar. Kettle holes can be present at the sandur's surfaces. They correspond to thermokarstic depressions resulting of the melting of ice blocks displaced by the jökulhlaups. Because of the recurrence of jökulhlaup events and their erosive capacity, the preservation of the deposits on sandar is relatively poor.

Jökulhlaups can discharge into the sea. When density is >1, the sediment-rich flow is transformed into an hyperpycnal flow that moves along the sea floor to distal gravity flow sedimentary systems. Submarine deposits related to the entrance of the 1996 jökulhlaup into the sea were recognized off the shore of the Skeidararsandur, Iceland (Maria *et al.*, 2000). During recurrent floods from Lake Missoula, turbidites were emplaced into the Tufts Abyssal Plain in the eastern Pacific Ocean, off the Columbia River inlet (Brunner *et al.*, 1999).

Jökulhlaups and climate: consequences or control?

Climate warming and jökulhlaups

Major glacial outbursts occur both during deglaciation phases (warm climatic periods) or stable climatic periods as the result of ice melting related to the local heat flow or volcanic activity beneath the englaciated area. Warm climatic phases lead to a negative mass balance of the ice bodies, and subsequently to their retreat and formation of glacial lakes by meltwater output. All these conditions increase the jökulhlaup events potential. Numerous present-day glacial outbursts in mountainous regions result of local warming (Korup and Clague, 2009).

The major known glacial outbursts occurred during the Late Pleistocene deglaciation phases and during the beginning of interglacial stages. Former Lake Missoula, Montana (U.S.A.) is an interesting example (Bretz, 1923, 1969; Baker and Bunker, 1985; O'Connor and Baker, 1992). It contained 2000 km^3 of water, and developed at the end of the Last Glacial Maximum (LGM) between 17.2 and 11 ka along the Clark Fork River (tributary of the Columbia River) at the southern edge of the Rocky Mountains ice sheet. During warm periods of the end of the LGM, the pressure induced by water level rise of the lake led to ice dam failures. Subsequently, recurrent large jökulhlaups flooded and eroded the large plain of the Channeled Scablands, and flowed into the Columbia River valley up to the Pacific Ocean. About 40 successive floods, with peak discharges up to $1.7.10^7$ $m^3.s^{-1}$ (*i.e.* ten times the discharge peaks during the largest hydrometeorological Amazon River floods) occurred during a 2000 years period (15 to 13 ka) with a frequency of 50 years in average, as attested by rhythmic slackwater deposits (Waitt, 1985).

Unusually warm weather facilitates and increases the flow of water at the sole of the glaciers. Consequently, glacier surge can be a result of warm conditions. Such surges can dam valleys with the subsequent development of a dammed lake. The October 8, 1986 Russell Fjord jökulhlaup in Alaska resulted of the drainage of a dammed-lake that formed during the May 1986 surge of Hubbard Glacier (Mayo, 1989). This outburst was the largest of the 20th century with a peak discharge of $1.1.10^5$ $m^3.s^{-1}$ during 3 hours. Conversely, Alley *et al.* (2006) proposed that glacial outbursts can be liberated after proglacial water trapping and overpressurization by ice-shelf grounding during glacial surges related to climatic cooling.

In Iceland, the volcanic activity enhanced after deglaciation at the end of the LGM. This activity was previously drastically reduced because of the load of the ice cap that enlarges the rift systems (Bourgeois, et al., 1998; Pagli and Sigmundsson, 2008). During deglaciation, the important strain

release favors dyke injection, aerial and subglacial volcanic activity (Björnsson, 2002), and an increase of the jökulhlaup activity, which is enhanced also by the increase of precipitations.

Can glacial large outburst floods exert a control on the climate?

Former Lake Agassiz provides a spectacular example of the control exerted by large-scale jökulhlaups on the global climate (Teller *et al.*, 2002). This lake developed along the southern edge of the Laurentide ice sheet in Canada during the Late Pleistocene. Its relics are represented today by Winnipeg, Winnipegosis, Manitoba and The Woods lakes in Canada. During the 4000 years of the lake's existence, its area was variable around 450,000 km^2 with a depth of 200 m in average, and a maximal extent around 11.5 ka. Its volume probably reached 114.10^6 km^3; it is equivalent to the total volume of the present-day lakes on Earth. Lake Agassiz outflows occurred recurrently during short periods, the five most important lasted less than one year, with peak discharges of about 10^6 $m^3.s^{-1}$. Outbursts runoff routes were through the Mackenzie River to the Arctic Ocean, the Mississippi River to the Gulf of Mexico, and the Saint-Laurent River, and Hudson Bay and Strait for the most recent, to the North Atlantic Ocean. It is very likely that these major floods induced successive global climatic cooling phases at the end of the Pleistocene and during the Holocene: (1) the Younger Dryas (12.8-11.5 ka; discharge of 9500 km^3 of water), (2) the Pre-Boreal climatic oscillation (10.3-9.6 ka; two successive discharges of 9300 and 5900 km^3, respectively), and (3) the 8.2 ka BP climatic event (outflow of up to 70,000 km^3 at the end of the maximal extent of the lake). These flood events induced a temperature decrease of about 1.5°C in the Northern Hemisphere during about 200 years. For each event, the rapid injection of fresh water within the North Atlantic Ocean led to a decrease of the surface waters density and, consequently, to a slowdown of the overall Atlantic thermohaline circulation. Correlatively, heat advection from the Southern Hemisphere decreased, and the North Atlantic area and, consequently, the North Atlantic area cooled.

It is suspected that Heinrich events, that are attested by ice-rafted debris layers in the sediments of the North Atlantic (Grousset *et al.*, 1993), could result of major glacial outbursts from the northern hemisphere retreating ice sheets. Such a process has been hypothetized by Johnson and Lauritzen (1995).

Conclusions

To occur, jökulhlaups necessitate large volume of meltwater that is previously stored with glacial lakes that form mainly during warmer climatic periods and, additionally, by the geothermal heat flow or subglacial volcanic eruptions (Iceland). Apart characteristic megaflood erosion structures that have a relatively good preservation potential, jökulhlaup slackwater, sandur and turbidite deposits can then be used as a potential proxy for warm climatic periods, but they need further studies. The potentiality of large glacial lake outburst flood events in Antarctica remains to be investigated (van Loon, 2009). Jökulhlaups mainly result of climate warming phases, but large-scale outbursts might also induce relatively short-term cooling periods of the global climate. Even if only the largest glacial flood events could have such climatic impacts, it is crucial to study, monitor and modelize smaller-scale jökulhlaups that occur in Iceland and in mountainous domains worldwide, because of their hazard potential.

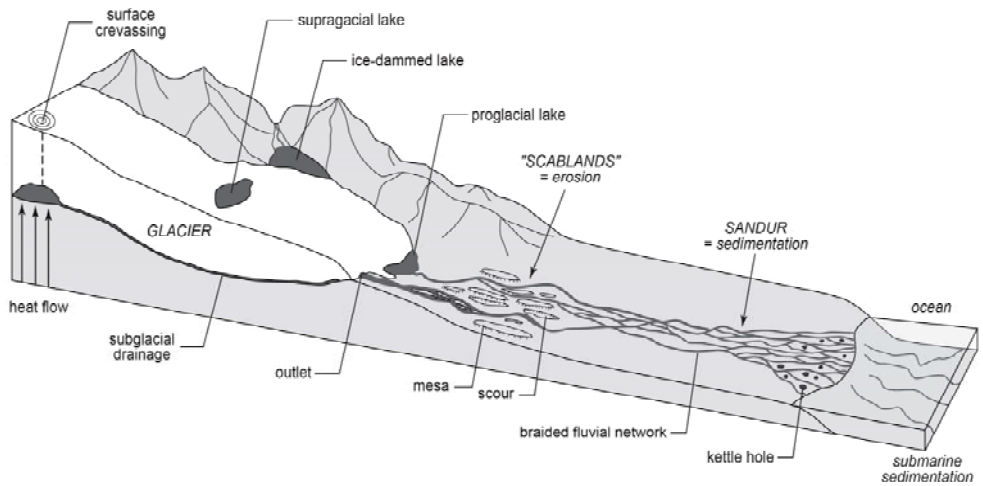

Figure 1: The main characteristics of glacial lakes and erosive and depositional structures by jökulhlaups (from Roberts, 2005, modified and completed).

Flood - River	Location	Date	Mechanism	Volume (m^3)	Peak discharge ($m^3.s^{-1}$)
Lake Kuray	Altai, Russia	Late Pleistocene	Ice-dam failure	$1.0 . 10^{12}$	$1.8 . 10^{7}$
Lake Missoula	Montana, USA	Late Pleistocene	Ice-dam failure	$2.2 . 10^{12}$	$1.7 . 10^{7}$
Tsangpo River	Tibet	Holocene	Ice-dam failure	$8.3 . 10^{11}$	$5.0 . 10^{6}$
Lake Agassiz	Alberta / Canada	12.8 - 11.5 ka	Proglacial-lake overflow	$9.5 . 10^{12}$	$1.2 . 10^{6}$
Lake Agassiz	Canada / USA	10.3 - 9.6 ka	Proglacial-lake overflow	$9.3 . 10^{12} + 5.9 . 10^{12}$	$2 . 10^{5}$
Lake Agassiz	Northcentral USA	8.2 ka	Ice-dam failure	up to $70 . 10^{12}$	$1.3 . 10^{5}$
Russel Fjord	Alaska, USA	October 8, 1986	Ice-dam failure	$5.4 . 10^{9}$	$1.1 . 10^{5}$
Jökulsá á Fjöllum	Iceland	Early Holocene	Subglacial eruption	?	$7.0 . 10^{5}$
Vatnajökull	Iceland	November 1996	Subglacial eruption	$3.8 . 10^{9}$	$5.3 . 10^{4}$

Figure 2: Examples of large glacial outburst floods with their hydrologic characteristics (data from the literature).

References

Alley, R.B., Dupont, T.K., Parizek, B.R., Anandakrishnan, S., Lawson, D.E., Larson, G.J., Evenson, E.B., 2006. Outburst flooding and the initiation of ice-stream surges in response to climatic cooling: A hypothesis. *Geomorphology*, 75, 76-89.

Baker, V.R., 1973. Paleohydrology and sedimentology of Lake Missoula flooding in eastern Washington. *Geol. Soc. Amer. Spec. Pap.*, 144, 79 p.

Baker, V.R., 2008. Paleoflood hydrology: Origin, progress, prospects. *Geomorphology*, 101, 1-13.

Baker, V.R., Bunker, R.C., 1985. Cataclysmic Late Pleistocene flooding from glacial Lake Missoula: a review. *Quatern. Sci. Rev.*, 4, 1-41.

Baker, V.R., Benito, G., Rudoy, A.N., 1993. Paleohydrology of Late Pleistocene superflooding, Altay Mountains, Siberia. *Science*, 259, 348-350.

Björnsson, H., 1992. Jökulhlaups in Iceland: prediction, characteristics, and simulation. *Ann. Glaciol.*, 16, 95-106.

Björnsson, H., 2002. Subglacial lakes and jökulhlaups in Iceland. *Global Planet. Change*, 35, 255-271.

Bourgeois, O., Dauteuil, O., Van Vliet-Lanoë, B., 1998. Pleistocene subglacial volcanism in Iceland: tectonic implications. *Earth Planet. Sci. Lett.*, 164, 165-178.

Bretz, J.H., 1923. The channelled scabland of the Columbia plateau. *J. Geol.*, 31,617-649.

Bretz, J.H., 1969. The Lake Missoula floods and the Channeled Scabland. *J. Geol.*, 77, 505-543.

Brunner, C.A., Normark, W.R., Zuffa, G.G., Serra, F., 1999. Deep-sea sedimentary record of the late Wisconsin cataclysmic floods from the Columbia River. *Geology*, 27(5), 463-466.

Carriwick, J.L., Russell, A.J., Tweed, F.S., 2004. Geomorphological evidence for jökulhlaups from Kverkfjöll volcano, Iceland. *Geomorphology*, 63, 81-102.

Costa, J.E., Schuster, R.L., 1988. The formation and failure of natural dams. *Geol. Soc. Amer. Bull.*, 100, 1054-1068.

Grousset, F.E., Labeyrie, L., Sinko, J.A., Cremer, M., Bond, G., Duprat, J., Cortijo, E., Huon, S., 1993. Patterns of ice-rafted debris in the glacial North Atlantic, 40°-55°N. *Paleoceanography*, 8, 175-192.

Gupta, S., Collier, J.S., Palmer-Felgate, A., Potter, G., 2007. Catastrophic flooding origin of shelf valley systems in the English Channel. *Nature*, 448, 342-346.

Johnson, R.G., Lauritzen, S.-E., 1995. Hudson Bay-Hudson Strait jökulhlaups and Heinrich events: a hypothesis. *Pal. Pal. Pal.*, 117, 123-137.

Kjær, K.H., Sultan, L., Krüger J., Schomacker, A., 2004. Architecture and sedimentation of outwash fans in front of the Myrdalsjökull ice cap, Iceland. *Sediment. Geol.*, 172, 139-163.

Korup, O., Clague, J.J., 2009. Natural hazards, extreme events, and mountain topography. *Quatern. Sci. Rev.*, 28, 977-990.

Maizels, J.K., 1997. Jökulhlaup deposits in proglacial areas. *Quatern. Sci. Rev.*, 16, 793-819.

Maria, A., Carey, S., Sigurdsson, H., Kincaid, C., Helgadóttir, G., 2000. Source and dispersal of jökulhlaup sediments discharged to the sea following the 1996 Vatnajökull eruption. *Geol. Soc. Amer. Bull.*, 112(10), 1507-1521.

Mayo, L.R., 1989. Advance of Hubbard Glacier and 1986 outburst of Russell Fiord, Alaska, U.S.A. *Ann. Glaciology*, 13, 189-194.

O'Connor, J.E., Baker, V.R., 1992. Magnitudes and implications of peak discharges from glacial Lake Missoula. *Geol. Soc. Amer. Bull.*, 104, 267-279.

O'Connor, J.E., Grant, G.E., Costa, J.E., 2002. The geology and geography of floods. *In*: House, P.K., Webb, R.H., Baker, V.R., Levish, D.R., Eds., Ancient floods, modern hazards – Principles and applications of paleoflood hydrology. *Water Science and Application* 5, AGU, Washington, DC, 359-385.

Pagli, C., Sigmundsson, F., 2008. Will present day glacier retreat increase volcanic activity? Stress induced by recent glacier retreat and its effect on magmatism at the Vatnajökull ice cap, Iceland. *Geophys. Res. Lett.*, 35, L09304, doi:10.1029/2008GL033510.

Roberts MJ (2005) Jökulhlaups: a reassessment of floodwater flow through glaciers. *Rev. Geophys.*, 43(1), RG1002, doi: 10.1029/2003RG000147.

Rudoy, A.N., 2002. Glacier-dammed lakes and geological work of glacial superfloods in the Late Pleistocene,Southern Siberia,Altai Mountains. *Quatern. Intern.*, 87, 119-140.

Russell, A.J., Marren, P.M., 1998. A Youger Dryas (Loch Lommond Stadial) jökulhlaup deposit, Fort Augustus, Scotland. *Boreas*, 27, 231-242.

Smith, A.J., 1985. A catastrophic origin for the palaeovalley system of the eastern English Channel. *Mar. Geol.*, 64, 65-75.

Teller, J.T., Leverington, D.W., Mann, J.D., 2002. Freshwater outbursts to the oceans from glacial Lake Agassiz and their role in climate change during the last deglaciation. *Quatern. Sci. Rev.*, 21, 879-887.

Tweed, F.S., Russell, A.J., 1999. Controls on the formation and sudden drainage of glacier-impounded lakes: implications for jökulhlaup characteristics. *Progr. Phys. Geogr*., 23, 79-110.

Van Loon, A.J., 2009. Reflections on subglacial megafloods: their possible cause, occurrence, and consequence for the global climate. *Geologos*, 15(2), 115-128.

Waitt, R.B., 1985. Case for periodic, colossal jökulhlaups from Pleistocene glacial Lake Missoula. *Geol. Soc. Amer. Bull.*, 96(10), 1271-1286.

Walder, J.S., Costa, J.E., 1996. Outburst floods from glacier-dammed lakes: the effect of mode of lake drainage on flood magnitude. *Earth Surf. Process. Landforms*, 21, 701-723.

Zielinski, T., van Loon, A.J., 2002. Present-day sandurs are not representative of the geological record. *Sediment. Geol.*, 152, 1-5.

INFLUENCE OF TECTONISM ON THE COMPOSITION OF ACID AND BASALTIC LAVA

Olgeir Sigmarsson
Laboratoire Magmas et Volcans, CNRS – Université Blaise Pascal, 63038 Clermont-Ferrand, France
et
Institute of Earth Sciences, University of Iceland, 101 Reykjavik, Iceland

Abstract

The Neovolcanic zones in Iceland are of threefold origin: the Mid-Atlantic rift-zone, the Snæfellsnes "leaky-transform fault", and South-Iceland transgressive volcanic zone or propagating rift segment. Basalt compositions range from alkali basalts through transitional basalts to tholeiites along the off-rift zones towards the centre of Iceland. Diminishing proportion of garnet-pyroxenite melts towards the centre of the mantle plume is the preferred explanation. The origin of silicic magmas reflects their tectonic settings and appears to be controlled by the crustal geothermal gradient.

Basaltic lavas

Mantle heterogeneity beneath oceanic islands can be inferred from basaltic bulk lava samples or glass inclusions. Lava samples represent the integrated magma formation processes (melting, mixing, contamination and fractionation) whereas glass inclusions record melts less affected by higher-level processes. Nevertheless, more precise analyses of compositional parameters can be obtained on bulk samples that permits thorough assessment of mantle heterogeneity from the final basalt composition at surface. This is especially true for well characterized sample suites from oceanic islands showing important compositional variability in their basalts. Here, we present new major-, trace element and Sr-Nd-Hf-Pb isotope results on post-glacial basalts from the Neovolcanic belt of Iceland: the Snæfellsnes Volcanic Zone (SNVZ), the South Iceland Volcanic Zone (SIVZ) and the Mid-Iceland Volcanic Zone (MIVZ). The results reveal systematic lateral variations. Along the strike of the off-rift zones (SNVZ and SIVZ), regular decrease is observed for alkalinity, La/Yb, Sm/Yb, HFSE/Y, $^{87}Sr/^{86}Sr$ and $^{206\text{-}207\text{-}208}Pb/^{204}Pb$ towards the centre of Iceland, where olivine-tholeïtes with depleted trace element compositions, low $^{87}Sr/^{86}Sr$ and $^{206\text{-}207\text{-}208}Pb/^{204}Pb$ (and high $^{143}Nd/^{144}Nd$ and $^{176}Hf/^{177}Hf$) are produced. These latter have similar composition as most mafic lavas along the rift zones that cut through the island from SW to NE. A clear compositional difference is thus observed for basalts erupting at the spreading axis compared to those from the non-rifting flank zones.

The systematic decrease of residual garnet signature (high La/Yb, Sm/Yb, HFSE/Y) and Sr and Pb isotope ratios (and the increase of Nd and Hf isotope ratios) in the off-rift lavas towards the assumed centre of the plume at Iceland's centre, is consistent with the occurrence of fertile garnet pyroxenites in the mantle source. Basalts from the periphery of the flank zones are probably generated by less total melting and thus sample the more enriched and fusible component(s) of the mantle beneath Iceland. Melts of this fertile mantle thus dominate the bulk melt composition at the periphery, and are progressively diluted towards the centre. In the Mid-Iceland Volcanic Zone, basalt compositions are dominated by melts derived principally from the more refractory component(s) of the mantle. The lateral variations of the basalt compositions and the proposed diminishing role of fertile pyroxenites towards the centre of the island is readily explained by increased total melting towards the hotter core of the Iceland mantle plume. Finally, the first-order observation of strong correlations between geochemical parameters and geographical location of the basaltic craters strongly suggests that mantle heterogeneity dominates the highly-incompatible trace element and radiogenic isotope ratios relative to other magma processes, such as crustal contamination and fractional crystallization forming the final basalt composition.

In-situ analysis of major- and trace elements in Holocene tephra produced during subglacial eruptions confirm the spatial variability of the basalt compositions as recorded in the lava samples . Furthermore, cross-correlations of the compositional variability permits to identify the very centre of the Iceland hot-spot, namely the most active Icelandic volcano, Grímsvötn. Moreover, eruption frequency of the principal tephra-forming volcanoes can be determined for the last 6 kyears, where robust age models for soil accumulation can be obtained from well-dated silicic key-layers.

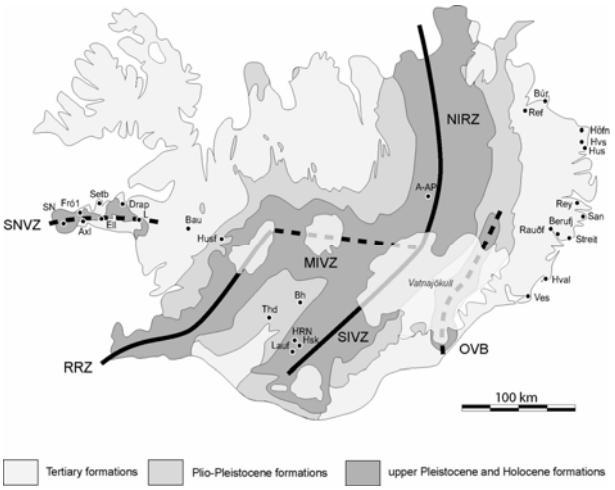

Figure 1 Map of Iceland showing sample locations. The Neovolcanic zones are the Snæfellsnes Volcanic Zone (SNVZ), Reykjanes Rift Zone (RRZ), Mid-Iceland Volcanic Zone (MIVZ), North-Iceland Rift Zone (NIRZ), South-Iceland Volcanic Zone (SIVZ) and the Öræfi Volcanic Belt (OVB). White areas correspond to the main glaciers.

Acid lavas

Pleistocene and Holocene peralkaline rhyolites from Torfajökull (South Iceland Volcanic Zone) and Ljósufjöll central volcanoes and trachytes from Snæfellsjökull (Snæfellsnes Volcanic Zone) allow the assessment of the mechanism for silicic magma genesis as a function of tectonic settings and variable crustal geothermal gradient. The low 18O (2.4‰) and low Sr concentration (12.2 ppm) measured in Torfajökull rhyolites are best explained by partial melting of hydrated metabasaltic crust followed by major fractionation of feldspar. In contrast, very high 87Sr/86Sr (0.70473) and low Ba (8.7 ppm) and Sr (1.2 ppm) concentrations measured in Ljósufjöll silicic lavas are best explained by fractional crystallisation and subsequent 87Rb decay. Snæfellsjökull trachytes are also principally generated by fractional crystallisation, with only small crustal contamination. The fact that silicic magmas within, or close to, the rift zone are principally generated by crustal melting whereas those from off-rift zones are better explained by fractional crystallisation clearly illustrates the controlling influence of the thermal state of the crust on silicic magma genesis in Iceland.

The origin of the Quaternary silicic rocks in Iceland thus appears to be linked to the thermal state of the crust, which in turn depends on the regional tectonic settings. This simple model can be tested on rocks from the Miocene to present, both to suggest an internally consistent model for silicic magma formation in Iceland and to constrain the link between tectonic settings and silicic magma petrogenesis. New major and trace element compositions together with O-, Sr- and Nd-isotope ratios have been obtained on silicic rocks from 19 volcanic systems ranging in age from 13 Ma to present (see sample location in Fig.1). This allows tracing spatial and temporal evolution of both magma generation and the corresponding sources. Low $\delta^{18}O$ (<5 ‰ SMOW) in most silicic rocks results from partial melting of hydrothermally altered metabasaltic crust, whereas low Ba and Sr concentrations (down to 9 and 1 ppm, respectively), in addition to Th concentrations higher than 9 ppm in the silicic rocks, indicate important role of fractional crystallisation during the final stage of magma formation. Trace element ratios, such as Th/U, Th/Zr and Th/La, record important role of accessory minerals during final differentiation. The $^{143}Nd/^{144}Nd$ proves to be an excellent marker of the silicic-magma source: high $^{143}Nd/^{144}Nd$ (0.51303 to 0.51296) characterizes a “rift-zone source”, from which the silicic magmas are generated by crustal anatexis, whereas low $^{143}Nd/^{144}Nd$ (0.51290 to 0.51297) is typical of an “off-rift source”, where rhyolites formed by fractional crystallisation of mantle-derived basaltic magma in a cooler environment far from the rift-zone.

The spatial and temporal distribution of samples having a “rift zone” Nd-isotope signature allows inferences to be drawn about the past tectonic regime. At Snæfellsnes Peninsula, silicic magmas younger than 5.5 Ma have an “off-rift” Nd-isotope signature, whereas those older than 6.8 Ma have typical “rift zone” characteristics. This suggests that before 6.8 Ma silicic rocks were generated in a rift-zone by crustal melting caused by high geothermal gradient. But later than 5.5 Ma they were produced in a flank zone environment by fractional crystallisation alone, probably due to decreasing geothermal gradient, of basalts derived from a mantle source with lower $^{143}Nd/^{144}Nd$. This is in agreement with an eastwards rift-jump, from Snæfellsnes towards the present Reykjanes Rift Zone , between 7 and 5.5 Ma. In the South Iceland Volcanic Zone (SIVZ), the intermediate Nd-signature observed in silicic rocks from the Torfajökull central volcano reflects the transitional character of the basalts erupted at this propagating rift segment. Therefore, the abundant evolved rocks at this major

silicic complex result from partial melting of the transitional alkaline basaltic crust (<3 Ma) generated in this propagating rift segment, suggesting rapid crustal recycling there.

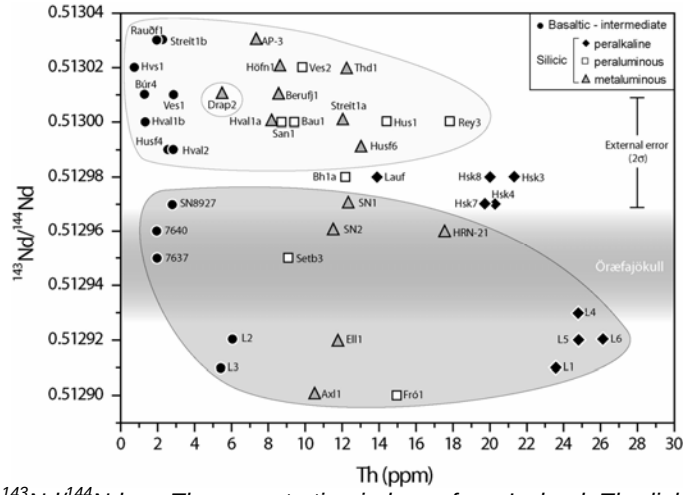

Figure 2. The isotope ratio $^{143}Nd/^{144}Nd$ vs. Th concentration in lavas from Iceland. The light and dark grey fields represent the ""rift-zone" and "off-rift" values, respectively (see text for further discussion). Note that all samples from the Snæfellsnes Peninsula (SNVZ) plot in the "off-rift" field with the exception of Drap 2. All other samples from this study plot in the "rift-zone" field with the exception of the samples from the SIVZ that fall in between. The DRAP 2 is a 6.8 Ma dacite that formed in a former rift-zone that was active from 15-6 Ma, hence its higher $^{143}Nd/^{144}Nd$ compared to other volcanics from the SNVZ . For comparison, range of $^{143}Nd/^{144}Nd$ from Öræfajökull volcanic system is also shown (Prestvik et al., 2001). The error bar (2σ) corresponds to the external error of our standard over the duration of this project.

Improved understanding of silicic magmatism in Iceland can, therefore, be used for deciphering past geodynamic settings characterized by rift- and off-rift zones resulting from interaction of a mantle plume and divergent plate boundaries.

References:

Carpentier, M. and Sigmarsson, O., 2010: Spacial variation of Holocene basalt compositions in Iceland. In revision for *G-cube*.

Martin, E. and Sigmarsson, O., 2007: Geographical variations of silicic magma origin in Iceland: the case of Torfajökull, Ljósufjöll and Snæfellsjökull volcanoes. *Contrib. Mineral. Petrol.*, 153, 593-605.

Martin, E. and Sigmarsson, O., 2010: Thirteen million years of silicic magma production in Iceland: links between petrogenesis and tectonic settings. *Lithos*, doi:10.1016/j.lithos.2010.01.005.

Oladottir, B., Sigmarsson, O., Larsen, G. and Thordarson, T., 2008: Temporal evolution of the magma plumbing system beneath Katla volcano Iceland. *Bull. Volcanol.,* 70, 475–493.

Oladottir, B., Larsen, G. and Sigmarsson, O., 2010: Holocene activity at the Grímsvötn, Bárdarbunga and Kverkfjöll subglacial volcanoes of Vatnajökull, Iceland. *Bull. Volc* accepted.

Oladottir, B., Sigmarsson, O., Larsen, G. and Devidal, J.-L., 2010: Provenance of basaltic tephra layers from the subglacial Vatnajökull volcanoes (Grímsvötn, Bárdarbunga and Kverkfjöll), Iceland. *Holocene*, accepted

HOLOCENE MAJOR ERUPTIONS

Erik Sturkell
University of Göteborg, Department of Earth Sciences, PO Box 460) SE-405 30 Göteborg, Sweden
Sturkel@hi.is

During the Holocene, Iceland has experienced more than 20 eruptions per century from about 30 active volcanoes. The magmatic production is completely dominated by basalts. Intermediary and rhyolitic rocks make up less than 10%. The distribution is calculated to 91:6:3 (basalt / intermediate / rhyolitic) by Thordarson and Höskulsson (2008). They estimate that 2,400 eruptions has occurred and about 566 ± 100 km^3 of erupted material has been generated the last 11,000 years. This is the estimate of erupted material, which is only a part of the magma activated in the crust. Experience from the Krafla eruption and rifting episode 1975-84 suggests about 25% of the material in circulation made it to the surface. Using this observation, more than 2,000 km^3 have been activated during the Holocene. Deglaciation in Iceland at the end of the Weichselian glaciation, about 10,000 years BP, was associated with rapid glacial rebound, apparently reaching completion in only about 1,000 years in coastal areas. This exceptionally fast postglacial rebound suggests an increased eruptive activity.

During the deglaciation of Iceland, at the Pleistocene-Holocene boundary, eruption rate is inferred to have been about 30-100 times its steady state. Increased decompressional mantle melting due to ice removal has been suggested as the main cause of the increase in melt production during deglaciation. The formation of more than ten lava shields with an erupted volume in the range of 20 km^3 were formed in a narrow time after the deglaciation. These lava shields are composed of numerous thin basaltic lava flows. Basaltic fissure eruptions are a common feature in Iceland as it is located on the mid Atlantic rift.

The Thjorsa lava flow in South Iceland originates from the Bardabunga volcanic system and is dated by Hjartarson (1988) to 8,600 BP and can be tied to the enhanced activity in the aftermath of the glaciation. This lava flow is the largest fissure eruption during the Holocene with a total volume of 25km^3 (Halldorsson et al., 2008). It originates from the Bardarbunga volcanic system - the most productive part of the eastern volcanic system during the Holocene (Halldorsson et al., 2008).

Two other fissure eruptions in the eastern volcanic zone which have occurred in historic times are the Eldgja eruption 934-940 AD and the Laki eruption 1783-84. Eldgja produced 19.6 km^3 and the Laki eruption 15.1 km^3 (Thordarson and Self, 2003). Despite the slightly less material produced, the Laki eruption had the most devastating impact on population and environment. The Laki eruption emitted 122 megatons of SO_2 into the atmosphere; this resulted in a sulfuric aerosol hanging over the northern hemisphere for more than five months (Thordarson and Self, 2003).

Large Plinian eruptions, often silicic, also take place in Iceland despite its location on a mid oceanic ridge. By volume, the basaltic eruptions are the largest and can impact a large area occasionally with ash and aerosols, but the explosive intermediate and silicic eruptions can disperse ash widely. One type of large silicic eruption take place in volcanoes with a developed shallow magma chamber, which is given time to differentiate and can result in an explosive eruption. It can be triggered by an intrusion of basaltic magma. Those explosive eruptions can be followed by the formations of a caldera. Several calderas have been formed in the Holocene, both the largest and the most recent can be found in the volcano Askja (northern Iceland). The largest with a diameter of 8 km formed in the beginning of Holocene producing a silicic (pumice) layer. The most recent caldera formation started 1875 with an explosive eruption ejecting 2.5 km^3 dense-rock equivalents (DRE), and it took thirty years until the present day caldera (4.5 km in diameter) reached its present shape. The pumice from the 1875 eruption devastated a farming district in eastern Iceland and the ash spread to Scandinavia.

The internationally best-known Icelandic volcano (until 17th April when Eyjafjallajökull started) with a name that is easier pronounced is Hekla. It is currently one of the three most active volcanoes in Iceland with twenty summit eruptions. The first traces of Hekla as an evolved volcanic centre (erupting basaltic andersite to rhyolite) probably occurred in early Holocene time (Sverrisdottir, 2007). The explosive magmatism in Hekla has produced several distinct silicic ash layers. The largest of these silicic ash layers are named H5, H4 and H3. These conspicuous ash layers are easy to recognize by

their white color. They are wide spread and are excellent marker horizons. The first recorded silicic eruption in Hekla is H5, with a volume of 0.7 km^3 DRE, and it is dated to roughly 7,000 years ago. The H4 ash layer has a volume of 1.8 km^3 and is dated to 4,200 BP. The most voluminous silicic ash from Hekla is the 3,900 BP old H3 layer with 2.2 km^3. All the volumes and datings above are taken from a compellation done by Sverrisdottir (2007). Despite all the large explosive silicic eruptions, no caldera has been formed in Hekla. A deep-seated magma chamber under the volcano can explain this. Hekla has a characteristic pattern, as the longer response time between eruptions the more silicic is the initial products in the explosive phase of the eruption. This is attributed to differentiation in a magma chamber, the longer time the more silicic material accumulated at its top. The response time of the most recent eruptions has been ten years giving pathetic eruptions with a short duration and low initial silicic contents. The next major eruption expected is a phreatomagmatic eruption in Katla that most likely will produce material in the cubic kilometer scale.

References

Halldorsson, S.A., Oskarsson, N., Gronvold, K, Sigurdsson, G., Sverrisdottir, G., and Steinthorsson, S., 2008. Isotopic-heterogeneity of the Thjorsa lava - implications for mantle sources and crustal processes within the Eastern Rift Zone, Iceland. Chemical Geology, 255 (1-3), 305-316. Doi: 10.1016/j.chemgeo.2008.06.050

Hjartarson, A., 1988.The Thjorsa lava the largest Holocene lava flow on earth (in Icelandic). Natturufraedingurinn 58 (1), pp. 116.

Sverrisdóttir, G., 2007. Hybrid magma generation preceding Plinian silicic eruptions at Hekla, Iceland; Evidence from mineralogy and chemistry of two zoned deposits. Geological Magazine, 144 (4), 643-659. doi:10.1017/S0016756807003470.

Thordarson, T., Höskuldsson, A., 2008. Postglacial volcanism in Iceland, Jökull (58), 197-228.

Thordarson, T., and Self, S., 2003. Atmospheric and environmental effects of the 1783–1784 Laki eruption: A review and reassessment. Journal Of Geophysical Research, Vol. 108, No. D1, 4011, doi:10.1029/2001JD002042, 2003

.

GLACIERS AND SEA ICE EXTENT IN ICELAND DURING THE QUATERNARY

Van Vliet Lanoe Brigitte [(1)], Guillou Hervé[(2)], Gudmundsson Agust[(3)] and Schneider Jean-Luc.[(4)]

(1) LDO, IUEM, Plouzané, University of Brest, FR; Brigitte.vanvlietlanoe@univ-brest.fr, (2) LSCE Gif/Yvette, FR
(3) JFS ,Geological Services Reykjavik, Iceland; (4) EPOC , Univ.Bordeaux, Talence,FR

In Iceland glacier development is closely related with the extent of the sea ice and the inland precipitation mostly controlled by the Irminger Current, a branch of the North Atlantic mild Current. Also the relief inherited from the volcanic activity of the hotspot favours the formation of the ice sheet, together with the cooling brought by the Eastern Cold Current derived from the Eastern Greenland current. This is the reason of the formation of an ice sheet in the South-East of the island where precipitation and the relief are the highest. The North is usually arid, a limiting factor for the glacial extent. During thermal optimum, glaciers usually vanish but restore during cooling events, especially late interglacials: it never reached a permanent volume as the Greenland or Antarctica ice sheets. Sea ice is for the moment absent, but developed along the Northern coast during the Little Ice Age. Sea ice extent prevent sea water vaporization and thus snow accumulation on land. Moreover, because of its position in the central northern Atlantic, Iceland is an intergrade between Greenland and the Eastern America, cooled by the Eastern Greeland Current and Scandinavia, warmed and sprayed thanks to the mild North Atlantic drift during interglacials.

Curiously, the Pleistocene stratigraphy of Iceland is very limited even about 20 glaciations are recorded for the whole Quaternary. Well constrain for the Plio-Pleistocene, almost no clear stratigraphy is given for the Quaternary, excepted since the Older Dryas (13-12ka) and the Last Deglaciation. A lot of controversies exist, easy by limited dating, especially for the Middle and Upper Pleistocene. K-Ar dating and detailed stratigraphical work has raised the possibility of a more detailed record, especially for the Middel and Upper Pleistocene, more in conformity with marine records around the island and in other Nordic countries than the favourite interpretations.

The first glaciations in Arctic.

Since 14 Ma, IRD in marine cores from the Northern Atlantic evidence the drift of icebergs on the Northern Atlantic (Bleil, 1989). Earlier events are speculative, only located on the eastern margins of Greenland, where glaciations are well recorded from 7 Ma (Larsen et al, 1994; Solheim et al., 1997); earlier events can be derived from local glaciers or even sea ice. Platform and inland evidences of glaciations are much younger, usually recorded from the Middle Pliocene (3.3 ma), as on the Barents Shelf, when the Bering Strait opened. The Yakataga glacio-marine Formation in the Gulf of Alaska was first interpreted as early Miocene (c.20 Ma), but now relocated into the Pliocene, even mountain glaciers were probably pre-existing in altitude since 38 Ma. A glacial intensification in the circum-Atlantic region occurred from c2.7 Ma (Jansen et al., 2000; Kleiven et al., 2002; Haug et al, 2005, Bartoli et al., 2006), with a distinct supply of IRD-rich sediments on the Yermak Plateau between c. 2.7 and 2.4 Ma .

The very first glaciations in Iceland.

The age of the Tertiary basalt formation ranges from 16 Ma. Iceland is thus a very good place to analyse the occurrence of early glaciations. Observations by Geirsdottir and Eiriksson (1994, Geirsdottir , 2004; Geirsdottir et al. 2007) have shown that the onset of glaciations in the North and in the East also give a similar answer as in most Arctic. Fossil fauna in sedimentary beds interlayered with basaltic floods attest of a progressive cooling from subtropical close to 16 Ma to temperate at 7 Ma. Glaciers have been developing in the southeast since the late Miocene (c. 9 Ma). Evidence of glaciers (tillites) are interbedded with basalts in the East (Jokulsa à Bru) since 5 Ma, attesting the intermittent development of a small ice cap in place of the southern (and highest) portion of the Vatnajökull. Island-wide glaciations spread from the Plio-Pleistocene transition with glacial-interglacial cyclicity indicated from ~2.6 Ma, followed by step-like amplifications at 2.2-2.1, 1.6 Ma and after 1 Ma.
The sedimentary sequence of Tjorness Group records continuously the crucial period between 4 and 2.5 Ma. Cooling and glacio-marine tillites are interbedded in the youngest *Serripes* serie, although the two older members are still temperate. The next fossiliferous group, the Furuvik Group, c.2.2 Ma, contents evidence of two major tillites, marking the onset of a real ice.sheet reaching the coast. The

next group, the Breidavik one (2.0-1.2 Ma), contents 6 tillite beds. Almost 20 glaciations are recorded in Iceland (fig.1).

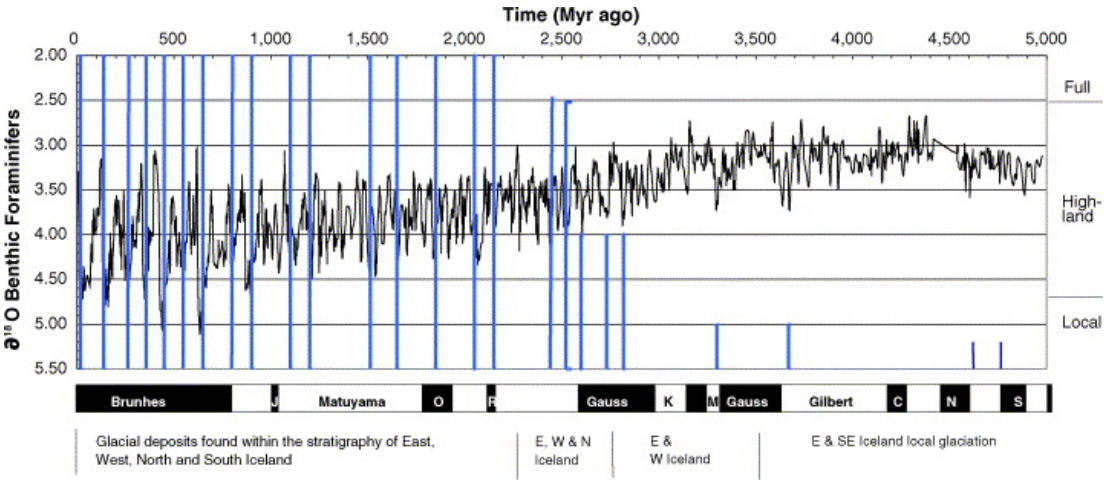

Figure 1: Correlation of identified glacial deposits in the Iceland stratigraphy with the Tropical Pacific benthic isotope record from core ODP849 for 0–5 Ma. Lines show the approximate position of glacial deposits found in the Icelandic stratigraphy. (Geirsdottir et al. 2007)

The Middle Pleistocene transition (MPT).

Evidences of large glaciations exist thus from 1.2 Ma. At the North edge of Skagi peninsula, glacio-marine sediments sealed by basalts yield this date. Huge volcanism existed in the rift from 1.2 to 1 Ma inland and along the Snaefelness ridge. At that time also the first móbergs (subglacial table volcanoes) are observed in Skjalfandi (Littla Saltvik), truncated by temperate based glaciers.
From an oceanic point of view, the Middle Pleistocene Transition can be divided into a first transition (1000 - 920 ka), the MPT s.s. (920 - 640 ka) and a second transition (640 - 530 ka; Schmieder et al., 2000). In the NE of Iceland, most hyaloclastite ridges formed during large glaciation formed from 1 Ma and mostly close to 750-700 ka. Glacial permanence of the Vatnajökull is indicated since only 790 ka (Helgason & Duncan, 2001).

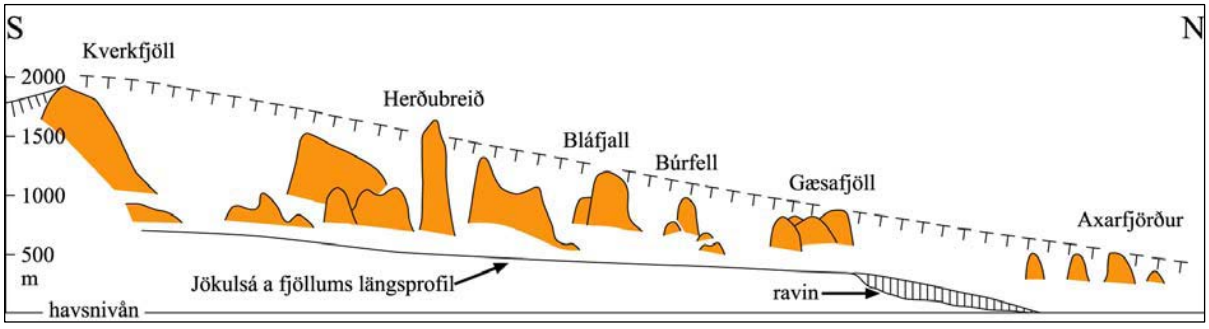

Fig.2 Altitude of the móbergs (transect Vatnajökull to Oxarfjodur) and the volume of the Icelandic ice sheet (Walker 1965). All these móbergs are supposed to belong to the Last glaciation.

After the onset of the MPT event, a main effusive event occurred from 750 to 700 ka in the NE of Iceland, damming the glacially shaped Jökudalur in the middle of the Jökuldalheidi allowing the formation of a hudge paleolake, the Múlalón (Guillou et al., 2009), recorded by 80 m of thick sandy glaciolacustrine deposits, the Laugarvalla sediments. Laugarvalla serie A, below the lower basalt (750 ka) corresponds to MIS 19 deglaciation, and the basal hyaloclastite probably traces MIS 22 (~920-880 ka), an important glaciation responsible for a basal nonconformity that marks the onset of very large glaciations, The main deposits, Laugarvalla B sediments, younger than 750 ka and including two glacial events correspond fairly well to the twinned stadial of MIS 18. Laugarvalla C, deposited during the onset of the major MIS 16 glaciation, also responsible for a major erosionnal discontinuity. After the complete levelling of the landscape by the MIS 16 glaciation, the overflowing by interglacial basalts was extensive from MIS 15 to MIS 13 (560-480 ka). Similar deposits exist in the East : the age of the lacustrine deposits of the Sinafellsfjall is though to yield c.700 ka.

This period is mild and characterised by limited glaciations (Lisiecki and Raymo, 2005).

The MIS 12.

The intensification in glacial conditions is indicated offshore by a marked increase in the accumulation rates of IRD in the Northern Atlantic during MIS 16 and 12 (Helmke et al., 2005; Hoddel et al., 2008) and by a weakening of the THC (Hoddel et al., 2008). The largest glacial extent in Iceland seems to occur during this MIS 12 glaciation (430 ka) with móberg formation on Snaefellness and very large móbergs inland as the Laufafell (south) or the Hagónga, south of the Hofsjökull (Guillou et al, 2009). During the last 500 kyr, rates of erosion increased to 50–175 cm kyr^{-1} (Geirsdottir et al., 2007). The ice sheet reaches the platform edge in SE Iceland (V.Bout Roumazeille, pers.com.).

The Saalian (MIS 8 & 6)

Saalian I (MIS 8 (280-240 ka) is not a major glaciation following the δ18 O isotopic curve of Liesencki & Raymo (2005). Nevertheless, major mobergs formed close to 250 ka, especially the eastern Snaefell (Guillou et al, 2009). Hyaloclastite ridge activity persisted under large ice sheets. MIS 7 is a cool complex interglacial, but no clear evidence of it is observed in Iceland. Some ice sheets are preserved at that time on Scandinavia.

Saalian II (MIS 6, 180-135 ka), was characterised by a major, temperate-base ice mass (Van Vliet-Lanoë et al., 2005) that probably covered most of the shelf. MIS 6 is associated with the storage of huge amounts of ice on land masses around the North Atlantic (Ehlers, 1983; Mangerud et al., 1998; Svendsen et al., 2004), due to the mild conditions in the Atlantic Ocean (Funnell, 1995). In Iceland this explains the erosional capability of the ice masses which mostly shaped the present-day morphology. The MIS 6 ice sheet was thick and extensive, and associated with ice-streams and major glacio-isostatic rebound in southern Iceland. Major subglacial activity occurred close to prior 150 ka, even in Eyafjordur (Guillou et al, 2009). Nevertheless, some deglaciation probably developed close to 150 ka a shown by subaerial lava flows. The glacial load on Iceland at the end of MIS 6 also explains the importance of the subglacial hyaloclastites, which were further reworked by Termination II.

The Last Interglacial and Termination II

Important lava flows and phreatomagmatism occurred during Termination II in the North Volcanic Zone as well as on Snaefelness, sealed by interglacial deposits. Also the Hekla volcano seems to be very early active, perhaps explaining the basaltic tephra described by Wastegard et al, 2005 at 132 ka in the Faeroe Island. Jökulhaups are common during deglaciation both in the North and the South . The sedimentary record of this period is widely spread in the North Volcanic zone, in the Vopnafjördur valley, in the upper Jökuldalur, in the Ranga valley (in the South), and east of Snaefellness, on the strandflat. This interglacial was one of the possible interpretations of the Fossvögur formation but also for the Ellivögur one (close to Reykjavik). First described in the North (van Vliet-Lanoë et al, 2005) it will be described now as the Ranga formation. The deposits formed during MIS 6 deglaciation and MIS 5e mainly derive hyaloclastitic sands. It records one lateglacial re-advance (Zeifen-Kategat oscillation), two climate optima with coastal highstands, interglacial paleosols interrupted by two successive glacial advances were correlated with the Middle Eemian cooling (van vliet-Lanoë et al, 2007). Permafrost certainly extended in altitude from the mid Eemian cooling.

The Weichselian

The precise timing of the Last Glacial Maximum (LGM) and the full extent of the Iceland ice sheet is poorly constrained, although the deglacial cycle is reasonably well defined. In Iceland, several authors have postulated the existence of a glacial extent that reached the outer border of the island platform or shelf during the Weichselian (e.g., Norðdalh and Halfidason, 1992; Ingólfsson et al., 1997). Móberg's data are also used to indicate the thickness of the ice sheet and to map the boundary of the ice during the Last Glacial Maximum (LGM) (fig.2 , Walker, 1965). Small ice-free (nunataks) areas may have existed along the coastal mountains, particularly in the northwest, north and east during the LGM. Accumulating data indicate that during its maximal extent, weichselian ice streams and outlet glaciers from ice divides in central Iceland terminated at or close to the shelf edge. Several datation show the existence of retracted ice sheet during 5a (aerial lava flow in Skardsengi at 80 ka BP K-Ar), limited deglaciation at 55-60 ka (Thorsmork ignimbrite, Lacasse et al., 2001; rockglaciers at the coast: A.Gudmunsson, 2000) maximum ice load and móberg formation close to 50-40 ka BP (Levi et al., 1991, Guillou et al , 2009). The age of the Latra moraine close to the western shelf edge somewhat older than 36 ka (Syvitski et al, 1999) seems to confirm this. An important retreat from 26 ka in the N & NE of Iceland, younger readvances close to 15 and 13 ka (Van Vliet-Lanoë et al, 2007). The northwestern peninsula seems to have supported an independent ice cap with valley glaciers with

outlet glaciers originating within an ice-divide near the centre of the peninsula (Principato et al., 2006). This is consistent with the absence of deposits from 26 ka to 17 ka ago offshore of Ejafjordur (North), mentioned by Andrews et al. (2000, 2003), and with the Middle Weichselian transgression reconstructed by Svendsen et al. (2004) for the Scandinavian Arctic. A limited LGM glaciation could also explain the characteristics of the Termination I-a sediments, which are poor in hyaloclastites.

The deglaciation: Termination Ia (Bölling) versus Termination Ib (Younger Dryas)

Classical literature describes deglaciation, with the ice retreating from the present-day coast line during the Younger Dryas or even the Preboreal (Norðdahl and Halfidason, 1992; Ingólfsson et al., 1997),. The classical Vedde Ash (11.8 cal ka BP) and the Saksunarvatn tephra (10.2 cal. ka BP) trace the termination Ib. (Grönvold et al., 1995). A shard like rhyolithic tephra (Skógar) found in secondary position at coastal sites, mostly in the North of the island where it has been correlated with the Vedde Ash, (Norðdahl and Halfidason, 1992): it is commonly used to date Termination Ib (Rundgren et al., 1997). The Vedde ash is a pellet-like marker tephra layer from the Katla Volcano, South Iceland, well known in marine sequences; it has been found on the top of the Mykjuness moraine close to Hella (+90m) and on the marine terrace at +15m in the North (Kaupangur, Eyafjordur) where it postdates clearly the Skógar (13 cal ka). In fact, 3 tephra with similar signature as the Vedde Ash exist. Correlated with an ignimbrite of the Katla (Solheimar ; Lacasse et al., 2001), the Skógar tephra seems older than the maximum deglaciation flooding surface and can be correlated with the Middle Vedde ash c.13.5 cal ka (IA2: in Mortensen et al., 2005; Van Vliet-Lanoë et al, 2007) .

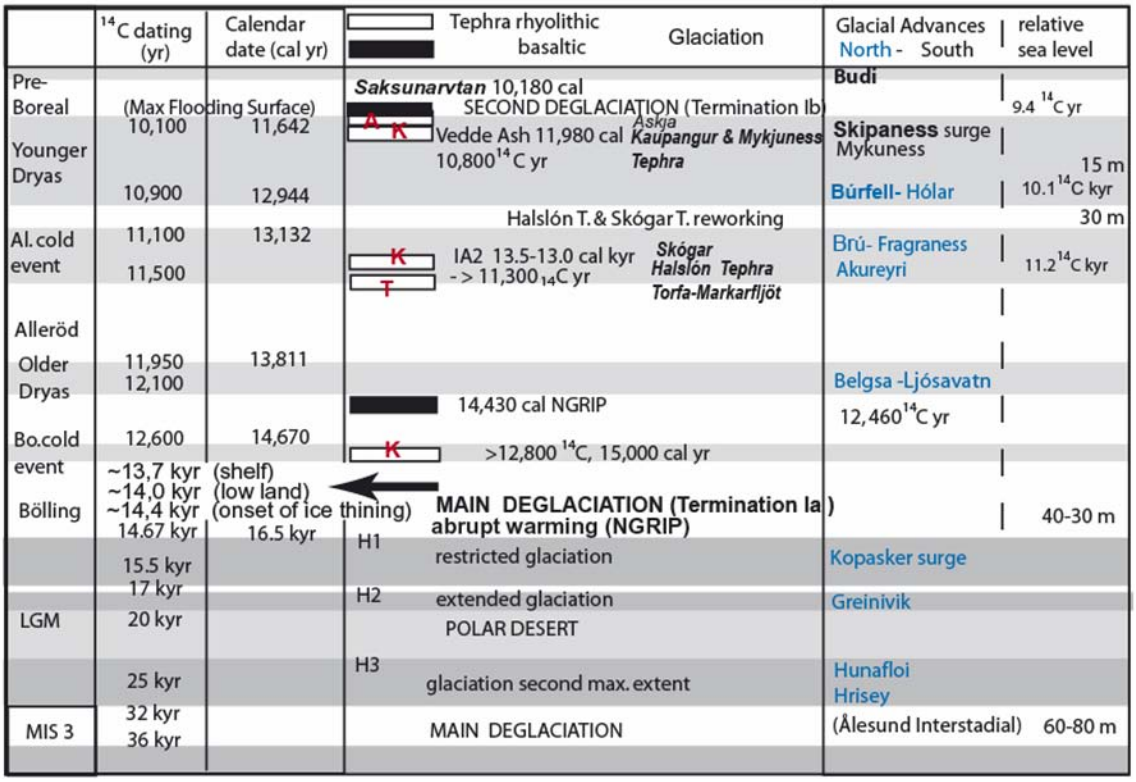

Figure 3; stratigraphical position of the main tephra markers and proposed glacial history of the Weichselian in Northern Iceland (completed from Van Vliet-Lanoë et al., 2007). Skipaness advance occurred c.11600 cal yr; Mykjunes one is slightly older.

The deposits of the Weichselian deglaciation (Termination I *sensu lato*) are much more limited in thickness that for the Termination II. Both in south and northern Iceland considerable deglaciation (Termination I-a) develop from the Bølling onward (cf. Geirsdóttir et al., 1997; Principato et al., 2006; Jennings et al., 2007; Licciardi et al., 2007). Deglaciation seems major as the Skógar tephra is found at the end of the Halslón sedimentation, prior to the Saksunarvatn tephra, 20 km North only of the Vatnajökull (Van Vliet-Lanoe et al., 2007). The occurrence of the Vedde Ash in lake sediment, shows that during the Younger Dryas (12.7–11.5 cal ka) outlet glaciers from a southern Icelandic already retracted icecap, surged locally to the current coastline. It is the case at Borgarfjôrdur where it calved on the strandflat and surged to Skypaness (Hvalfjördur). Deglaciation definitively proceeded from

10.299 cal yr, in the SW of Thingvellir (Mykjunes moraines) or in the North Western peninsula. In northern Iceland, the YD glaciers did not reached the coast but remained already inland as in Eyjafjörður or Oxarfjordür, as shown by the limited importance of the glacial rebound in the North, re-interpreted from the Rundgren et al., 1997 data or by the Kaupangur section (Ejafjördur) . In the North, glaciers were starved in precipitation by a re-extent of the sea-ice and a retracted Irminger current. A limited glacier advance in Southern Iceland occurred during the early Preboreal time from 11.5 to 10.1 cal ka, when the Búði moraines were formed, after the maximum flooding related to glacio-isotsatic rebound. In conclusion, Iceland record an early maximum ice extent during the Weichselian (MIS3), a limited glaciation during the LGM and a major deglaciation in NE Iceland from the Bølling onward are major differences from the interpretations presented in previous works about Iceland .

References

Bleil, U., 1989. Magnetostratigraphy of Neogene and Quaternary sediment series from the Norwegian Sea, Ocean Drilling Program , Leg 104, *Proc.ODP Sci.Res.* 104: 289-901

Einarsson and Albertsson, 1988 T. Einarsson and K.J. Albertsson, The glacial history in Iceland during the past three million years, Philos. Trans. R. Soc. Lond. *B* **318** (1988), pp. 637–644.

Funnell, B.M., 1995. Global sea-level and the (pen)insularity of late Cenozoic Britain. In: Preece, R.C. (Ed.), Island Britain: a Quaternary perspective. Geol. Soc., London, Spec. Publ. 96, 3-13.

Geirsdóttir A., J. Hardardóttir and A.E. Sveinbjörnsdóttir, 2000 Glacial extent and catastrophic meltwater events during the deglaciation of Southern Iceland, Quat. Sci. Rev. **19** , 1749–1761

Geirsdóttir A., J. Hardardóttir and J. Eiriksson, 1997 Depositional history of the Younger Dryas(?)—Preboreal sediments, South Central Iceland, *Arct. Alp. Res.* **29**, 13–23.

Geirsdottir, A . and Eirıksson, J., 1994. Growth of an intermittent ice sheet in Iceland during the late Pliocene and early Pleistocene. Quat.Res., 42, 115 -130.

Geirsdóttir, Á. 2004. Extent and chronology of Glaciations in Iceland. In Ehlers, J. and Gibbard, P. eds., Quaternary Glaciations — Extent and Chronology of Glaciations. Part 1 Europe. INQUA Commission on Glaciation. Elsevier B.V. 175-182.

Geirsdóttir, A., Miller, G.H. and Andrews, J.T., 2007. Glaciation, erosion, and landscape evolution of Iceland. J.Geodyn. 43 , 170 -186.

Grönvold K., N. Oskarsson, S.J. Johnsen, H.B. Clausen, C.U. Hammer, G. Bond and E. Bard, 1995Ash layers from Iceland in the Greenland GRIP ice core correlated with oceanic and land sediments, *Earth Planet. Sci. Lett.* **135** (1995), pp. 149–155.

Guðmundsson, A., 2000. The relict periglacial face of the Héradsfloí area-East Iceland. [In:] Russel, A. & Marren, P. (Eds): Iceland 2000 - modern processes and past environments. *Keele University, Department of Geography Occasional Papers Series* 21, 44-47.

Guillou H., Van Vliet-Lanoë-B., Guðmundsson A. and S.Nomade. Climate-related Quaternary volcanic activity in Iceland? Insights from new unspiked K-Ar ages. Quaternary Geochronology, 5, 10-19.

Haug G.H., Ganopolski A., Sigman D. M., Rosell-Mele A., Swann G. E. A., Tiedemann R.,. Jaccard S. L, Bollmann J.,. Maslin5 M.A, Leng M. J. & Eglinton G. 2005 North Pacific seasonality and the glaciation of North America 2.7 million years ago. Nature 433, 821 -825.

Helgason, J., Duncan, R.A., 2003. Ekkra Geological Consulting, Ar-Ar age dating of the Kárahnjúkar volcanic formation, Kárahnjúkar. Hydroelectric Project, Age dating performed by dr. Robert A. Duncan, Jarðfræðistofan, EKKRA Rept. LV-2003/090, Unpublished Report 39 pp.

Helmke J. P., Bauch H. A., Röhl U., Mazaud A. 2005. Changes in sedimentation patterns of the Nordic seas region across the mid-Pleistocene. Marine Geol., 215, 107-122.

Hodell, D. A., Channell, J. E. T., Curtis, J. H., Romero, O. E., and Röhl, U. ,2008. Onset of "Hudson Strait" Heinrich events in the eastern North Atlantic at the end of the middle Pleistocene transition (~640 ka)? Paleoceanography, 23, PA4218, doi:10.1029/2008PA001591.

Ingólfsson Ó, Björck S., Haflidason H., Rundgren M.1997. Glacial and climatic events in iceland reflecting regional north atlantic climatic shifts during the Pleistocene-Holocene transition. 16, 1135-1144

Knies, J., Matthisen, Vogt, Laberg, J.S., Hjelstuen, B.O., Larsen, E., Andreassen, K., Eidvin, T., Vorren, T.O., 2009. A new Plio-Pleistocene ice sheet model for the Svalbard-Barents Sea region. Quat.Sc.Rev, 28, 812-828.

Lacasse C., Garbe-Schönberg C.D. 2001, Explosive silicic volcanism in Iceland and the Jan Mayen area during the last 6 Ma: sources and timing of major eruptions J.Volc.Geoth.Res., 107, 113-147.

Larsen H. C, A. D. Saunders, P. D. Clift, J. Begét, W. Wei, S. Spezzaferri, J. Ali, H. Cambray, A. Demant, G. Fitton, M. S. Fram, K. Fukuma, J. Gieskes, M. A. Holmes, J. Hunt, C. Lacasse, L. M. Larsen, H. Lykke-Andersen, A. Meltser, M. L. Morrison, N. Nemoto, N. Okay, S. Saito, C. Sinton, R. Stax, T. L. Vallier, D. Vandamme, and R. Werner (The ODP Leg 152 Scientific Party) 1994 Seven Million Years of Glaciation in Greenland. *Science*, , 264, ,952-955.

Levi, S., Audunsson, H., Duncan, R. A., Kristjansson, L., Gillot, P.Y., Jakobsson, S.P. 1990. Late Pleistocene geomagnetic excursion in Icelandic lavas: confirmation of the Laschamp excursion. Earth Plan..Sc. Lett., 96, 443-457.

Licciardi, J.M., Kurz, M.D., Curtice, J.M., 2007. Glacial and volcanic history of Icelandic table mountains from cosmogenic ^{3}He exposure ages: Quat. Sc. Rev. 26, 1529-1546.

Lisiecki, L. E., and M. E. Raymo, 2005. A Pliocene-Pleistocene stack of 57 globally distributed benthic $\delta^{18}O$

records. Paleoceanography, 20, PA1003, doi:10.1029/2004PA001071.
NGRIP North Greenland Ice Core Project members. 2004. High-resolution record of Northern Hemisphere climate extending into the last interglacial period. Nature, 431, 7005, 147-151.
Norðdahl H., Halfidason H., 1992. The Skógar tephra, a YD marker in North Iceland. Boreas, 21, 23-41.
Syvitski, J.P.M., Jennings, A., and Andrews, J.T., 1999, High-resolution seismic evidence for multiple glaciations across the southwest Iceland Shelf. Arctic, Antarctic and Alpine Research, 31: 50-57.
Van Vliet-Lanoë, B., Bourgeois, O., Dauteuil, O. Embry, J.C, Schneider, J.L., Guillou, H., 2005. Deglaciation and volcano-seismic activity in Northern Iceland: Holocene and Early Eemian. Geodyn. Acta 18, 81-100.
Van Vliet-Lanoë, B., Guðmundsson, A., Guillou, H., Duncan, R.A., Genty, D., Gassem, B., Gouy, S., Récourt, P., Scaillet, S., 2007 Limited glaciation and very early deglaciation in central Iceland: Implications for climate change. CRAS Géosciences 339, 1-12.

EARTH RESPONSES TO ICE MASS CHANGING IN ICELAND

Thierry VILLEMIN
EDYTEM, Université de Savoie, 73376 Le Bourget du Lac, Thierry.Villemin@univ-savoie.fr

Abstract

The reological properties of the crust and the upper mantle beneath Iceland make the earth surface sensitive to recent ice mass changing. On a short time scale, strong correlation exists between seasonal variations in continuous GPS time series and snow covering. The overall retreat of Icelandic glaciers is causing uplift of over 2 cm/yr around Vatnajökull, the largest Icelandic ice cap. Recent modelling also suggests that the same phenomena is causing increased mantle melting and magma generation under Vatnajökull

RIFT AND ICE CAP CONJUNCTION

In Iceland, the plate boundary crosses Iceland from S to N and links with the Mid-Atlantic ridge through two south and north transform zones, the South Iceland Seismic Zone and the Tjörnes Transform Zone respectively (SISZ and TFZ). The rift zone outcrops along volcanic zones, most active of them being the Eastern Volcanic Zone and the Northern Volcanic Zone (EVZ and NVZ). Both of them are shifted eastward with regard to the axis of the oceanic ridge (RR and KR). This particular situation is known as resulting of the global movement of the lithospheric plate system relative to the Icelandic mantle plume.

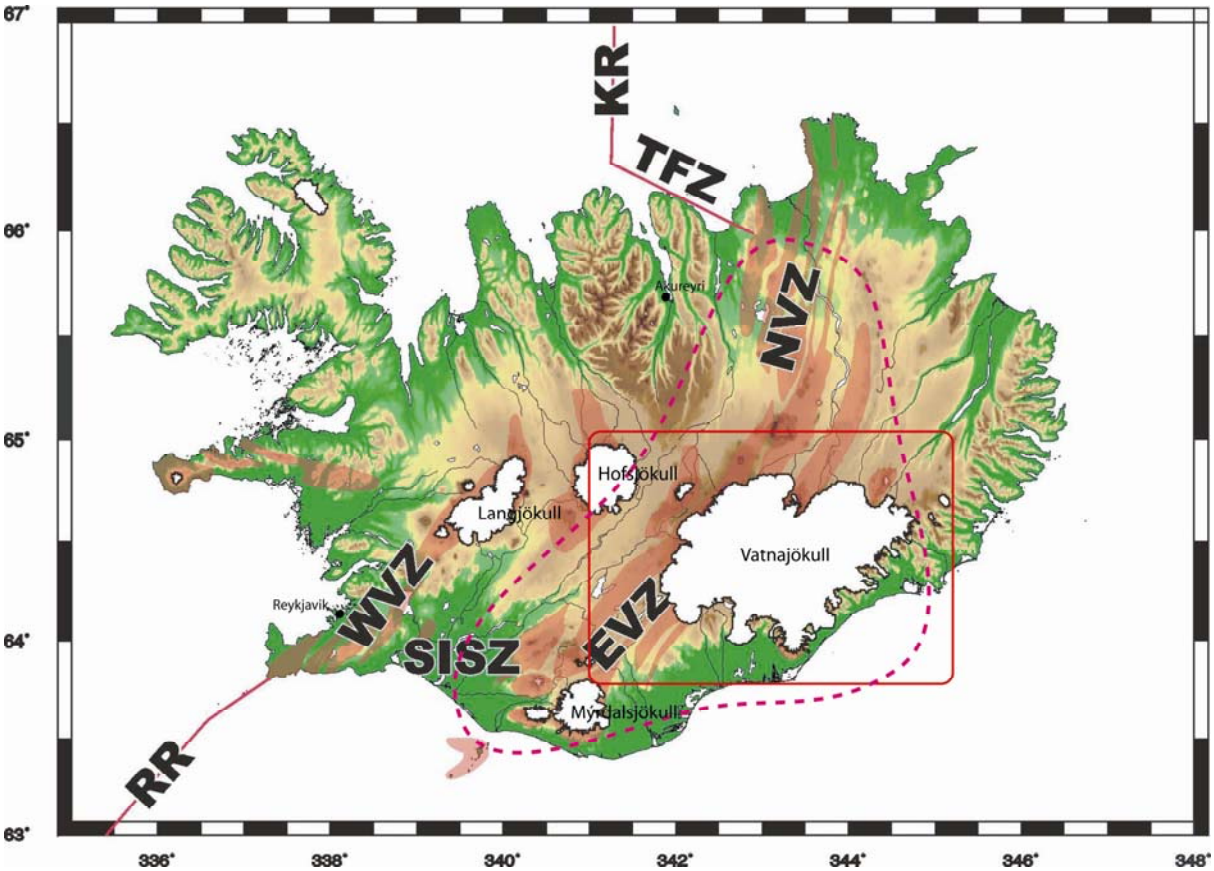

Figure 1 : Iceland general overview : plate boundary and ice caps.
EVZ : eastern Volcanic Zone ; KR : Kolbeinsey Ridge; NVZ :Northern Volcanic Zone ; RR : Reykjanes Ridge; SISZ :South Iceland Seismic Zone; TFZ : Tjörnes Fracture Zone; WVZ : Western Volcanic Zone.
Purple dotted line figures the hotspot trace whose apex is located below Vatnajökull.

The junction between the EVZ and NVZ is covered by the western half of **Vatnajökull**.

Vatnajökull is the largest ice cap in Iceland (Björnsson, 1988), covering an area of about 8100 km2 with a mean radius of 50.7 km and a maximum thickness of about 900 m (e.g. Björnsson et al., 2002). The ice volume loss at Vatnajökull since 1890 is estimated to be about 400 km3 and ongoing glacio-isostatic deformations around Vatnajökull has been reported by several geodetic studies. The average altitude of the glacier is around 1500 m. The ice cap is maintained by strong annual precipitation, exceeding locally 4 m. The feedback between mass balance and altitude settles the ice cap to steady state for the recent past (last millennium). Nevertheless, this steady state is bounded by a critical elevation line as shown by (Aðalgeirsdóttir et al., 2005).

There are three other ice caps of smaller volume and surface west and southwest of Vatnajökull:

- **Langsjökull** (the "long glacier") covers the northern end of the Western volcanic zone (WVZ). The glacier is following more or less the direction of the active volcanic zone. Under Langjökull there are two volcanic systems with caldeiras well discerned from air. Langjökull is the second-largest of the glaciers of Iceland (1021 km^2), after Vatnajökull. Its highest peak reaches 1360 metres.
- **Hofsjökull** is the third largest glacier in Iceland. It situates at the west of the Highlands of Iceland between, outside the active rift zone. It covers an area of 925 km^2, reaching 1,765 m at its summit. The subglacial volcano is a shield type with caldera.
- **Mýrdalsjökull** is situated south of Iceland, at the southern end of the EVZ and is connected to the smaller glacier Eyjafjallajökull. The top of Mýrdalsjökull reaches 1493 m in height and the ice extends on an area of 595 km^2. The icecap covers the active volcano Katla. The eruption cycle range 40 – 80 years. Eldgjá, a fissure swarm of about 30 km length, erupting in 936, is part of the same volcanic system.

All ice caps in Iceland have negative mass balances and are retreating since the end of the Little Ice Age (16th to mid 19th century). This tendency is likely accelerated nowadays due to global climatic change.

EARTH RESPONSE TO ICE MASS CHANGING

The response of the Earth to stress loading imposed on the surface of the Earth, or within the Earth, depends on the rheology of the Earth. This rheology can be constrained by measuring geodetically the response to various loading of different spatial extent and different time scales. On a short time scale, the Earth behaves elastically whereas on a long time scale the Earth behaves as a viscoelastic body, with an elastic outermost layer. The rheological structure of crust and mantle under Iceland has been constrained by modelling of various geodetic results, e.g. evaluated by modeling spreading across the plate boundary in Iceland, and studies of co-seismic and post-seismic deformation. Studies of the response of the Earth to changing ice mass on the surface of Iceland have addressed the following topics:

• “Icelandic rhythmics” - the annual Earth response to change in ice mass at Icelandic glaciers. Strong correlation has been found between seasonal variations in continuous GPS time series (peak-to-peak amplitude of more than 10 millimeters) and predicted response to annual snow load in Iceland [Graphenthin et al., 2006]. The load has been modeled using Green’s functions for an elastic halfspace and a simple sinusoidal load history on Iceland’s four largest ice caps, constraining the elastic Young’s modulus of the Earth response.

• The overall retreat of Icelandic glaciers that is causing uplift of over 2 cm/yr. Glaciers in Iceland began retreating around 1890, and since then the Vatnajökull ice cap has lost over 400 km3 of ice. The associated unloading of the crust induces a glacio-isostatic response. From 1996 to 2004 a GPS network was measured around the southern edge of Vatnajökull. These measurements, together with more extended time series at several other GPS sites, indicate vertical velocities around the ice cap ranging from 9 to 25 mm/yr, and horizontal velocities in the range 3 to 4 mm/yr. The vertical velocities have been modeled using the Finite Element Method (FEM) in order to constrain the viscosity structure beneath Vatnajökull [Pagli et al., 2007]. An axisymmetric Earth model with an elastic plate over a uniform viscoelastic halfspace was used in modeling. The observations are consistent with predictions based on an Earth model made up of an elastic plate with a thickness of 10-20 km and an underlying viscosity in the range $4-10\times10^{18}$ Pa s. Knowledge of the Earth structure allows us to predict uplift around Vatnajökull in the next decades. According to the estimates of the rheological parameters, and assuming that ice thinning will continue at a similar rate during this century (about 4 km^3/year), a minimum uplift of 2.5 meters between 2000 to 2100 is expected near the current ice cap edge. If the thinning rates were to double in response to global warming (about 8 km^3/year), then the

minimum uplift between 2000 to 2100 near the current ice cap edge is expected to be 3.7 meters.

• Sudden redistribution of ice mass due to glacial surges. Mass redistribution on the surface of the Earth may induce deformation and flexure at the site of loading. However, this general uplift may be interrupted by sudden subsidence next to ice caps. Instability in ice flow at outlet glaciers can cause sudden glacial surges, when large volumes of ice flow from accumulation areas on the ice caps towards their edges. InSAR observations have revealed subsidence associated with such glacial surges [Sigmundsson et al., 2006].

• Influence on volcanic systems. Recent modelling suggests that the ice reduction is causing increased mantle melting and magma generation under the largest ice cap in Iceland. Global warming causes retreat of ice caps and ice sheets. Can melting glaciers trigger a higher frequency of magmatic events? Since 1890 the largest ice cap of Iceland, Vatnajökull, has been continuously retreating losing about 10% of its mass during last century. Present-day uplift around the ice cap is as high as 25 mm/yr. Interactions between ongoing glacio-isostasy and current changes to mantle melting and in crustal stresses at volcanoes underneath Vatnajökull have been evaluated. The modeling indicates that a substantial volume of new magma, 0.014 km^3/yr, is produced under Vatnajökull in response to current ice thinning.

• Ice retreat also induces significant stress changes in the elastic crust that may contribute to high seismicity, unusual focal mechanisms, and unusual magma movements in NW-Vatnajökull.

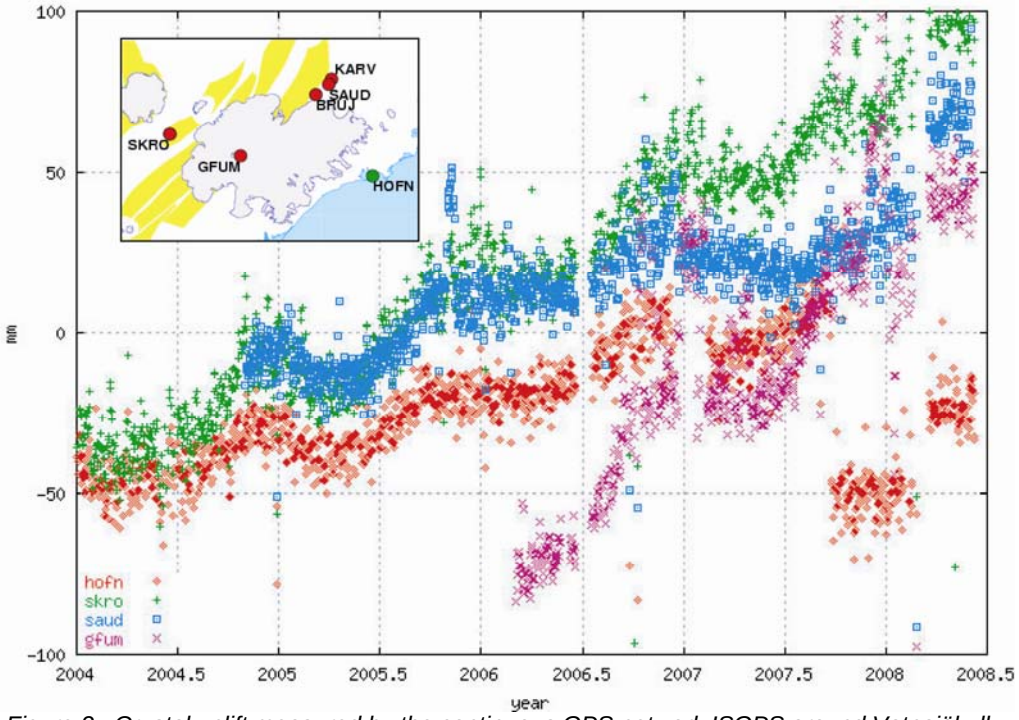

Figure 2 : Crustal uplift measured by the continuous GPS network ISGPS around Vatnajökull. This diagram shows the evolution of the vertical component at four places, relative to REYK, a station set up in Reykjavik, SW Iceland. Stations show velocities of 27 mm/yr (SKRO), 18 mm/yr (SAUD), 17 mm/yr (HOFN) et 60 mm/yr (GFUM) in the ITRF2005 reference frame.

Deglaciation in Iceland at the end of the Weichselian glaciation, about 10000 14C years BP, was associated with rapid glacial rebound, apparently reaching completion in only about 1000 years in coastal areas. This exceptionally fast postglacial rebound suggests a viscosity under Iceland on the order of 10^{19} Pa s or less (e.g. Sigmundsson, 1991). Such a low viscosity results in the rapid response of the Earth to contemporary changes in ice volume. Major ice retreat is currently ongoing at ice caps in Iceland in response to a warmer climate.

Previous studies of the rheological structure under Vatnjökull are based on geodetic measurements around the glacier edge (e.g. Thoma and Wolf, 2001; Sjöberg et al., 2004; Pagli et al., 2007). From 1996 to 2004, a GPS network was measured around the southern edge of Vatnajökull (Pagli et al., 2007). These measurements, together with more extended time series at several other

GPS sites, indicate vertical velocities around the ice cap ranging from 9 to 25 mm/yr, and horizontal velocities in the range 3 to 4 mm/yr. Recently, a nationwide network of GPS stations, the Isnet network, was used to investigate glacial isostatic adjustment in all of Iceland (Árnadóttir et al., 2009). The IsNET data confirms high uplift rates all around Vatnajökull and the need to consider all the larger glaciers and ice caps when analyzing the rebound signal.

Lake leveling measurements at Lake Langisjór at the SW edge of Vatnajökull were performed in 1959, 1991 and in 2002. The measurements show a relative uplift rate of about 4 mm/yr between benchmarks spaced 15 km perpendicular to the ice edge (Sigmundsson and Einarsson, 1992).
The GPS station at Jökulheimar on the western edge of Vatnajökull has the highest uplift rate observed outside an active volcano. The uplift at JOKU relative to the REYK station is 28 5 mm/yr, and is interpreted to be mostly caused by glacio-isostatic adjustment around Vantajökull.

The velocities derived from GPS measurements have been modeled using the Finite Element Method (FEM) in order to constrain the viscosity structure beneath Vatnajökull (Pagli et al., 2007; Arnadottir et al., 2009). Pagli et al., 2007 used an axisymmetric Earth model with an elastic plate over a uniform viscoelastic halfspace was used. The observations are consistent with predictions based on an Earth model made up of an elastic plate with a thickness of 10-20 km and an underlying viscosity in the range $4\text{-}10\times10^{18}$ Pa.s (Pagli et al., 2007). Knowledge of the Earth structure allowed them to predict uplift around Vatnajökull in the next decades. According to their estimates of the rheological parameters, and assuming that ice thinning will continue at a similar rate during this century (about 4 km3/year), a minimum uplift of 2.5 meters between 2000 to 2100 is expected near the current ice cap edge. If the thinning rates were to double in response to global warming (about 8 km3/year), then the occurring minimum uplift 2000 - 2100 near the current ice cap edge is expected to be 3.7 meters.

Árnadóttir et al. (2009) have modeled GPS nation-wide measurements of crustal uplift 1993-2004 with glacial isostatic adjustments due to thinning of the five largest ice caps in Iceland, using a 3D model. An Earth model with a 10 km thick elastic upper crust, underlain by a 20 km thick viscoelastic lower crust with viscosity of 10^{20} Pa.s, over a mantle with viscosity of 10^{19} Pa.s, can explain the measurements well. The authors also stresses that in order to model the crustal uplift at Vatnajökull, it is necessary to include the ice thinning at the smaller glaciers of Langjökull, Hofsjökull, Mýrdalsjökull and Eyjafjallajökull. The uplift signals taking place at the various glaciers interact with each other and with the uplift around Vatnajökull, i.e. causing a broad uplift signal in western Vatnajökull.

Since 1890 the mass balance of Vatnajökull has been negative and the entire ice cap lost about 11% of its total volume. The net loss has been equal to 1 m/yr on the average over the entire area, but in the marginal regions of the southern outlets (Breiðamerkurjökull and Skeiðarárjökull terminating below 100 m elevation) the loss equal to 8 m/yr and to 3 m/yr in the western and northern edge. The retreat of the outlet glaciers has been extensive over the last century, and areas at the southern edge of the ice cap that were covered with 200 m thick ice at the beginning of the 20th century are now ice free.

The retreat will lead to changes in the drainage pattern of the glacier. This will lead to continuous challenges for structures such as roads, bridges, power dams and power lines around Vatnajökull. One striking example of rapid change in drainage patterns is at Jökulsárlón in southern Vatnajökull. Prior to 1992, Jökulsárlón and Stemárlón were two separate lagoons at the margin of the same outlet glacier (Breiðamerkurjökull), with separate drainage systems. As Breiðamerkurjökull retreated the barrier between the two lagoons disappeared and one larger lagoon was formed. The river that used to drain Stemárlón dried up and now all the water drains from the river flowing from Jökulsárlón. Such increased water discharge can lead to accelerate erosion, and this may be a future threat to the bridge and the road.

In 1996 a GPS campaign of 15 stations was performed around the Öraefajökull volcano at the southern edge of the Vatnajökull ice cap. In 2002, four GPS points were re-measured. In 2003, all the stations from the 1996 campaign were re-measured. In 2004, three GPS points were re-measured. The results from these GPS campaigns are presented by Pagli et al. (2007), showing vertical velocities around the ice cap ranging from 9 to 20 mm/yr –campaign measurements show vertical velocities max 20 mm/yr, higher rates are obtained at STEM-HAMA-JOKU, maybe add that-, and horizontal velocities in the range 2 to 4 mm/yr.

On a still larger scale, it is known that ice unloading can influence eruptive activity. During the deglaciation of Iceland, at the Pleistocene-Holocene boundary, eruption rate is inferred to have been about 30-100 times its steady state. Increased decompressional mantle melting due to ice removal has been suggested as the main cause of the increase in melt production during deglaciation.

A similar situation, on a smaller scale, exists in Iceland today. According to Pagli and Sigmundsson (2008) a substantial volume of new magma, 0.014 km3/yr, is produced under Vatnajökull in response to current ice thinning. They also suggest that ice retreat induces significant stress changes in the elastic crust that may contribute to high seismicity, unusual focal mechanisms, and unusual magma movements in NW-Vatnajökull.

References

Adalgeirsdóttir, G., Björnsson, H., Pálsson, F., and Magnússon, E., (2005). Analyses of a surging outlet glacier of Vatnajökull ice cap, Iceland, Ann. Glaciol., 42, 23–28, doi:10.3189/17275640578181293.

Árnadóttir, T., Lund, B., Jiang, W., Geirsson, G., Björnsson, H., Einarsson, P., and Sigurdsson, T., (2009), Glacial rebound and plate spreading: Results from the first countrywide GPS observations in Iceland, Geophys. J. Int., 177(2), 691–716, doi: 10.1111/j.1365-246X.2008.04059.x

Björnsson, H., (1988). Hydrology of ice caps in volcanic regions, Soc. Sci. Islandica, 139 pp., University of Iceland, Reykajvik.

Björnsson, H., Pálsson, F., and Haraldson, H. H., (2002). Mass balance of Vatnajökull (1991–2001) and Langjökull (1996–2001), Iceland, Jökull, 51, 75–78.

Geirsson, H., Árnadóttir, T., Völksen, C., Jiang, W., Sturkell, E., Villemin, T., Einarsson, P., Sigmundsson, F., and Stefánsson, R., (2006). Current plate movements across the Mid-Atlantic Ridge determined from 5 years of continuous GPS measurements in Iceland, J. Geophys. Res., 111, B09407, doi:10.1029/2005JB003717.

Grapenthin, R., Sigmundsson, F., Geirsson , H., Arnadottir, T., and Pinel, V., (2006). Icelandic rhythmics: Annual modulation of land elevation and plate spreading by snow load, Geophys. Res. Lett., 33, L24305, doi:10.1029/2006GL028081.

Pagli, C., Sigmundsson, F., Lund, B., Sturkell, E., Geirsson, H., Einarsson, P., Árnadóttir, T., and Hreinsdóttir, S., (2007). Glacio-isostatic deformation around the Vatnajökull ice cap, Iceland, induced by recent climate warming: GPS observations and Finite Element Modeling, J. Geophys. Res., 112, B080405, doi:10.1029/2006JB004421.

Pagli, C., and F. Sigmundsson, Will present day glacier retreat increase volcanic activity? Stress induced by recent glacier retreat and its effect on magmatism at the Vatnajökull ice cap, Iceland, Geophys. Res. Lett., 35, L09304, doi:10.1029/2008GL033510, 2008.

Sigmundsson, F. (1991). Post-glacial rebound and asthenosphere viscosity in Iceland, Geophys. Res. Lett., 18, 1131–1134.

Sigmundsson, F., and Einarsson, P., (1992). Glacio-isostatic crustal movements caused by historical volume change of the Vatnajökull ice cap, Iceland, Geophys. Res. Lett., 19, 2123–2126.Sjöberg, L.E., Pan, M., Erlingsson, S., Asenjo, E., and Arnason, K., (2004). Land uplift near Vatnajökull, Iceland, as observed by GPS in 1992, 1996 and 1999, Geophys. J. Int., 159, 943–948, doi: 10.1111/j.1365-246X.2004.02353.x.

Sigmundsson, F., R. Pederesen, K. L. Feigl, V. Pinel, H. Björnsson, Elastic Earth responset to glacial surges: Crustal deformation associated with rapid ice flow and mass redistribution at Icelandic outlet glaciers observerd by InSAR, European Geosciences Union General Assembly, April 2-7, 2006, Geophysical Research Abstracts, 8, 07822, 2006.

Sturkell, E., and P. Einarsson, F. Sigmundsson, S. Hreinsdottir, and H. Geirsson, Deformation of Grímsvötn volcano, Iceland: 1998 eruption and subsequent inflation, Geophys. Res. Letters, 30, 1182, doi: 10.129/2002GL016460, 2003

Thoma, M., and Wolf, D., (2001). Inverting land uplift near Vatnajökull, Iceland, in terms of lithosphere thickness and viscosity stratification, in Gravity, Geoid and Geodynamics 2000, 97–102, Springer-Verlag, Berlin, Germany.

POSTERS SESSION

FOCAL MECHANISMS, STRESS FIELD AND CRUSTAL RHEOLOGY IN THE NORTH TANZANIAN DIVERGENCE (EAST AFRICAN RIFT) INFERRED FROM LOCAL SEISMICITY ANALYSIS

Julie Albaric[1], Maxime Godano[2], Jacques Déverchère[1], Julie Perrot[1], Anne Deschamps[2], Christian Sue[1], Bernard Le Gall[1], Richard W. Ferdinand[3], Carole Petit[4], Christel Tiberi[5].

1 CNRS - UMR 6538 – Domaines Océaniques, IUEM-UBO, Plouzané, France
2 CNRS - UMR 6526 – Géoazur, IRD-UNS-OCA, Sophia-Antipolis, France
3 University of Dar Es Salaam, Geology Department,Tanzania
4 CNRS- UMR 7072 – Laboratoire de Tectonique, UPMC, Paris, France
5 CNRS - UMR 5243 – Géosciences Montpellier, UM2, Montpellier, France

We deployed a temporary local seismic network in the North Tanzanian Divergence (NTD) for 6 months in 2007 (35 stations, SEISMOTANZ'07 experiment). The region is characterized by major changes in the magmatic/tectonic nature of the rift, at the place where the eastern branch of the East African Rift enters the Tanzanian craton. More than 200 earthquakes were accurately located south of Lake Manyara (**Figure 1**, Albaric et al., in press).

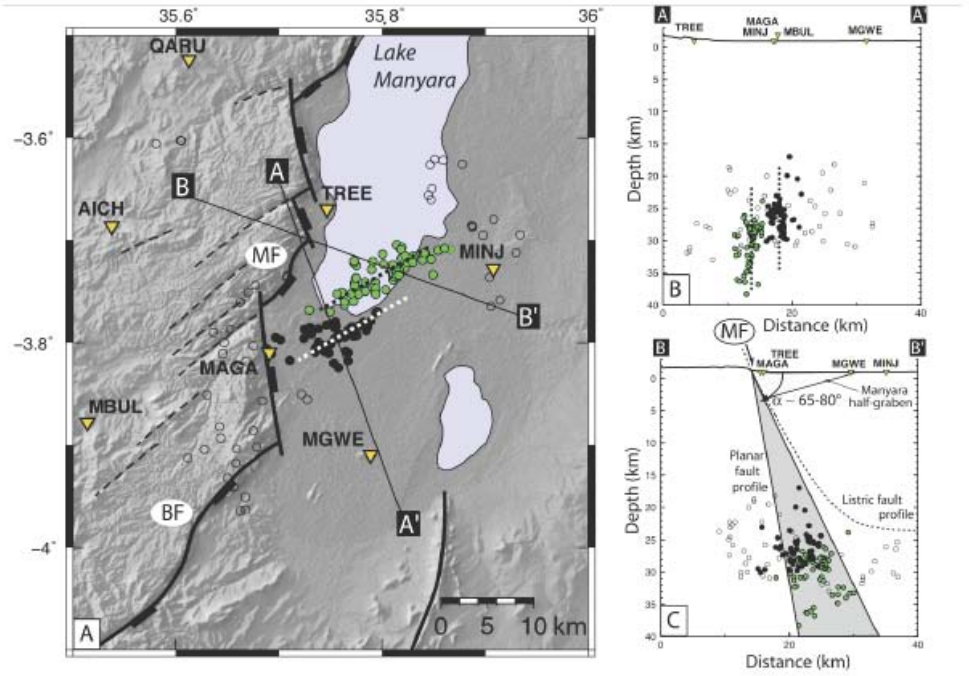

Figure 1 : *A: Map of the seismicity in Lake Manyara. Thick lines delineate major faults and thin dashed ones the main N-E direction. Green and black circles refer to two distinguishable clusters while the rest of the seismicity is plotted with empty circles. The earthquakes are aligned along the N60°E direction (dashed line across clusters). B: Cross-section perpendicular to the direction of the clusters. arthquakes are arranged along two vertical zones (dashed lines) between 25 and 40 km for the northern one (green circles) and between 20 and 30 km for the southern one (black circles). C: Cross-section perpendicular to the mean direction of the segmented Manyara fault. The latter is projected downward into the earthquake sequence either as planar (thick line) or as listric (dashed line) profile. The "planar fault" hypothesis implies a fault surface dip in the range 65-80°, according to the location of the earthquakes. MF, Manyara fault; BF, Balangida fault. (From Albaric et al., in press).*

They form two main clusters rooted at ca. 20-35 km depth, i.e. significantly deeper than the neighbouring Natron-Gelai seismo-magmatic crisis of July-November 2007 (Calais et al., 2008). This apparently long-lasting seismic activity is surprisingly associated with significant NE-SW strike-slip faulting.

The preliminary stress field determined in Manyara is transtensive, with the minimum principal stress oriented WNW-ESE. From a non-linear inversion method using direct P, SV and SH wave amplitudes (Simulated Annealing algorithm, Godano et al., 2009), we improve the double-couple focal mechanisms database, preliminarily determined with P wave polarities. The active structures determined depict clear links with the inherited structures of the basement, at the contact of the Tanzanian cratonwith the Proterozoic belt.

We also model the yield stress envelope of the crust from the depth frequency distribution of earthquakes. The results are consistent with the presence of a mafic lower crust and further support the overall tendency of strength increase of the rifted crust from south Kenya to the NTD (Albaric et al., 2009). It is suspected that deep fluid injections at subcrustal levels may trigger this anomalous activity in the lower crust.

References

Albaric J., J. Perrot, J. Déverchère, A. Deschamps, B. Le Gall, R. W. Ferdinand, C. Petit, C. Tiberi, C. Sue and M. Songo. Contrasted seismogenic and rheological behaviours fromshallow and deep earthquake sequences in the North Tanzanian Divergence, East Africa. *Journal of African Earth Sciences*. In Press.

Albaric J., J. Déverchère, C. Petit, J. Perrot and B. Le Gall. 2009 Crustal rheology and depth distribution of earthquakes: Insights from the central and southern East African Rift System. *Tectonophysics*, 468(1-4), 28-41, doi:10.1016/j.tecto.2008.05.021,.

Calais E., N. d'Oreye, J. Albaric, A. Deschamps, D. Delvaux, J. Déverchère, C. Ebinger, R. W. Ferdinand, F. Kervyn, A. S. Macheyeki, A. Oyen, J. Perrot, E. Saria, B. Smets, D. S. Stamps and C. Wauthier. 2008.Strain accommodation by slow slip and dyking in a youthful continental rift, East Africa*. Nature*, 456, 783-787, doi:10.1038/nature07478,

Godano M., M. Regnier, A. Deschamps, T. Bardainne, and E.Gaucher. 2009 Focal Mechanisms from Sparse Observations by Nonlinear Inversion of Amplitudes: Method andTests on Synthetic and Real Data. *Bulletinof the Seismological Society of America*,99(4):2243–2264

,.

A LARGE ROCK AVALANCHE ONTO MORSÁRJÖKULL GLACIER, SOUTH-EAST ICELAND. ITS IMPLICATIONS FOR ICE-SURFACE EVOLUTION AND GLACIER DYNAMICS

Armelle Decaulne[1,2], Þorsteinn Sæmundsson[3], Halldór G. Pétursson[4], Helgi Páll Jónsson[3], Ingvar A. Sigurðsson[5]

(1) Clermont Université, Université Blaise Pascal, GEOLAB, BP 10448, F-63000 Clermont-Ferrand, France (armelle.decaulne@univ-bpclermont.fr)
(2) CNRS, UMR 6042, GEOLAB, F-63057 Clermont-Ferrand, France
(3) Natural Research Centre of Northwestern Iceland, Aðalgata 2, IS-550 Sauðárkrókur, Iceland
(4) Icelandic Institute of Natural History, Borgum við Norðurslóð, IS-600 Akureyri, Iceland

Abstract

In spring 2007, a large rock avalanche descended onto the Morsárjökull valley glacier in southeast Iceland, leaving one fifth of the glacier buried. The insulating effect of the deposit on the ice was quickly observed as a difference in the ablation between the exposed ice and that under the deposit. After three melt seasons, the ice surface under the deposit was 29 m above the surrounding glacier surface. A reduced rate of ice melting beneath the area of the deposit would likely alter the longitudinal profile of the glacier.

Introduction

Mass movements from oversteepened mountain slopes adjacent to glaciers are a common source of debris on ice surface (Benn and Evans, 1998; Hambrey and Alean, 2004), resulting from paraglacial adjustment of rock slopes (Ballantyne, 2002). Spectacular examples of large-scale rock avalanches falling onto glaciers are documented in the literature, mainly from Alaska, United States, the Himalaya and New Zealand. A characteristic of such rock avalanches is the exceptionally long distances reached by the deposits on the ice surface. On March 20 2007, a large avalanche of rock covered the valley glacier Morsárjökull, in southeast Iceland. About one fifth of the glacier surface was then buried by about 4×10^6 m^3 of debris covering an area of over 720,000 m^2. It corresponds to one third of the eastern part of the glacier. Among the questions that arose after this event are: how will the debris mass affect the movement of the glacier and how will the glacier incorporate and/or distribute the debris mass? The purpose of this study is to evaluate the effects of the rock avalanche insulation on the future morphology and movement of the glacier, based on the 3-melting season observations and measurements, but also based on a review of previous case studies.

The Morsárjökull case study

Yearly measurements of the glacier front since 1933 indicate a total retreat of over 1300 m, although small advances have also occurred during that time (Sigurðsson, 2007). As the glacier front retreats the glacier becomes thinner and narrower in its basin, and the surrounding steep slopes become more unstable. The bedrock is palagonite and pillow breccia, interlain by basaltic lava flows and cut by faults and numerous thin dykes. The scar from the rock avalanche is located on the north face of the headwall that dominates the ice fall area of the eastern Morsárjökull glacier, between 720 m and 1120 m a.s.l. A part of the northwest facing slope, 400 m high and 500 m long, collapsed onto the glacier, partially burying the medial moraine. The material then flowed southwest onto the eastern section of the glacier, reaching a horizontal length of 1400 m and a maximum drop of 660 m, for a friction coefficient of 0.47. The deposit fell onto the glacier at approximately 760 m and its lower part was located by 460 m a.s.l., over a length of 1700 m. On July 2007 the upper margin of the debris mass was located approximately 3513 m from the glacier snout and the lower margin approximately 2050 m. The contact between the ice and the deposit was sharp, and no deformation of the glacier ice was visible at the contact with the deposit or in the close surroundings, indicating a rapid process.

Photogrammetric studies of the source-area estimates the volume of the rock avalanche to be 4×10^6 m^3. Analyses of available aerial photographs show that the largest clast sizes are found in the peripheries of the deposit. The central part consists of smaller clasts. The deposit thickness is also highly variable. It changes from 1.5 to 3 m at the front to over 7 m elsewhere.

The rock avalanche deposit is located within the mid ablation zone of the glacier. Since the debris cover insulates the glacier ice from solar radiation, differential melting occurred on the surface. At the front, the deposit standed 10 m above the exposed glacier surface in early July 2007, as measured on

the field with an inclinometer, 22 m in early August 2008, and 29 m in early August 2009. This caused local collapses of boulders on the boundaries of the deposit. This process contributes to widen the size of the deposit, increasing the buried surface of the glacier. According to measurements made on Skeiðarár jökull (Icelandic Meteorological Office, unpublished information), the ablation rate of Morsárjökull glacier can be estimated to 8-10 m.a^{-1}. This seems to be in accordance with the non-ablated ice under the deposit after the two melting seasons during the summers 2007, 2008 and 2009. From 07/2007 to 08/2009, the front of the debris mass progressed down glacier to a distance of about 200 m.

Fig. 1: The Morsarjökull glacier partially buried under the rock avalanche deposit.

Fig. 2: The variety of material size constituting the rock avalanche deposit: clast supported on the upper layer, the deposit is enriched in fine material (gravel to coarse sand) at the contact with ice. Observers as scale are outlined on the photographs, providing scales.

Discussion on the future implications of the avalanche deposit onto the Morsárjökull glacier

According to previous case studies of rock avalanche that have fallen onto glaciers, the glaciers reacted in several ways after a part of the ice had been buried. From 1920 to 1942, the Brenva glacier in the Italian Alps encountered an advance prolongation up to *c.* 600 m following a rock avalanche that occurred in 1920. Its thickness relatively increased at the snout and farther up-glacier, while the surrounding glaciers retreated about 65 m during the same period (Deline, 2002). The Bualtar glacier in the Karakoram Range in Pakistan surged after three huge landslides partly buried the ablation zone and affected the under-glacial drainage (Gardner and Hewitt, 1990). The Sioux glacier (Alaska) experienced a significant ice thickness increase after a third of the lower part of the glacier was insulated by the debris cover. An ice mass transfer that lowered the upper unburied part of the glacier and raised the insulated lower one (Reid, 1969) resulted in an advance of the glacier snout.

Historically, two rock avalanches onto glaciers are known from southern Iceland. The rockslide that covered the terminus of the Jökulsárgilsjökull outlet glacier (south Mýrdalsjökull ice cap) in 1972 or 1973 caused substantial differential melting and the glacier snout underwent significant thickening (Sigurðsson and Williams, 1991). Part of the snout of the Steinsholtsjökull glacier, an outlet of the north Eyjafjallajökull ice cap, was covered by a 15 x 10^6 m^3 rockslide in January 1967 (Kjartansson, 1968). The rock avalanche also impacted a proglacial lake, causing a flood that flowed 35 km to the sea.

From these case studies, we underline that the effects of a rock avalanche affecting a glacier are a function of the magnitude of the event *versus* the size of the glacier, i.e. the surface and thickness of the debris cover *versus* the ice surface and thickness. Another important factor is the location of the deposit on the glacier body.

In the Morsárjökull case study, the deposit covers the mid ablation area and the snout of the glacier is mostly free of debris. Though, changes were observed soon after the rock avalanche

occurred. The most obvious implication of the deposit on the glacier is the effectiveness of its insulation property on the buried ice, significantly decreasing its melting rate. Presumably, the ice that is not ablated from under the deposit will sooner or later favour an ice transfer down-glacier, as observed in other cases (Reid, 1969). The result will then be to speed down the retreat and thinning of the glacier.

The incorporation of the rocky material within the glacier should also be considered. A first possibility is that the material will be buried by snow and ice; the rock avalanche material is very coarse so it will require an abundant supply of ice and snow to be buried. This seems unlikely as the deposit is located within the ablation zone of the glacier. Nevertheless, the location of the head of the deposit in the free-falling ice avalanches part of the glacier caused the uppermost one fifth of the deposit to be buried within a thick apron of ice and snow by falling snow and ice avalanches after only 3 months. The ice apron progresses over the deposit with time. Another possibility is that the material could be incorporated into the ice by falling down crevasses in the glacier surface. As the deposit covers a part of the glacier with a poor crevasse network, it makes unlikely the incorporation of the debris into the glacier as englacial sediment. Therefore, the main part of the deposit will remain supraglacial.

From a supraglacial hydrological point of view, a few minor changes can be expected, mainly involving the western part of the Morsárjökull glacier. On the eastern side of the glacier, the deposit buried an area of relatively low channel network. On the western side, the deposit obstructs the entry of melt water into the medial moraine. Depending on the crevasse network in the western area, the drainage of supraglacial meltwater into the glacier will occur further up on the glacier.

We then assume that the main effect of the debris cover on the eastern part of the Morsárjökull glacier will be a significant reduction of the ablation along with enhanced ice transfer due to the formation of steep ice slopes and overburden pressure under the deposit. This could create an asymmetry between the two parts of the glacier: the eastern one having a less negative mass balance than the western one.

Conclusion

The collapse of the rock slope that caused the rock avalanche on the Morsárjökull glacier is a major event in the Icelandic glacial environment. Such events are rare onto glaciers. Several implications of the deposit onto the glacier can be emphasized. The part affected by the deposit is located within the ablation zone, so its impact on ice dynamics is immediate. The lower melting rate beneath the deposit is evident by a relative rise in comparison with the exposed ice reaching 29 m after 29 months. As a result, the ice surface will pursue to steepen, increasing the driving stresses and causing the down-glacier region to advance. The Morsárjökull glacier is not known as debris-mantled. Except for the present event, neither major rockfall nor rock avalanche has been recorded in the past. The present debris input to the ice surface, though large, will therefore not have a long-lasting effect, contrary to the case of the Brenva glacier which involved repeated rockfall and rock avalanches for several centuries. The debris cover onto the Morsárjökull glacier may reduce the retreat of its eastern part while its western part will probably not be similarly affected, leading to an asymmetrical front position in the future. However, the Morsárjökull glacier is presently within a retreat phase that has lasted for at least eight decades. Further slope destabilisation is therefore possible.

References

Ballantyne C.K., 2002, Paraglacial geomorphology. *Quaternary Science Reviews*, 21, 1935-2017.

Benn D.I., Evans D.J.A., 1998, *Glaciers and Glaciations*. Arnold, London, 734 p.

Deline P., 2002, *Etude géomorphologique des interactions écroulements rocheux/glaciers dans la haute montagne alpine (versant sud-est du massif du Mont Blanc)*. Unpublished PhD thesis, Department of Geography, University of Savoie, Chambéry, 365 p.

Gardner J.S. and Hewitt K., 1990, A surge of Bualtar Glacier, Karakoram Range, Pakistan: a possible landslide trigger. *Journal of Glaciology* 36, 159-162.

Hambrey M., Alean J., 2004, *Glaciers*. Cambridge University Press, Cambrige, 376 p.

Kjartansson G., 1968, The Steinsholtshlaup, central south Iceland on January 15, 1967. *Jökull 17*, 249-262.

Reid J., 1969, Effects of a debris slide on “Sioux Glacier”, South-Central Alaska. *Journal of Glaciology* 8-54, 353-367.

Sigurðsson O., 2007, Jöklabreytingar 1930-1970, 1970-1995, 1995-2005 og 2005-2006 (glacier variations). *Jökull* 57, 91-97.

Sigurðsson O., Williams R., 1991, Rockslides on the terminus of “Jökulsárgilsjökull”, Southern Iceland. *Geografiska Annaler* 73A, 129-140.

LATE ORDOVICIAN CLIMBING DUNE ASSEMBLAGES, THE SIGNATURE OF GLACIAL OUTBURST ?

F. GIRARD1, J.F. GHIENNE1, J.MOREAU2, J.L. RUBINO3 ,Y. BOUJAZIA41

CNRS, CGS, Strasbourg, France, ghienne@eost.u-strasbg.fr, flavia.girard@eost.u-strasbg.fr
2Aberdeen University, Scotland, j.moreau@abdn.ac.uk3Total, CSTJF, ISSC, jean-loup.rubino@total.com4NOC, Libya, Y-Boujazia@yahoo.com

Meltwater-related processes have long been recognized as first-order geomorphic mechanisms in both subglacial and proglacial environments. Among them, glacial outburst or jökulhlaups (the Icelandic term for “glacial flood”) represent short-term events (1-15 days, e.g. Snorrason et al., 2002) with major erosional and depositional impacts. They emanate either from the catastrophic drainage of glacially dammed lakes or from the drainage or collapse of subglacial reservoirs.
At the end of the Ordovician, a continental-scale ice sheet extended on present-day West and North Africa, as well as Arabia, possibly joining South Africa. Glacial depositional sequences essentially comprise fluvial, deltaic and shallow-marine sandstones and pelitic facies grading distally into turbidites succession (Le Heron et al., 2006; Ghienne et al., 2007). One of the most striking and conspicuous glacially-related Late Ordovician depositional facies is constituted by recurrent assemblages of aggrading, stoss-depositional 2D or 3D dunes. Based on data of outcrops from the paraglacial successions of the Western Murzuq Basin/ Tassili n’Ajjer area (southern Libya – Algeriaboundary), this presentation aims to describe climbing dunes assemblages (facies, geometries and depositional model), and to relate them to outburst events affecting the fluvio-glacial outwash plains at the periphery of the retreating Late Ordovician ice sheet (Ghienne et al., 2003; Ghienne et al., 2007, Ghienne et al., 2010).

Climbing dune-scale cross-stratification depositional facies is comprised of medium-grained to coarse-grained sandstones that typically involve 0,3 to 1 m high, 3 to 5 m in wavelength, asymmetrical laminations. Most often stoss-depositional structures have been generated, with preservation of the topographies of formative bedforms. Climbing-dune cross-stratification related to the migration of lower-flow regime dune trains is thus identified. Related architecture and facies sequences are described from two case studies: (i) erosion-based sandstone sheets; and (ii) a deeply incised channel. The former characterized the distal outwash plain and the fluvial/ subaqueous transition of related deltaic wedges, while the latter formed in an ice-proximal segment of the outwash plain. In erosion-based sand sheets, climbing-dune cross-stratification results from unconfined mouth-bar deposition related to expanding, sediment-laden flows entering a water body. Within incised channels, climbing-dune cross-stratification formed over eddy-related side-bars reflecting deposition under recirculating flow conditions generated at channel bends.

Associated facies sequences record glacier outburst floods that occurred during early stages of deglaciation and were temporally and spatially linked with subglacial drainage events involving tunnel valleys. The primary control on the formation of climbing-dune cross stratification is a combination between high-magnitude flows and sediment supply limitations, which lead to the generation of sediment-charged Stream flows characterized by a significant, relatively coarse-grained,
sand-sized suspension-load concentration, with a virtual absence of very coarse to gravelly bedload. The high rate of coarse-grained sand fallout in sediment-laden flows following flow expansion throughout mouth bars or in eddy-related side bars resulted in high rates of transfer of sands from suspension to the bed, net deposition on bedform stoss-sides and generation of widespread climbing dune cross-stratification. The later structure has no equivalent in the glacial record, either in the ancient or in the Quaternary literature, but analogues are recognized in some flood-dominated depositional systems of foreland basins.

References

Le Heron D., Craig J., Sutcliffe O., Whittington R. (2006) Ordovician glaciogenic reservoir heterogeneity : an example from the Murzuq Basin Libya. Mar.Petrol. Geol, 23, 655–677

Ghienne J.-F., Le Heron D., Moreau J., Denis M., Deynoux M. (2007) The Late Ordovician glacial sedimentary system of the North Gondwana platform. In: Hambrey, M., Christoffersen, P., Glasser, N., Janssen, P., Hubbard, B. And Siegert, M. (eds.) Glacial Sedimentary Processes and Products. Special Publication n°39, IAS, Blackwells, Oxford, 295-319.

Ghienne J.F., Deynoux M., Manatschal G., Rubino J.L. (2003) Palaeovalleys and fault-controlled depocenters in the Late Ordovician glacial record of the Murzuq Basin (Central Libya), C.R. Geosciences, 335, 1091-1100.

Snorrason A., Jonsson P., Sigurosson O., Palsson S., Arnason S., Vikingsson S., Kaldal I. (2002) November 1996 jökulhlaup on Skeiararsandur outwash plain, Iceland. Special publication N°32, IAS, Blackwells, Oxford, 55-65.

Ghienne J.F., Girard F., Moreau J., Rubino J.L. (2010) Late Ordovician climbing-dune cross stratification: a signature of outburst floods in proglacial outwash environments?. Sedimentology, in press.

AMSTERDAM - ST. PAUL HOTSPOT HISTORY

Myriam Janin[1,2], Christophe Hémond[1,2], Marcia Maia[1,2]
(1) Université Européenne de Bretagne, 6 avenue Le Gorgeu, 29200 Brest, France,(2) Université de Brest, CNRS Domaines Océaniques, Institut Universitaire Européen de la Mer, Place Copernic, 29280 Plouzané, France - Myriam.Janin@univ-brest.fr

Abstract (Arial 10)

The Amsterdam St. Paul hotspot (Indian Ocean) interacts with a regional depleted mantle containing some DUPAL-like blobs. Its lateral motion velocity is about 1-2 cm/yr. The plume induced the construction of a volcanic chain and of an oceanic plateau through two pulses of more intense magmatic activity. The intraplate plate activity appears partially controlled by some tectonic stress induced by the diverging motion of the Australian and Capricorn plates along a diffuse boundary.

Introduction

The Amsterdam-St Paul (ASP) plateau results of the excess of melting induced by the interaction between the ASP hotspot and the South-East Indian Ridge. The ASP plume was originally located beneath the Capricorn-Australian plates and its interaction with the SEIR began about 10 Ma ago. The intraplate activity of the ASP hotspot resulted into the construction of the chain of seamounts (the Chain of the Dead Poets: CDP) (cf. fig.). This volcanic chain is thus a unique opportunity to study the hotspot chemical characteristics prior to its interaction with the SEIR and its evolution since. A sorrow inspection shows that CDP is built near by the diffuse opening boundary between Capricorn and Australian plate, which has consequences on its morphology.

Main

An exhaustive study of the ASP hotspot products prior to its interaction with the SEIR provides acces to its geochemical composition while studying products of its interaction with the SEIR (i. e. ASP plateau) provides indirect knowledge on the Indian Ocean regional upper mantle.

The ASP plume exhibits a very variable enriched isotope composition with $^{86}Sr/^{87}Sr \approx 0.7039$, $^{143}Nd/^{144}Nd \approx 0.51280$, $^{206}Pb/^{204}Pb \approx 18.8$ to19.5 and $^{208}Pb/^{204}Pb \approx$ 39.1 to 39.8 for the extreme endmember. In addition, a large variation at volcano scale is also observed i. e. $^{208}Pb/^{204}Pb$ varying from 39.13 to 39.43 for La Fontaine seamount. This variability is interpreted in terms of contamination of hotpot derived melts with the heterogeneous Indian Ocean upper mantle. As proposed by Maia et al. [2008] the ASP hotspot seems to be weak plume that had pulses of activity within the last 10 My. Two periods of increased magmatic production have been identified between 10 and 6 My and during the last 3 My years. These two periods has resulted with the construction of two generations of seamounts northward of the ASP. Their elongated morphologies suggest a construction influenced by tectonic stress and likely due to the regional diverging motion between the Australian and Capricorn plates oriented N150°.

The isotopic compositions of the ASP plateau have reveal that the Indian Ocean upper mantle is extremely heterogeneous. The hotspot related melts mixed variably with the local Depleted Mantle which containing a poor component in radiogenic Pb, having a DUPAL-type composition. Nicolaysen et al. [2007] have shown that the DUPAL-type signature in the SEIR lavas is spatially limited to the segment I2 and J1/J2 crossing ASP plateau. They proposed that (1) the ASP hotspot is partially zoned, (2) the hotspot source contains components with different solidus temperatures or (3) a high proportion of DUPAL-type material is present within or beneath the plateau. Our data support the last model because we evidenced the existence of long-lived component with a restricted lateral extension from SW to NE, which has contaminated the plateau and SEIR lava during the 1 M. Consequently, we assume that the local upper mantle might resemble the “Plum-pudding” of Morgan & Morgan [1999]. When the SEIR approaches the ASP hotspot, some plume derived material mixes with the depleted surrounding mantle and/or DUPAL blobs, leading to the variability formed in ASP plateau lavas.

K-Ar dating on ASP samples reveals that the absolute motion of the Australian plate calculated with respect with a fixed ASP plume is of about 77 km/My toward the NE. With a spreading rate of about 6-7 cm/yr the accretion at the SEIR axis cannot account for this velocity. In consequence, an absolute motion of the ASP plume of about 10-20km/My to the SW, comparable in velocity to that of Hawaii [Tarduno et al. 2003], could account for this discrepancy.

In summary, the ASP hotspot is a plume, emplaced in an heterogeneous upper mantle, showing pulses of activity and partially controlled by regional tectonic settings….

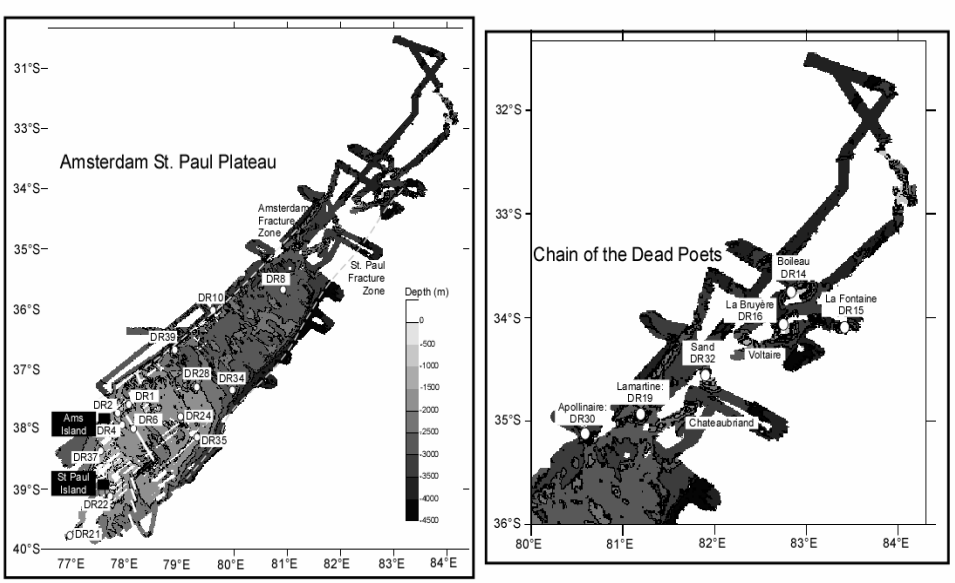

Bathymetry (in grey scale) of the ASP plateau with a focus on CDP mapped during the MD157/PLURIEL cruise. White circles represent basalts samples with the related dredge (DR) number. On the CDP name of seamounts are given. Seamounts without dredge could not be successfully dredged. Black squares are Amsterdam (Ams) and St Paul islands. Grey dotted lines are the Fracture Zones limiting the ASP plateau to the NW and the SE.

References

Maia, M., Courreges, E., Pessanha, I., Hemond, C., Janin, M., Bassoullet, C., Brachet, C., Chavrit, D., Gente, P., Humler, E., Johnson, K., Loubrieu, B., Martin, C., Mudholkar, A., Oldra, J., Patriat, M., Raquin, A., Richard, M., Royer, J., Vatteville, J., (2008). Evolution of the Saint Paul Amsterdam Plateau in the Last 10 m.y. *Eos Trans. AGU, 89*(53), Fall Meet. Suppl., Abstract T54B-06.

Morgan, J.P., Morgan , W. J., (1999). Two-stage melting and the geochemical evolution of the mantle: a recipe for mantle plum-pudding - Earth Planet Sci Lett - 1999

Nicolaysen, K. P., Frey, F. A., Mahoney, J. J., Johnson, K. T. M., Graham, D.W., (2007). Influence of the Amsterdam/St. Paul hot spot along the Southeast Indian Ridge between 77° and 88°E: Correlations of Sr, Nd, Pb and He isotopic Variations with ridge segmentation, *Geochem. Geophys. Geosyst., 8*, Q09007, doi:10.1029/2006GC001540.

Tarduno, J. A., Duncan, R. A., Scholl, D. W., Cottrell, R. D., Steinberger, B., Thodarson, T., Kerr, B. C., Neal, C. R., Frey, F. A., Torii, M., Carvallo, C., (2003). The Emperor Seamounts: Southward motion of the Hawaiian hotspot plume in Earth's mantle. *Science 301*, 1064-1069.

HIGH-RESOLUTION LATE PLEISTOCENE PALEOMAGNETIC SECULAR VARIATION RECORD FROM LAGUNA POTROK AIKE, SOUTHERN PATAGONIA (ARGENTINA): PRELIMINARY RESULTS FROM THE ICDP-PASADO DRILLING

Agathe Lisé-Pronovost (1,2,*), Guillaume St-Onge (1,2), Torsten Haberzettl (1,2,3), and the PASADO science team (4)

(1) Institut des sciences de la mer de Rimouski (ISMER), Université du Québec à Rimouski (UQAR), 310 allée des Ursulines, Rimouski (QC) G5L3A1, CANADA
(2) GEOTOP research center, (QC) CANADA
(3) Physical Geography, Institute of Geography, Friedrich-Schiller-University Jena, Löbdergraben 32, 07743 Jena, GERMANY
(4) http://www.pasado.uni-bremen.de/index.html
*agathe.lisepronovost@uqar.qc.ca

Abstract

Here we present preliminary results of a high-resolution full vector paleomagnetic reconstruction from the southernmost continental scientific drilling site Laguna Potrok Aike, Argentina (52°S). Magnetic analyses of the long PASADO-ICDP composite record are currently underway at the Sedimentary paleomagnetism laboratory of the Institut des sciences de la mer de Rimouski (ISMER) and reveal high quality paleomagnetic data.

Introduction

High-resolution paleomagnetic reconstructions from sedimentary sequences are scarce in the Southern Hemisphere. Therefore, the millennial- to centennial-scale variability of the geomagnetic field is under-represented in the Southern Hemisphere relative to the Northern Hemisphere and the possible global nature of that variability cannot be assessed. Here we present the first high-resolution Late Pleistocene paleomagnetic secular variation (PSV) reconstruction from the continental archive Laguna Potrok Aike south of 42°S in South America. Laguna Potrok Aike (51°58'S, 70°23'W) is a maar lake located in the Pali Aike Volcanic Field in southern Patagonia (Argentina) (Figure 1). Previous studies revealed very high Holocene sedimentation rates (> 100 cm/ka; Haberzettl et al., 2007) in the center of the lake. Because of its geographic location in the mid-latitudes of the southern hemisphere and its high sedimentation rates, Laguna Potrok Aike is a key site for paleoenvironmental and paleomagnetic studies. During the austral spring 2008, the multi-national Potrok Aike maar lake Sediment Archive Drilling prOject (PASADO) science team successfully drilled two ~100 m holes under the framework of the International Continental scientific Drilling Program (ICDP) (Zolitschka et al., 2009).

Main

A preliminary Holocene age model of the PASADO-ICDP core based on comparison of magnetic susceptibility data from that core with a well-dated (radiocarbon-and tephra-based chronology) core located nearby in the center of the lake (PTA03-12; Haberzettl et al., 2007) indicates a deposition of ~19 m of lacustrine sediments since 16 ka cal BP. Hysteresis measurements using an alternating gradient force magnetometer were completed on 64 samples from the uppermost 25 m of the composite sequence. The results indicate a magnetic assemblage dominated by magnetite grains in the pseudo-single domain range. Principal component analysis (PCA) inclination and declination profiles were constructed from the stepwise alternating field demagnetization of the natural remanent magnetization (NRM) measured on u-channel samples at 1 cm intervals using a 2G Enterprises cryogenic magnetometer. The PCA inclinations vary around the expected geocentric axial dipole (GAD) inclination for the latitude of the coring site and the maximum angular deviation (MAD) values are generally lower than 5°, indicating high quality paleomagnetic data. Furthermore, the PASADO-ICDP paleosecular variation (PSV) record for the last 16 ka cal BP displays similar variations as the available records from marine sediments in the South Atlantic, South Pacific and Southern oceans, as well as from lacustrine sediments further north in Argentina. Altogether, the preliminary results indicate a genuine geomagnetic origin of the signal and indicate the great potential of the drilled core for further paleomagnetic investigations which will be accomplished within the next year.

These preliminary results are part of a PhD project with the following main scientific objectives: 1)

reconstruct the full geomagnetic vector (inclination, declination and relative paleointensity) of the PASADO-ICDP composite profile (~106 m), 2) use magnetostratigraphy as a regional chronostratigraphic tool for Laguna Potrok Aike, in addition to radiocarbon, luminescence, uranium isotopes series and tephrochronology dating approaches, 3) develop paleoenvironmental proxies of rapid climate changes using magnetic properties of the sediment.

Figure 1. *Laguna Potrok Aike (51°58'S, 70°23'W) is a maar lake located in the the Pali Aike Volcanic Field of southern Patagonia (Argentina). The maximum lake diameter is ~3.5 km and the maximum water depth is ~100 m. The picture was taken from a nearby scoria cone named the "Mexican hat". Typical volcanic rocks of this geologic structure are visible on the lower right.*

References

Haberzettl, T., Corbella, H., Fey, M., Janssen, S., Lücke, A., Mayr, C., Ohlendorf, C., Schäbitz, F., Schleser, G.H., Wille, M., Wulf, S., Zolitschka, B., 2007. Lateglacial and Holocene wet-dry cycles in southern Patagonia: chronology, sedimentology and geochemistry of a lacustrine record from Laguna Potrok Aike, Argentina, The Holocene 17(3), 297-310.

Zolitschka, B., Anselmetti, F., Ariztegui, D., Corbella, H., Francus, P., Ohlendorf, C., Schäbitz, F and the PASADO Scientific Drilling team, 2009. The Laguna Potrok Aike Scientific Drilling Project PASADO (ICDP Expedition 5022), Scientific Drilling 8, 29-34.

LIST of PARTICIPANTS

Agranier Arnaud	LDO, Plouzané	arnaud.agranier@univ-brest.fr
Amman Jérôme	LDO, Plouzané	jerome.amman@univ-brest.fr
Bassoulet Claire	UMS 3113 Plouzané	claire.bassoulet@univ-brest.fr
Babonneau Nathalie	LDO, Plouzané	nathalie.babonneau@univ-brest.fr
Barrat Jean-Alix	LDO, Plouzané	jean-alix.Barrat@univ-brest.fr
Bellon Hervé	LDO, Plouzané	herve.bellon@univ-brest.fr
Beaumais Aurélien	Student , LDO, Plouzané	Aurelien.beaumais@univ-brest.fr
Bergerat Françoise	LGS, UMPC, Paris	francoise.bergerat@upmc.fr
Bjornsson Helgi	University Reykjavik, Is.	hb@raunvis.hi.is
Chazot Gilles	LDO, Plouzané	Gilles.chazot@univ-brest.fr
Courrèges Esther	Student, LDO & Ifremer	esther.courreges@ifremer.fr
Dauteuil Olivier	Géosciences Rennes 1	olivier.dauteuil@univ-rennes1.fr
David Christine	Dir Adjointe IPEV	dirpol@ipev.fr
Decaulne Armelle	Geolab, Clermont	mailto:Armelle.Decaulne@univ-bpclermont.fr
Delacourt Christophe	LDO, Plouzané	Christphe.delacourt@univ-brest.fr
Deschamps Anne	LDO, Plouzané	anne.deschamps@univ-brest.fr
Devèrchère Jacques	LDO, Plouzané	jacques.deverchere@univ-brest.fr
Droz Laurence	LDO, Plouzané	Laurence.Droz@univ-brest.fr
Eynaud Frédérique	EPOC Bordeaux	f.eynaud@epoc.u-bordeaux1.fr
Fagel Nathalie	Univ.Liège, Belgique	nathalie.fagel@ulg.ac.be
Frank Norbert	LSCE-CEA Giff	Norbert.Frank@lsce.ipsl.fr
Garcia Sébastien	Univ.Berlin , BRD	sgarcia@zedat.fu-berlin.de
Geoffroy Laurent	Géologie, Univ.Le Mans	laurent.geoffroy@univ-lemans.fr
Giraudeau Jacques	EPOC Bordeaux	j.giraudeau@epoc.u-bordeaux1.fr
Girard Flavia	Student, Eost Strasbourg	flavia.girard@eost.u-strasbg.fr
Guégan Solène	Student , LDO, Plouzané	solene_guegan@hotmail.fr
Goiran Jean Phillipe	UMR 5133 Clermont	jean-philippe.goiran@mom.fr
Goslin Jean	LDO, Plouzané	jean.gosselin@univ-brest.fr
Gudmundsson Agust	Royal Holloway, London	rock.fractures@googlemail.com
Gudmundsson Agust	JFS Reykjavik	jardis@geoice.net

Guillou Hervé	LSCE-CEA Giff	herve.guillou@lsce.ipsl.fr
Gutscher Marc André	LDO, Plouzané	marc-andre.gutscher@univ-brest.fr
Hémond Christophe	LDO, Plouzané	Christophe.hemond@univ-brest.fr
Huck Thierry	LPO Brest	thierry.huck@univ-brest.fr
Janin Myriam	Student , LDO, Plouzané	Myriam.janin@univ-brest.fr
Kirkbride Martin	Univ. Dundee , Scotland	m.p.kirkbride@dundee.ac.uk
Legall Bernard	LDO, Plouzané	bernard.legall@univ-brest.fr
Lisé Pronovost Agathe	Student GEOTOP, Rimouski	agathe_lp@hotmail.com
Massé Guillaume	LOCEAN, Univ.Paris 6	Guillaume.Masse@locean-ipsl.upmc.fr
Maia Marcia	LDO, Plouzané	marcia.maia@univ-brest.fr
Ménard Gabrielle	Student , LDO, Plouzané	gabrielle-menard@hotmail.fr
Menzies Martin	Royal Holloway, London	m.menzies@es.rhul.ac.uk
Mercier Denis	Géolittomer , Nantes	denis.mercier@univ-nantes.fr
Nonnotte Philippe	LDO, Plouzané	Philippe.nonnotte@univ-brest.fr
Paulet Yves-Marie	Dir. IUEM, Plouzané	yves-marie.paulet@univ-brest.fr
Perrot Julie	LDO, Plouzané	julie.perrot@univ-brest.fr
Popescu Spéranta	LDO, Plouzané	Speranta.Popescu@univ-brest.fr
Rabineau Marina	LDO, Plouzané	Marina.rabineau@univ-brest.fr
Royer Jean Yves	LDO, Plouzané	Jean-yves.royer@univ-brest.fr
Roussel Erwan	Student Clermont	erwan.roussel@univ-bpclermont.fr
Safra Anissa	Student , LDO, Plouzané	safraanissaa@gmail.com
Schneider Jean Luc	EPOC, Bordeaux	jl.schneider@u-bordeaux1.fr
Ségard Mélanie	Student, Univ. Nantes	melanie.segard@univ-nantes.fr
Sigmarsson Olgeir	Labo Magma & Volcans, Univ. Clermont	O.Sigmarsson@opgc.univ-bpclermont.fr
Sturkell Erik	Earth Sc.Centre Göteborg	sturkell@hi.is
Thomas Marine	Student , LDO, Plouzané	marinechloe.thomas@laposte.net
Tréguer Paul	LEMAR, Plouzané	Paul.treguer@univ-brest.fr
Tréguier Anne Marie	LPO-Brest	Anne-Marie.treguier@univ-brest.fr
Van Vliet-Lanoe Brigitte	LDO, Plouzané	Brigitte.vanvlietlanoe@univ-brest.fr
Van Welden Aurélien	Trondheim	aurelien.vanwelden@gmail.com

Villemin Thierry	EDYTEM, Univ.Chambéry	Thierry.Villemin@univ-savoie.fr